CHARACTERISATION AND PERFORMANCE ASSESSMENT OF SEMI-SOLID DISPERSIONS USING SURFACE ACTIVE LIPIDIC CARRIERS

SARAH OLADEINDE OTUN

A THESIS PRESENTED FOR THE DEGREE OF DOCTOR OF PHILOSOPHY
AT THE UNIVERSITY OF EAST ANGLIA, NORWICH, UK

SEPTEMBER 2011

ABSTRACT

Semi-solid dispersions offer many advantages in the delivery of poorly soluble drugs. However, there is limited understanding of the mechanisms by which in vitro dissolution and in vivo bioavailability is enhanced. Low melting point lipidic carrier excipients demonstrate properties beneficial to formulation of these systems despite presenting further challenge in their characterisation. The physicochemical properties of semi-solid dispersions comprising the lipidic carrier Gelucire 44/14 with the poorly soluble drugs ibuprofen, indometacin and piroxicam were investigated.

Conventional differential scanning calorimetry demonstrated dissolution effects, the slow rate allowing crystalline drug to dissolve within the molten lipid during analysis giving unreliable data regarding the presence of solid crystalline drug in proportion to that existing as a molecular dispersion. Hyper DSC was not definitively found to eliminate these effects, however they were reduced, giving a more accurate estimation of the drug solubility within the lipid. The drugs demonstrated different affinities for the lipid with subsequent effects on the extent of interaction. The presence of drug in the lipid demonstrated a significant inhibitory effect on the lipid crystallisation temperature, with QIMTDSC demonstrating a more extended crystallisation than expected. The dissolution properties of all drugs were enhanced when formulated into semi-solid dispersions with Gelucire 44/14, most notably with the low loaded systems. These low loaded systems, however, demonstrated an increased affinity for atmospheric moisture. Aging effects on the semi-solid dispersions were observed with ibuprofen and indometacin systems in which the drug was found to exist partially as a molecular dispersion. Piroxicam however, which had very limited miscibility with the lipid, was found to exhibit few aging effects over time. Overall, the formulated semi-solid dispersions with Gelucire 44/14 achieved the ultimate goal of successfully enhancing the aqueous dissolution of poorly soluble drugs, however more research is needed in order to relate this successfully to in vivo bioavailability.

ACKNOWLEDGMENTS

My PhD experience over the last three years has been enjoyable, rewarding, often entertaining and frequently very challenging! There are many people to whom I would like to take this opportunity to extend my gratitude and thanks.

I was privileged to work under the supervision of Professor Duncan Craig and Dr Sheng Qi. Sincere thanks for your guidance, vast knowledge and technical assistance throughout. My thanks go to my industrial supervisor Dr Liz Meehan at AstraZeneca for your guidance and input. Thank you to Dr Helen Blade for her help with the very temperamental hyper DSC, and to the rest of Dr Meehan's team at AstraZeneca for welcoming me into your lab. Many thanks also to AstraZeneca for funding my whole PhD experience. Thank you to my dear friends, Nicole Hunter, Carl Rivett, Louise Grisedale, Janine Morris and Bahijja Raimi-Abraham. Thank you for the laughs, the tears and the tea breaks! Thanks to all the past and present members of the UEA Pharmaceutics Research Group, and to all those who have trained me on instruments, taught me software and generally made my PhD life easier than it could have been.

I would like to extend my deepest gratitude to my wonderful parents, Joy and Harry, for your unconditional love, support and encouragement. Thank you for your strength in my times of crisis and your capacity to always solve my problems. Thank you to all my amazing family for always having faith in me, particularly my one of a kind brother Dominic, Auntie Jill (my second mother!) and my cousin Kate. A special mention should also be made to my lovely little Nana. I would also like to take this opportunity to remember my wonderful Gran, and also Nanny Wicks, who both passed away whilst this thesis was being written.

And finally to my wonderful and unshakable husband Gary. Thank you for keeping me sane throughout and for always being on hand with a smile and a cuddle (and the odd sarcastic comment!) whenever I needed. I couldn't have done it without you.

TABLE OF CONTENTS

FIGURES AND TABLES

CHAPTER ONE INTRODUCTION

CHAPTER TWO MATERIALS AND METHODS

CHAPTER THREE CHARACTERISATION OF SURFACE ACTIVE LIPIDIC CARRIERS

CHAPTER SIX HYDRATION STUDIES OF SEMI-SOLID DISPERSION SYSTEMS

CHAPTER SEVEN EFFECT OF AGING ON SEMI-SOLID DISPERSION SYSTEMS

ABBREVIATIONS

DSC	Differential scanning calorimetry
DVS	Dynamic vapour sorption
HSM	Hot stage microscopy
MDT-50%	Mean dissolution time for drug release up to 50%
MTDSC	Modulated temperature differential scanning calorimetry
QIMTDSC	Quasi-isothermal modulated temperature differential scanning calorimetry
RH	Relative humidity
SSD	Semi-solid dispersion
SSD(4)	Fridge cooled semi-solid dispersion (4^{o}C)
SSD(20)	Room temperature cooled semi-solid dispersion (20^{o}C)
Tc	Crystallisation temperature
$Tc_{(end)}$	End of crystallisation exotherm
$Tc_{(max)}$	Maximum of crystallisation exotherm
$Tc_{(onset)}$	Extrapolated onset of crystallisation exotherm
Tm	Melting temperature
$Tm_{(max)}$	Maximum of melting endotherm
$Tm_{(onset)}$	Extrapolated onset of melting endotherm
ΔH	Transition enthalpy / energy

CHAPTER ONE

INTRODUCTION

1.1 BACKGROUND OF THE PROJECT

Whilst surface active lipidic carriers appear to offer advantages for the formulation and delivery of poorly soluble drugs in solid dispersions, there is a limited understanding of the key performance parameters required in the choice of semi-solid carrier for a particular active pharmaceutical ingredient (API) or drug. Furthermore, low melting point excipients present significant challenge in terms of characterising the solid dispersion. Internal development work carried out by AstraZeneca on these types of formulation has exposed areas which require more rigorous analytical approaches to improve our fundamental understanding of the physicochemical properties and the subsequent impact on the dissolution mechanism, and the effects of processing variables and storage conditions on these solid dispersion formulations.

1.2 POOR DRUG SOLUBILITY

A drug may be defined "as 'poorly soluble' when its dissolution rate is so slow that dissolution takes longer than the transit time past its absorptive sites, resulting in incomplete bioavailability" (Horter and Dressman 1997). Approximately 40% of all newly discovered drugs display limited solubility in water and therefore poor and often greatly variable oral bioavailability (Gursoy and Benita 2004). Drugs can also be classed as poorly soluble if they exhibit solubility in water below 100µg/ml (Horter and Dressman 1997).

1.2.1 Biopharmaceutics Classification System

The Biopharmaceutics Classification System is a prognostic tool by which drugs can be classified in terms of their gastrointestinal absorption, proposed by Amidon et al (1995). This classification was proposed through the recognition that the fundamental parameters upon which the rate and extent of drug absorption depend are drug solubility in aqueous media and permeability through the gastrointestinal cell wall.

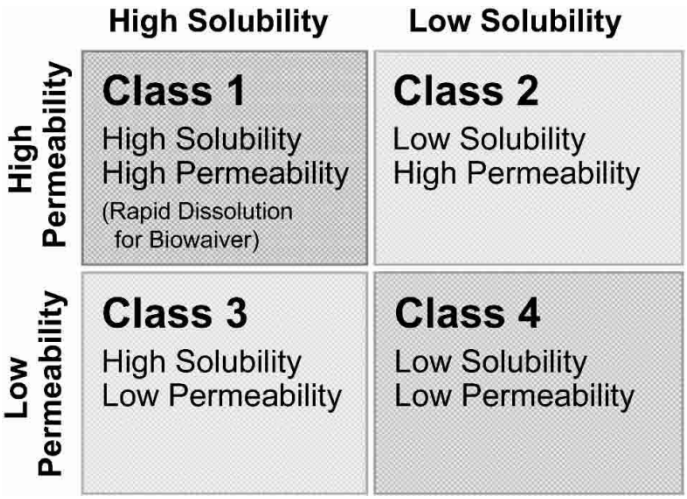

Figure 1.1 *The Biopharmaceutics Classification System (Wu and Benet 2005).*

In vitro / in vivo correlation is only expected for Class II drugs if the in vitro and in vivo dissolution rates are similar. Care must be taken however, as classification into this system is dependent upon the limits set for permeability and solubility. High permeability is classed as absorption up to or greater than 90% across the human jejunum, with no instability within the gastrointestinal tract. Solubility is defined as

the minimum drug solubility at 37^{o}C ± 0.5 over pH 1 to 8, with high solubility being a dose to solubility volume ratio less than or equal to 250ml (Martinez and Amidon 2002).

Further consideration is also required for drugs which exhibit pH dependent solubility (as the pH varies throughout the gastrointestinal tract), drugs that display instability in the gastrointestinal tract, and also those who exhibit complexation with gastrointestinal contents (Amidon et al. 1995).

Since the development of the BCS, the system has been adapted by Wu and Benet (2005) who proposed the Biopharmaceutics Drug Disposition Classification System (BDDCS). The BDDCS hopes that by classifying drug compounds by their mechanism of metabolism it may allow for more accurate prediction of disposition in vivo.

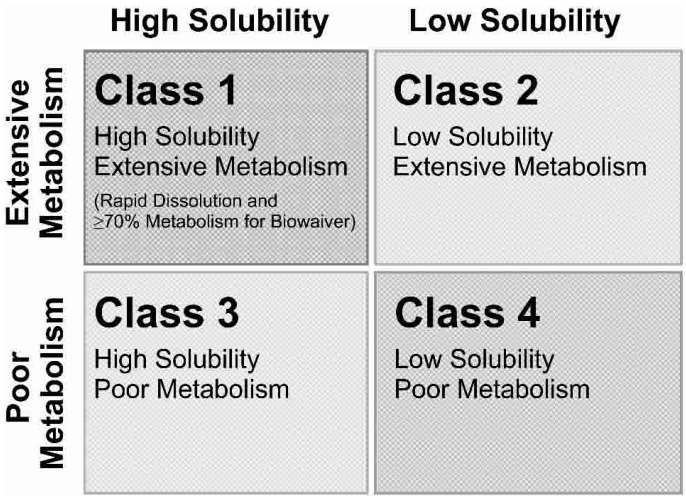

Figure 1.2 *The Biopharmaceutics Drug Disposition Classification System (Wu and Benet 2005).*

The system takes into account a number of factors:

1) Route of elimination.
2) Effect of efflux and absorptive transporters on oral absorption.
3) Clinically significant effect of transporter-enzyme interaction e.g. low bioavailability and drug-drug interactions.
4) Direction and importance of food effects.
5) Transporter effects on systemic levels after absorption following oral and intravenous dosing (Wu and Benet 2005).

It has however been suggested that this revised system does not apply in all cases with some drugs classed as highly permeable by BCS being found not to be extensively metabolised (Chen and Yu 2009).

For the purposes of this project, the BCS terminology will be utilised.

1.2.2 Factors Affecting Drug Dissolution

1.2.2.1 Noyes-Whitney Equation

The chemists Arthur Noyes and Willis Whitney carried out the first dissolution experiments using lead chloride and benzoic acid. They subsequently published the Noyes-Whitney equation in a paper entitled “The rate of solution of solid substances in their own solution” in 1897 (Dokoumetzidis and Macheras 2006; Leuner and Dressman 2000). The equation as it is used today is shown below (York 2002):

$$\frac{dm}{dt} = kA(C_s - C) \qquad \textbf{Equation 1.1}$$

where *m* is the mass of solute passed into solution at time *t*, *A* is the surface area of solid, C_s is the solubility of the compound in the dissolution media, *C* is the concentration of the compound in the dissolution media at time *t* and *k* is the dissolution rate constant. The value of *k* is defined by:

$$k = \frac{D}{Vh} \qquad \textbf{Equation 1.2}$$

where *D* is the diffusion coefficient, *V* is the volume of the dissolution media and *h* is the thickness of the boundary layer.

The Noyes-Whitney equation highlights the factors which contribute to the dissolution of a poorly soluble drug, therefore suggesting a means of improving its solubility. These are:

1) Increasing the surface area of the poorly soluble drug compound by decreasing the particle size.
2) Enhancing the wetting properties of the drug compound surface.
3) Reducing the boundary layer thickness.
4) Ensuring sink conditions.
5) Increasing drug solubility in physiologically relevant dissolution media (Leuner and Dressman 2000).

1.2.2.2 Drug Physicochemical Properties

Crystalline drugs display great order of their constituent molecules which is repeated indefinitely in three dimensions. The most favoured and therefore common crystalline forms of drugs are polymorphs and solvates. Polymorphs are chemically identical species however they possess different crystalline packing arrangements or conformations and thus different physicochemical properties. These drugs are of low energy therefore dissolution can often be reduced. Solvates contain solvent molecules within the crystalline structure and can be known as pseudopolymorphs (Hancock and Zografi 1997; Vippagunta et al. 2001).

The formation of the amorphous phase of a crystalline drug can often dramatically increase dissolution rate. Amorphous substances display liquid structural characteristics i.e. disordered molecular arrangements, but greater viscosity, and can be formed by the supercooling of a molten substance below its melting point (see Figure 1.3) (Hancock and Zografi 1997). The amorphous state is, however, thermodynamically metastable and much higher energy than the crystalline state, meaning that conversion back to the more stable and molecularly ordered crystalline phase is always a possibility. This conversion may be facilitated by mechanical processing, temperature, humidity, additive concentration and time i.e. aging (Hancock and Zografi 1997; Schamp et al. 2006). Storage conditions therefore play a key role in the degradation of dosage forms.

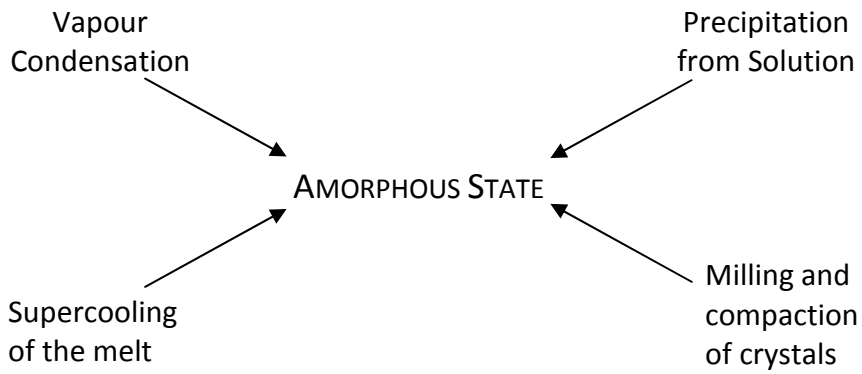

Figure 1.3 *The most common ways in which amorphous character can be introduced into a pharmaceutical system, reproduced from Hancock and Zografi (1997).*

Particle size can affect drug dissolution. The smaller the particle size the greater the surface area in contact with the dissolution media and therefore in theory, greater dissolution. Particles in the range 3 to 5µm can often effectively increase solubility (Horter and Dressman 1997). This is especially important when considering poorly soluble drug substances. If the drug displays poor wetting properties then agglomeration of the small particles may occur, further decreasing the dissolution. The poor wetting characteristics of water insoluble drugs are due to their high contact angle. The presence of surfactants in dissolution media or in vivo can however act to decrease the contact angle, promoting wetting and dissolution, and preventing agglomeration (Horter and Dressman 1997).

The pKa of a drug is its ability to partition from a lipidic to an aqueous environment, and it is this property which allows estimation of its aqueous solubility. The pKa determines the ionisation state of the drug based upon the pH of the solvent solution. Drugs in the ionised form tend to demonstrate greater aqueous solubility in

comparison to those in the unionised form. Weakly basic drugs will exhibit greater solubility in low pH environments, with weakly acidic drug compounds demonstrating greater solubility at high pH (Martinez and Amidon 2002). The pH of the gastrointestinal tract environment changes drastically upon transit throughout, therefore influencing the saturation solubility of ionisable drugs.

1.2.2.3 Physiological Factors

As well as drug physicochemical properties, physiological conditions can also greatly influence the absorption of drug substances during their transit through the gastrointestinal tract. Gastrointestinal pH varies depending upon the area of the tract involved and the presence or absence of food (Table 1.1) (Horter and Dressman 1997).

Table 1.1 *Average pH values in healthy humans in the fasted and fed state at various sites in the upper gastrointestinal tract (Horter and Dressman 1997).*

Location in GI Tract	Fasted State pH	Fed State pH
Stomach	1.3	4.9
Duodenum (mid-distal)	6.5	5.4
Jejunum	6.6	5.2-6.0
Ileum	7.4	7.5

The pKa of the drug substance can therefore determine the optimum area of the gastrointestinal tract for dissolution. It must be taken into account however that other factors such as drug therapy, pathophysiological conditions and age can also play a role in the pH of luminal fluids (Horter and Dressman 1997).

As well as influencing the gastrointestinal pH, the presence of food can facilitate direct interactions with the drug. These interactions, which can often occur during emulsification of the fatty foods into mono- and diglycerides, have sparked interest in the formulation of insoluble drug substances with lipophilic excipients in order to improve solubility and absorption (Schamp et al. 2006).

The caloric content of food is known to have the potential to impact on the extent of food effect demonstrated on certain drug entities, however in some cases it may have a limited effect. The gastric emptying time is greatly increased by the fluid volume in the upper gastrointestinal tract meaning that any oral dosage forms present will be subjected to the environmental conditions for extended periods of time. This effect may be advantageous or detrimental depending upon the drug physical properties (Martinez and Amidon 2002). The intake of certain food components can influence the viscosity of gastrointestinal fluids which can act to decrease the diffusivity of the drug. The presence of food and fluid in the upper gastrointestinal tract can also increase the contents volume, stimulating the secretion of gastric acid, bile and pancreatic fluid. Gastrointestinal fluid also contains naturally occurring surfactants for example bile salts and lecithin, the concentrations of which do not compare to the unphysiologically high concentrations present in in vitro dissolution media (Horter and Dressman 1997). The development of accurately simulated gastric and intestinal

fluid in vitro for dissolution testing is a complex process, highlighted by the varying physiological conditions outlined above. The inability of in vitro dissolution media to compare to physiological conditions is the principal reason why there is currently no reliable correlation between the two.

The bioavailability of drugs can also be significantly influenced by first pass metabolism. This is a process by which the drug molecule is metabolised and deactivated before reaching the systemic circulation, meaning therefore that the drug will have no therapeutic effect (Martinez and Amidon 2002)

1.2.3 Measures to Improve Drug Dissolution

Poorly water soluble drug compounds, provided formulation-dependent bioavailability issues are identified early in the development phase, can be prime candidates for the measures and technologies currently available to enhance in vivo activity. Provided these drugs are classified as BCS II then absorption will be dissolution limited, and therefore once in solution, the drug will be readily absorbed across the gastrointestinal cell wall. BCS IV compounds however are known to exhibit poor aqueous solubility as well as poor permeability, and therefore the limitations to achieving good in vivo bioavailability cannot be solved using formulation alone. In this case, a return to the lead optimisation phase of discovery is required in order to select a candidate with more favourable physicochemical properties (Pouton 2006).

There are a number of methods of formulation which have been shown in the literature to enhance the dissolution properties and therefore the in vitro release, and often in vivo bioavailability, of poorly soluble drugs, and these methods have been outlined in a review by Pouton (2006). Overall, they generally fall within the following categories: crystalline solid formulations, amorphous formulations and lipid formulations, and Table 1.2 below highlights the main methods.

Table 1.2 *Options for formulation of poorly water-soluble drugs (Pouton 2006).*

Technology	Potential advantage	Potential disadvantage
Conventional micronization	Known technology, freedom to operate, solid dosage form	Insufficient improvement in dissolution rate
Nanocrystals obtained by ball-milling	Established products on the market, experienced technology provider (Elan), solid dosage form possible	Available only under license, secondary process required to avoid aggregation of nanocrystals
Nanocrystals obtained by dense gas technology	Alternative nanocrystal processing method, still room to develop new IP	Unproven technology, secondary process required to avoid aggregation of nanocrystals
'Solid solutions'—drug immobilized in polymer	Freedom to operate, new extrusion technology offers solvent-free continuous process	Physical stability of product questionable—drug or polymer may crystallize
Self-dispersing 'solid solutions' with surfactants	Steric hindrance to aggregation built into product, amenable to extrusion	Physical stability of product questionable—drug or polymer may crystallize
Lipid solutions (LFCS Type I lipid systems)	Freedom to operate, safe and effective for lipophilic actives, drug is presented in solution avoiding the dissolution step	Limited to highly lipophilic or very potent drugs, requires encapsulation
Self-emulsifying drug delivery systems (SEDDS) and SMEDDS (LCFS Type II or Type III lipid systems)	Prior art available, dispersion leads to rapid absorption and reduced variability, absorption not dependent on digestion	Surfactant may be poorly tolerated in chronic use, soft gel or hard gel capsule can be used in principle but seal must be effective
Solid or semi-solid SEDDS	Could be prepared as a free flowing powder or compressed into tablet form	Surfactant may be poorly tolerated in chronic use, reduced problem of capsule leakage, physical stability of product questionable—drug or polymer may crystallize
Surfactant-cosolvent systems (LFCS Type IV 'lipid' systems)	Relatively high solvent capacity for typical APIs	Surfactant may be poorly tolerated in chronic use, significant threat of drug precipitation on dilution

1.3 SOLID DISPERSION SYSTEMS

1.3.1 Definition and Mechanism of Drug Release

Solid dispersions were first demonstrated in 1961 by Sekiguchi and Obi (Chiou and Riegelman 1971; Sekiguchi and Obi 1961; Serajuddin 1999). The term solid

dispersion is used to describe the mixture of a poorly soluble drug in an inert, water soluble carrier, usually prepared via the melt or solvent methods which are explained later (Serajuddin 1999). Solid dispersions are able to enhance the dissolution behaviour of poorly water soluble drugs and also therefore improve their in vivo bioavailability (Broman 2001). BCS Class II drugs are those most likely to benefit from solid dispersion formulation, as once they are solubilised in the gastrointestinal tract they will achieve an absorption profile similar to that of a Class I drug. Class III and IV drugs however are limited by poor membrane permeability and therefore require chemical modification (Pouton 2006).

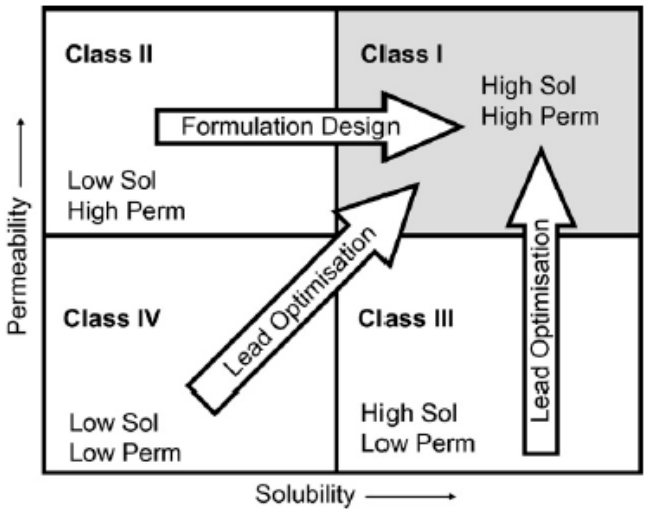

Figure 1.4 *A typical representation of the biopharmaceutical classification system, indicating that absorption of a class II drug can be markedly improved by attention to the formulation (Pouton 2006).*

The drug in the solid dispersion may be dispersed as fine crystalline or amorphous particles, a combination of both, or be molecularly dispersed within the carrier excipient forming a solid solution (Craig 2002; Leuner and Dressman 2000).

There are a number of proposed mechanisms of enhanced drug dissolution from solid dispersions, some of which include:

1) Reduction of particle size.
2) Inhibition of drug aggregation.
3) Increased drug wettability and dispersibility by the carrier.
4) Drug solubilisation effect of the carrier.
5) Conversion of drug to the metastable amorphous state.
6) Dissolution of drug in the carrier.
7) A combination of the above (Abdul-Fattah and Bhargava 2002; Damian et al. 2000; Karatas et al. 2005).

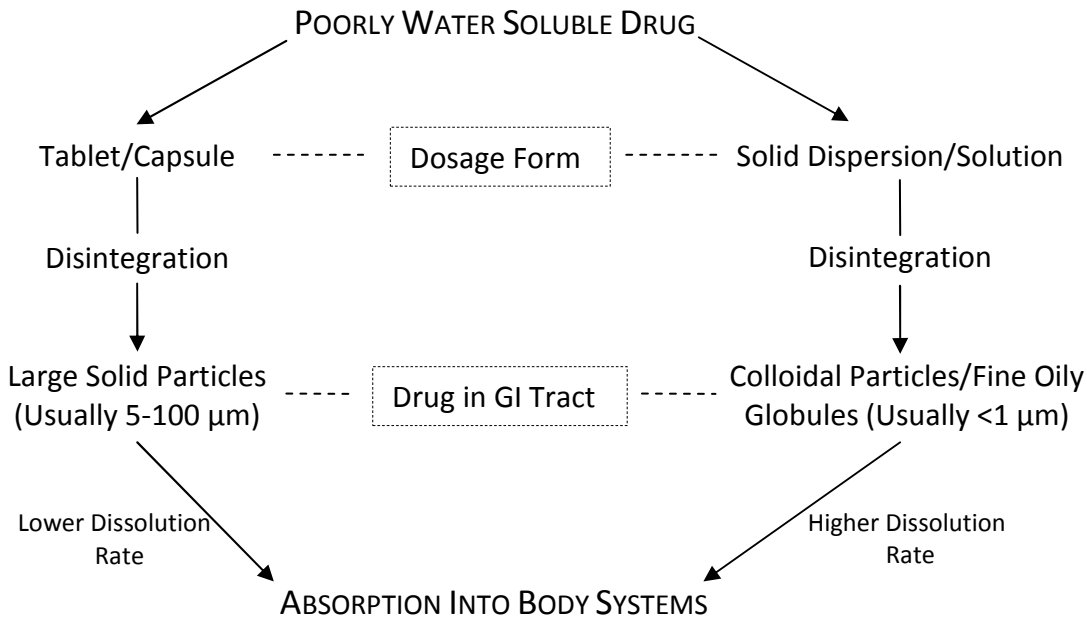

Figure 1.5 *A schematic representation of the bioavailability enhancement of a poorly water soluble drug by solid dispersion compared with conventional tablet or capsule, reproduced from Serajuddin (1999).*

When in contact with aqueous media such as gastrointestinal fluid, the carrier contained within the solid dispersion dissolves, exposing the poorly soluble drug to the aqueous environment as fine, colloidal particles. The drug surface area is greatly increased therefore enhancing dissolution (Serajuddin 1999).

An example of a solid dispersion recently brought to market is Intelence®. Intelence is a formulation containing the novel second generation non-nucleoside reverse transcriptase inhibitor (NNRTI), etravirine, used in the treatment of HIV. Etravirine is a BCS class IV drug and is spray dried with HPMC in order to render it amorphous in combination with the glassy polymer, thus enhancing its in vivo bioavailability (Weuts et al. 2010).

1.3.2 Methods of Solid Dispersion Formulation

There are a number of methods which can be used to formulate solid dispersions. The hot melt method (Sekiguchi and Obi 1961) involves heating the carrier above its melting point so that a molten liquid is formed. The drug is added under continuous stirring to the molten carrier until a homogenous mix is obtained. The mix is then filled into hard gelatin capsules (ensuring that its temperature is below 70^{o}C which is the maximum tolerated by the capsule shells) and cooled either rapidly for example in an ice bath, or left to cool at room temperature (Chambin and Jannin 2005; Leuner and Dressman 2000; Serajuddin 1999). Carriers with low melting points are most advantageous for this method as there is less chance of the drug degrading when being held at the carrier melting temperature for any length of time.

Hot melt extrusion (Hüttenrauch 1974) has also been used in the formulation of solid dispersions. This involves the simultaneous melting, homogenisation, extrusion and shaping of the drug and carrier into tablets, granules, pellets, sheets, sticks or powder. The drug and carrier are only subjected to high temperatures for a very short time which is an advantage when using thermolabile substances (Leuner and Dressman 2000). The dispersion is however subjected to mechanical processing which can facilitate the conversion of amorphous drug back into its crystalline form.

The solvent method (Tachiban and Nakamura 1965) involves the dissolution of both drug and carrier in a common solvent. The solvent is then removed either via evaporation, freeze-drying or spray-drying. It must be ensured however that all traces of solvent have been removed as it has the potential to affect product performance (Leuner and Dressman 2000).

1.3.3 Factors Influencing Solid Dispersion Behaviour

1.3.3.1 Carrier Properties

The use of surface active carriers over non-surface active carriers has the advantage of preventing drug rich surface layers of undissolved drug by dispersing or emulsifying it in a finely divided state (Serajuddin 1999). Surface active agents, or surfactants, possess the ability to aggregate into micelles above the critical micelle concentration (CMC).

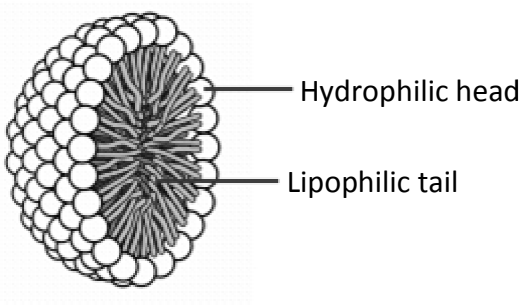

Figure 1.6 *The structure of a micelle (Kumar 2009).*

Poorly soluble or lipophilic drugs can be solubilised within the lipophilic centre of the micelle, enhancing drug wetting properties by decreasing the contact angle, preventing aggregation and increasing the surface area of the drug particles, therefore increasing dissolution.

The formation of a drug rich surface layer hinders drug dissolution and absorption as it prevents the uptake of water by the formulation. Drug rich surface layers can be formed by the aggregation of small water insoluble particles, therefore it is of benefit to use a surface active carrier during formulation in order to prevent this occurring. The surface active carrier is able to rapidly emulsify the solid drug particles on liberation from the solid dispersion, ensuring dispersion as fine, colloidal particles with a large surface area for dissolution (Figure 1.7) (Serajuddin 1999).

If formulating via the melt method it is advantageous to use a carrier with a low melting point to avoid drug degradation during melt preparation, however the long term stability of the preparation may be compromised (Serajuddin 1999).

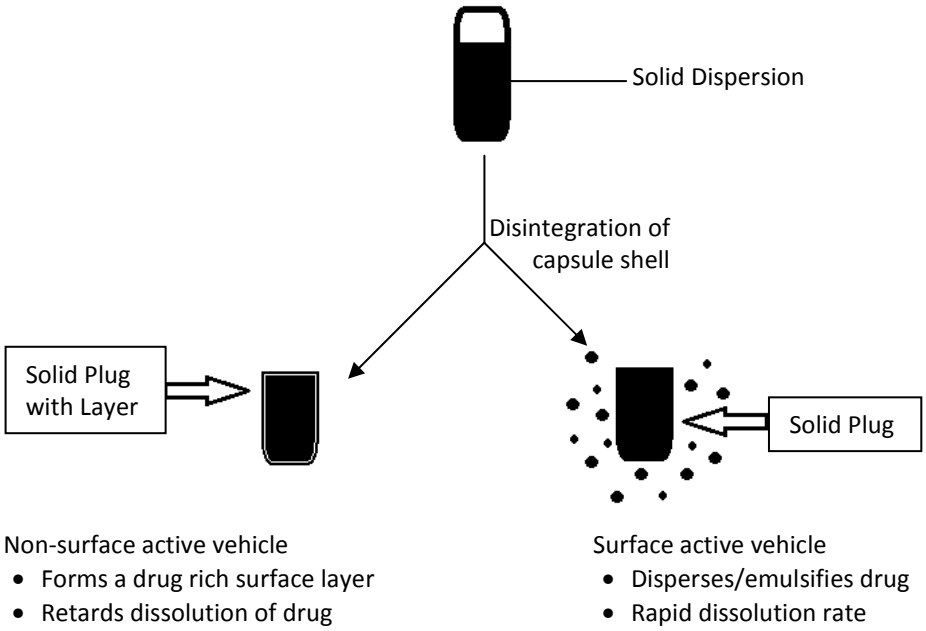

Figure 1.7 *A schematic representation of the comparative dissolution of a poorly water soluble drug from surface active versus non-surface active vehicles, reproduced from Serajuddin (1999).*

1.3.3.2 Drug Properties

The drug properties influencing solubility have been outlined previously, however the physical phase in which the drug is present can also play an important role in the effectiveness of solid dispersions. The two phases in which a solid drug substance can exist are crystalline and amorphous, and both display very individual characteristics. The molecules in the crystalline phase are highly ordered in three dimensions, and are bound tightly together by secondary interactions such as hydrogen bonding and ionic interactions. This is a very stable, low energy and unreactive phase. The molecules in the amorphous phase however have no ordered arrangement or crystal lattice. The amorphous phase is unstable, high energy and

therefore reactive, so will readily undergo conversion back into its most stable form (crystalline). This phase can be referred to as a supercooled liquid (Bottom 1999; Hancock and Zografi 1997; Zhang et al. 2004). The amorphous phase is more water soluble and hence it is advantageous for any drug contained within a solid dispersion to be in this form. It does however mean that the solid dispersion formulation is more susceptible to degradation during storage.

Interaction between the drug and carrier material will also play a significant role in the physical state of the drug in the formulation. If the drug is found to exhibit high miscibility in the carrier then dissolution of the drug may occur during manufacture. This will therefore mean that the drug may be present as a molecular dispersion within the carrier (although not necessarily 100%), and therefore may in part be classified as a solid solution.

1.3.3.3 Processing and Storage Variables

It is essential to identify the appropriate form for the drug in the formulation and ensure it remains unchanged in the final product. The processes drug and carrier are subjected to during manufacture can greatly influence the final performance of the solid dispersion formulation. These processes generally involve the modification of crystalline into amorphous form which can affect chemical, physical and mechanical properties of the solid dispersion (Zhang et al. 2004).

A review carried out by Zhang et al (2004) investigated the effect of process development of solid oral dosage forms on phase transformation. The greatest

increase in dissolution of poorly soluble drugs in solid dispersions occurs when they are in the amorphous form. The amorphous form, being high-energy, is unstable and has a tendency to convert back to the more stable crystalline form on processing and storage. The amorphous form can be created via the melt method i.e. when the carrier and drug are melted together, however the cooling rate of the melt can influence if the crystalline form is regenerated in the final dosage form. Cooling at room temperature has been found to encourage crystal growth as it allows the drug time to attain a suitable orientation for crystal nucleation. However, rapid cooling appears to prevent crystal growth, maintaining the amorphous state (Khoo 2000; Zhang et al. 2004).

Preparing solid dispersions via the solvent method only encourages conversions of the metastable phase into the stable phase when the metastable phase comes into contact with the saturated solvent solution. This process involves:

1) Initial dissolution of the metastable phase into the solution to reach and exceed the solubility of the stable phase.
2) Nucleation of the stable phase.
3) Crystal growth of the stable phase with the continuous dissolution of the metastable phase (Zhang et al. 2004).

Additional mechanical processing such as pulverisation and compression can also influence the conversion of amorphous drug into crystalline, therefore filling of the molten melt via the melt method into hard gelatin capsules and cooling rapidly is the most optimum method to maintain amorphous drug (Khoo 2000).

Phase conversions of the drug and carrier can occur in the solid state and can be influenced by factors such as particle size and distribution, impurities, crystalline defects and environment. Environmental factors come into play on storage of the finished solid dispersion dosage forms (Zhang et al. 2004). High temperature (especially if low melting point excipients are used) and high humidity can both encourage conversion of the amorphous form back into the crystalline.

1.3.4 Lipid-Based Carrier Excipients

Developments in the last 10 to 15 years have shown drug delivery systems composed of lipidic excipients to be a promising technology in the enhancement of the bioavailability of poorly soluble drugs. They have been shown to be successful in increasing solubility, lymphatic transport targeting, modulation of enterocyte-based drug transport and disposition, sustained release, and coating for either taste masking or protection of the drug (Jannin et al. 2008). They have also been found to have the capability of normalising drug absorption across the GI tract which can be advantageous for the formulation of drug compounds with a low therapeutic index (Hauss 2007). Lipids, which are fatty acids and their derivatives and also substances which are functionally or biosynthetically related, can be further classified into oils, waxes, fats, and more complex lipids including phospholipids and lipoproteins which have involvement in biological processes. The enhancement of oral bioavailability does however tend to be dominated by vegetable or dietary oils and their derivatives, which encompasses TPGS and Gelucire 44/14 which will be discussed later in the Chapter (Jannin et al. 2008).

A survey carried out by Strickley found that in the UK, lipid-based formulations account for 2% of commercially available drug products (Strickley 2007). These systems are however, known for their complexity of physicochemical properties, stability issues, difficulties with manufacture scale up, limited solubility of some drugs within lipid carriers, pre-absorptive gastrointestinal processing, a lack of knowledge regarding in vivo behaviour, a lack of understanding of the influence of co-administered drug formulations and also limitations in methods of in vitro / in vivo correlation (Chakraborty et al. 2009). Nonetheless research is continuing to expand the knowledge base available in order to take further advantage of this promising technology.

1.3.5 Current Place in the Pharmaceutical Industry and Future Prospects

The development of solid dispersions has proved an effective method of increasing drug solubility. However despite their advantages, the commercial production of water insoluble drugs in these formulations is limited by difficulties relating to preparation, reproducibility, formulation, scale-up and stability (Serajuddin 1999). Additional development is needed in these areas however the utilisation of solid dispersions is a promising tool in the enhancement of drug dissolution.

1.4 SURFACE ACTIVE LIPIDIC CARRIERS

1.4.1 Gelucire 44/14

Gelucire 44/14 is an inert, amphiphilic excipient which belongs to the lauryl macroglyceride group of compounds. It consists of a combination of fatty acid esters of polyethylene glycol (PEG) and glycerides, the combinations of which determine its physical characteristics (Damian et al. 2000; Serajuddin et al. 1988; Svensson et al. 2004).

1.4.1.1 Contact with Aqueous Media

Gelucire 44/14 displays a number of interesting properties on contact with water, to which its different components contribute. It contains mono- and di-esters of PEG which act as surfactants, monoglycerides which act as cosurfactants, and di- and triglycerides which comprise the oily phase (Chambin and Jannin 2005). Gelucire 44/14 overall is classified as a non-ionic surfactant (Abdul-Fattah and Bhargava 2002).

Gelucire 44/14's well balanced proportion of short, medium and long chain fatty acids means it has the unique property of spontaneously emulsifying on contact with aqueous solutions, for example gastrointestinal fluids at 37^{o}C, forming a stable fine emulsion (Gattefossé 2007). The oil in water emulsion droplets formed during this process are approximately 3 to 300nm in size (Chambin and Jannin 2005). In the presence of large volumes of aqueous media at ambient temperature, glycerol and

PEG dissolve immediately as they are the most hydrophilic, followed by the other crystals i.e. PEG esters and trilaurin, the resulting liquids being mesophases. Dissolution is found to be a slow process due to mesophase formation, however they are found to melt at physiological temperature making dissolution a faster process (Svensson et al. 2004). This is a unique characteristic, different from all other Gelucires which remain essentially intact when in contact with aqueous media (Karatas et al. 2005).

Gelucire 44/14 is also thought to have the capability of forming micelles. The CMC is known to be difficult to determine due to its many components, nonetheless the initiation of micelle formation is thought to occur at either 2µg/ml or 10µg/ml (Kawakami 2004; Schamp et al. 2006). The ability of Gelucire 44/14 to form micelles may allow it to be effectively utilised for increasing the solubility of lipophilic substances in aqueous media by micellar solubilisation. Gelucire 44/14 is able to decrease the interfacial tension of poorly soluble compounds with water, in turn decreasing the contact angle between the insoluble solid surface and the dissolution media, promoting wetting and dissolution by preventing aggregation and agglomeration (Damian et al. 2000; Tashtoush et al. 2004).

1.4.1.2 Oral Delivery Applications

Gelucire 44/14 has been established as an effective excipient for pharmaceutical formulations. Gelucire 44/14 does however lend itself to formulation as the sole excipient, particularly into self-emulsifying drug delivery systems (SEDDS) such as semi-solid dispersions (SSD) in hard gelatin capsules of poorly water soluble drugs.

This method, as well as increasing bioavailability of insoluble drugs, can also enhance stomach tolerance (Chambin and Jannin 2005). There are a number of published data looking at the formulation, characterisation, dissolution and effect of storage conditions of Gelucire 44/14 solid dispersions, generally in comparison with solid dispersions containing other excipients, physical mixtures and pure drug, which will be discussed.

1.4.1.3 Enhancement of Dissolution Rate by Semi-Solid Dispersion Formulation

The low melting temperature of Gelucire 44/14 lends it to formulation into semi-solid dispersion systems via the melt method. This involves heating the pure Gelucire 44/14 to a temperature above its melting point. There is, however, conflicting information with regards the best temperature to use for this purpose. A number of studies suggest 2^{o}C and others suggest 5^{o}C above melting point (Karatas et al. 2005; Pillay and Fassihi 1999; Serajuddin et al. 1988). Other studies have suggested between 60 and 80^{o}C (Chambin and Jannin 2005; Schamp et al. 2006). However the manufacturer Gattefossé has demonstrated, using hot stage microscopy, that temperatures in the range 53-56^{o}C were necessary in order to obtain a fully molten liquid thus ensuring that all crystals have melted. The solid drug is then added to the molten Gelucire 44/14 under continuous stirring and the mixture is filled into hard gelatin capsules at less than 70^{o}C, which is the maximum tolerated by the capsule shells (Serajuddin 1999). The semi-solid dispersion formulations then undergo a rapid cooling process between 5-8^{o}C or are left to cool at room temperature.

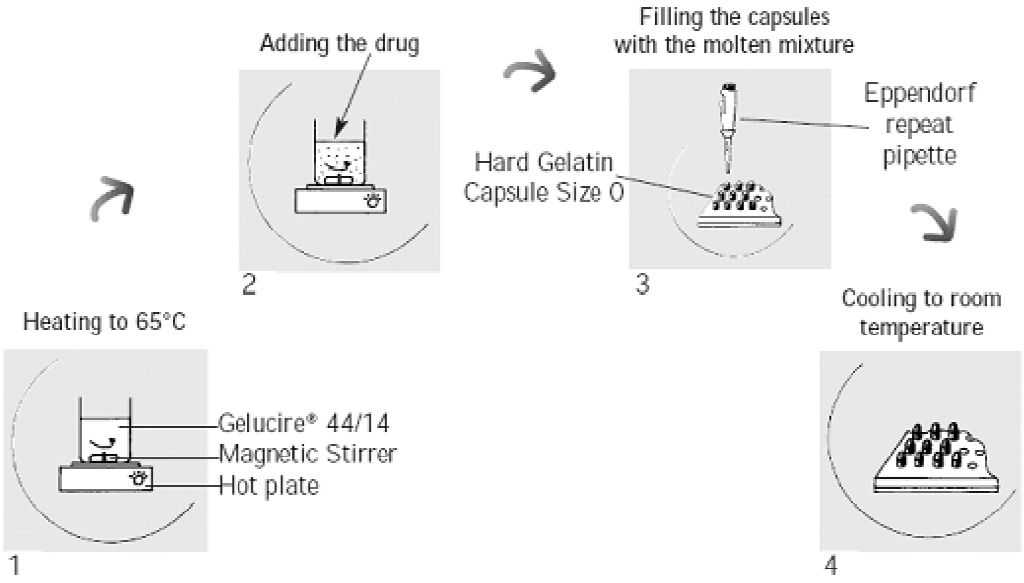

Figure 1.8 *Formulation of Gelucire 44/14 semi-solid dispersions via the melt method (Gattefossé 2007).*

Cryogenic grinding of Gelucire 44/14 and formulation into sold dosage forms such as tablets and pellets has been investigated by Chambin and Jannin (2005) in order to overcome the need for time consuming melting and the requirement for high temperatures. Cryogenic grinding, in this case, involved grinding of the carrier at low temperatures, brought about by liquid nitrogen, into a powder form. The main concern was the chance of the mechanical activation and generation of energy affecting the crystalline structure of Gelucire 44/14. After characterisation and in vitro dissolution studies it was concluded that, although cryogenic grinding appeared to have no affect on the crystalline structure of Gelucire 44/14, there appeared to be no advantage of one manufacturing method over the other.

On disintegration of the hard gelatin capsule, dissolution of the semi-solid dispersion occurs via erosion by the dissolution media (Khoo 2000). Gelucire 44/14

spontaneously emulsifies on contact with aqueous media which in turn has been shown to increase drug wettability and dispersibility, protecting the particles from aggregation, agglomeration and precipitation (Tashtoush et al. 2004). It was suggested by Barker et al (2003) that the improvement in drug dissolution may, in part, be due to the incorporation of drug into the hydration layer of Gelucire 44/14 during self-emulsification.

Drug/carrier interactions may also play a role in the enhancement of drug dissolution, which can be characterised by techniques such as DSC and IR spectroscopy. A study carried out by Karatas et al (2005) highlighted that chemical interactions between drug and Gelucire 44/14, specifically the mono-, di- and triglycerides, fatty alcohols and polyglycolised fatty acid esters, can lead to increased solubility of the poorly soluble drug. Physical mixtures of the drug and Gelucire 44/14 also brought about an increase in dissolution, possibly due to close physical contact contributing to increased solubilisation and wettability on self-emulsification of Gelucire 44/14 (Damian et al. 2000).

1.4.1.4 Inhibition of P-glycoprotein Efflux Transporter

P-glycoprotein or P-gp is a polarised multidrug resistance ATP-dependent efflux transporter (Figure 1.9). It is highly expressed on the apical membranes (luminal surface) of most epithelial tissues, such as intestine, liver, kidney, colon and blood brain barrier. P-gp belongs to the ATP binding cassette (ABC) superfamily of protein membrane transporters and it is expressed by the MDR or multidrug resistance gene (Collnot et al. 2007). It actively transports a wide range of substances out of the cell

against a concentration gradient, thus keeping intracellular levels low. It can therefore be a barrier against potentially toxic substances, protecting the cell from damage (Collnot et al. 2007).

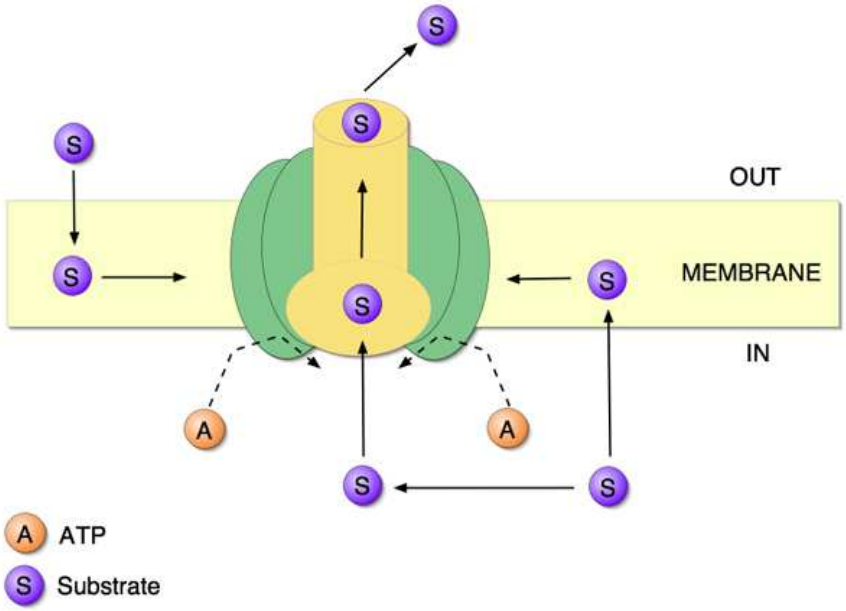

Figure 1.9 *P-glycoprotein efflux transporter (Edwards 2003).*

Overexpression of the P-gp efflux transporter can lead to multidrug resistance which is observed in cancerous cells against chemotherapy treatments. It also leads to the limitation of adequate bioavailability of certain chemically unrelated drugs such as digoxin, antibiotics and steroids. The inhibition of P-gp by lipidic excipients therefore has the potential to increase the activity of chemotherapy agents against resistant cancers when administered in a combined formulation such as a solid dispersion (Collnot et al. 2007).

The effect of Gelucire 44/14 on the P-gp efflux transporter has been investigated in a study conducted by Sachs-Barrable (2007). They established that Gelucire 44/14, at a

concentration of 0.02% w/v, was capable of achieving an intracellular concentration of the P-gp substrate Rh123, greater than that of the control. Gelucire 44/14 appeared to suppress the active secretion of Rh123 across a Caco-2 cell monolayer via inhibition of the P-gp efflux transporter. It was also noted that, after exposure to Gelucire 44/14, the cells down-regulated P-gp expression on the lipid membrane.

1.4.1.5 Effect of Aging and Storage Conditions

A number of studies have investigated the influence of varying storage conditions i.e. temperature and humidity on Gelucire 44/14 and its formulations. Humidity plays a vital role in the possible degradation of Gelucire 44/14 formulations. A study carried out by Svensson et al (2004) investigated the hydration of pure Gelucire 44/14 by humid air at ambient temperature in detail, and characterised the physical changes involved in the process. Below 70% relative humidity (RH) only free glycerol absorbed water up to approximately 1% w/w which is the maximum permitted by the European Pharmacopoeia. The conditions experienced during processing and storage would generally be between 30 and 60% RH meaning that Gelucire 44/14 would not exceed 1% w/w water absorption under normal storage circumstances. However, above 80% RH the PEG esters dissolve and the viscosity of Gelucire 44/14 begins to change from a white gel at 11% w/w water, to a white dispersion at 25 to 31% w/w water, to a white gel at 50 to 61% w/w water, to white dispersions again at 71 to 75% w/w water, and then finally to separate white and transparent liquid phases. Svensson et al (2004) also highlighted that water uptake by Gelucire 44/14 can be effectively replicated by assuming independent uptake by each individual component.

Studies carried out by the manufacturer Gattefossé, highlighted that, above 30^{o}C at 75% relative humidity, Gelucire 44/14 will absorb approximately 10% water, indicating that temperature does play a role. It has also been demonstrated, via methods such as X-ray diffraction and scanning electron microscopy, that Gelucire 44/14 does not undergo any change in crystalline structure upon aging at varying temperatures (below 30^{o}C) and humidities (below 80%) (Chambin and Jannin 2005; Gattefossé 2007).

The effect of aging has also been carried out on semi-solid dispersion formulations containing Gelucire 44/14. Tashtoush et al (2004) found no significant change in the release of drug from the formulations after aging for two months at room temperature. Damian et al (2002) however found that dissolution from Gelucire 44/14 semi-solid dispersions decreased as a function of storage time, possibly due to a reorganisation of crystalline structure. Increasing temperature appeared to favour the conversion of the triglyceride fraction into a more stable form. X-ray diffraction studies indicated that the decreasing dissolution properties of the semi-solid dispersions were due only to changes in Gelucire 44/14 physical state and not that of the drug.

Joshi et al (2004) found that storage at temperatures above 40^{o}C caused leakage from the Gelucire 44/14 semi-solid dispersion capsules due to its low melting temperature of 44^{o}C. Stability of the formulations could therefore not be guaranteed at high temperatures.

Serajuddin et al (1988) highlighted that drug concentration in the semi-solid dispersion may also play a part in the decrease in extent of dissolution. High drug concentrations were found to encourage drug recrystallisation in short periods of time (i.e. less than 7 days) becoming more stable and less water soluble.

1.4.2 TPGS

TPGS, or D-alpha tocopheryl polyethylene glycol 1000 succinate, is a water soluble derivative of fat soluble vitamin E. It is a non-ionic surfactant with amphiphilic properties (Eastman 2005).

1.4.2.1 Contact with Aqueous Media

TPGS molecules, due to their amphiphilic nature, spontaneously self associate in water to form micelles when present above the critical micelle concentration (CMC). The CMC for TPGS is relatively low at 0.02% w/v in water at 37^{o}C. This property allows the effective solubilisation of lipophilic molecules in an aqueous environment, facilitating absorption (Eastman 2005).

Figure 1.10 illustrates the liquid crystalline phases (mesophases) of increasing TPGS concentrations in water at 37^{o}C. Above the CMC, TPGS micellar solutions remain low-viscosity until approximately 20% w/v, above which the liquid crystalline structure evolves through the following:

1) Isotropic globular micellar.
2) Isotropic cylindrical micellar.
3) Mixed isotropic cylindrical micellar and hexagonal.
4) Mixed hexagonal and reversed hexagonal.
5) Reversed globular micellar.
6) Lamellar phase (Eastman 2005).

At the extremes of concentration the solutions remain liquid-like, however between approximately 20 and 90% w/v the solutions demonstrate gel-like properties.

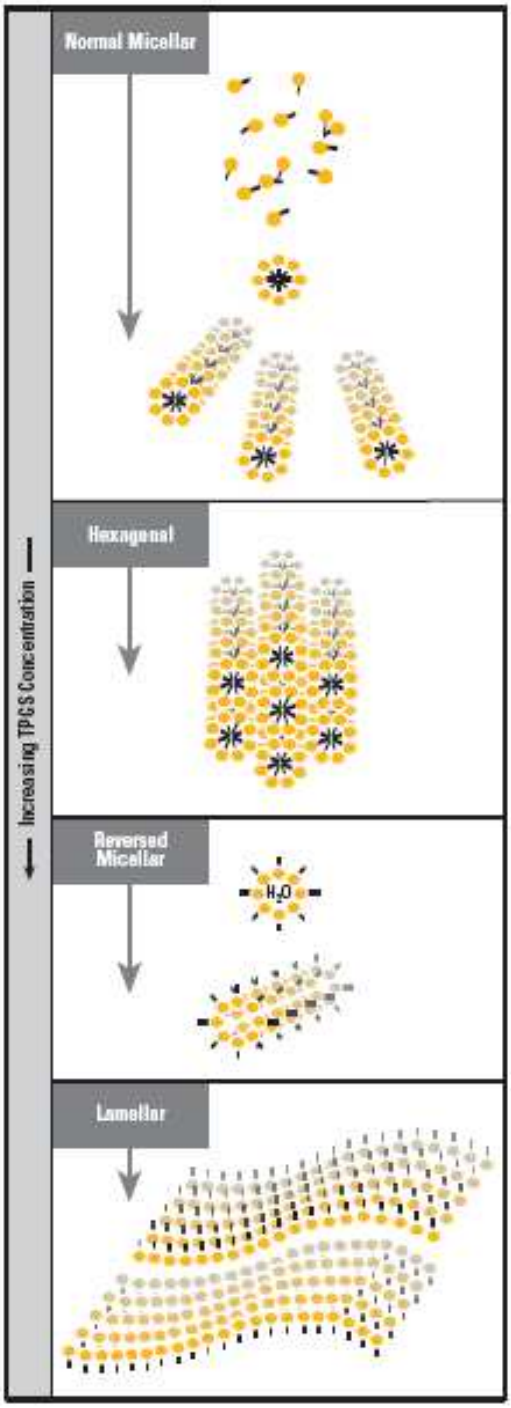

Figure 1.10 *Liquid crystalline phases of TPGS / water systems at 37°C (Eastman 2005).*

1.4.2.2 Absorption and Excretion

TPGS micelles are thought to readily pass through cellular membranes where they are broken down and hydrolysed releasing the metabolites alpha-tocopherol and PEG 1000. Alpha-tocopherol is secreted into the lymphatic system via chylomicrons, whereas the PEG 1000 is rapidly excreted in the urine (Eastman 2005; Traber et al. 1988). The use of TPGS in vivo has demonstrated no detectable clinical or laboratory evidence of hepatic, renal, bone marrow, gastrointestinal or metabolically toxic effects however it has been noted that the long term toxicity of chronic absorption of PEG 1000 should be monitored (Sokol et al. 1991; 1988).

Vitamin E plays an essential role in the antioxidant system and deficiency can cause varying degrees of damage to the peripheral nervous system (Traber et al. 1988). The ability of TPGS to form micelles has been shown to enhance intraluminal absorption, therefore increasing plasma levels of alpha-tocopherol, thus making it a possible source of vitamin E for malabsorbing patients. TPGS does however only provide one of the eight tocols comprising vitamin E in foods and at high doses alpha-tocopherol can actually deplete other essential tocols (Papas et al. 2007).

1.4.2.3 Oral Delivery Applications

The characteristics of TPGS lend it to use as a solubiliser and absorption enhancer of poorly water soluble or lipophilic drugs i.e. those in BCS class II. Studies present in the literature to date have been carried out investigating concomitant administration of liquid TPGS with poorly soluble drugs, physical mixtures and semi-solid

dispersions, to discover which is the most effective method of increasing the solubility and absorption of these drugs. These methods are nearly always compared to the solubility and absorption of pure drug alone.

1.4.2.4 Enhancement of Dissolution Rate by Semi-Solid Dispersion Formulation

There are a number of methods of preparing semi-solid dispersion formulations which have been mentioned previously. In general, semi-solid dispersion systems containing TPGS are formulated using the melt method due to its low melting point of between 37 and 41^{o}C and high degradation temperature of 199^{o}C (Shin and Kim 2003). TPGS is melted to between 60 and 80^{o}C to ensure complete melting of crystals (Schamp et al. 2006). The drug is then added to the molten TPGS and stirred to ensure a homogenous mixture. The mixture is then poured into hard gelatin capsules at a temperature less than approximately 70^{o}C and the capsules are either cooled rapidly (between 5-8^{o}C) or allowed to cool at room temperature.

The method of enhanced absorption of poorly soluble drugs by TPGS in semi-solid dispersion systems appears to be two fold; incorporation of the drug into micelles, and inhibition of the P-glycoprotein efflux transporter, provided the drug is a substrate. There is evidence to suggest however that formulation into a semi-solid dispersion may also cause conversion of crystalline drug into the more soluble amorphous form (Shin and Kim 2003). This may indicate an interaction on a molecular level although this should possibly be evaluated on a case by case basis.

The nature of TPGS means it is able to form micelles on contact with aqueous media i.e. it can prevent the formation of a water insoluble drug rich surface layer on dissolution of semi-solid dispersion formulations by acting as a dispersing or solubilising agent (Barakat 2006). TPGS spontaneously disperses and dissolves releasing drug particles throughout the aqueous media. This increase in surface area of solid drug in turn increases its dissolution and subsequent absorption and bioavailability. The media becomes saturated with dissolved drug therefore the remaining drug precipitates as fine colloidal drug particles (Serajuddin 1999). These remaining drug particles are thought to be incorporated into TPGS micellular structures, increasing both the solubilisation into the aqueous environment of the gastrointestinal tract and absorption by intestinal cells into the systemic circulation. The TPGS molecules dissolve the lipophilic drug molecules in their lipophilic tocopheryl tail groups, exposing the hydrophilic PEG 1000 head groups to the aqueous environment, provided TPGS is present at a concentration above the CMC.

TPGS has been shown to bring about limited increase in drug dissolution below the CMC, however above this concentration, dissolution has been observed to increase linearly. Once the drug molecule is incorporated into the micelle, one proposed mechanism is that the complete structure enters the cell and the drug is released by intracellular hydrolysis of the TPGS molecules (Eastman 2005; 1994; Varma and Panchagnula 2005; Yu et al. 1999).

It is possible, after formulation of a semi-solid dispersion, to discover during characterisation that a solid solution has been formed instead of a solid dispersion, or even a combination of the two (Leuner and Dressman 2000). This means that the

drug will have been molecularly dispersed throughout the TPGS during melting. Therefore, on dissolution of the water soluble TPGS on contact with aqueous media, the drug will be present in a supersaturated solution. The presence of TPGS in solution may also prevent precipitation (Leuner and Dressman 2000). It is thought, however, that solid solutions are more prone to formation of drug rich surface layers (Serajuddin 1999).

1.4.2.5 Inhibition of P-glycoprotein Efflux Transporter

TPGS has been shown to be a potent inhibitor of the P-glycoprotein efflux transporter. The exact mechanism of inhibition of P-gp efflux by TPGS is currently unknown. P-gp inhibition has been observed at TPGS concentrations well below the CMC suggesting that it is not only restricted to micellar activity but also that of free TPGS molecules. TPGS appears to be a potent inhibitor of P-gp, with concentrations approximately 10 fold lower than the measured CMC demonstrating almost complete inhibition. Inhibition has also been found to be highly temperature dependent indicating that an active energy transport system is involved (1999; Yu et al. 1999).

TPGS has been observed to bring about P-gp inhibition via energy source depletion. This occurs by steric hindrance of the ATPase enzyme of the Pgp transporter therefore obstructing substrate binding or causing allosteric modulation. This steric hindrance may be a result of either a direct interaction of TPGS with allosteric Pgp sites or incorporation of surfactant molecules into the cell membrane causing blockage of substrate binding sites. Unspecific membrane fluidisation or rigidification brought about by TPGS is thought not to be responsible for any P-gp

inhibition observed (Collnot et al. 2007). TPGS does however appear to cause rigidification of the cell membrane both above and below the CMC which should not be discounted as a possible method of P-gp inhibition (Rege et al. 2002).

1.4.2.6 Effect of Aging and Storage Conditions

Aging of semi-solid dispersion formulations containing TPGS and poorly soluble drugs is thought to cause instability in the system, bringing about conversion of amorphous drug into the more stable crystalline form. This was found to significantly reduce the dissolution on in vitro testing after one month of storage at room temperature (Schamp et al. 2006).

Conversion of amorphous drug (and carrier) into the crystalline form has been found not to occur at room temperature and below, at 0% RH, although evidence of crystallinity was found as the temperature and humidity increased. It is thought that this is due to the PEG portions present in TPGS encouraging hydrogen bonding with water, therefore facilitating drug-carrier segregation and crystallisation (Barakat 2006).

1.4.3 Comparison of the Effectiveness of Gelucire 44/14 and TPGS in Semi-Solid Dispersion Formulations

There are three key papers which highlight the effectiveness of TPGS and Gelucire 44/14 in comparison with each other, these papers are detailed below.

Barakat (2006) investigated the effectiveness of solid dispersions, formulated via the fusion method, of etodolac with either Gelucire 44/14 or TPGS as the sole excipient. Using FTIR spectroscopy it was identified that there was a probable interaction between the imino group of etodolac and the carboxyl group of the Gelucire 44/14 and TPGS. DSC data also suggested the formation of amorphous etodolac within the solid dispersions. Dissolution studies were carried out in simulated gastric fluid and simulated intestinal fluid. Both Gelucire 44/14 and TPGS showed enhanced dissolution in comparison with pure etodolac, and both solid dispersions displayed greater dissolution concentrations in simulated intestinal fluid, probably due to etodolac being weakly acidic (pKa 4.65). TPGS, in all studies, appeared to demonstrate enhanced solubilising properties when compared to Gelucire 44/14, as a greater proportion of Gelucire 44/14 was required to produce similar results. A solid dispersion formulation containing both Gelucire 44/14 and TPGS did however provide faster release profiles in both aqueous dissolution media than each excipient alone.

A study carried out by Schamp et al (2006) investigated the development of an in vitro / in vivo correlation for solid dispersions of a poorly water soluble drug EMD 57033. The solid dispersions were prepared via the melt method and it must also be taken into account that, in order to achieve complete dissolution of the drug in the carrier melt, 2-vinylpyrrolidone was added to Gelucire 44/14 and labrafil and PEG 1000 to TPGS. Dissolution testing was carried out in simulated gastric fluid, FeSSIF and FaSSIF. Gelucire 44/14 produced a release profile of approximately 100% within 30 minutes in all media and this did not significantly change after 2 years storage at room temperature. TPGS however released approximately 85% drug after

180 minutes and this decreased to less than 40% after one month storage at room temperature.

The in vivo studies were carried out on four male beagle dogs after an overnight fast of 16 hours. TPGS produced drug plasma levels fourfold higher than the IV standard, however Gelucire 44/14 produced plasma levels 10 fold higher. These results coincided with the in vitro studies and it was therefore concluded that there was "a very strong rank order correlation" and that evaluation of solid dispersion formulations of poorly soluble drugs can be done at least partly on an in vitro basis.

Khoo et al (2000) studied the absolute bioavailability of the poorly soluble drug halofantrine in lipid based solid dispersions containing TPGS and Gelucire 44/14. Dissolution studies were carried out in hydrochloric acid and water at 37^{o}C. Both excipients increased the dissolution profile of halofantrine compared to the pure sample. However TPGS appeared to demonstrate slightly enhanced solubilising properties compared to Gelucire 44/14, as a higher proportion of Gelucire 44/14 was required to produce a similar result. It was also noted that a solid dispersion containing halofantrine, Gelucire 44/14 and TPGS in a ratio of 1:3:3 gave the most optimum dissolution results.

1.8 AIMS OF THIS RESEARCH

As detailed previously, lipid based solid dispersion formulations offer great potential in the enhancement of dissolution of poorly soluble drug compounds. The complexity of these systems along with stability issues, difficulty with scale up and

little knowledge of their in vivo performance makes their successful journey to market challenging (Chakraborty et al. 2009). The main aim of this project was to gain a greater understanding of the physicochemical properties of the chosen lipidic carrier excipients, with a view to relating these to and also explaining the physicochemical properties of their formulated lipid-based semi-solid dispersions. It was also hoped that these properties, as well as determination of the physical state of the model drug within the semi-solid dispersion system, could be successfully related to their behaviour in vitro, during hydration, and also during aging under differing humidity conditions.

Chapter Two outlines the materials and methods used in the project and can be referred to throughout for methods such as sample preparation which will not be repeated in subsequent chapters. A more detailed methodology is given in further Chapters specific to the data presented. Chapter Three demonstrates characterisation data of the surface active lipidic carrier materials as a background prior to analysis of the formulated dosage forms being investigated. All subsequent Chapters are concerned with characterisation of the semi-sold dispersion systems of Gelucire 44/14 with model drugs (ibuprofen, indometacin and piroxicam). Chapter Four is concerned with the overall characterisation of the semi-sold dispersion formulations, consisting of thermal analysis techniques including conventional, hyper (fast-speed) and quasi-isothermal differential scanning calorimetry, and also hot stage microscopy. Chapter Five presents in vitro release data of the drug from the semi-sold dispersion systems. Chapter Six outlines hydration data of the semi-sold dispersion systems carried out using dynamic vapour sorption analysis in relation to the affinity with atmospheric moisture, and Chapter Seven demonstrates aging and

storage effects upon these formulations. Finally, Chapter Eight aims to summarise the project findings as well as drawing definitive conclusions from the data presented in this thesis.

CHAPTER TWO

MATERIALS AND METHODS

The way in which pharmaceutical formulations behave depends upon the physicochemical properties of the constituents. In order to develop a complete understanding of these properties it is essential to fully characterise each component alone and also the formulation as a whole. It is therefore beneficial to employ a multi-instrumental approach to ensure comprehensive characterisation. This project employs a variety of techniques, ranging from thermoanalytical to in vitro dissolution, in order to gain an in depth understanding of the physicochemical properties of the systems, and therefore be able to predict how these properties will influence the behaviour of the final formulation.

In this chapter, an outline of the materials used in the project is given, as well as background to the techniques and methods of sample preparation.

2.1 MATERIALS

2.1.1 Surface Active Lipidic Carriers

Two surface active lipidic carriers, Gelucire 44/14 and TPGS, were selected for the purposes of this project. They were chosen on the basis that they demonstrate an ability to enhance the dissolution profile of poorly soluble active drug compounds when formulated into semi-solid dispersion systems. These materials are detailed below.

2.1.1.1 Gelucire 44/14

Gelucire 44/14 (Lot Number 103201) was kindly provided by Gattefossé (Lyon, France) and was used as received.

Structure and Formation

Gelucires are amphiphilic excipients belonging to the group of compounds lauryl macroglycerides (Serajuddin et al. 1988; Svensson et al. 2004). They consist of fatty acid esters of polyethylene glycol (PEG) and glycerides, the combinations of which determine their physical characteristics (Damian et al. 2000). Gelucires are categorised according to their melting points and hydrophilic-lipophilic balance (HLB) values which are denoted by numbers at the end of 'Gelucire'. They are totally inert compounds which are used as excipients in a wide variety of pharmaceuticals worldwide (Gattefossé 2007).

Gelucire 44/14 belongs to the larger group of 'Gelucires'; however it possesses the unique ability to spontaneously emulsify on contact with aqueous media, which has been explained in detail in Chapter One. It is approved as a food additive by the FDA and its raw components are of food grade. It is considered to be non-toxic and can be safely administered orally up to 1440mg/day based on an adult of 60kg. It is formed via the polyglycolysis of hydrogenated palm kernel oil with PEG 1500 (Gattefossé 2007). Being derived from vegetable oil it is well tolerated by the body and is 'generally regarded as safe' (GRAS) (Chambin and Jannin 2005; Sheen et al. 1995). The constituents of Gelucire 44/14 are shown in Tables 2.1 and 2.2 below.

Table 2.1 *Constituents of Gelucire 44/14 and their percentages (Gattefossé 2007; Svensson et al. 2004).*

Constituent	Percentage (%)
Free PEG 1500	8
PEG 1500 esters (mono- and di-fatty acid esters)	72
Glycerides (mono-, di- and tri-)	20
Glycerol	0-3

Table 2.2 *Constituent fatty acids of Gelucire 44/14 and their percentages (Gattefossé 2007).*

Fatty Acid	Percentage (%)
C8 (caprylic acid)	<15
C10 (capric acid)	<12
C12 (lauric acid)	30-50
C14 (myristic acid)	5-25
C16 (palmitic acid)	4-25
C18 (stearic acid)	5-35

At room temperature Gelucire 44/14 exists as a white semi solid waxy material of approximately 83% crystallinity. It has been found to exist in a single crystalline form, the crystals thought to be formed by lamellae of PEG esters and some pure PEG, separated by layers of fatty acid chains. There may also be amorphous regions, trilaurin crystals and liquid glycerol (Gattefossé 2007; Svensson et al. 2004).

Characteristics and Thermal Properties

As explained above, '44/14' denotes the melting point and HLB value for this particular Gelucire. This indicates Gelucire 44/14 has a melting point of approximately 44^{o}C (although in reality it melts over a range of temperatures) and an HLB value of 14 (Barakat 2006). DSC plots produced by Gattefossé and Damian et al (2000) show that, on melting, Gelucire 44/14 crystals display a broad leading shoulder (Figure 2.1). This is thought to be brought about by the separation of Gelucire 44/14 components into fractions with different melting points (Gattefossé 2007).

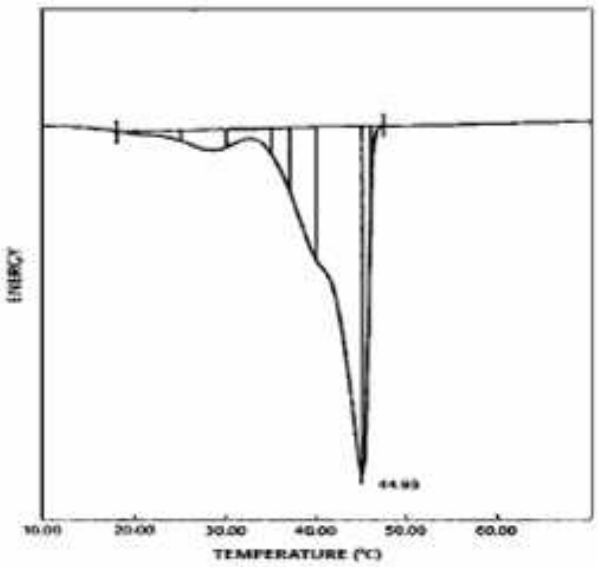

Figure 2.1 *DSC melting profile of Gelucire 44/14 (Gattefossé 2007).*

2.1.1.2 TPGS

TPGS (Batch Number 50037000) was kindly provided by AstraZeneca (Macclesfield, UK) and was used as received.

Structure and Formation

TPGS is a water soluble derivative of the fat soluble vitamin, vitamin E. It has the classification of 'generally regarded as safe' (GRAS) by the FDA and is effective to be used as a pharmaceutical excipient. It has the chemical name D-alpha tocopheryl polyethylene glycol 1000 succinate and is synthesised via the esterification of the acid group of vitamin E (crystalline D-alpha tocopheryl succinate) by polyethylene glycol (PEG) 1000 (Eastman 2005). At room temperature TPGS is a white to light brown / pale yellow waxy solid substance.

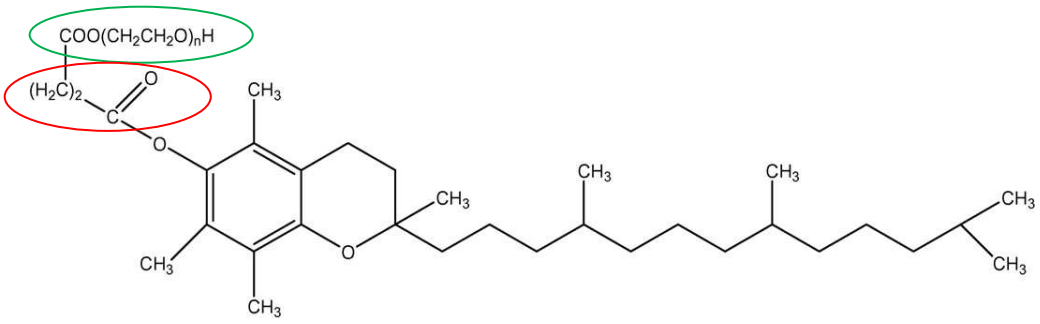

Figure 2.2 *General structure of TPGS analogues; n = 23 (Li et al 2008).*

Characteristics and Thermal Properties

TPGS is a non-ionic surfactant which has amphiphilic properties and a hydrophilic-lipophilic balance (HLB) of approximately 13 (Eastman 2005). It consists of a hydrophilic polar head group (PEG) illustrated by green in Figure 2.2, a lipophilic tail group (tocopheryl) illustrated by black and a succinate linker illustrated by red (Collnot et al. 2007). These bulky groups give the molecule a large surface area making TPGS an effective emulsifier. It also functions as a solubiliser, absorption enhancer and stabiliser (Shin and Kim 2003).

TPGS has a low melting point between 37 and 41^{o}C, however it is heat stable below 200^{o}C and has a degradation temperature of approximately 199^{o}C (Figure 2.3). It therefore displays good thermal stability during pharmaceutical formulation when subjected to normal processing temperatures.

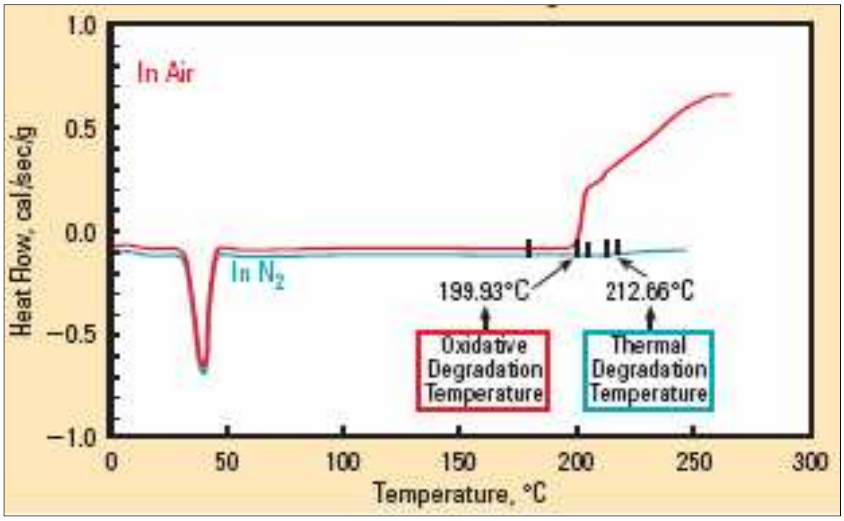

Figure 2.3 *The DSC melting profile and oxidative thermal degradation of TPGS (Eastman 2005).*

2.1.2 Active Pharmaceutical Ingredients (Model Drugs)

The model drugs used in this project are all BCS Class II compounds and therefore by their nature have low aqueous solubility and high permeability across the gastrointestinal cell wall. BCS Class II drugs are prime candidates for dissolution enhancement using solid dispersion systems, as once they are in solution in the GI fluids they will be readily absorbed into the systemic circulation, thus improving their in vivo bioavailability.

2.1.2.1 Ibuprofen

Ibuprofen is used pharmaceutically as a non-steroidal anti-inflammatory drug and is widely available as a 'General Sales List' or 'Over the Counter' formulation for its analgesic and anti-inflammatory effects. It is a non-selective cyclo-oxygenase inhibitor and exists as a white, crystalline powder. It has the systematic name (2RS)-2-[4-(2-Methylpropyl)phenyl]propanoic acid, a molecular weight of 206.3 g/mol and a melting point of 75-78°C (British Pharmacopoeia 2010). Its glass transition temperature is thought to be -45.15°C (Domanska et al. 2009).

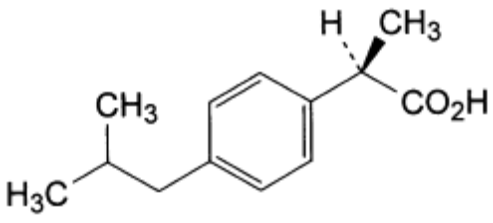

Figure 2.4 *Structural formula of ibuprofen (British Pharmacopoeia 2010).*

It has been shown to be highly insoluble in water (0.01mg/ml (Kasim et al. 2003)) but freely soluble in acetone (British Pharmacopoeia 2010). The solubility of ibuprofen is also pH dependent as it is acidic in nature. It is thought to fall within BCS II due to its low solubility but high permeability. It is also thought, as with all NSAIDS, to promote its own transport across the GI tract (Potthast et al. 2005). It is for this reason that ibuprofen is a valuable model drug in the development of oral dosage forms to improve the bioavailability of poorly soluble drugs.

Ibuprofen is usually administered as the free acid and as a racemic mixture of two enantiomers, S (+) and R (-), however the R (-) enantiomer has little activity (Potthast et al. 2005). Commercially available formulations of ibuprofen are often film or sugar coated and are known to demonstrate variation in terms of in vitro dissolution and in vivo bioavailability (Saville 2001). This will be brought about by the poor aqueous solubility of ibuprofen which is the rate limiting step on oral administration.

Ibuprofen can exist as plate or needle-shaped crystals which are characterised by melting points of 75.1 and 75.2^{o}C (Moneghini 2008). Despite not exhibiting genuine polymorphism, the crystal habit of ibuprofen has been found to change with pharmaceutical processing, and once mixed with excipients, the interactions between molecules can become destabilised (Romero et al. 1993).

2.1.2.2 Indometacin

Indometacin is a cyclo-oxygenase inhibitor and is a 'Prescription Only Medicine' used as a non steroidal anti-inflammatory analgesic in capsule or suppository formulations. It has the systematic name 1-(4-chlorobenzoyl)-5-methoxy-2-methyl-1H-indol-3-acetic acid (molecular mass 357.81 g/mol), a melting point of between 158 and 162^{o}C and a decomposition temperature of 220°C (British Pharmacopoeia 2010; Okumura et al. 2006).

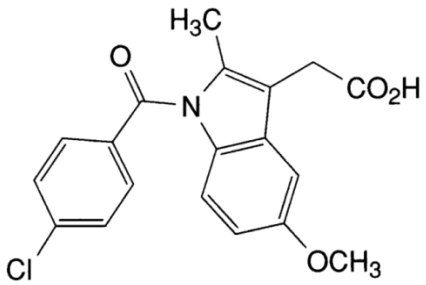

Figure 2.5 *Structural formula of indometacin (British Pharmacopoeia 2010).*

Indometacin is a white / yellow crystalline powder and can exist in a number of different polymorphic forms. It is virtually insoluble in water, with a solubility recorded as 0.0025mg/ml (Bandi et al. 2004), and only sparingly soluble in alcohol (British Pharmacopoeia 2010). Amorphous indometacin has a glass transition temperature (T_g) of 43^{o}C, below this temperature amorphous indometacin crystallises to the stable γ polymorphic form (m.p. 162^{o}C), however above the T_g the metastable α form (m.p. 155^{o}C) is favoured (Andronis and Zografi 2000; Otsuka et al. 2001).

Indometacin, like ibuprofen, is a BCS Class II compound i.e. low solubility but high permeability across the cell wall of the gastrointestinal tract. This means that it demonstrates a low and often erratic bioavailability when taken orally caused by its poor solubility in the GI fluids (El-Badry et al. 2009).

2.1.2.3 Piroxicam

Piroxicam is a 'Prescription Only Medicine' belonging to the same group of non-steroidal anti-inflammatory drugs as ibuprofen and indometacin. It is not utilised for its analgesic, anti-inflammatory and antipyretic properties due to its delayed onset of action which is caused by slow and gradual absorption and a long half life of elimination. Its use is therefore reserved for the acute and long term treatment of osteo and rheumatoid arthritis symptoms (Prabhu 2005; Qi et al. 2010a). It is a cyclo-oxygenase inhibitor and has the systematic name 4-Hydroxy-2-methyl-N-(pyridine-2-yl)-2H-1,2-benzothiazine-3-carboxamind 1,1-dioxide. It exists as a white crystalline powder with a limited water solubility of 0.0198mg/ml (Karatas et al. 2005),.

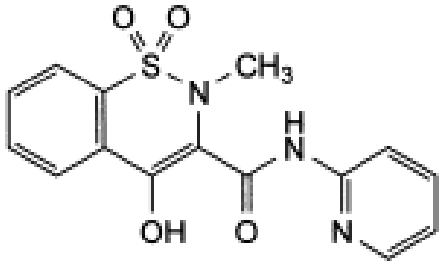

Figure 2.6 *Structural formula of piroxicam (British Pharmacopoeia 2010).*

Piroxicam is known to show polymorphism however it is unknown how many different forms exist. An investigation carried out by Vrečer et al (1991) was able to isolate four polymorphic forms with melting points 201.6^{o}C, 195.5^{o}C, 178.4^{o}C and 164.1^{o}C, and at least one pseudopolymorphic (monohydrate) modification.

Piroxicam is classified as BCS II (high permeability, low solubility) and its bioavailability has been successfully increased using solid dispersions formulations in the past (Yuksel 2003).

2.2 METHODS

2.2.1 Physical Mix Preparation

Physical mixes of the crystalline model drugs and lipidic carrier were created for the purpose of comparison with the SSD systems of the same components. Known amounts of crystalline drug were physically mixed with the carrier, the resulting melting transitions of which acted as a calibration (control) in order to calculate the quantity of drug dissolved in carrier during the formulation process, as opposed to that present as crystalline particles in the SSD.

Physical mixes were created in the DSC pan by weighing the crystalline drug on top of the lipidic carrier, then sealing. This method was chosen in preference to making larger quantities as that would pose the difficulty of achieving an evenly distributed mix. Uneven distribution would result in unreliable data and the small quantities required for analysis would be likely to contain varying amounts of crystalline drug. The kinetic energy created by the process of mixing could also render the crystalline

drug amorphous. Placing the crystalline drug on top of the carrier in the DSC pan is able to ensure mixing when the lipid melts at lower temperatures.

2.2.2 Semi-Solid Dispersion Formulation

There are a number of methods available for the preparation of SSD systems, as described in Chapter One, such as solvent evaporation by spray or freeze-drying, or by hot melt extrusion. The method chosen ultimately depends upon the drug and excipient involved and also the physicochemical properties required of the final product. The properties of the carriers used in this project, being low melting point lipids, lend them to formulation via the hot melt method. This involves heating of the carrier to approximately 60^{o}C until molten and the addition of the crystalline drug with continuous stirring for 5 minutes until the mix is homogeneous. The dispersions were then allowed to cool, protected from light, for 48 hours at either 4^{o}C (denoted as SSD(4)) or 20^{o}C (denoted as SSD(20)) before being analysed.

2.2.3 Capsule Preparation

Due to the viscous nature of the molten SSD systems on preparation and the resulting difficulty in accurately measuring the required quantity by volume, the formulations were allowed to cool before being filled into size 0 hard gelatin capsules. This allowed an accurate quantity by weight to be put into each capsule corresponding to the required amount of drug for each system; 25mg of ibuprofen, 25mg of indometacin, and 10mg of piroxicam, the total weight of SSD depending upon the drug loading.

2.2.4 Thermal Analysis Techniques

2.2.4.1 Conventional Differential Scanning Calorimetry

Differential scanning calorimetry (DSC) is the most widely used of the thermal analytical techniques. It is a technique by which the thermal transitions of a substance, such as melting, re-crystallisation, glass transition or decomposition, are investigated, providing quantitative and qualitative information about the samples physicochemical properties. Samples are subjected to a linear temperature programme, heating, cooling or isothermal in nature, and the response is measured in terms of the energy transfer to or from the sample over time or temperature. The energy changes which occur within the sample during these transitions are measured in comparison to an empty reference, generating a trace of heat flow or heat capacity signals against temperature which displays transitions as exothermic or endothermic peaks (Gabbott 2008).

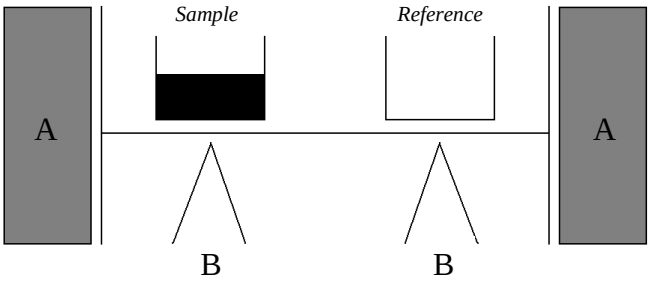

Figure 2.7 *Schematic of a heat flux DSC. A = furnace, B = thermocouple (Reproduced from Reading and Craig (2007)).*

There are two different approaches to DSC analysis, one being heat flux and the other power compensation. Heat flux DSC consists of only one furnace containing both sample and empty reference pans which are placed symmetrically within the cell. This furnace heats the sample and reference pans equally and the temperature difference between the two is measured by thermocouples placed underneath the pans. Heat flow from the furnace can be calculated using this equation:

$$\frac{dQ}{dt} = \frac{\Delta T}{R} \qquad \textbf{\textit{Equation 2.1}}$$

where dQ / dt represents heat flow, ΔT is the temperature difference between the furnace and the pan and R is the thermal resistance in the heat flow between the furnace and pan (Reading and Craig 2007).

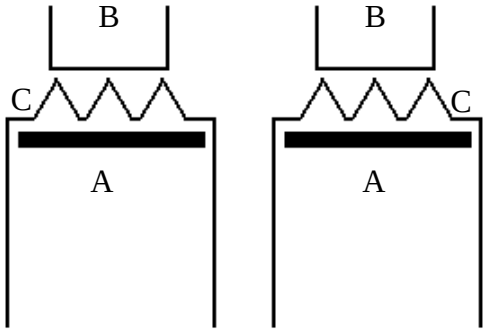

Figure 2.8 *Schematic of a power compensation DSC. A = furnace, B = sample and reference pans, C = sample and reference platinum resistance thermometers (Reproduced from Reading and Craig (2007)).*

The concept of power compensation DSC is more complex than that of heat flux. This approach makes use of two separate furnaces, one for each of the sample and reference pans. The temperature programme is the same for each furnace, however the difference in power required to maintain both pans at the same temperature is measured (Reading and Craig 2007).

Heat capacity (C_p) represents the energy required to increase the sample temperature by 1K, and heat flow is consequently a function of heat capacity (Reading and Craig 2007). Therefore, taking into account heat capacity and the occurrence of any kinetic responses of the sample, the DSC signal may be expressed as:

$$\frac{dQ}{dt} = C_p.\frac{dT}{dt} + f(t,T) \qquad \textbf{\textit{Equation 2.2}}$$

where *dQ/dt* represents the heat flow, C_p is the heat capacity, *dT/dt* is the heating rate and *f*(*t*,*T*) is a function of time and temperature representing any kinetic response (Hill et al. 1998)

Modulated temperature differential scanning calorimetry (MTDSC) is an extension of conventional DSC in the fact that a modulated sinusoidal heating wave is applied to the standard linear temperature programme. Due to the modulating temperature, the heating rate also modulates accordingly, instead of remaining constant. This allows separation of the reversible (heat flow associated with heat capacity) and irreversible (heat flow associated with a chemical event) processes, making it easier to distinguish between phases.

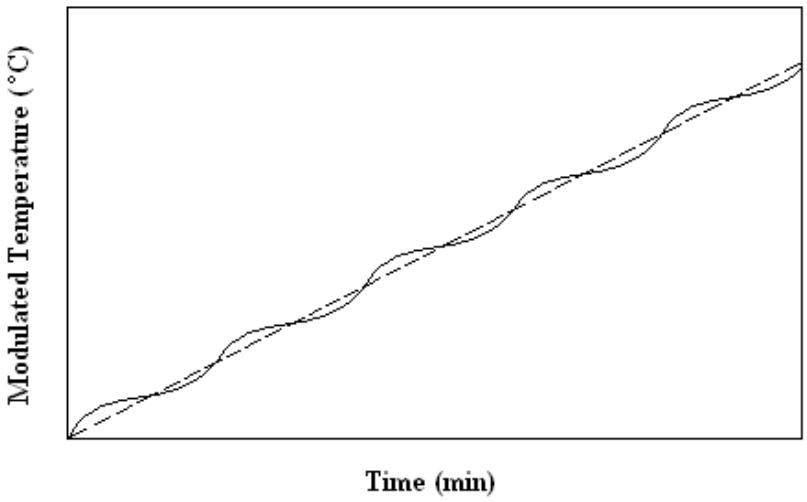

Figure 2.9 *Comparison between an MTDSC temperature profile (unbroken line) and that of conventional DSC (broken line) (Coleman and Craig 1996) .*

Reversible processes are thought to be in equilibrium with the surrounding temperature programme and are therefore dependent upon heating rate, for example crystallisation. Irreversible processes are those which are kinetically controlled and are therefore dependent upon absolute temperature, such as melting (Coleman and Craig 1996).

The modulated temperature programme can be expressed as:

$$T = T_o + qt + A.\sin(\omega t) \qquad \textbf{Equation 2.3}$$

where T represents temperature, T_o is the starting temperature, t is time, A is the amplitude of oscillation, q is the average heating rate and ω is the frequency of oscillation. Therefore taking Equation 2.2 into account, the heat flow of MTDSC experiments can be expressed as:

$$\frac{dQ}{dt} = C_p(q + A\omega.\cos(\omega t)) + f(t,T) + C.\sin(\omega t) \quad \textbf{\textit{Equation 2.4}}$$

where (q+$A\omega$ cos(ωt)) represents the derivative modulated temperature, $f'(t,T)$ is the kinetic response excluding the effect of the modulation and C is the amplitude of the kinetic response to the modulation (Hill et al. 1998).

Interaction between the drug and carrier of an SSD formulation can be characterised using DSC. It is known, however, that the heating rates capable of standard DSC instruments are slow enough to allow further dissolution of crystalline drug into the molten carrier during analysis. This allows false interpretation of data and may lead to the incorrect assumption of the presence of a solid solution. This effect could potentially be overcome by employing faster heating rates which is explained in section 2.2.4.3.

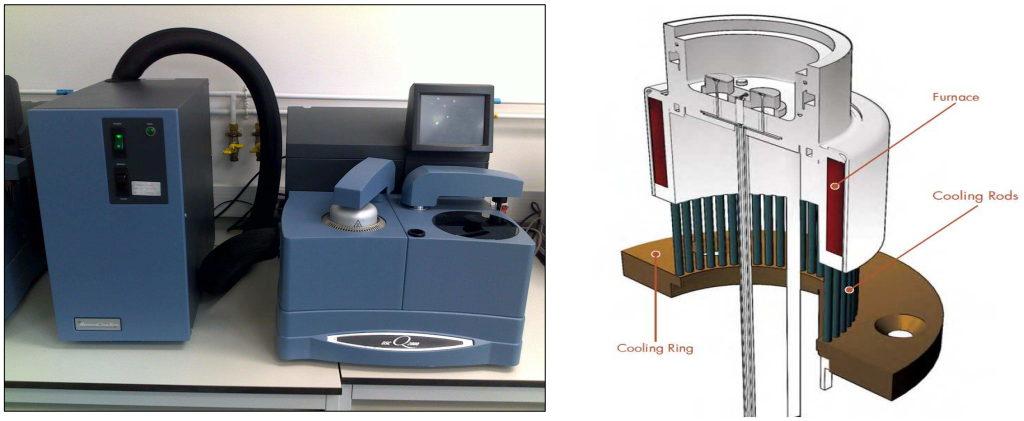

Figure 2.10 *TA Instruments Q2000 DSC and schematic of the heat flux cell (TA Instruments 2010).*

All conventional DSC experiments were performed using a TA Q1000 or Q2000 DSC instrument in TA Tzero or standard aluminium pans. These instruments perform using heat flux technology.

2.2.4.2 Quasi-Isothermal Modulated Temperature Differential Scanning Calorimetry

The technique of quasi-isothermal modulated temperature differential scanning calorimetry (QIMTDSC) is a variant of traditional MTDSC which involves the holding and sinusoidal modulation of the temperature programme around a specific temperature for extended periods of time. The temperature can be incrementally increased or decreased through a sample transition, eliminating the influence of heating or cooling rate. This method can be used in such a way as to accurately characterise a thermal transition, independent of rate. A disadvantage to this technique however is that QIMTDSC methods generally take a minimum of 12 hours to run which can extend to days. The outcome parameter of this method is the reversing "apparent" heat capacity which takes into account the reversing heat capacity and the effects of latent heat (Wunderlich 2003).

Transitions can be detected using Lissajous analysis, whereby the modulated heat flow is plotted against the modulated temperature. This allows observation of the reproducibility of the sine wave heat flow modulations within a single isothermal period. The transition can be observed in real time by noting the deviation of the sine wave curves from the steady state through the course of the process, thereby providing a novel means of de-convoluting the heat flow processes associated with

the thermal event as a function of time, in the absence of kinetic effects. The major slope of the Lissajous sine wave modulations gives an indication of heat capacity. Any change in this slope therefore suggests a change in heat capacity of the sample over the course of the experiment, with a steeper slope corresponding to a greater heat capacity. A change in the width of the Lissajous sine wave ellipses suggests a difference in phase between the sample response to heat flow and the applied stimulus or temperature fluctuation which could be as a result of a thermal transition. This difference is known as phase lag however its interpretation is known to be very difficult.

All Quasi-Isothermal MTDSC experiments were performed using a TA Q1000 or Q2000 DSC instrument in TA Tzero or standard aluminium pans.

2.2.4.3 Hyper (Fast Speed) Differential Scanning Calorimetry

Hyper DSC works under the same principles as conventional DSC however it involves the heating of samples at much faster rates than those possible using conventional DSC. The capability of achieving these high heating rates is attributed to the use of power compensation technology which employs a much smaller furnace as outlined in Section 2.2.4.1. Commercially available hyper DSC instruments can heat at rates up to 750^{o}C/minute. Advantages of using increased heating rates include reduced run times and improved sensitivity. The sensitivity enhancement observed is attributable to the time lag between the sample and reference achieving the same temperature after a thermal transition has occurred. This time lag is the same for slow and fast rates, however at faster rates, the transition peak will increase in size

due to a greater input of energy per unit time i.e. the energy changes occur over a significantly shorter time period, allowing visualisation of weak transitions (Gaisford 2008). This is useful in the detection of weaker or low energy process such as glass transitions. A disadvantage of enhanced sensitivity however is poor resolution. The increase in size of the thermal transitions can conceal other smaller transitions which may be occurring.

It is possible in some cases, by heating at accelerated rates, to inhibit kinetic transitions such as crystallisation and glass transition. The temperature of these processes is known to increase with increasing heating rate, therefore, if the heating rate is fast enough it is possible to inhibit them completely. The sample is still able to respond to the input of energy, and thermodynamically controlled events such as melting are not affected (Gaisford 2008; Gramaglia 2005). A study carried out by Gramaglia (2005) found that fast heating rates are also capable of reducing further dissolution of drug into polymeric film matrices and thus giving a more accurate determination of its solubility in the polymer. Hyper DSC has, however, been found to be less robust than conventional DSC due to increased variability in measured enthalpies (McGregor and Bines 2008).

For the purposes of this project, the main advantage of using hyper DSC was the reduced dissolution of drug in the molten lipidic carrier during analysis, allowing a more accurate determination of drug solubility within the carrier, and also quantification of crystalline drug present in the SSD systems after formulation. All hyper DSC experiments were performed using a Perkin Elmer Diamond DSC, based at AstraZeneca, Macclesfield, in 40µl aluminium pinhole pans.

2.2.4.4 Hot Stage Microscopy

Hot Stage Microscopy (HSM) technique can be used for the physical characterisation of pharmaceutical samples and involves the observation of thermal transitions occurring in a sample as a function of temperature and time. HSM is a useful visual method which allows evaluation of the physical properties of pharmaceutical compounds and complete formulations and which can be used to complement and confirm processes which are observed using other thermal analytical techniques such as DSC and TGA (Vitez et al. 1998). The apparatus consists of a camera mounted above a polarised light microscope, into which the hot-stage, containing the sample on a glass slide, is placed.

HSM was used in this project to characterise melting and crystallisation of the lipidic carriers on heating and cooling, as well as characterisation of the crystalline drugs and evaluation of these thermal processes when in combination as SSD systems. HSM experiments were performed using a Mettler Toledo FP90 Central Processor and an FP82HT Hot Stage, a Leica DM LS2 Microscope and a JVC digital colour video camera connected to a PC.

2.2.5 Dynamic Vapour Sorption

Dynamic Vapour Sorption is a technique by which the response of a sample material is measured in relation to changes in temperature and humidity over time. The loss or uptake of water is accurately recorded gravimetrically in comparison to an empty reference. It is important to understand the effect of temperature and humidity on

pharmaceutical excipients and active ingredients in order to predict the behaviour of the final formulation upon storage. The humidity in the sample and reference chambers is regulated by three mass flow controllers which adjust the nitrogen purge gas flow through the system. Humidity reservoirs are used to generate nitrogen purge gasses of the required moisture content, from 0 to 98%. A heat exchanger is used to control the temperature of the sample and reference environment between 5 and 85^{o}C (TA Instruments 2010).

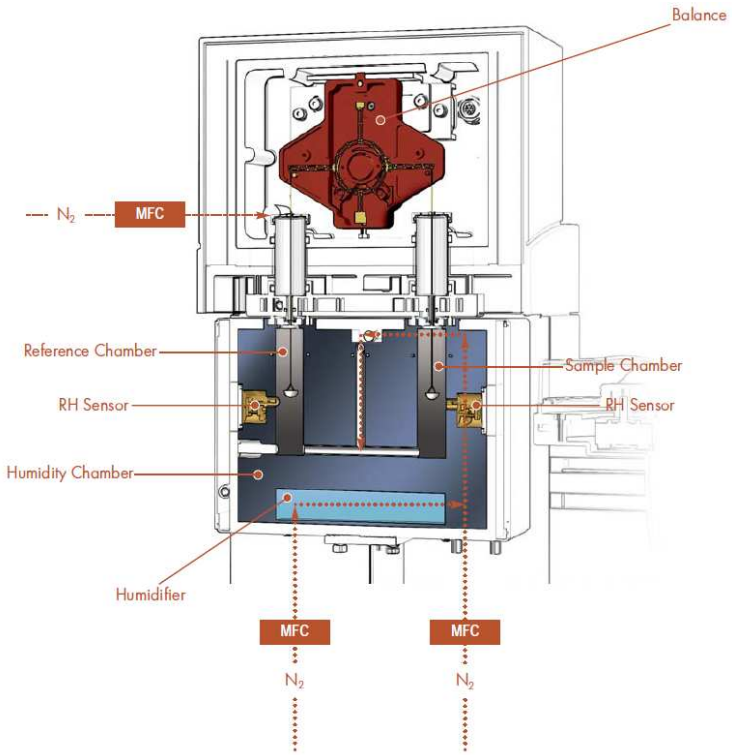

Figure 2.11 *The internal components of a typical DVS instrument; MFC = Mass Flow Controller (TA Instruments 2010).*

The most common analyses performed using this technique are isotherm experiments which involve the sample material being subjected to increasing or decreasing humidity at constant temperature, and isohume experiments where the sample is

subjected to increasing or decreasing temperature at constant humidity (TA Instruments 2010). In most cases the sample is dried before analysis and the weight is allowed to equilibrate at each isothermal step before moving on to the next.

Samples for analysis by DVS were prepared as detailed previously and all experiments were performed using a TA Instruments Q5000SA in 180µl quartz crucibles. DVS was used in this project to determine the hydration behaviour of the lipidic carrier material and drugs alone and in combination after formulation into SSD systems at varying temperature and humidity.

2.2.6 In Vitro Dissolution

In vitro dissolution testing is used in the pharmaceutical industry for a number of applications, for example in formulation science to assess the dissolution properties of a drug in order to aid selection of appropriate excipients for combination into oral dosage forms or to discriminate between formulation candidates to aid selection (Dressman 1998); however on the whole, dissolution testing allows characterisation of the release profile of immediate and modified release solid oral dosage forms. Ultimately, in vitro dissolution testing of pharmaceuticals is used to predict and assess in vivo performance i.e. bioavailability. In order to achieve a more accurate in vitro / in vivo correlation, the tests must be carried out under the appropriate conditions, and simulated gastrointestinal fluids are often used for this purpose.

Figure 2.12 *Copley dissolution bath.*

Drug dissolution into the gastrointestinal fluids is an essential part of the processes which occur after oral administration of a solid oral dosage form, and for poorly soluble drugs, this is the rate limiting step. In this project, dissolution was utilised purely to investigate the improvement, if any, of the dissolution rate of the three poorly soluble drug SSD systems formulated with the chosen lipidic carrier material. All experiments were performed using a Copley Scientific DIS8000 dissolution bath attached to a Copley Scientific FH16-D heating unit.

CHAPTER THREE

CHARACTERISATION OF SURFACE ACTIVE LIPIDIC CARRIERS

3.1 INTRODUCTION

The physicochemical properties of the chosen surface active lipidic carriers, such as melting and crystallisation temperatures, can undergo alterations during manufacture into formulations, and also upon storage. It is important to fully characterise these properties prior to formulation in order to predict their behaviour when in combination with the drug, and also in the final product as a whole. The lipidic carrier materials under investigation are largely crystalline in structure. Crystalline materials display significant or complete structural order which is repeated indefinitely in three dimensions. As well as characterisation of the physicochemical properties of the carriers upon heating, in order to demonstrate the changes undergone during manufacture, the crystallisation transition was also investigated. On cooling from a molten state, for example during SSD formulation, the carriers crystallise, however not necessarily forming the same crystalline structure as before. Any alteration in the crystalline packing arrangement will alter the carrier's physicochemical properties. This may become a disadvantage as the behaviour of the final formulation will be unknown and therefore unpredictable.

In this chapter, structural properties of the lipidic carrier materials are determined using DSC methods by observing thermal transitions upon heating and cooling. HSM is used to complement DSC data by visually mirroring these transitions. The technique of quasi-isothermal MTDSC is further developed as part of this project in order to characterise crystallisation of lipidic materials. The technique allows isolation of the temperature at which crystallisation occurs, independent of heating rate. DVS has also been used to investigate the water sorption properties of the

carriers, as such characteristics may be extremely important in determining the performance of the final formulation.

3.2 METHODOLOGY

3.2.1 Conventional Differential Scanning Calorimetry

Conventional DSC experiments were performed under a nitrogen environment, with a purge rate of 50ml/minute. Calibration of the instrument was conducted prior to experimentation. This involved cell resistance and capacitance (baseline) calibrations with an empty cell and sapphire disks (Tzero calibration), cell constant calibrations using indium standard (Tm 156.6°C, heat of fusion 28.6J/g), and finally temperature calibrations using benzoic acid (Tm 122.4°C) and n-octadecane (Tm 28.2°C). Temperature calibrations were carried out at the same rate as intended for sample analysis. Samples for analysis were taken directly from the container, loaded and crimped into TA standard aluminium pans or Tzero aluminium pans, all of similar weight.

Heating and cooling experiments were conducted in TA standard aluminium pans with a sample weight range of 2 to 2.5mg. Samples were heated from 0^{o}C to 60^{o}C, held isothermally for 10 minutes to ensure complete melting, and then cooled back to 0^{o}C or -10°C at a rate of 0.5, 2, 10 or 20^{o}C/minute. Samples were also heated to 200^{o}C at 10^{o}C/minute. Experiments were repeated up to four times.

As part of the aging study, samples were heated and cooled at 10°C/minute as described above, then aged in the pan for 1, 2, 3, 5, 24 and 72 hours under ambient conditions, after which time the method was repeated.

3.2.2 Quasi-Isothermal Modulated Temperature Differential Scanning Calorimetry

Quasi-isothermal MTDSC experiments were performed under a nitrogen environment at a purge rate of 50ml/minute. Calibration of the instrument was conducted prior to experimentation, as per conventional DSC. An additional calibration using aluminium oxide was also carried out in order to calibrate for the required QIMTDSC method, determining the total and reversing heat capacity constants. Samples in the weight range 2 to 2.5mg were prepared into TA standard aluminium pans or Tzero aluminium pans, all of similar weight.

All samples were heated above the melting temperature at 10°C/minute to 60°C, held for 10 minutes to ensure complete melting, and then cooled to the point of QIMTDSC. All methods employed an amplitude of ±1°C and a period of 60 seconds.

Method One – Cooled from 40 to -10°C in 5°C increments, with an isotherm of 60 minutes at each increment.

Method Two – Cooled from 35 to 5°C in 1°C increments, with an isotherm of 20, 40 or 60 minutes at each increment.

Method Three – Held isothermally for 720 minutes (12 hours) at 29, 30, 31, 32, 33, 35 or 40°C.

Method Four – Held isothermally for 2880 minutes (48 hours) at 29°C.

3.2.3 Hot Stage Microscopy

Samples for analysis were applied to glass microscope slides and heated from 30 to 50°C at 10°C/minute, cooled to room temperature, then re-heated to 50°C. Images were captured at x20 magnification, under polarised light. It should be noted that the apparatus has no control over the rate of cooling, however it was calculated to be approximately 2°C/minute.

3.2.4 Dynamic Vapour Sorption

Samples were taken directly from the container to be analysed gravimetrically using DVS in quartz crucibles against an empty reference. Three different methods, under nitrogen environment, were used to characterise the hydration behaviour of the lipidic carrier.

Method One – 75% RH, temperature ramped from 25 to 55°C, 60 minutes at each step.

Method Two – 75% RH, held isothermally for 60 minutes at a single temperature (25, 30, 35, 40, 45, 50 or 55°C).

Method Three – 40°C, RH ramped from 0 to 90%, 60 minutes at each step.

All samples were dried at 25°C and 0% RH for 60 minutes prior to experimentation. Desorption or absorption of water was measured as weight loss or gain respectively.

3.3 GELUCIRE 44/14

3.3.1 Assessment of Thermal Properties using Conventional Differential Scanning Calorimetry

Conventional DSC is the most widely used of the thermal analytical techniques. It is a fast and convenient method of determining the fundamental thermal properties of pharmaceutical samples and therefore an indirect indication of their structural properties. In this section it is used to characterise the melting and crystallisation transition of Gelucire 44/14 and also the dependence of these transitions upon rate changes, thermal history and aging.

3.3.1.1 Melting

The most accurate method of determining the melting temperature (Tm) of crystalline materials is to calculate the extrapolated onset temperature ($Tm_{(onset)}$). The peak max ($Tm_{(max)}$) is affected by the broadness of the transition which is dependent upon the particle size, sample mass and heating rate (Saunders 2008). On heating, Gelucire 44/14 exhibits a characteristic double melting endotherm (Figure 3.1). The smaller leading peak (secondary peak) displays a $Tm_{(onset)}$ of 28.3°C ± 0.3 ($Tm_{(max)}$ 34.5°C ± 0.2; ΔH 21.1 J/g ± 0.3), with the main melt (primary peak) occurring at 39.9°C ± 0.1 ($Tm_{(max)}$ 45.0°C ± 0.07; ΔH 91.4 J/g ± 3.2). The secondary peak, which appears to consist of 2 phases, is contributed by lower melting point fractions of the lipid (Gattefossé 2007). The larger primary melt endotherm also appears to have a slight shoulder. MTDSC studies carried out by the manufacturer, Gattefossé (2007), found the reversing and non-reversing signals to demonstrate a similar melting

endotherm to that of the total heat flow, thus suggesting that the broad endotherm observed is attributable to a single melting transition only, and not a number of different thermal events occurring over the same temperature range. Due to the many components of the lipid and their complex interaction, which are not yet fully understood, the broad double melting endotherm and its various peaks and shoulders cannot be assigned to any specific components (Sutananta et al. 1994b).

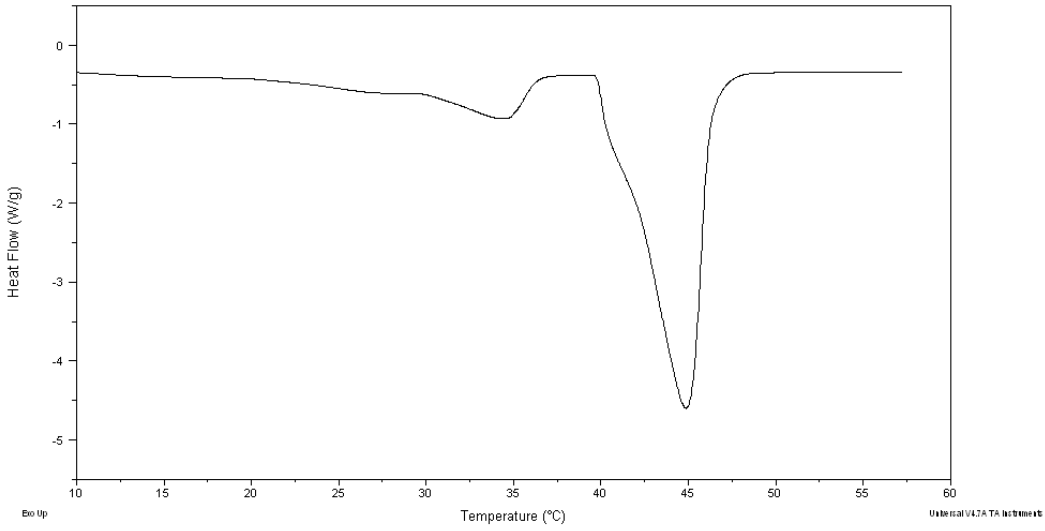

Figure 3.1 *Heat flow against temperature signal on heating at 10°C/minute of the Gelucire 44/14 melting endotherm.*

On heating above the melting temperature of Gelucire 44/14 (Figure 3.2), an exotherm is observed at onset 144.14°C ± 0.2 (max 157.8°C ± 0.3; ΔH 9.0 J/g ± 1.4). It is possible that this exotherm is some form of decomposition of the lipid; however it is unlikely to be oxidative in nature. The sample pan was crimped and not hermetically sealed therefore any oxygen present within the pan will have been driven off by the nitrogen gas purge flowing through the cell during analysis. Dordunoo et al (1991), whilst investigating solid dispersions of Gelucire 44/14 with

triamterene, suggested the decomposition of Gelucire 44/14 at approximately 170^{o}C however offered no suggestion as to the nature of the process. As this is not the focus of this study, the nature of this exotherm was not further investigated.

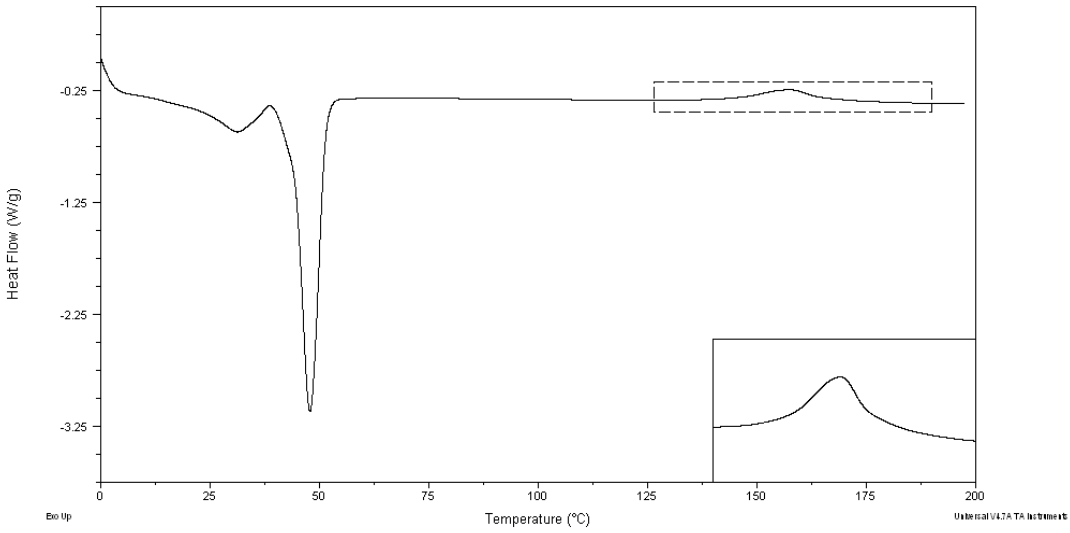

Figure 3.2 *Heat flow against temperature signal on heating at 10^{o}C/minute of Gelucire 44/14. Inset: Magnification of decomposition exotherm.*

3.3.1.2 Crystallisation

Lipids in general consist of multiple components making the process of crystallisation, and subsequently its characterisation, complex. The carriers investigated are doubly complex since, despite being of a lipidic nature, they also contain polymeric elements or properties which will inevitably have an effect on the overall behaviour of the material. General lipidic and polymer crystallisation theory will however give an insight into the processes which occur upon cooling from the molten state.

Lipids are known to retain some molecular order when in the liquid phase. This order is lost upon heating to extreme temperatures above the melting point of the lipid. The temperature from which the lipid is cooled is a determining factor on the form of the lipid once crystallised. If the lipid order is lost then a less stable form is known to crystallise from the melt (Metin and Hartel 2005). This will have an impact on the structure of the final formulation depending upon the temperatures used during manufacture.

The process of crystallisation relies upon two independent phenomena; nucleation and crystal growth. Before crystallisation can occur, the solution is required to be in a supersaturated or subcooled state, generally achieved once the temperature drops below the melting point of the lipid. The phase transformation process of crystallisation is dependent upon the Gibbs free energy barrier to nucleation. Crystallisation begins with nucleation which involves the association of molecules into a solid crystalline phase, i.e. a crystal lattice. Only those nuclei large enough to overcome the barrier of free energy will remain, those too small will disperse back into the supersaturated or subcooled solution (Long et al. 1995). Once a nucleus is formed, energy is released known as the latent heat of fusion, allowing the molecules to exist in a lower energy state. Upon cooling at a slow rate, the associating molecules have sufficient time to organise into ordered lamellae structures, whereas during fast cooling, a diffuse crystalline phase of low energy is known to form (Metin and Hartel 2005).

There are three methods by which nucleation is thought to occur, as outlined by Long et al (1995):

1) Spontaneous homogeneous nucleation which involves the association of only a single species from a supercooled homogeneous melt. This is rarely the case.
2) Heterogeneous nucleation around the surface of a foreign particle or phase present in the solution acting as a catalyst, known to reduce the free energy required for nucleation to occur.
3) Orientation induced nucleation which involves the alignment of macromolecules and spontaneous crystallisation.

Once nuclei are present in solution, greater numbers of molecules from the liquid phase begin to associate causing growth of the crystal which continues until equilibrium or complete crystallisation is achieved (Metin and Hartel 2005).

One method of modelling the process of crystallisation is with the Avrami equation which takes the form:

$$(1 - X) = exp(-kt^n) \qquad \textbf{\textit{Equation 3.1}}$$

where *X* is the crystal fraction at time *t*, *k* is a crystallisation rate constant and *n* is the Avrami exponent (Avrami 1939). The application of this model can give an indication as to the mechanism by which nucleation and crystal growth occurs. The value of *n* can be expressed as

$$n = n_d + n_n \qquad \textbf{\textit{Equation 3.2}}$$

where n_d relates to the dimensionality of crystal growth, and n_n is the time dependence of nucleation. n_d can be calculated to the value of 1, 2 or 3 corresponding to one dimensional growth, two dimensional lamellar aggregates (axialites) or three dimensional aggregate superstructures of radial lamellae (spherulites) respectively. The value of n_n can assume the integers 0 or 1 signifying instantaneous nucleation or spontaneous nucleation respectively (Lorenzo et al. 2007). Overall therefore, total values of n suggest:

$n = 4$ Heterogeneous nucleation and spherulitic crystal growth from sporadic nuclei in three dimensions; Constant nucleation rate which is independent of time.

$n = 3$ Heterogeneous nucleation and spherulitic crystal growth from instantaneous nuclei in three dimensions; The majority of nuclei are formed at the beginning of the crystallisation process; The rate of crystallisation decreases with time.

$n = 2$ Two dimensional, plate-like crystal growth; A very rapid nucleation rate at the outset of crystallisation which decreases with time (Metin and Hartel 1998).

$n = 1$ One dimensional crystal growth from instantaneous nuclei.

Melting, as a first order thermodynamic process, is not affected by increasing heating rate. Crystallisation, however, is kinetically controlled and therefore the temperature at which it occurs is reduced with increasing rate of cooling. Modification of lipid mechanical properties upon variation of cooling rate due to the formation of mixed glyceride crystals is well known (Sutananta et al. 1994b). Increasing the cooling rate

also enhances sensitivity making transitions appear larger. This effect is due to an increase in energy flow per unit time. This is demonstrated by Figure 3.3 in which the crystallisation exotherm increases considerably in size. The $Tc_{(onset)}$ reduces in temperature from 28.8°C ± 0.9 ($Tc_{(max)}$ 27.4°C ± 0.9; ΔH 98.7 J/g ± 8.4) cooling at 0.5°C/minute, to 20.0°C ± 2.3 ($Tc_{(max)}$ 12.5°C ± 3.0; ΔH 100.6 J/g ± 1.8) at 20°C/minute.

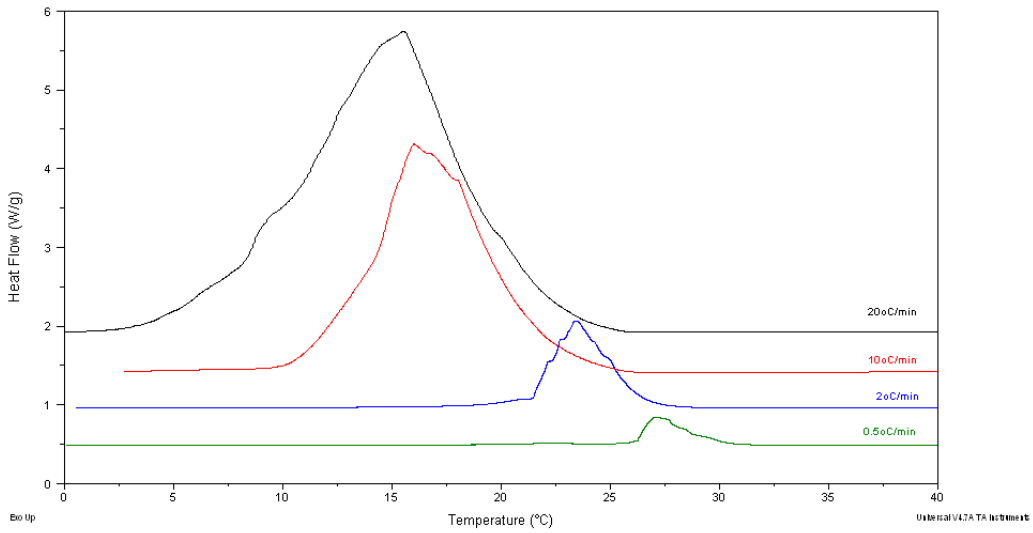

Figure 3.3 *Heat flow against temperature signal on cooling at varying rates of Gelucire 44/14 crystallisation.*

The physical state of the lipid in the formulated SSD will have implications on the physicochemical properties of the final product. Cooling rate has been shown to impact crystallisation of lipids greatly by the modification of the solid fat content and also the crystal habit. Slow rates of crystallisation can encourage the aggregation of small crystals into larger particles and therefore the formation of more stable polymorphs (Bourlieu et al. 2010). This can therefore affect the physical state of the lipid at room temperature. It is important, therefore, to have an understanding of

these processes in order to select the most appropriate formulation method and storage conditions as the formulation may have to be cooled to much lower temperatures than anticipated in order to achieve a fully solidified system.

It is noted by Sutananta et al (1994a) that since the manufacturing of Gelucire formulations, in the main, involves its transformation into the liquid state before undergoing some form of solidification, due to the complex crystallisation behaviour of the lipidic material, this process may affect the physical structure and therefore the performance of the final product. Another paper by the same author (Sutananta et al. 1994b) also highlights that cooling rate has a profound effect on the physical state of the lipid, with a faster cooling rate forming a homogeneous system and a slower cooling rate encouraging fractionation of the various lipid components into different microscopic regions.

The crystallisation exotherm appears to be greatly variable in shape between repeats of the same sample, often demonstrating a double $Tc_{(max)}$ (data not shown). This may in part be due to the nature of the different melting point fractions of the lipid. Crystallisation is also very dependent upon nucleation and crystal growth and the rate of these processes, which can vary extensively, as therefore can the shape of the exotherm. The crystallisation of Gelucire 44/14 was observed to be comparable between those samples cooled at the same rate however melted at different rates (data not shown), implying that crystallisation is independent of the prior rate of melting and therefore that it is not necessarily dependent upon the thermal history of the lipid.

Solid Fat Content Calculation

The solid fat content illustrates the proportion of the crystallisation exotherm, and therefore the proportion of lipid in the crystalline state, at any particular temperature (Bourlieu et al. 2010). It can also be used to plot the progression of the endothermic melting transition. The data is generally plotted against temperature; however plotting versus time can also give information about the crystallisation process. The solid fat content of Gelucire 44/14 crystallisation was calculated as a function of temperature using the area under the re-crystallisation plots at various temperature points, expressing them as percentages of the total on complete crystallisation, assuming that the total peak represents 100% crystallisation. This technique allows visual simplification of the crystallisation process. By plotting the percentage solid fraction against temperature, for each individual cooling rate, it is possible to identify the amount of Gelucire 44/14 present in the solid state at any temperature point during the crystallisation process.

Figure 3.4 illustrates the percentage of solid Gelucire 44/14 during crystallisation after standard heating at 10^{o}C/minute. The cooling rate has a significant effect on the crystallisation kinetics of the lipid. It can be observed that the crystallisation temperature decreases with increasing cooling rate. This will have a great impact on the physical state of the lipid at room temperature. Taking this into account and referring to Figure 3.4, it suggests that at cooling rates above 0.5^{o}C/minute, the lipid may not be completely solidified at room temperature as the crystals have insufficient time to form. This does however make the assumption that the area of the

crystallisation DSC endotherm is directly proportional to the content of solid in the system (Sutananta et al. 1994a).

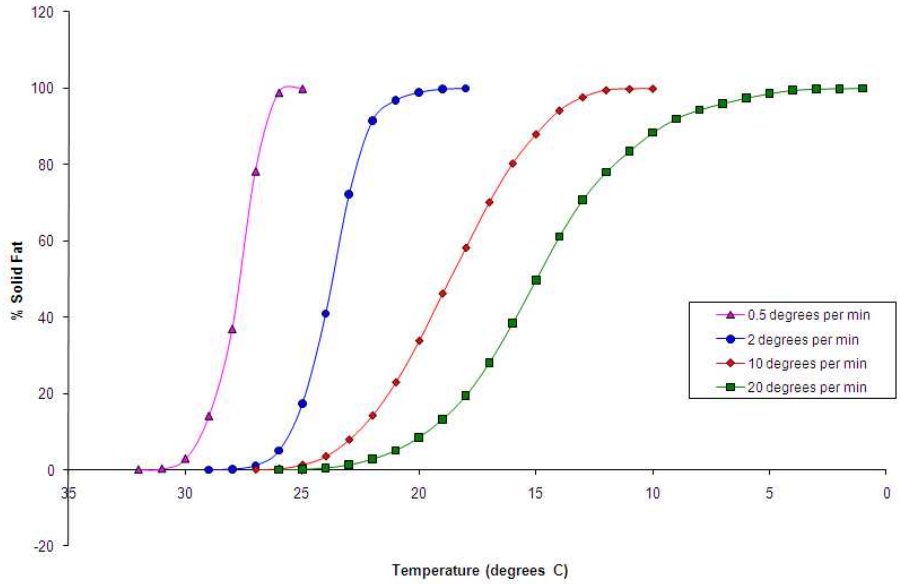

Figure 3.4 *Percentage solid fat of Gelucire 44/14 during crystallisation versus temperature on cooling at varying rates.*

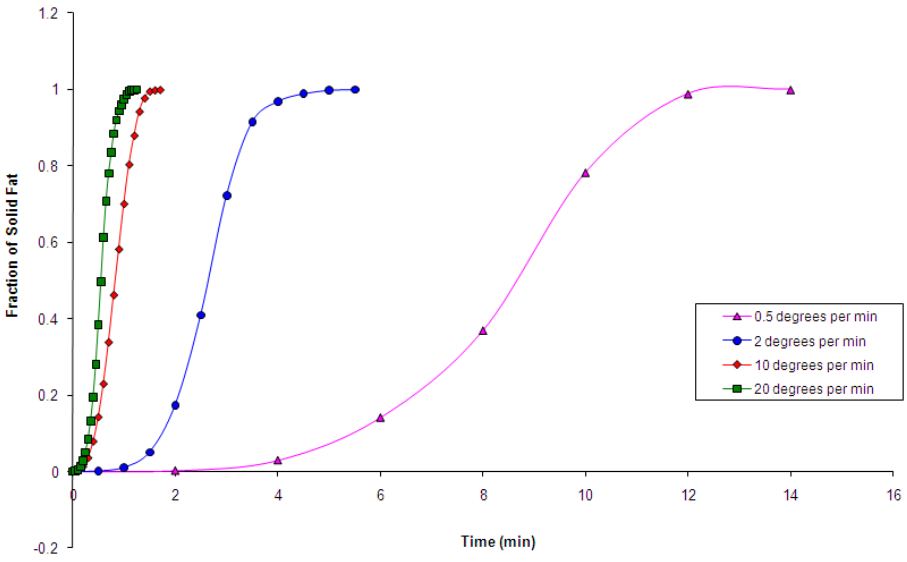

Figure 3.5 *Fraction of solid fat of Gelucire 44/14 during crystallisation versus time on cooling at varying rates.*

Using the solid fat fraction at time *t* against time data (Figure 3.5) it was possible to perform Avrami analysis. The Avrami modelling parameters are illustrated in Table 3.1. The data was found to fit well, with R^2 values between 0.9934 and 0.9998. The crystallisation rate constant, k, was observed to increase with increasing cooling rate. The rate of crystallisation was also seen to have a positive relationship with the cooling rate on observation of the fraction of solid fat in relation to time in Figure 3.5 above. The increase in crystallisation rate with cooling rate is attributable to a greater driving force for crystallisation, thus effecting nucleation and crystal growth (Bourlieu et al. 2010).

Table 3.1 *Avrami modelling parameters for the solid fat data of Gelucire 44/14.*

Cooling Rate (^oC/minute)	***n***	***k*** **(min^{-n})**	**R^2**
0.5	4	0.0001	0.9934
2	4	0.015	0.9981
10	3.05	1.22	0.9998
20	3.24	4.67	0.9991

The value of the calculated *n* gives an indication as to the time dependence of nucleation and also the dimensionality of the crystal growth. Slower cooling rates illustrated an *n* value of 4 suggesting heterogeneous nucleation and spherulitic growth from sporadic nuclei. This also indicates that the rate of nucleation was constant and independent of time. Cooling rates of 10 and 20^{o}C/minute demonstrated an *n* value of 3 (to the nearest integer) also suggesting spherulitic growth however

from instantaneous nuclei, with the rate of nucleation decreasing with time. Heterogeneous nucleation is expected in the case of Gelucire 44/14, as in most lipids, due to the presence of many different components. The slower cooling rates may allow spontaneous nuclei formation throughout the crystallisation process however faster rates reduce the amount of time for crystallisation to occur suggesting that nuclei may be instantaneously formed only at the start of the process.

3.3.1.3 Temperature Cycling

On re-melting after first crystallisation, with a standardised thermal history, the endotherm was altered in both size and shape (Figure 3.6). The secondary melt of the lower melting point fraction was reduced from $Tm_{(onset)}$ 28.3^{o}C ± 0.3 ($Tm_{(max)}$ 34.5°C ± 0.2; ΔH 21.1 J/g ± 0.3) to 23.4^{o}C ± 0.6 ($Tm_{(max)}$ 28.3°C ± 1.0; ΔH 4.3 J/g ± 2.1). The $Tm_{(onset)}$ of the primary melting endotherm remained relatively constant and could be seen to occur at 39.9^{o}C ± 0.1 ($Tm_{(max)}$ 45.0°C ± 0.07; ΔH 91.4 J/g ± 3.2) first melt and 40.4^{o}C ± 0.5 ($Tm_{(max)}$ 44.0°C ± 0.07; ΔH 70.7 J/g ± 1.0) second melt. A significant change in the ΔH of the peak could however be observed.

The second, third and fourth melting endotherms appeared to be identical and reproducible. This suggests an initial alteration in the lipid's physicochemical properties, which are maintained on heating and cooling thereafter.

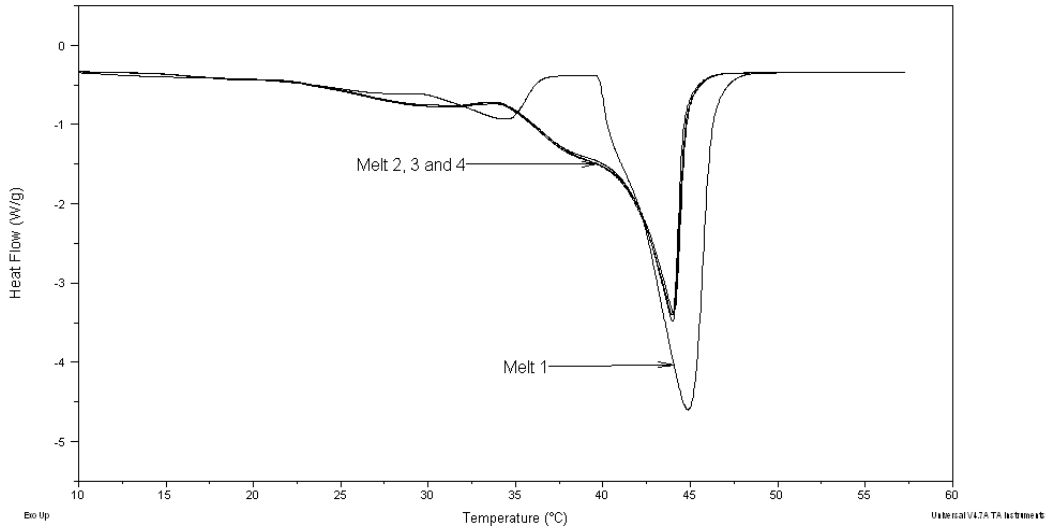

Figure 3.6 *Heat flow against temperature signal of Gelucire 44/14 heated multiple times at 10°C/minute (crystallisation data excluded).*

Gelucire 44/14 contains a large proportion of PEG esters (72%) and it is known that PEGs can exist in different polymorphic forms corresponding with different chain folding arrangements, which are structurally dependent upon the thermal history (Sutananta et al. 1994b). Lipids can also exist in varying polymorphic forms due to their generally complex nature, particularly natural fats which consist of multiple components, such as palm kernel oil (hydrogenated) which is polyglycolysed with PEG 1500 in the manufacture of Gelucire 44/14 (Metin and Hartel 2005). Overall crystallisation of Gelucire 44/14 will be a complex mixture of different crystal forms however the possible capacity of Gelucire 44/14 components to exist in different polymorphic forms may be the cause of the alteration of the melting endotherm upon temperature cycling. The process of the first melt may initiate this polymorphic change which therefore brings about a consequent change in the shape of the second and subsequent melts.

The shape of the second melting endotherm was found to be influenced by the cooling rate of the first crystallisation. As the rate of crystallisation increased, the secondary melting peak became broader, the primary peak became sharper and the $Tm_{(max)}$ increased in temperature (Figure 3.7). The rate at which the lipid crystallises therefore appears to have an effect upon the thermal properties of both the lower and higher melting point fractions. This must be taken into account when considering the rate of cooling of the final product after formulation. Gattefossé, the manufacturer of Gelucire 44/14, however, state that the structure of Gelucire 44/14 is not affected by cooling rate.

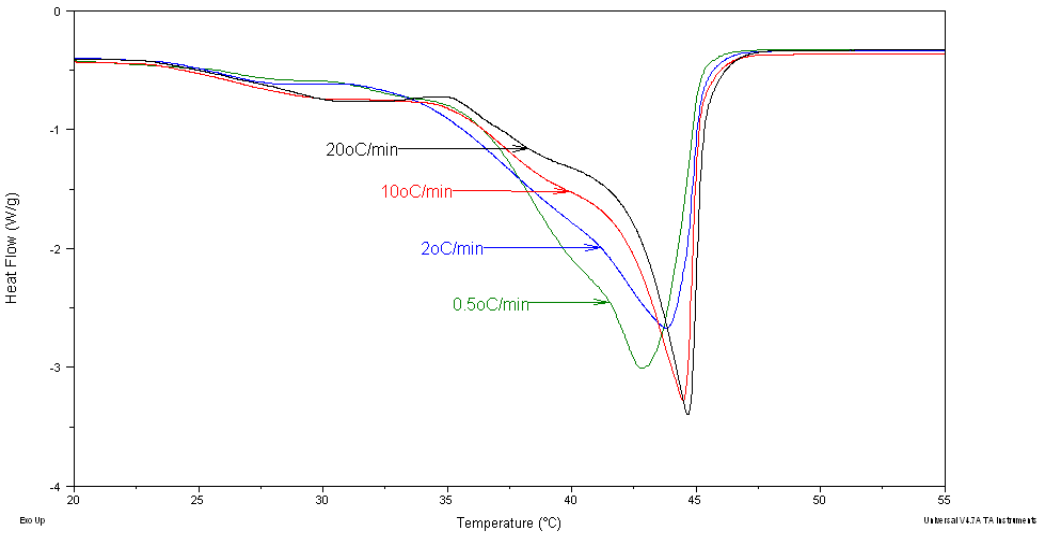

Figure 3.7 *Heat flow against temperature signal on heating at 10°C/minute of Gelucire 44/14 second melting after cooling at different rates (noted on the plot).*

3.3.1.4 Aging

The melting endotherm of Gelucire 44/14 was observed to change during temperature cycling i.e. the second melting endotherm (after heating and cooling) had altered in shape as demonstrated above. In the light of this finding, the lipid was heated and cooled, then aged for varying lengths of time under ambient conditions before being heated for a second time in order to establish if the lipid remained in this altered state (Figure 3.8).

After one hour, the shape of the second Gelucire 44/14 melting endotherm almost completely transformed back to that of the first; from $Tm_{(onset)}$ 27.4^{o}C ($Tm_{(max)}$ 33.6^{o}C; ΔH 18.6 J/g) to 24.5^{o}C ($Tm_{(max)}$ 31.3^{o}C; ΔH 27.8 J/g) for the secondary peak, and $Tm_{(onset)}$ 40.0^{o}C ($Tm_{(max)}$ 44.4^{o}C; ΔH 73.6 J/g) to 18.6^{o}C ($Tm_{(max)}$ 14.6^{o}C; ΔH 99.0 J/g) for the primary peak. The slight differences between endotherms became less and less pronounced with aging, particularly that of the primary peak. The differences in the secondary peak, however, appeared to remain. The two phases seen at time zero were reduced, as was the $Tm_{(max)}$.

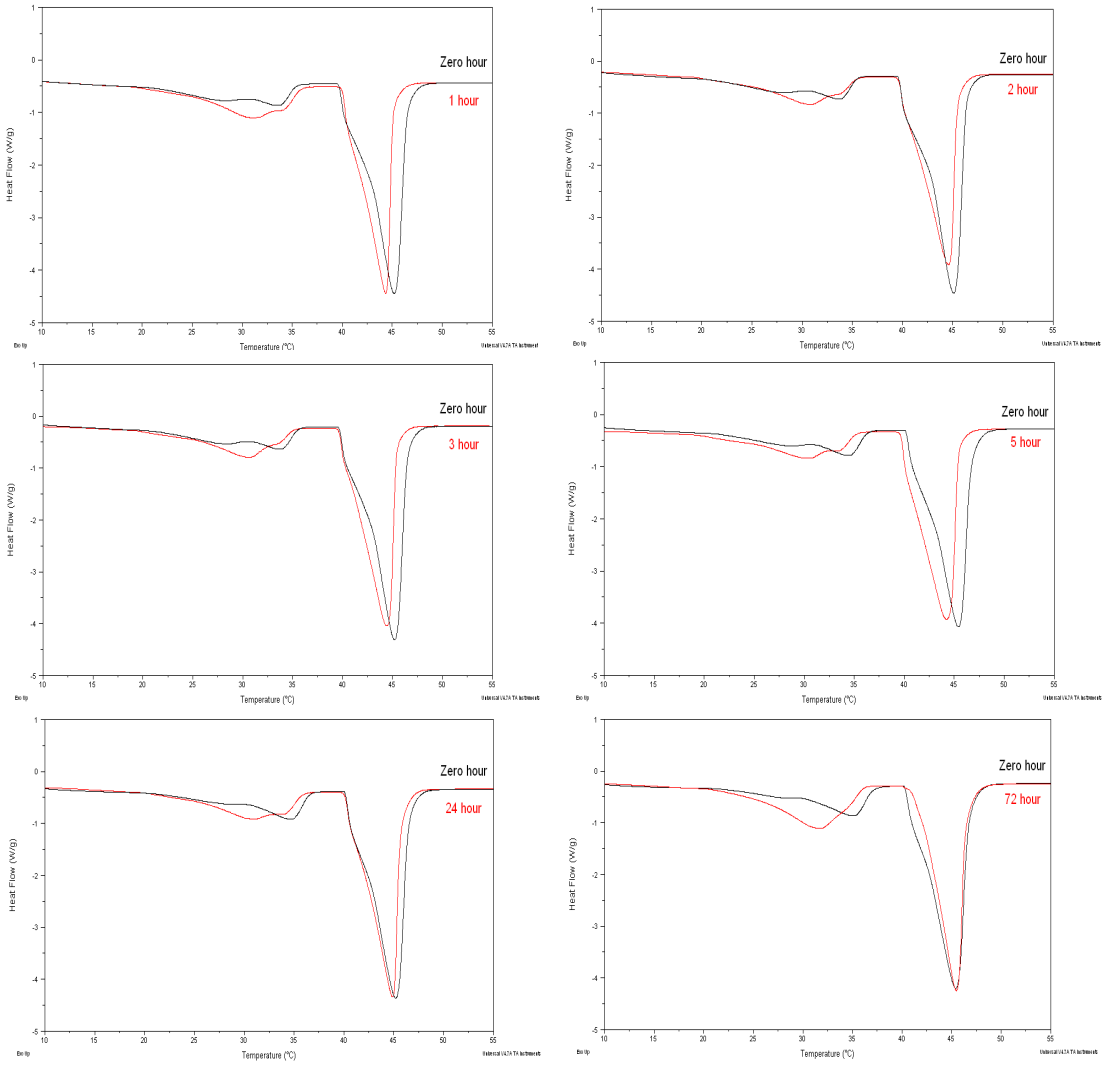

Figure 3.8 *Heat flow against temperature signal of Gelucire 44/14 first melt at 10°C/minute (black) before aging and second melt at 10°C/minute (red) after aging under ambient conditions for 1 to 72 hours.*

This suggests that any alterations to the thermal properties of the lipidic carrier after first melting, as observed previously, may not be permanent, and almost complete conversion back to its original state, i.e. that observed upon first melting taken directly from the container, is rapid, with the slight exception of the lower melting point fraction thermal properties. As discussed above, the change noted in the Gelucire 44/14 melting endotherm upon temperature cycling may be attributable to

the possible capacity of Gelucire 44/14 components to exist in different polymorphic forms after the first melt and crystallisation. The fact that the shape of the melting endotherm can be observed to be time limited may suggest that the new polymorphic form(s) is unstable and therefore upon aging, rapidly converts back to its original state.

3.3.1.5 Continuity throughout the Container

Since Gelucire 44/14 is formed directly in the container during manufacture and is composed of multiple constituents, it was felt necessary to ensure that continuity throughout could be assumed, by assessment of thermal properties by conventional DSC. The melting endotherm of samples obtained from the top, middle and bottom of the container were analysed. The $Tm_{(onset)}$ of the secondary melting endotherm of all samples was found to occur at 28.2^{o}C, being reproducible to within ± 0.1 standard deviations ($Tm_{(max)}$ 34.2^{o}C ± 0.4; ΔH 19.5 J/g ±1.4), with the main melt at 40.4^{o}C ± 1.1 ($Tm_{(max)}$ 45.4^{o}C ± 0.4; ΔH 92.5 J/g ± 1.4). Crystallisation occurred at 21.8^{o}C ± 0.1 ($Tc_{(max)}$ 15.9^{o}C ± 0.8; ΔH 101.6 J/g ±1.0) (data not shown). Samples taken from throughout the container demonstrated good reproducibility of the melt and crystallisation transition suggesting that all samples analysed in the subsequent studies should show good continuity and be independent of its position in the original container.

3.3.2 Crystallisation Analysis using Quasi-Isothermal Modulated Temperature Differential Scanning Calorimetry

The technique of QIMTDSC is a variant of traditional MTDSC which involves the holding and modulation of a sample around a specific temperature for extended periods of time. The temperature can be incrementally increased or decreased through a transition, eliminating the influence of rate and therefore investigating time dependent processes. Crystallisation is a kinetic process and therefore highly dependent upon the rate at which the sample is cooled. QIMTDSC can be used in such a way as to accurately characterise crystallisation, independent of cooling rate, giving an indication of the true temperature at which it occurs. In the case of MTDSC, the kinetic nature of nucleation and crystal growth means that the single modulation enthalpic change can be sufficiently small that the system is rendered non-reversing, with the heat capacity of the system being observed in the reversing signal (Reading et al. 2007). The crystallisation process can also be observed through the creation of Lissajous figures, whereby the modulated heat flow is plotted against modulated temperature. This allows observation of the reproducibility of the sine wave heat flow modulations within a single isothermal period. The crystallisation can be observed in real time by noting the deviation of the sine wave curves from the steady state through the course of the crystallisation process, thereby providing a means of de-convoluting the heat flow processes associated with the thermal event as a function of time, in the absence of kinetic effects.

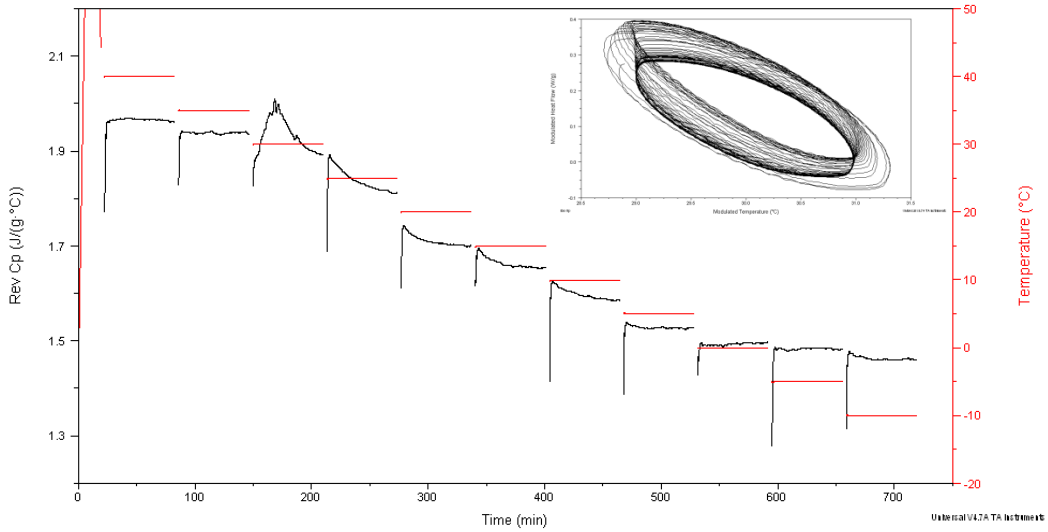

Figure 3.9 *Reversing heat capacity versus time signal for Gelucire 44/14 QIMTDSC 60 minute isotherm on cooling with 5°C increments. Inset: Lissajous plot (modulated heat flow against modulated temperature) of the sine wave heat flow modulations at 30°C.*

After analysis of Gelucire 44/14 using *Method One*, which involved cooling from 40 to -10°C in 5°C increments with an isotherm of 60 minutes at each increment, crystallisation appeared to occur during the 30°C isothermal period. This is indicated by the abrupt increase in reversing heat capacity and also the deviation of the sine wave modulations from steady state or equilibrium in the Lissajous analysis (Figure 3.9). The distortion in shape of the sine wave ellipses correspond with a change in phase lag of the sample which can also suggest the occurrence of crystallisation. This therefore implies that the Tc of Gelucire 44/14, independent of cooling rate, lies between 30 and 35°C. The exact temperature could not however be determined from this analysis as the temperature increment was too large.

Deviation of the Lissajous plot from the steady state was at its maximum during the first 31 minutes of the 60 minute modulation at 30°C, after this period the sine wave

curves reached equilibrium (see inset Figure 3.9). The change in shape of the ellipses indicated that the latent heat of the sample was changing at this isothermal temperature i.e. a thermal transition is occurring. The reversing heat capacity signal appeared to reduce over the course of the experiment. This suggested crystallisation was on going until the 0^{o}C increment where it began to reach steady state. The crystallisation of Gelucire 44/14 therefore appeared to consist of an initial or primary energetic crystallisation, followed by a secondary slower, more extended period of crystallisation which continued to much lower temperatures than previously expected. Despite melting of Gelucire 44/14 consisting of two separate endotherms attributable to the lower and higher melting point fractions of the lipid, the crystallisation transition did not demonstrate a two step process.

This phenomenon was also demonstrated by *Method 2* which subjected Gelucire 44/14 samples to a much reduced temperature increment of 1^{o}C, from 35 to 5^{o}C, for a more accurate determination of the true Tc (Figures 3.10, 3.12 and 3.13).

When held isothermally for 20 minutes at 1^{o}C increments, deviations from the equilibrium sinusoidal response and a change in shape and size of the sine wave ellipses in the Lissajous analyses were found to occur at 31^{o}C (see inset Figure 3.10). Before and after this temperature, sine waves were superimposable suggesting steady state of the sample and therefore the absence of any thermal or energetic transition at these temperatures.

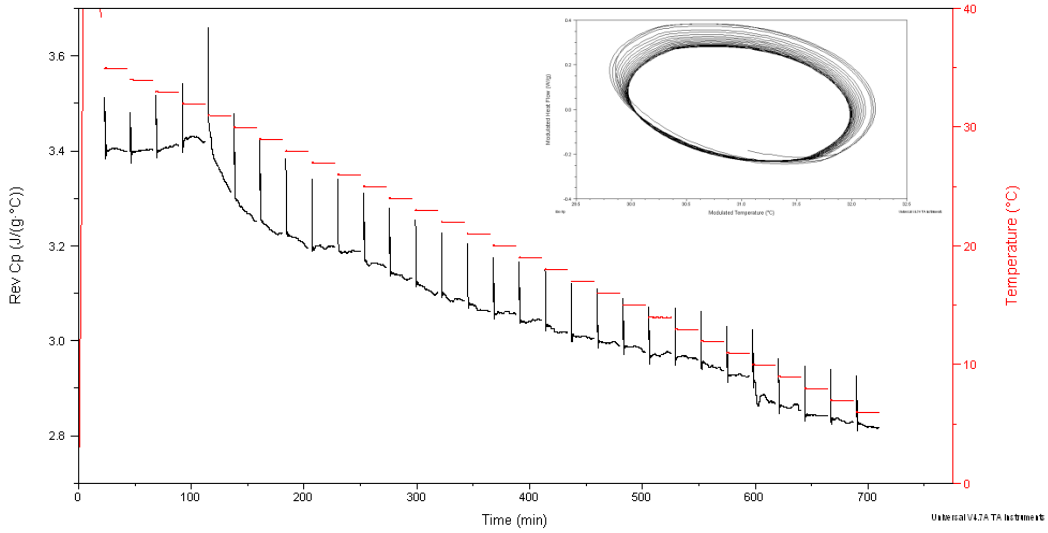

Figure 3.10 *Reversing heat capacity versus time signal for Gelucire 44/14 QIMTDSC 20 minute isotherm on cooling with 1°C increments. Inset: Lissajous plot (modulated heat flow against modulated temperature) of the sine wave heat flow modulations at 31°C.*

It was found however, as previously, that a secondary, more extended period of slow crystallisation was present after 31°C in the reversing heat capacity signal, continuing until the conclusion of the experiment at 5°C. This is demonstrated in Figure 3.11 where the major slope of the sine wave ellipses can be seen to decrease, suggesting a subsequent decrease in the heat capacity of the sample over the course of the experiment. In this case the modulated heat flow was plotted against the modulated temperature derivative time so that the ellipses were superimposed.

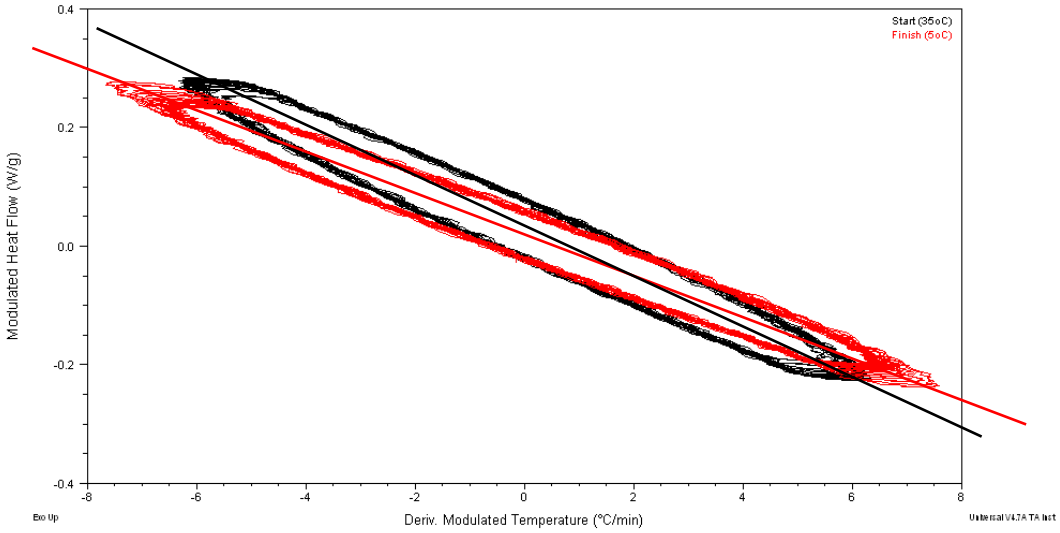

Figure 3.11 *Lissajous figures of the sine wave heat flow modulations of Gelucire 44/14 at the start (35^{o}C, black) and finish (5^{o}C, red) of the cooling experiment showing the major slope of each plot.*

Gelucire 44/14, when subjected to QIMTDSC 1^{o}C increments with a 40 minute isotherm, Tc was found to occur at 32^{o}C. The crystallisation transition was noted to be significantly more subtle that those noticed previously as the sine wave deviations were much less pronounced (see inset Figure 3.12). There also appeared to be a double peak occurring during both the 32 and 31^{o}C increments in the reversing heat capacity signal, suggesting that primary crystallisation may be taking place over both temperature increments. This may be attributable to crystallisation of the lower and higher melting point fractions of the lipid at slightly different temperatures.

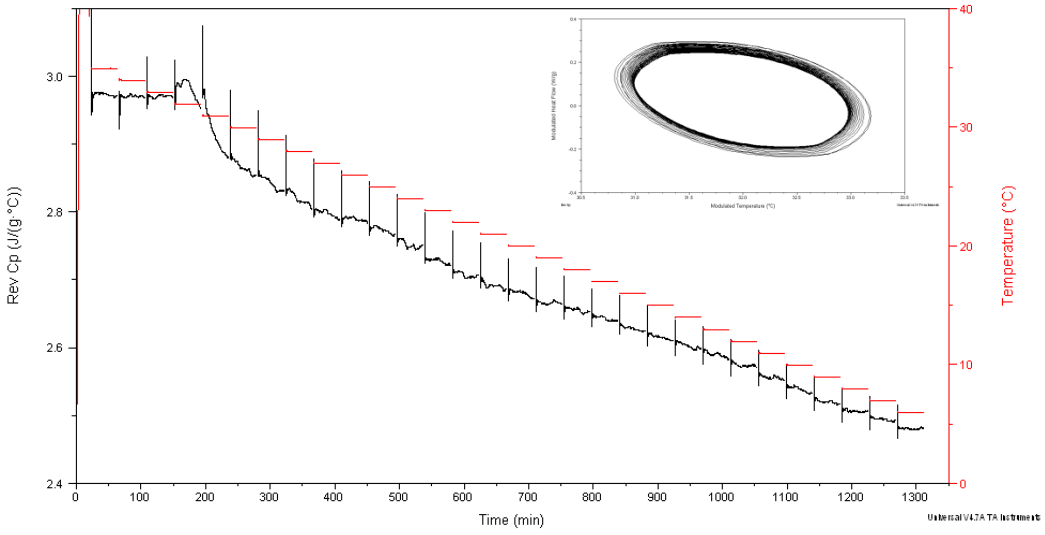

Figure 3.12 *Reversing heat capacity versus time signal for Gelucire 44/14 QIMTDSC 40 minute isotherm on cooling with 1°C increments. Inset: Lissajous plot (modulated heat flow against modulated temperature) of the sine wave heat flow modulations at 32°C.*

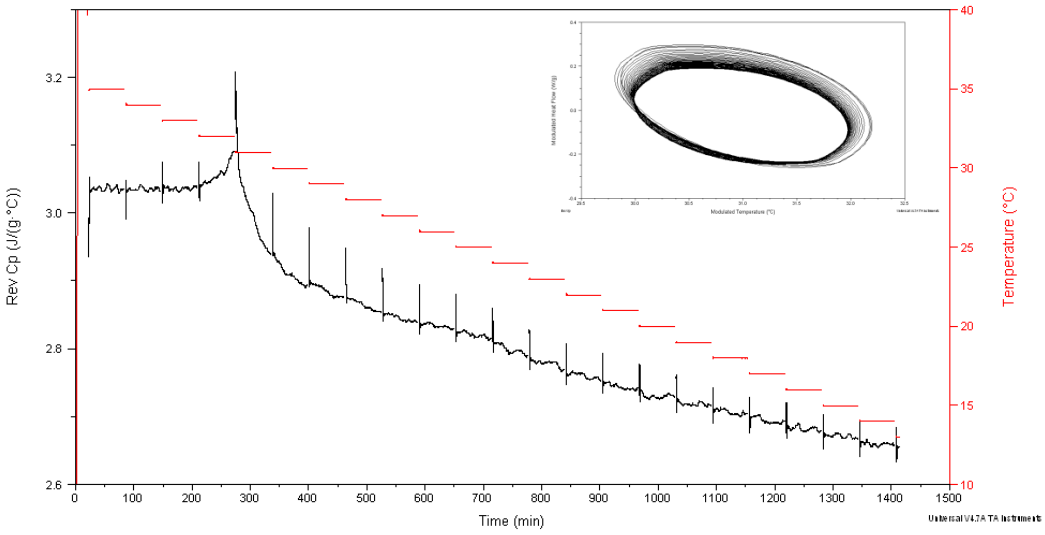

Figure 3.13 *Reversing heat capacity versus time signal for Gelucire 44/14 QIMTDSC 60 minute isotherm on cooling with 1°C increments. Inset: Lissajous plot (modulated heat flow against modulated temperature) of the sine wave heat flow modulations at 31°C. It should be noted that the experiment only ran to the 14°C increment due to instrument inability to store the large data file during collection.*

A similar trend was also demonstrated by the 60 minute isotherm (Figure 3.13). Lissajous analysis displayed primary crystallisation at 31°C, with secondary crystallisation continuing until the conclusion of the experiment in the reversing heat capacity signal.

Method Three involved holding the sample isothermally for 720 minutes (12 hours) at temperatures from 29 to 40°C. Crystallisation was found to occur when held isothermally for 12 hours at 29, 30, 31 and 32°C, above this temperature however, no obvious transition was present in the reversing heat capacity signal over 12 hours (Figure 3.14). The time to $Tc_{(max)}$ was calculated to be 24.91, 50.18, 25.36 and 39.67 minutes at 29, 30, 31 and 32°C respectively.

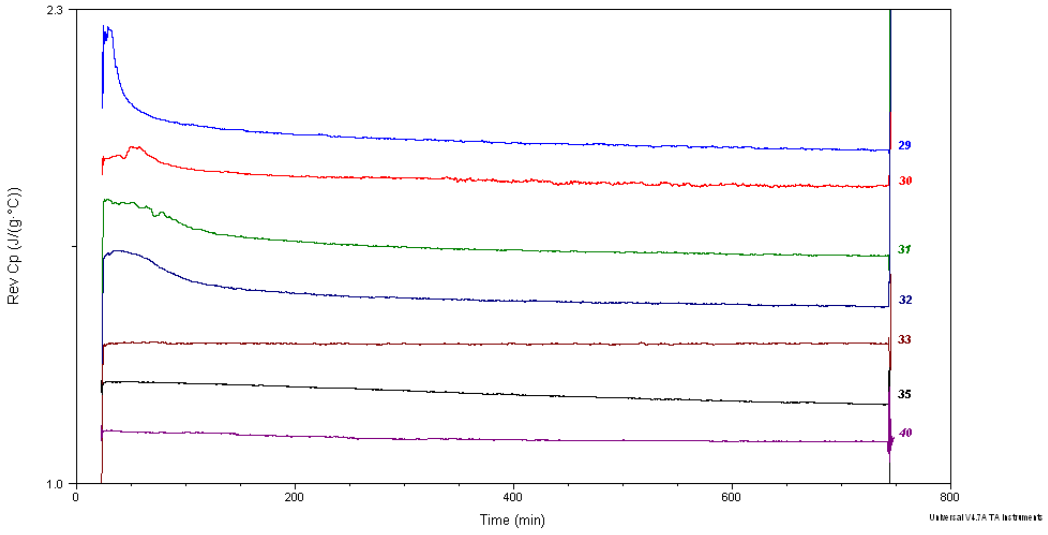

Figure 3.14 *Reversing heat capacity versus time signal for Gelucire 44/14 12 hour QIMTDSC at 29 to 40°C.*

The shape was found to be variable between samples, possibly due to the variable nature of the crystallisation process and the complexity of the sample as described

previously. Broadness, as well as peak smoothness, increased with temperature until 31^{o}C, which was similar to that at 32^{o}C. This effect may be due to the rate at which crystallisation occurs at each individual temperature. The further below the crystallisation temperature the sample is held isothermally, the faster the crystallisation process will be on commencement of QIMTDSC methodology, provided crystallisation did not occur prior to this point whilst cooling with conventional DSC (there was no evidence of this in the presented data).

Method Four extended the isothermal time period Gelucire 44/14 was subjected to at the lowest temperature investigated, 29^{o}C (Figure 3.15). This was to explore the extent of secondary crystallisation, and the time period over which this may occur. Samples were held at 29^{o}C for 48 hours. Primary crystallisation was seen, as expected, at commencement of the experiment at this low temperature. There was also a continuous decrease in the reversing heat capacity signal over the course of the experiment.

The present evidence suggests that Gelucire 44/14 undergoes an initial crystallization followed by a secondary, slower process that may potentially be extremely extensive and hence alter processing or performance characteristics immediately following manufacture into solid oral dosage forms.

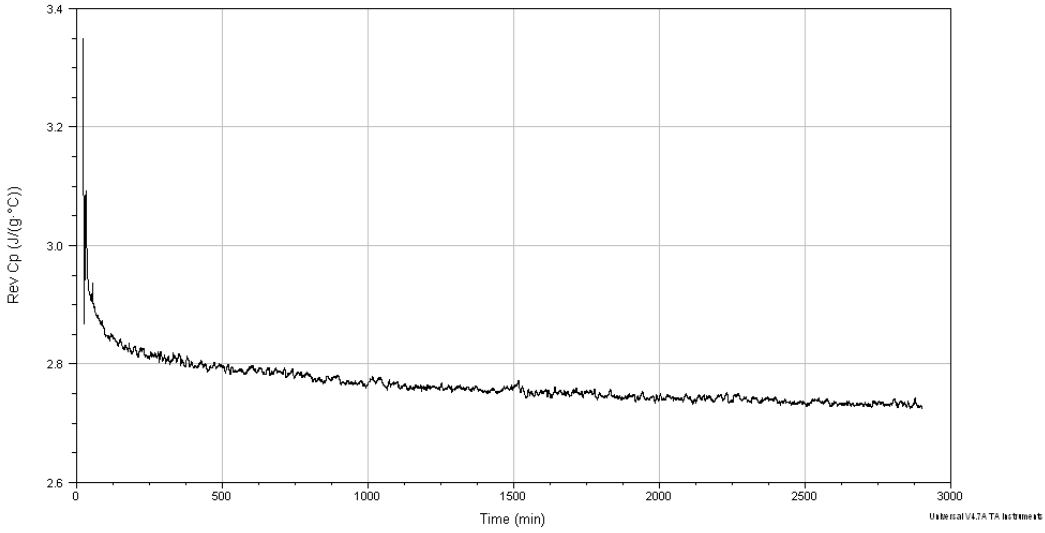

Figure 3.15 *Reversing heat capacity versus time signal for Gelucire 44/14 QIMTDSC over 48 hours at 29°C.*

3.3.3 Observation of Thermal Transitions by Hot Stage Microscopy

HSM was employed to visualise the melting and crystallisation transitions of Gelucire 44/14, previously characterised using conventional and QIMTDSC. Figure 3.16 shows images of these processes. Melting of Gelucire 44/14 appeared to occur over a wide temperature range, beginning at approximately 36°C until completion at 46°C. This follows with the nature of Gelucire 44/14 characterised by the DSC studies Upon cooling, nucleation began at 30°C followed by crystal growth until 28°C. The crystals appeared to be spherulitic and radial in nature, growing outwards in finger-like projections.

On re-heating, melting commenced at 39°C and was completely molten by 46°C. The crystallisation of other Gelucires, investigated by Sutananta (1994b) suggested that

the crystals were formed of complex mixtures of components rather than particular pure components. Comparing this to data obtained from conventional and QIMTDSC, it is apparent that neither melting of the lower melting point fractions, or the extended slow crystallisation of Gelucire 44/14 are visible using HSM. It should however be noted that comparison of HSM and DSC is difficult due to the nature of the thermal transitions in both cases i.e. HSM demonstrates crystal growth in two dimensions however DSC illustrates bulk thermal behaviour and crystal growth in three dimensions.

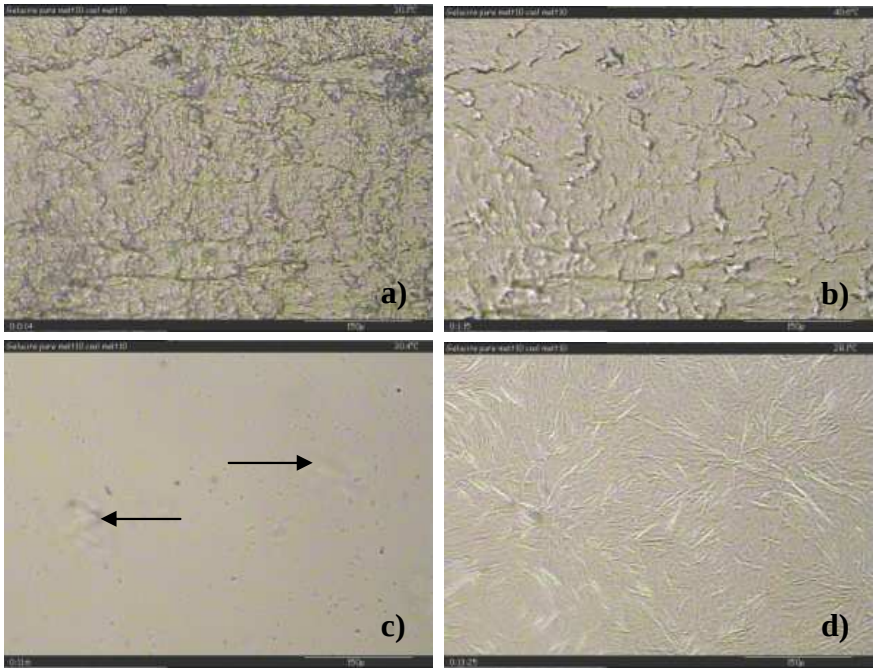

Figure 3.16 *HSM Images of Gelucire 44/14; a) Start; b) Melting at 36.0^{o}C; c) Nucleation on cooling at 30.4^{o}C; d) Crystal Growth end at 28.8^{o}C.*

3.3.4 Hydration Behaviour Analysis using Dynamic Vapour Sorption

Hydration of Gelucire 44/14, as described by Svenssen et al (2004), was outlined in Chapter Two. This section, however, aims to establish the temperature and humidity parameters below which the lipidic carrier will remain stable. This is important for consideration of storage conditions of Gelucire 44/14 formulations. A series of experiments were carried out using dynamic vapour sorption in order to determine the response of the lipidic Gelucire 44/14 to atmospheric temperature and humidity. Samples undergoing all three methods were subjected to a drying period which consisted of 60 minutes at 25^{o}C and 0% RH.

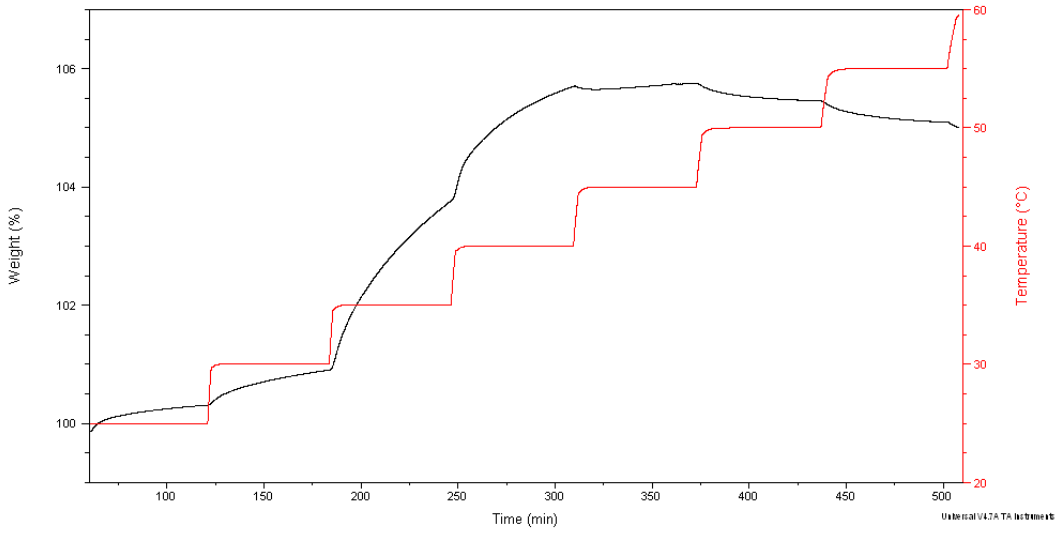

Figure 3.17 *Weight percent versus time signal for Gelucire 44/14 at 75% RH with a temperature ramp from 25 to 55^{o}C.*

Method One held each sample at 75% RH and ramped from 25 to 55^{o}C with 60 minutes at each step. Gelucire 44/14 was found to lose a small amount of water during the drying stage (0.09%, data not shown) suggesting that the lipid contains a

proportion of water (unknown) which can be removed, albeit very slowly, when held at 0% RH. At 75% RH the sample absorbed only small amounts of moisture when held at 25 and 30°C to a total of 0.9% (Figure 3.17). On increasing temperature up to 40°C, larger amounts of moisture were taken up, to a total of 5.7%, with the maximum observed at 35°C (2.5%). At 45°C Gelucire 44/14 could be seen to begin losing this moisture, a loss which continued to the conclusion of the experiment at 55°C. The crystalline lipidic carrier undergoes melting on heating which has been found to peak at 45°C. This suggests that Gelucire 44/14 absorbs the greatest quantity of moisture whilst it is undergoing melting, until it is completely molten, at which point it begins to lose this moisture. In all, this implies that, on storage, Gelucire 44/14 is relatively stable at high RH provided it remains below its melting temperature.

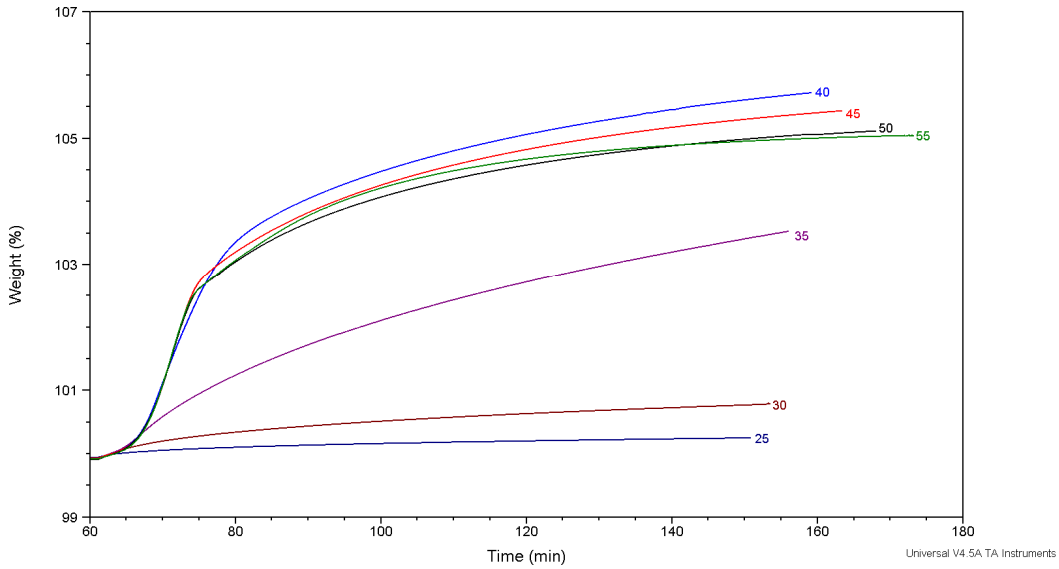

Figure 3.18 *Weight percent versus time signal for Gelucire 44/14 at 75% RH isothermal at 25 to 55°C for 60 minutes.*

Method Two, which involved holding each sample isothermally for 60 minutes at a single temperature from 25 to 55^{o}C at 75% RH, provided similar data to that of *Method One* above, however each sample was held isothermally at one temperature only, the temperatures ranging throughout the melt transition (Figure 3.18).

At 25 and 30^{o}C the lipidic samples appeared only to absorb small amounts of moisture at 75% RH, as observed above. The isotherms also appeared to level out suggesting a maximum was reached. At 35^{o}C, moisture was absorbed steadily over the course of the experiment. Unlike that shown in *Method One*, Gelucire 44/14 could be seen to absorb the greatest weight percentage of moisture at 40^{o}C. This change may possibly be attributable to the amount of water previously taken up. In *Method One*, moisture had already been absorbed due to the 60 minute isotherms at lower temperatures, whereas in *Method Two*, the sample had no previous high RH exposure. At this temperature and above there is, however, a distinct change in the shape of the absorption. After initial increase in RH from 0 to 75% there is a steep increase in moisture uptake to a point which falls at approximately 2.5 to 3.5% weight increase, moisture uptake then begins to slow.

Gelucire 44/14 appeared to absorb the greatest amount of atmospheric moisture at either 35 or 40^{o}C, depending upon the sample history. *Method Three* was chosen to observe moisture uptake with increasing RH from 0 to 90% at 40^{o}C with 60 minutes at each step (Figure 3.19). Gelucire 44/14 was observed to absorb increasing amounts of atmospheric moisture with increasing RH, the maximum weight increase occurring at 90% RH (4%).

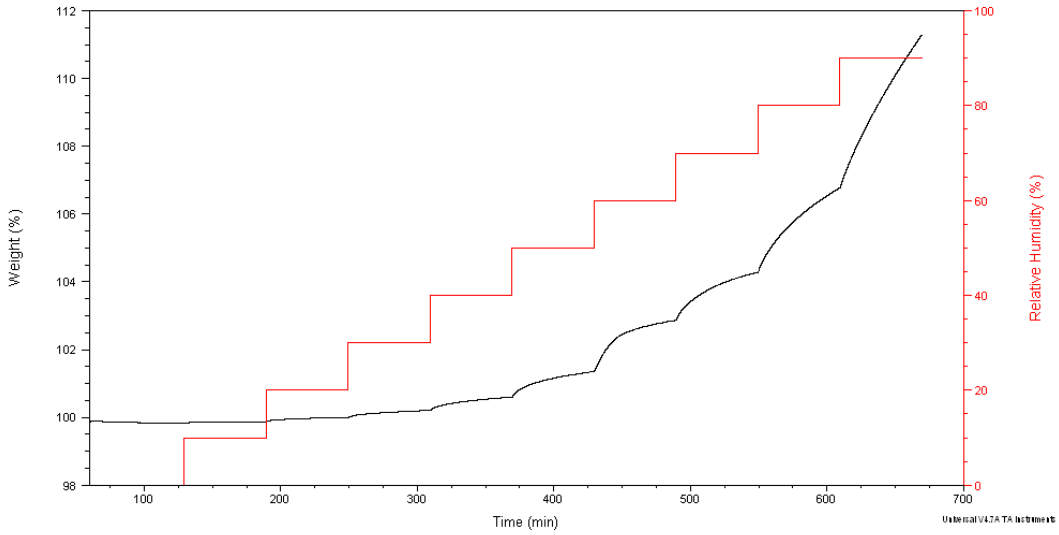

Figure 3.19 *Weight percent versus time signal for Gelucire 44/14 at 40°C with an RH ramp from 0 to 90%.*

As shown by Svensson et al (2004), the hydration process of Gelucire 44/14 appears to be equivalent to the sum of the hydrations of all of the individual components. Upon exposure to increasing RH, Svensson demonstrated that at low RH, free glycerol absorbs large amounts of atmospheric moisture. This remains relatively insignificant due to the low Gelucire 44/14 content of glycerol (approximately 3%), thus allowing it to stay below the recommended limit of 1% w/w moisture uptake as specified by the European Pharmacopoeia. As part of their investigation, it was suggested that up to 70% RH (at room temperature) a 2% weight increase in the Gelucire 44/14 sample could be attributed solely to the absorption of moisture by free glycerol. In this case, however, when conducted at 40^{o}C, over double the amount of moisture is absorbed by this point. The Gelucire 44/14 sample, at this temperature will be almost completely molten, suggesting that in this state, the affinity of Gelucire 44/14 for atmospheric moisture is significantly greater than at room temperature. This will be attributable to the completely disordered nature of the

Gelucire 44/14 molecules, increasing its reactivity and therefore its capacity to absorb atmospheric moisture. Above 70% RH, PEG is known to begin absorbing moisture, and at 80% and above, PEG esters contribute to the total weight increase observed over the course of the experiment (Svensson et al. 2004).

3.3.5 Summary of Gelucire 44/14 Characterisation Studies

This section has attempted to characterise the physicochemical properties of the lipid Gelucire 44/14 using a number of different techniques. Thermal analytical methods have confirmed thermal transitions which occur during heating and cooling. On heating, a clear double melting endotherm is observed, the $Tm_{(onset)}$ of which were found to be 28.3°C ± 0.3 and 39.9°C ± 0.1. Above the melting temperature, an exotherm can be noticed at onset 144.14°C ± 0.2 which may be attributable to decomposition.

On cooling, crystallisation of Gelucire 44/14 can be observed. This transition is found to be greatly dependent upon the rate at which cooling occurs, the $Tc_{(onset)}$ reducing from 28.8°C ± 0.9 cooling at 0.5°C/minute, to 20.0°C ± 2.3 at 20°C/minute. It should be noted that cooling at rates above 2°C/minute demonstrates incomplete crystallisation by the time room temperature is reached which must be taken into account when considering the manufacturing parameters of pharmaceutical formulations. Re-melting of Gelucire 44/14 demonstrates an alteration in the shape of the characteristic double melting endotherm. This altered shape was found to be maintained on heating and cooling thereafter. After aging at room temperature, however, the shape appears to regress back to that of the original. This may be

attributable to the formation of different polymorphs of the Gelucire 44/14 components, for example PEG, which are unstable and quickly convert back to the most stable form.

QIMTDSC is a novel method in the characterisation of crystallisation. Gelucire 44/14 was found to display a crystallisation temperature of 31^{o}C, without the influence of heating rate using Lissajous analysis. The crystallisation was found to occur over only a single temperature increment, despite melting of the lipid demonstrating two fractions with different melting points. Examination of the reversing heat capacity time plot suggested that after an initial energetic primary crystallisation, the lipid undergoes a slower, more extended period of crystallisation which continues to much lower temperatures than previously expected. HSM allowed the visualisation of the fundamental thermal transitions observed using conventional and QIMTDSC.

DVS studies suggested that Gelucire 44/14 has a great capacity to absorb atmospheric moisture at high temperatures and relative humidities due to its many different components. On storage it appears that below 35^{o}C and 40% RH, the moisture content of Gelucire 44/14 remains below the limit set by the European Pharmacopoeia of 1% weight increase. It has however been shown that at ambient temperature, Gelucire 44/14 absorbs only limited moisture below 70% RH (2% weight increase).

3.4 TPGS

3.4.1 Assessment of Thermal Properties using Conventional Differential Scanning Calorimetry

Conventional DSC is used in this section to characterise TPGS thermal properties i.e. melting, and also crystallisation at varying rates of cooling.

3.4.1.1 Melting

Upon heating, the melting endotherm of TPGS was found to consist of two distinct peaks, the first generally being the most prominent (Figure 3.20). The sizes of these peaks were found to vary between samples. The $Tm_{(onset)}$ was observed to occur reproducibly at 34.79^{o}C ± 0.07, the $Tm_{(max)}$ being dependent upon which of the two peaks was most dominant ($Tm_{(max)}$ 37.29°C ± 0.2; ΔH 101.1 J/g ± 0.5).

No published evidence of the presence of this double melting peak has been found in the literature to date, with evidence only of a single melt endotherm. It does however, in this case, suggest the incidence of two separate chemical or physical (crystal) forms of the lipidic carrier being present at varying degrees from sample to sample.

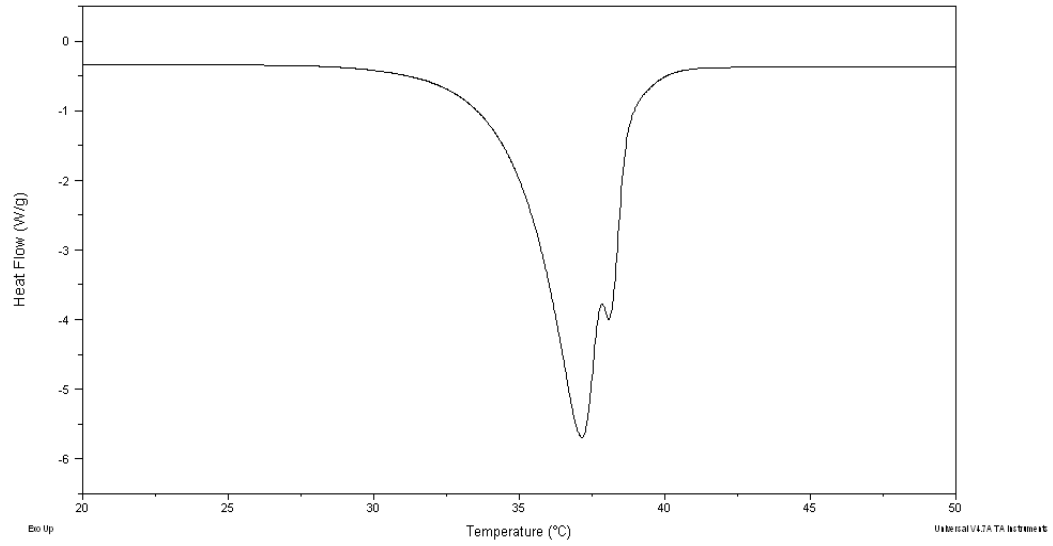

Figure 3.20 *Heat flow against temperature signal of TPGS on heating at 10°C/minute.*

Data collected internally at AstraZeneca, investigating the molecular weight distribution of TPGS, found evidence of both low and high molecular weight tocopheryl tails present in the sample. Both mono and di substituted PEG 1000 chains with tocopheryl succinate groups were identified, which may be responsible for the observed double melting endotherms (Meehan et al. 2007). Double melt endotherms could also be attributable to poor contact between sample and DSC pan. Due to the hard waxy nature of TPGS at room temperature it is possible that movement during heating could bring about the appearance of two melt transitions. This possibility of this effect could be eliminated by temperature cycling which is investigated later in the Chapter.

3.4.1.2 Crystallisation

The crystallisation exotherm of TPGS can be observed as a single peak occurring upon cooling. Crystallisation is highly dependent upon the rate at which the sample is cooled. The temperature of the transition, therefore, can be seen to reduce on cooling from $Tc_{(onset)}$ 31.9°C ± 0.6 ($Tc_{(max)}$ 30.4°C ± 0.4; ΔH 96.9 J/g ± 2.1) at 0.5°C/minute to $Tc_{(onset)}$ 23.9°C ± 0.3 ($Tc_{(max)}$ 22.7°C ± 0.2; ΔH 97.5 J/g ± 0.8) at 20°C/minute.

Figure 3.21 demonstrates that on cooling at elevated rates i.e. 20°C/minute and to some extent 10°C/minute, the lipidic carrier may not have reached complete crystallisation by the time it has reached room temperature. This will have implications on the manufacturing process of SSD systems and also the physicochemical properties of the final product.

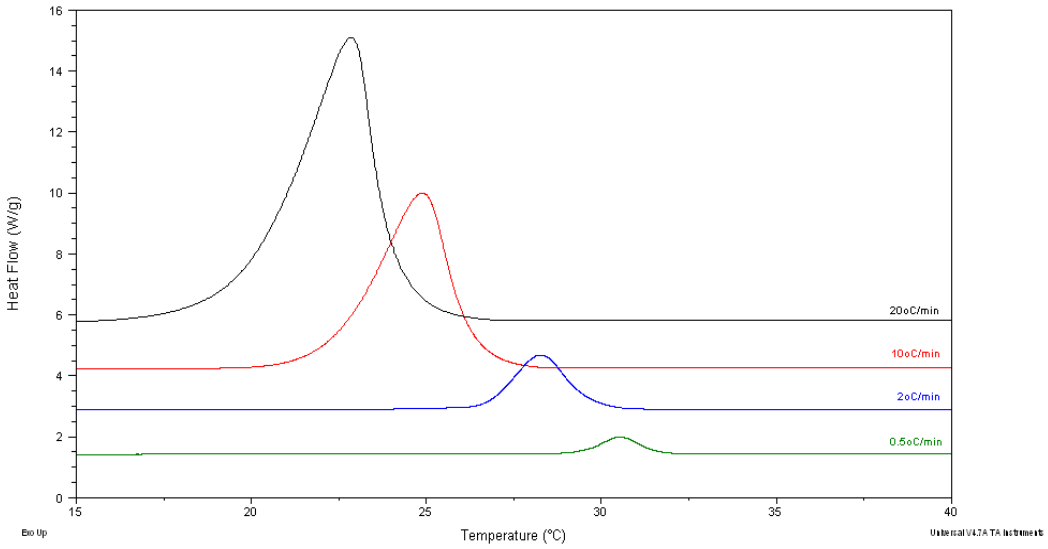

Figure 3.21 *Heat flow against temperature signal of TPGS crystallisation at varying rates after melting at 10°C/minute.*

Crystallisation of TPGS was found not to be greatly dependent upon the thermal history of the carrier. A similar trend to that shown above was also noted after melting at varying rates (data not shown), with the $Tc_{(onset)}$ and $Tc_{(max)}$ coinciding accurately.

Solid Fat Content Calculation

The amount of TPGS present in the solid state at any point during crystallisation was determined by calculating the area under the crystallisation exotherm on cooling at each $1^{o}C$ increment throughout the transition and plotting this as percentage of the total solid, against temperature (Figure 3.22).

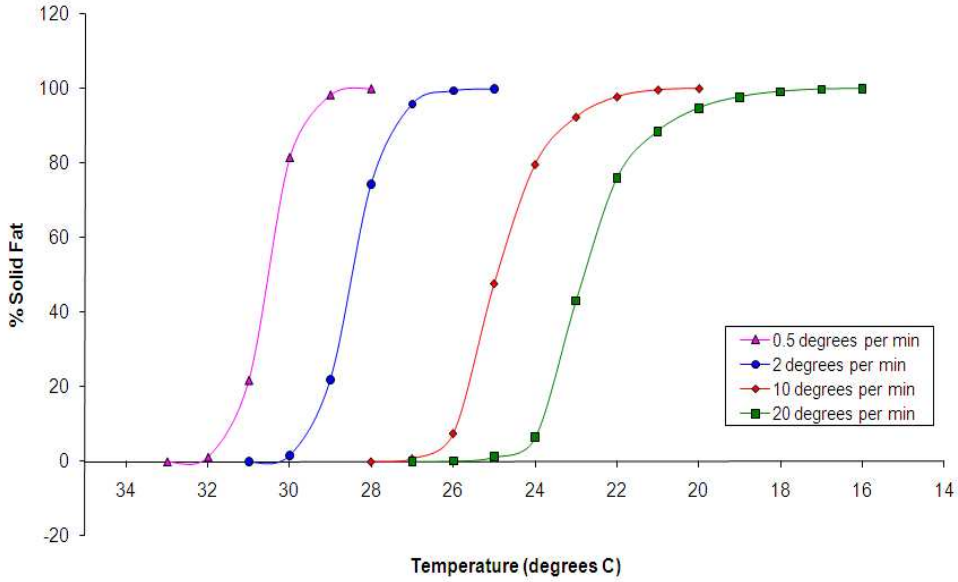

Figure 3.22 *Percentage solid fat of TPGS during crystallisation versus temperature on cooling at varying rates.*

The temperature at which crystallisation occurs decreased notably with increased rate of cooling since it is a kinetic process. The range of temperature over which crystallisation occurred however did not appear to be greatly affected by the change in cooling rate. A much broader exotherm would be expected due to the increased transfer of energy per unit time associated with increasing rates. This effect may be attributable to the fact that TPGS is a much purer lipid in comparison to Gelucire 44/14.

In order to observe and compare the rate at which crystallisation occurred, the solid fat data was plotted as a fraction against time (Figure 3.23). This illustrated, as expected, that the rate of progression of crystallisation was considerably quicker for those higher cooling rates.

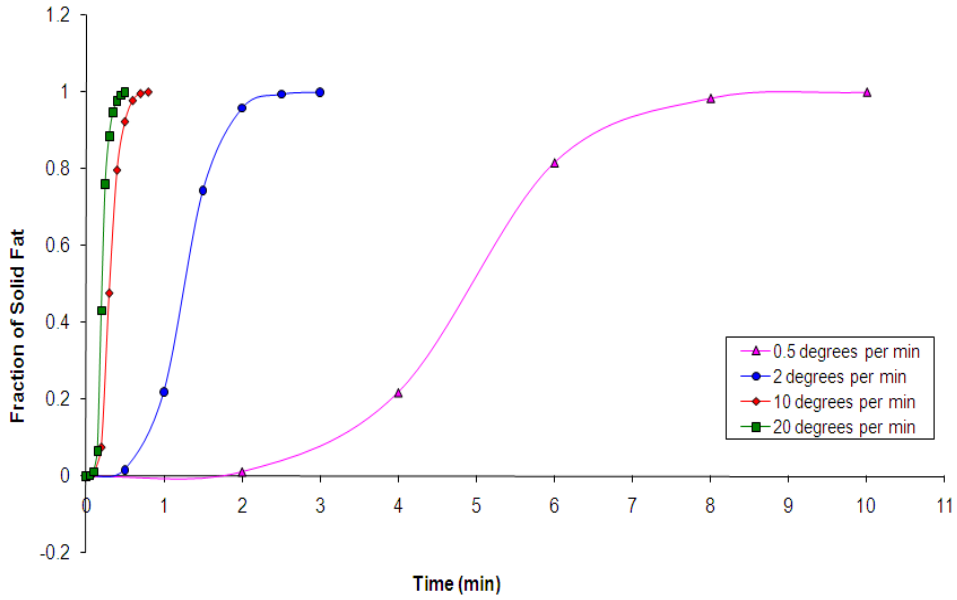

Figure 3.23 *Fraction of solid fat of TPGS during crystallisation versus time on cooling at varying rates.*

The data in Figure 3.23 fitted well with the Avrami model, with R^2 values between 0.9921 and 0.9991. Modelling allowed calculation of the *n* parameter as an indication of the time dependence of nucleation and also the dimensionality of the crystal growth (Table 3.2). All cooling rates demonstrated an *n* value of 4 (to the nearest integer) corresponding with heterogeneous nucleation and spherulitic growth from sporadic nuclei. It also indicated that the rate of crystallisation was constant and independent of time. The value of the crystallisation rate constant, *k*, sharply increased with cooling rate attributable to the subsequent increased driving force for the reaction.

Table 3.2 *Avrami modelling parameters for the solid fat data of TPGS.*

Cooling Rate (^oC/minute)	*n*	*k* (min^{-n})	R^2
0.5	4	0.0012	0.9967
2	4	0.26	0.9991
10	3.52	40.24	0.9951
20	4	327.52	0.9921

3.4.1.3 Temperature Cycling

Upon re-heating after the first crystallisation, the $Tm_{(onset)}$ fell accurately at 35.1^{o}C ± 0.04 ($Tm_{(max)}$ 37.0°C ± 0.1; ΔH 102.1 J/g ± 0.4) in comparison to that of the first melting transition at 34.79^{o}C ± 0.07 ($Tm_{(max)}$ 37.29°C ± 0.2; ΔH 101.1 J/g ± 0.5) suggesting no significant alteration to the thermal kinetics of TPGS (Figure 3.24).

The shape of the peak, however, did not accurately follow that of the first. The double peaks remained, but the ratio and distribution of these peaks altered after heating and cooling.

The presence of double peaks on second melting suggests that this is not attributable to sample movement or poor contact with the DSC pan, as suggested previously, as this would have been resolved after first heating. It does however imply that two separate forms of the lipid may be present, as suggested by Meehan et al (2007), in the existence of both mono and di substituted PEG 1000 chains with tocopheryl succinate groups. The process of heating may bring about conversion of one form to another causing a shift in the peak distribution. This could be investigated using other techniques such as IR or Raman Spectroscopy; however this was outside the scope of this project.

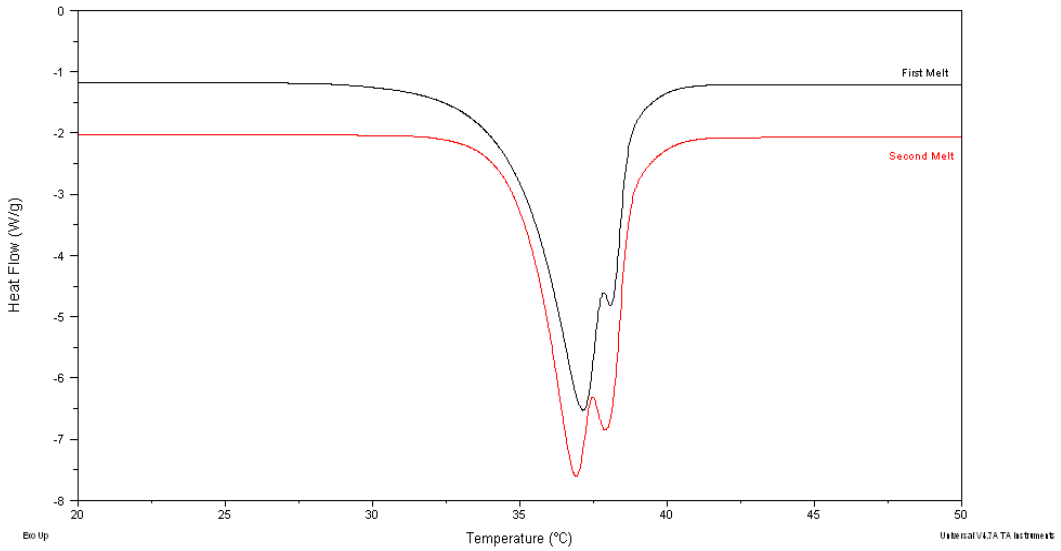

Figure 3.24 *Heat flow against temperature signal of TPGS on first heating and also second heating at 10°C/minute after cooling at 10°C/minute.*

3.4.1.4 Continuity throughout the Container

The continuity of TPGS throughout the container was investigated using conventional DSC to illustrate the reproducibility of its thermal properties. Samples taken from the top, middle and bottom of the container were found to demonstrate good continuity, with the melting endotherm $Tm_{(onset)}$ occurring at 34.5°C, being reproducible to within ± 0.3 standard deviations ($Tm_{(max)}$ 37.6°C ± 0.2; ΔH 103.0 J/g ± 1.7). Crystallisation was found to occur at 26.6°C ± 0.5 ($Tc_{(max)}$ 25.2°C ± 0.5; ΔH 101.1 J/g ± 1.9).

3.4.2 Crystallisation Analysis using Quasi-Isothermal Modulated Temperature Differential Scanning Calorimetry

The crystallisation transition of TPGS was further characterised using QIMTDSC. Samples were analysed using *Method Two,* cooling throughout crystallisation at 1°C increments, in order to establish the true Tc. When held isothermally for 20 minutes at each increment, Lissajous analysis of the acquired data suggested crystallisation at 33°C by deviation of the isolated sine wave modulations from the steady state (see Figure 3.25 inset). The shape of the ellipses were also observed to change in shape, demonstrating a corresponding change in the latent heat of the sample, which also confirmed that a thermal transition may be occurring. The reversing heat capacity versus time plot (Figure 3.25), however, demonstrated an increase beginning at 33°C, peaking at 31°C and continuing to decrease until the completion of the experiment at 5°C.

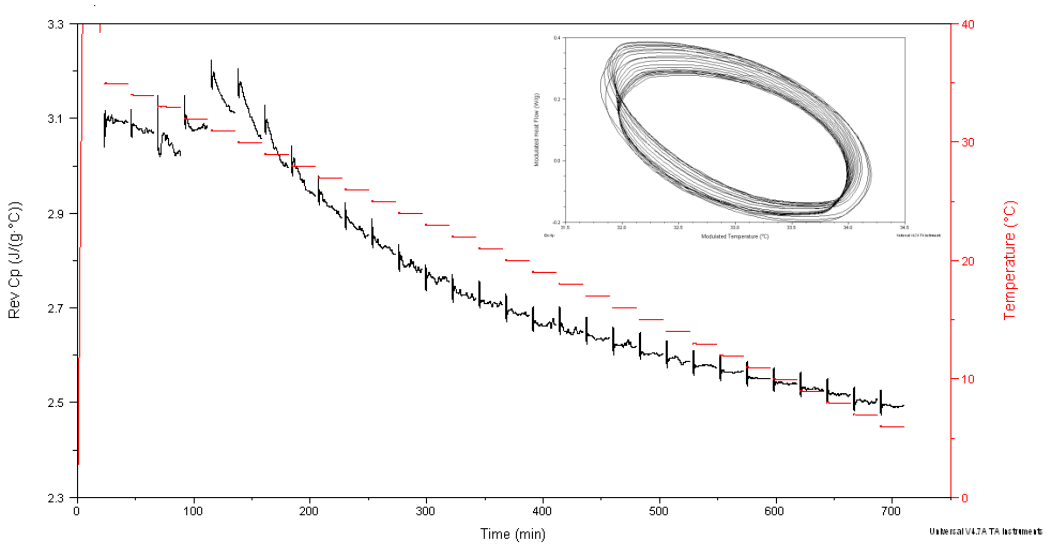

Figure 3.25 *Reversing heat capacity versus time signal for TPGS QIMTDSC 20 minute isotherm on cooling with 1°C increments. Inset: Lissajous plot (modulated heat flow against modulated temperature) of the sine wave heat flow modulations at 33°C.*

This decrease in heat capacity, as seen with Gelucire 44/14, suggests that the crystallisation transition consists of an initial or primary energetic phase, followed by a secondary slower, more extended phase, continuing to much lower temperatures than previously expected. This is demonstrated in Figure 3.26 where the major slope of the sine wave ellipses can be seen to decrease, suggesting a decrease in the heat capacity of the sample over the course of the experiment. This will have implications on the physicochemical properties of the final formulation. On cooling to room temperature during manufacture, it is possible that TPGS may not be present in its fully crystalline form.

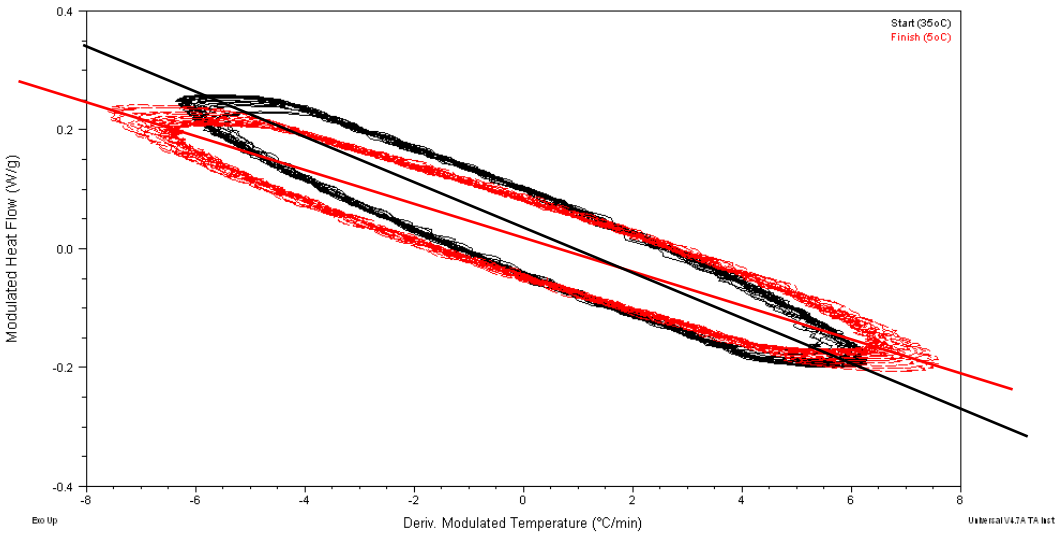

Figure 3.26 *Lissajous figures of the sine wave heat flow modulations of TPGS at the start (35°C, black) and finish (5°C, red) of the cooling experiment showing the major slope of each plot.*

When held for 40 minutes at each 1°C increment, Lissajous analysis indicated an increased level of sine wave deviation during the 33°C increment in accordance with the 20 minutes isotherm data shown above. The reversing heat capacity time plot demonstrated two energetic crystallisations, peaking at 35 and 32°C (Figure 3.27). This may be attributable to the possible presence of two crystal forms of the lipid relating to mono and di substituted PEG 1000 chains with tocopheryl succinate groups, this was not observed, however, using conventional DSC. The reversing heat capacity was also seen to decrease over time with reducing temperature suggesting continuation of the crystallisation transition.

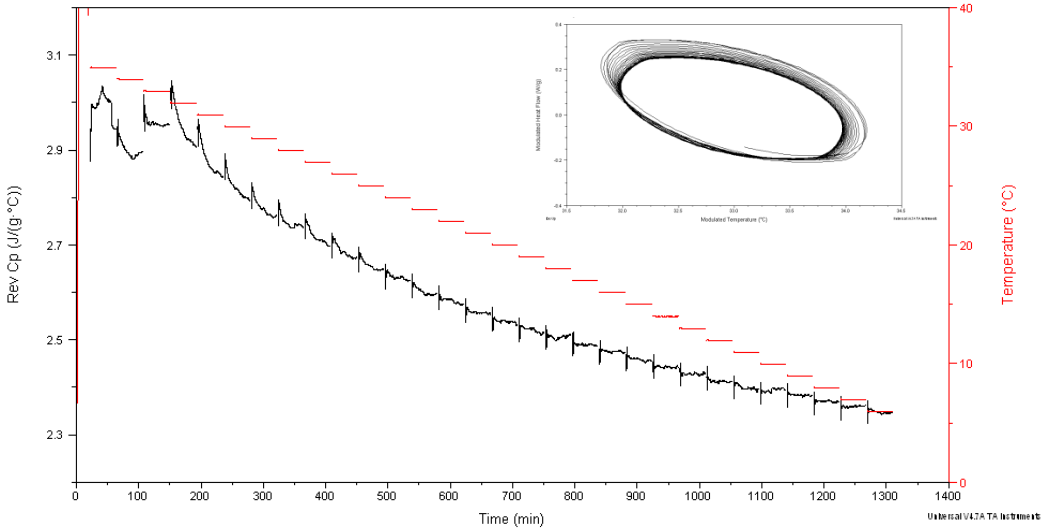

Figure 3.27 *Reversing heat capacity versus time signal for TPGS QIMTDSC 40 minute isotherm on cooling with 1°C increments. Inset: Lissajous plot (modulated heat flow against modulated temperature) of the sine wave heat flow modulations at 33°C.*

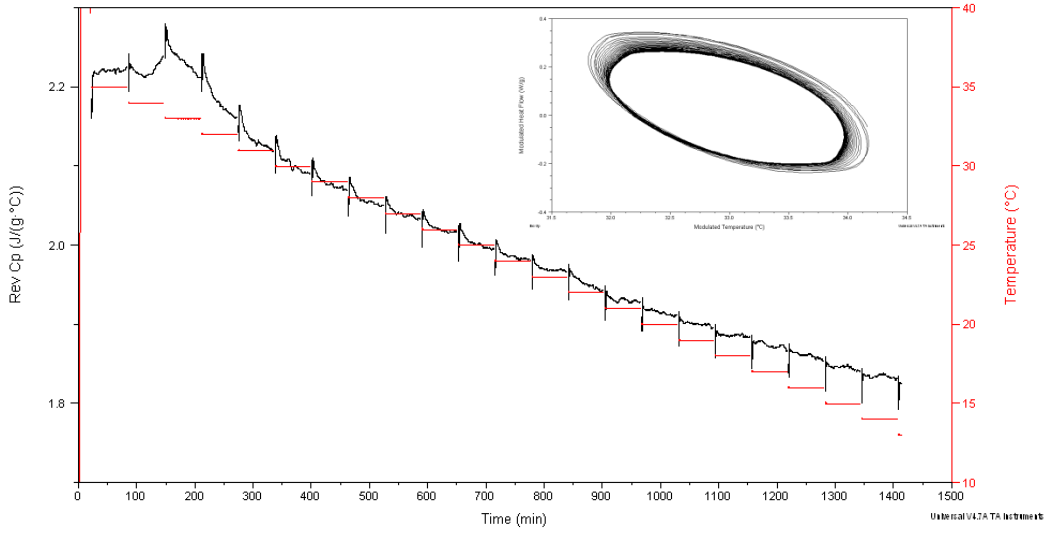

Figure 3.28 *Reversing heat capacity versus time signal for TPGS QIMTDSC 60 minute isotherm on cooling with 1°C increments. Inset: Lissajous plot (modulated heat flow against modulated temperature) of the sine wave heat flow modulations at 33°C. It should be noted that the experiment only ran to the 14°C increment due to instrument inability to store the large data file during collection.*

With an isotherm of 60 minutes at each increment, crystallisation was found to occur at 33^{o}C using Lissajous analysis, as above. The reversing heat capacity also demonstrated a peak at this temperature (Figure 3.28).

Lissajous analysis of all TPGS QIMTDSC data gave an indication that the true crystallisation temperature of the lipid, minus the effect of heating rate, may lie at 33^{o}C.

3.4.3 Observation of Thermal Transitions by Hot Stage Microscopy

Melting and crystallisation of TPGS was further characterised using HSM. Figure 3.29 demonstrates images of the lipid during heating and cooling. Melting appeared to begin at 34.3^{o}C, being completely molten by 40.6^{o}C. Nucleation became visible at 31^{o}C on cooling, with crystal growth continuing until 28.5^{o}C. Growth of the crystals were seen to be very spherulitic in nature with defined edges, unlike the more sporadic finger-like projections observed for Gelucire 44/14. On re-heating, melting appeared at 35.2^{o}C until 40.4^{o}C. The visible $Tm_{(onset)}$ followed closely with that demonstrated using conventional DSC (34.79^{o}C ± 0.07) however the biphasic melting endotherm could not be detected using this method. It should be noted that the relationship of crystallisation observed using this technique with other methods such as DSC is difficult due to the two dimensional nature of crystal growth. DSC analysis gives crystals the opportunity to grow in three dimensions and therefore cannot be directly compared.

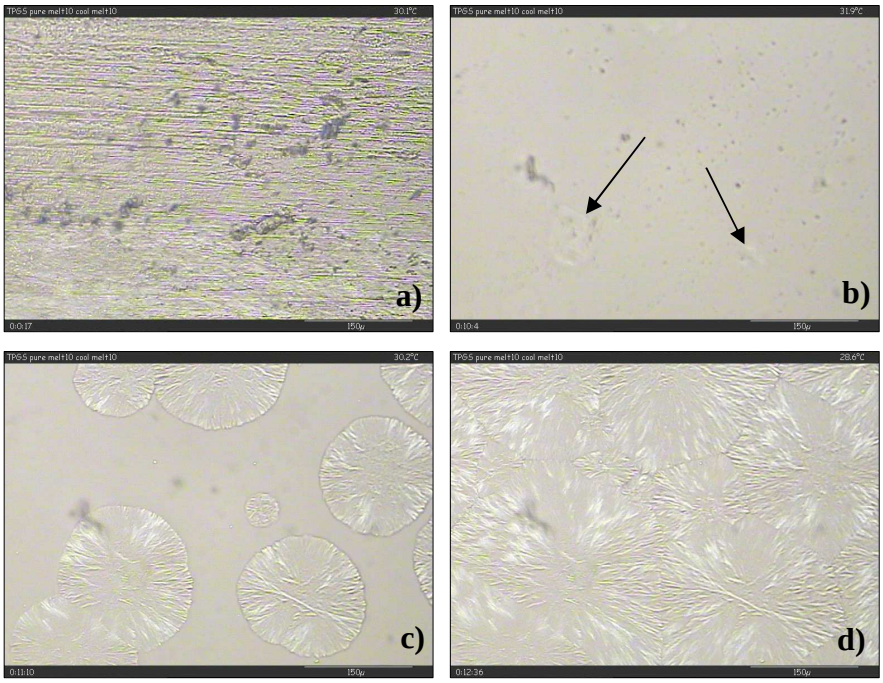

Figure 3.29 *HSM images of TPGS: a) Start; b) Nucleation on cooling at 31.0°C; c) Crystal growth and d) Crystal Growth end at28.5°C.*

3.4.4 Summary of TPGS Characterisation Studies

Characterisation of the lipidic carrier TPGS is essential in order to predict the physicochemical properties of the final formulation when combined with drug as part of an SSD system. Thermal analysis techniques discovered the melting of TPGS to occur at 34.79°C ± 0.07 on heating. The transition was however found to consist of two distinct peaks, which may be attributable to the presence of both mono and di-substituted PEG chains (Meehan et al. 2007). Crystallisation of the lipid was observed on cooling, which was highly dependent upon the rate at which this took place. The $Tc_{(onset)}$ was found to reduce in temperature from 31.9°C ± 0.6 at 0.5°C/minute to 23.9°C ± 0.3 at 20°C/minute. On temperature cycling of TPGS, the

$Tm_{(onset)}$ was found to be reproducible however the distribution of the double peaks appeared to shift.

QIMTDSC analysis of TPGS crystallisation suggested that the transition occurred at 33^{o}C when isolated using Lissajous plots. The decrease in reversing heat capacity over time observed in all cases, however, suggested that crystallisation continued until the conclusion of the experiment at 5^{o}C, to much lower temperatures than previously anticipated.

3.5 CONCLUSIONS

Characterisation of the physicochemical properties of excipients is essential before progressing to the investigation of formulations incorporating active model drugs. These properties can and will have impact on the properties of this final product, and full characterisation can therefore allow prediction of its behaviour.

The studies carried out in this chapter have demonstrated a number of issues which should be taken into consideration when deciding upon manufacturing parameters of the final formulation. These include:

1) Unexpected properties such as the alteration of the Gelucire 44/14 melting endotherm upon temperature cycling and also the double peak max of the TPGS melting endotherm suggests that further investigation into the chemical composition may be required in order to fully characterise the systems.

2) The rate at which the lipids are cooled appeared to impact greatly on the physical state at room temperature. Cooling at slower rates was found to promote a more complete crystallisation unlike faster rates which were found to create larger and broader crystallisation exotherms, being complete by much lower temperatures.

3) Crystallisation of both lipids, independent of cooling rate, was also found to continue to lower temperatures than expected. This could result in crystallisation / solidification of the formulated SSD system being incomplete at room temperature.

CHAPTER FOUR

CHARACTERISATION OF SEMI-SOLID DISPERSION SYSTEMS

4.1 INTRODUCTION

Active pharmaceuticals present in semi-solid dispersion systems can exist as crystalline or amorphous particles, as a molecular dispersion or as a mixture. The physical state of the SSD is dependent upon a number of factors: the physicochemical properties of both the drug and the carrier, the interaction between the two components and also the method of formulation (Janssens and Van den Mooter 2009). This being the case, the release properties of drug from these formulations is subsequently determined by these factors. The understanding of how drugs are dispersed within and throughout SSD formulations is therefore a major priority within the field. In this study, SSD systems were formulated using the melt method, more specifically only the lipidic carrier was molten during mixing, at a temperature below the melting point of the model drug. For this reason it is the likely situation that the drug is either dispersed as solid crystalline particles, or as a molecular dispersion i.e. solid solution, dependent upon the solubility of the drug within the carrier.

Care must be taken during the investigation and characterisation of SSD formulations using thermoanalytical methods. An investigation carried out by Lloyd et al (1997) into binary mixes and also SSD formulations of paracetamol and PEG 4000 demonstrated that the melting behaviour of these systems was highly dependent upon the heating rate employed. They noted that crystalline drug dispersed within the SSD formulations had the potential to dissolve into the molten carrier during heating. The drug was therefore observed to demonstrate broad low temperature melting endotherms, if any at all. This was attributed to the dissolution of paracetamol into

the molten PEG over a wide range of temperatures, thus broadening the peak, in some cases to such an extent that it could not be distinguished from the baseline. At slow rates the drug appeared to have time to dissolve into the molten carrier during analysis, thus reducing or eliminating the drug melting peak. At faster rates of heating the paracetamol melting endotherm became apparent, attributable to the drug having less time to dissolve. Taking this into account, misinterpretation of DSC data has the propensity to lead to inaccurate estimation of drug solubility within the carrier and incorrect identification of solid solutions.

This effect was also investigated by Gramaglia et al (2005). They highlighted that heating rates as low as 10^{o}C/minute allow time for the drug crystal molecules to detach from the lattice in response to the input of energy, thus dissolving into the molten carrier. This has the effect of increasing the apparent drug solubility within the carrier material, attributable to the increased temperature. Heating at faster rates does not prevent the sample responding to the input of energy, however increasing the rate of heating to the order of 100-500^{o}C/minute does allow the inhibition of kinetically controlled processes such as dissolution of the drug into the carrier, thereby allowing for a more accurate estimation of the true solubility.

In a paper published by Qi et al (2010b), the authors propose a novel mathematical model suggesting a method by which the concentration dependence of drug crystallinity in hot-melt extruded SSD preparations can be interpreted in terms of the miscibility of the drug with the carrier material. Upon heating, it is suggested that the ΔH of the drug melting endotherm is composed of two simultaneously occurring processes; crystalline drug melting, as well as drug dissolution into the molten

carrier. It is also suggested that depending upon the drug loading, different processes may manifest on heating. At low drug concentrations, below the saturation solubility in the carrier, drug dissolution into the carrier may take place. At high proportionate drug loadings, carrier dissolution into the drug will dominate. Between these extremes of concentration, both drug dissolution into the carrier, and carrier dissolution into the drug may take place simultaneously. With this in mind, plotting the drug melting ΔH from physical mixes of the two components against the solid weight content of the drug in the mix, a profile of these three phases can be observed (Figure 4.1).

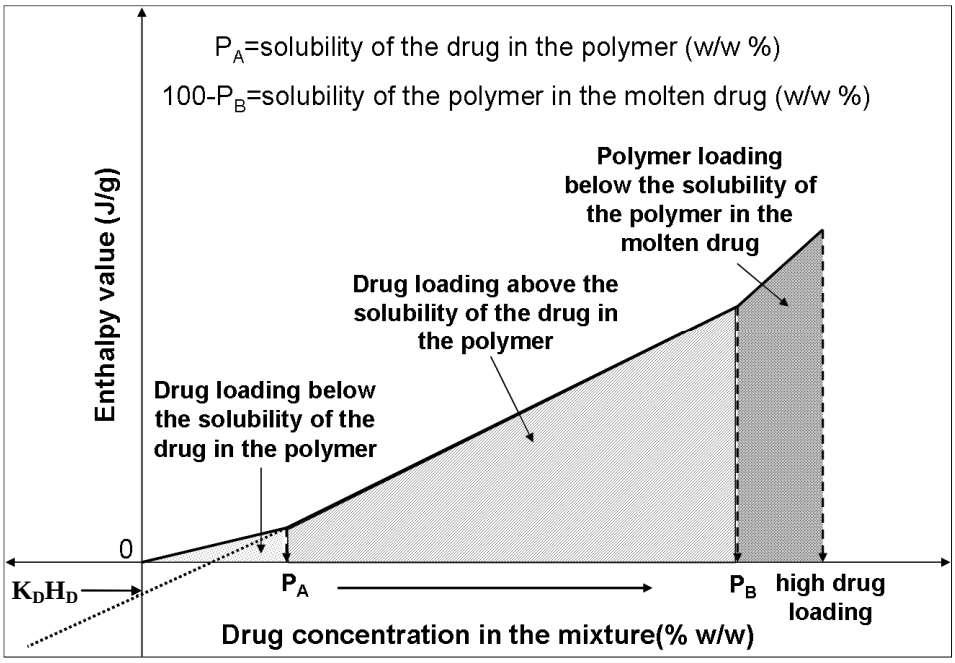

Figure 4.1 *Illustration of the enthalpy-drug concentration plot for the range of drug-polymer mixes (Qi et al. 2010b).*

The processes occurring at low drug loading (Phase 1) can be represented by:

$$\frac{H_t}{(M_D+M_P)} = X_D\left(H_f + H_D\right) \qquad \textbf{\textit{Equation 4.1}}$$

where H_t is the total amount of heat change of the exothermic peak, M_D is the mass of drug dissolved in the carrier, M_P is the mass of the polymer, X_D is the weight fraction of the drug in the whole mixture, H_f is the heat of fusion of the drug and H_D is the heat of dissolution of drug in the carrier (thought to be exothermic).

The intermediate phase of drug concentration is represented by:

$$\frac{H_t}{(M_D+M_P)} = X_D\left(H_f - K_D H_D + K_P H_P\right) + K_D H_D \qquad \textbf{\textit{Equation 4.2}}$$

where K_D is the solubility of the drug in the carrier, K_P is the solubility of the carrier in the molten drug and H_P the enthalpy of dissolution of the carrier into the molten drug.

High drug loading (Phase 2) is thought to obey the following:

$$\frac{H_t}{(M_D+M_P)} = X_D\left(H_f - H_P\right) + H_P \qquad \textbf{\textit{Equation 4.3}}$$

The solubility of the drug in the carrier (K_D) and the solubility of the carrier in the drug (K_P) can be further defined (as mass ratios) by:

$$K_D = \frac{M_{D1}}{M_{P1}} \qquad \textit{Equation 4.4}$$

$$K_P = \frac{M_{P2}}{M_{D2}} \qquad \textit{Equation 4.5}$$

where 1 and 2 are used to denote the Phase.

The solubility of the drug in the polymer is thought to be at the point whereby the Phase 1 and intermediate regions join, denoted by P_A in Figure 4.1, with carrier solubility in the molten drug being at point P_B where the intermediate and Phase 2 regions intersect.

From the literature, it is apparent that SSD systems are capable of enhancing the dissolution properties of poorly soluble drugs. The poor uptake of this technology onto the market is in part due to the lack of understanding of the mechanisms by which these systems work, with the current knowledge being relatively limited. The primary objective of this Chapter was therefore to form a greater understanding of the compatibility of the chosen model drugs with the lipidic carrier when formulated into SSD systems. This can be further defined as:

a) Characterisation of the model SSD systems using conventional DSC and comparison to that of the lipidic carrier alone.

b) Development of a method to more accurately estimate solubility of the model drug within the carrier of the SSD systems using fast heating rates.

c) Investigation of the effect of drug on the crystallisation process of the lipidic carrier.

d) Visualisation of the formulated SSD systems using HSM to investigate drug distribution and phase separation.

It was decided at this point to confine all subsequent SSD formulations to those including Gelucire 44/14, due to the possibility of further production of TPGS being terminated. The following results therefore only include SSD formulations of poorly soluble model drug with Gelucire 44/14.

4.2 METHODOLOGY

4.2.1 Conventional Differential Scanning Calorimetry

Conventional DSC experiments were performed under a nitrogen environment, with a purge rate of 50ml/minute. Calibration of the instrument was conducted, prior to experimentation which involved cell resistance and capacitance (baseline) calibrations with an empty cell and sapphire disks (Tzero calibration), cell constant calibrations using indium standard (melting point 156.6°C, heat of fusion 28.6J/g), and finally temperature calibrations using benzoic acid (melting point 122.4°C) and n-octadecane (melting point 28.2°C). Temperature calibrations were carried out at the same rate as intended for sample analysis. Samples for analysis, in the weight

range 2 to 2.5mg, were taken either directly from the container or formulated into physical mixes or SSD systems, the preparation of which has been outlined in Chapter Two, then prepared into Tzero aluminium pans.

All conventional DSC experiments were conducted at 10^{o}C/minute, heating throughout the melting transition; to 60^{o}C for Gelucire 44/14, 100^{o}C for ibuprofen alone and its formulations, 200^{o}C for indometacin alone and its formulations, and 220^{o}C for piroxicam alone and its formulations. All SSD samples, after initial melting, were cooled to -30^{o}C before being heated through the melt for a second time. Experiments were repeated up to four times.

4.2.2 Hyper (Fast Speed) Differential Scanning Calorimetry

Hyper DSC experiments were performed under a helium environment, with a purge rate of 20ml/minute. Calibration of the instrument was conducted using indium and tin standards. Samples for analysis, taken directly from the original container or formulated as outlined in Chapter Two, were prepared into 40µl aluminium pin holed pans in the weight range 2 to 2.5mg. All experiments were carried out in triplicate at 500^{o}C/minute from -50^{o}C to 150^{o}C for Gelucire 44/14 alone, to 200^{o}C for ibuprofen alone and its formulations, to 250^{o}C for indometacin alone and its formulations, to 260^{o}C for piroxicam and 300^{o}C for the formulations of piroxicam.

4.2.3 Quasi-Isothermal Modulated Temperature Differential Scanning Calorimetry

Quasi-isothermal MTDSC experiments were performed under a nitrogen environment at a purge rate of 50ml/minute. Calibration of the instrument was conducted prior to experimentation, as per conventional DSC. An additional calibration using aluminium oxide was also carried out in order to calibrate for the required QIMTDSC method, determining the total and reversing heat capacity constants. Samples with the approximate weight of 2mg were prepared into Tzero aluminium pans.

Samples were heated to either 100^{o}C for ibuprofen SSD systems, 200^{o}C for indometacin and 220^{o}C for piroxicam at 10^{o}C/minute. They were then cooled to 25^{o}C, at which point QIMTDSC was initiated in 1^{o}C increments to 0^{o}C, with an isotherm of 20 minutes, an amplitude of ±1^{o}C and a period of 60 seconds.

4.2.4 Hot Stage Microscopy

Samples for analysis were applied to glass microscope slides and enclosed with a glass cover slip. Samples were heated from room temperature through the melt transitions of both the lipidic carrier and the model drug at 10^{o}C/minute. Capture was terminated on visualisation of complete melting. Images were captured at x20 magnification under polarised light.

4.3 IBUPROFEN AND GELUCIRE 44/14 SEMI-SOLID DISPERSION SYSTEMS

In this section, formulations of the lipidic carrier Gelucire 44/14 with the model drug ibuprofen, a BSC Class II drug, were investigated, with the aim being to characterise, using thermal analysis techniques, the physical properties of their SSD systems as a whole and any subsequent interactions resulting from their combination.

4.3.1 Assessment of Thermal Properties using Conventional Differential Scanning Calorimetry

4.3.1.1 Analysis of Raw Materials

The melt of the lipidic carrier Gelucire 44/14 can be observed as a characteristic and reproducible double endotherm displaying a $Tm_{(onset)}$ at 28.3°C ± 0.3 and a $Tm_{(max)}$ at 45.0°C ± 0.07 (see Chapter Three, Section 3.3.1.1). The melting transition of the model drug, ibuprofen, can be observed to occur reproducibly at $Tm_{(onset)}$ 74.8°C ± 0.05, and $Tm_{(max)}$ 76.4°C ± 0.07 (Figure 4.2), complying well with data presented in the literature (British Pharmacopoeia 2010; Moneghini 2008).

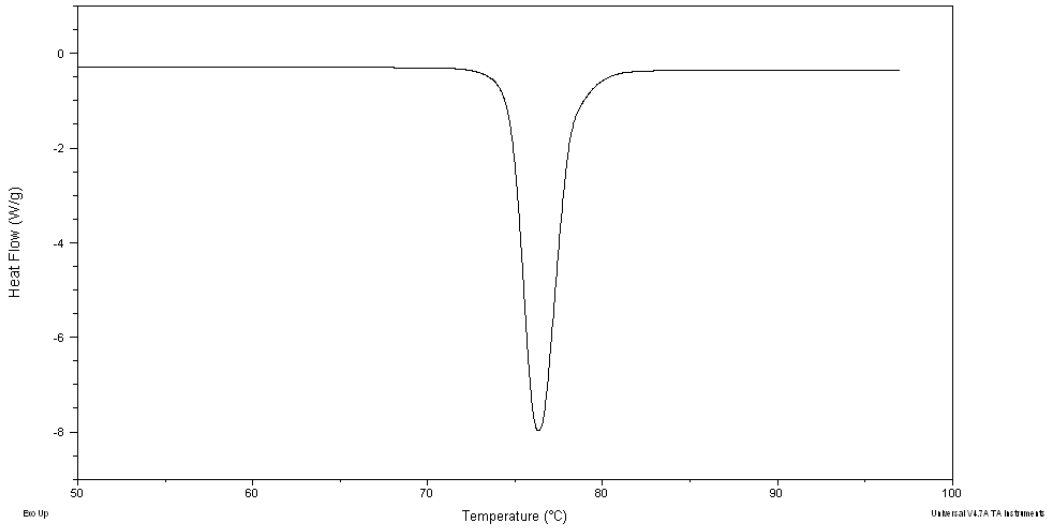

Figure 4.2 *Heat flow against temperature signal of the ibuprofen melting endotherm on heating at 10°C/minute.*

4.3.1.2 Analysis of Physical Mixes

The melt transitions of ibuprofen and Gelucire 44/14, as a physical mix, were analysed using conventional DSC, the purpose being to characterise combinations of the two compounds prior to formulation. The drug melt ΔH data from the physical mix DSC traces also served as a calibration plot, allowing calculation of the amount of crystalline drug remaining in the final SSD formulation. This is outlined in section 4.3.3.

The characteristic double Gelucire 44/14 melting peak was observed, occurring reproducibly at $Tm_{(onset)}$ 26°C and $Tm_{(max)}$ 44°C for all drug loadings, 5 to 50% w/w (Figure 4.3). This confirmed the absence of any interaction between the two components at this point.

On increasing the temperature, an ibuprofen melt endotherm would be expected in all samples, which was indeed the case (highlighted in Figure 4.3), with the exception of 5% w/w. Absence of the drug melting peak at 5% suggests one of two things. That the crystalline ibuprofen present is completely dissolving into the lipidic Gelucire 44/14 during analysis, therefore leaving no crystalline particles for melting point detection by DSC; or that the ibuprofen melting peak is undetectable in this case due to its small mass in the mix.

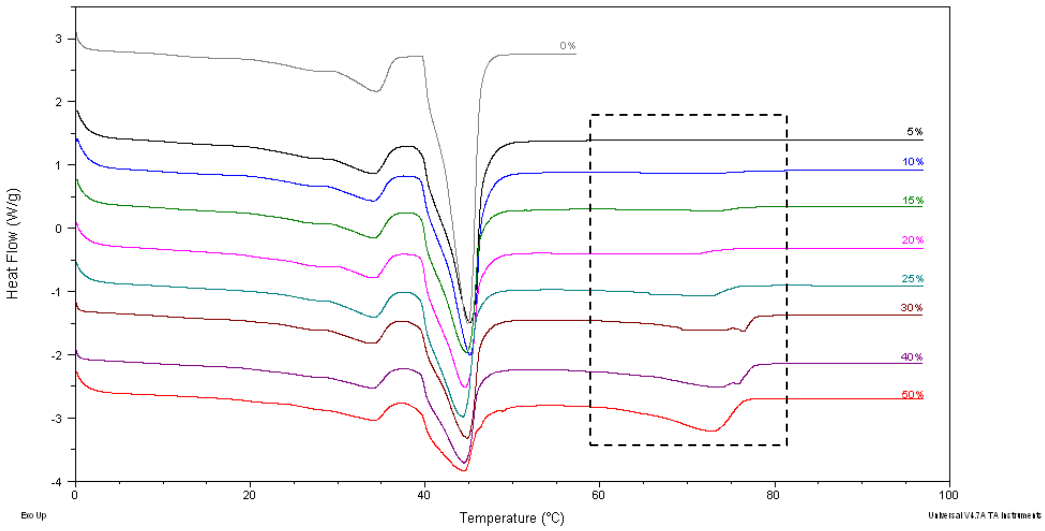

Figure 4.3 *Heat flow against temperature signal of ibuprofen and Gelucire 44/14 physical mixes on heating at 10°C/minute.*

The detected ibuprofen melting endotherms were measured above 70°C. The transition increased in size and ΔH with increasing drug loading. Taking into consideration the absence of an ibuprofen melt in the 5% w/w physical mix, and the possibility of drug dissolution into the lipid during analysis, the crystalline ibuprofen seen to melt in the higher loading samples may thus only be accountable for that

remaining after an amount of dissolution into Gelucire 44/14, given time to occur during the slow heating rate.

The $Tm_{(onset)}$ and $Tm_{(max)}$ of the ibuprofen melt transitions were observed to vary in temperature, in the range of 8^oC and 5^oC respectively, from one drug loading to another. Upon analysis of SSD systems using DSC, a shift in the melting peak of either component, or a change in the ΔH value of the transition, can indicate an interaction between the SSD components (Abdul-Fattah and Bhargava 2002). This observed change in $Tm_{(onset)}$ and $Tm_{(max)}$ may therefore suggest an interaction of some kind between the remaining crystalline ibuprofen and the molten Gelucire 44/14 during analysis.

Gelucire 44/14 has the capacity to facilitate hydrogen bonding interactions, attributable to its many components i.e. PEG 1500, PEG 1500 fatty acid esters (mono- and di-), glycerides (mono-, di- and tri-) and free glycerol, in particular the presence of PEG (Barakat 2006). The ibuprofen molecule contains one hydrogen donor group and two hydrogen acceptor groups, suggesting that the two components may be capable of forming a large number of hydrogen bonds with each other during analysis (Knox et al. 2011). The calculated ΔH values of the repeated samples were also found to vary in size between repeats which may be caused by variations in the amount of dissolution able to occur during analysis.

In the cases where an ibuprofen melting transition was present, the peak was very broad in nature, with the $Tm_{(onset)}$ being reduced from that of the drug alone (74.8^oC) by up to 12°C. This suggests that the melting peak may comprise drug melting

energy, plus that of its dissolution into the lipid. This effect was also noted by Lloyd et al (1997) who attributed it to the dissolution of drug into the molten carrier over a wide range of temperatures.

4.3.1.3 Analysis of Semi-Solid Dispersion Systems

Upon heating of the ibuprofen and Gelucire 44/14 SSD systems, the characteristic Gelucire 44/14 double melting peak was observed, with the exception of 50% w/w drug loading, in both formulations i.e. those cooled at 20^{o}C (SSD(20)) and at 4^{o}C (SSD(4)) (Figure 4.4). In comparing this melt with that of the lipid alone (0%) or the physical mixes, there is little variation in either the $Tm_{(onset)}$ or $Tm_{(max)}$ of the secondary endotherm however there is an obvious reduction in temperature of the primary $Tm_{(max)}$. The primary melting peak also appears to reduce in ΔH with increasing drug loading. This may be attributable to decreasing lipid mass, however the secondary melting peak does not reduce in proportion, suggesting it may be caused by interaction between iburofen and the higher melting point fractions of the Gelucire 44/14. Chambin et al (2004) also observed a depression in temperature of the Gelucire 44/14 primary melting endotherm when formulated into an SSD with ketoprofen. It was suggested that this was brought about by solubilisation of the drug into Gelucire 44/14 when in the molten state. This was backed up by X-ray diffraction analysis which showed the disappearance of the crystalline ketoprofen peaks when in the SSD formulation.

At 50% w/w, the primary Gelucire 44/14 melting peak is completely absent in both systems, with the secondary peak being shifted to a lower temperature. It is also

possible that the primary peak Tm may have reduced to an extent to which it is incorporated into that of the secondary or possibly that it is sufficiently small that it is hidden by that of the ibuprofen melting endotherm. With either being the case, it indicates an interaction with the high concentration of ibuprofen not previously detected with lower concentrations.

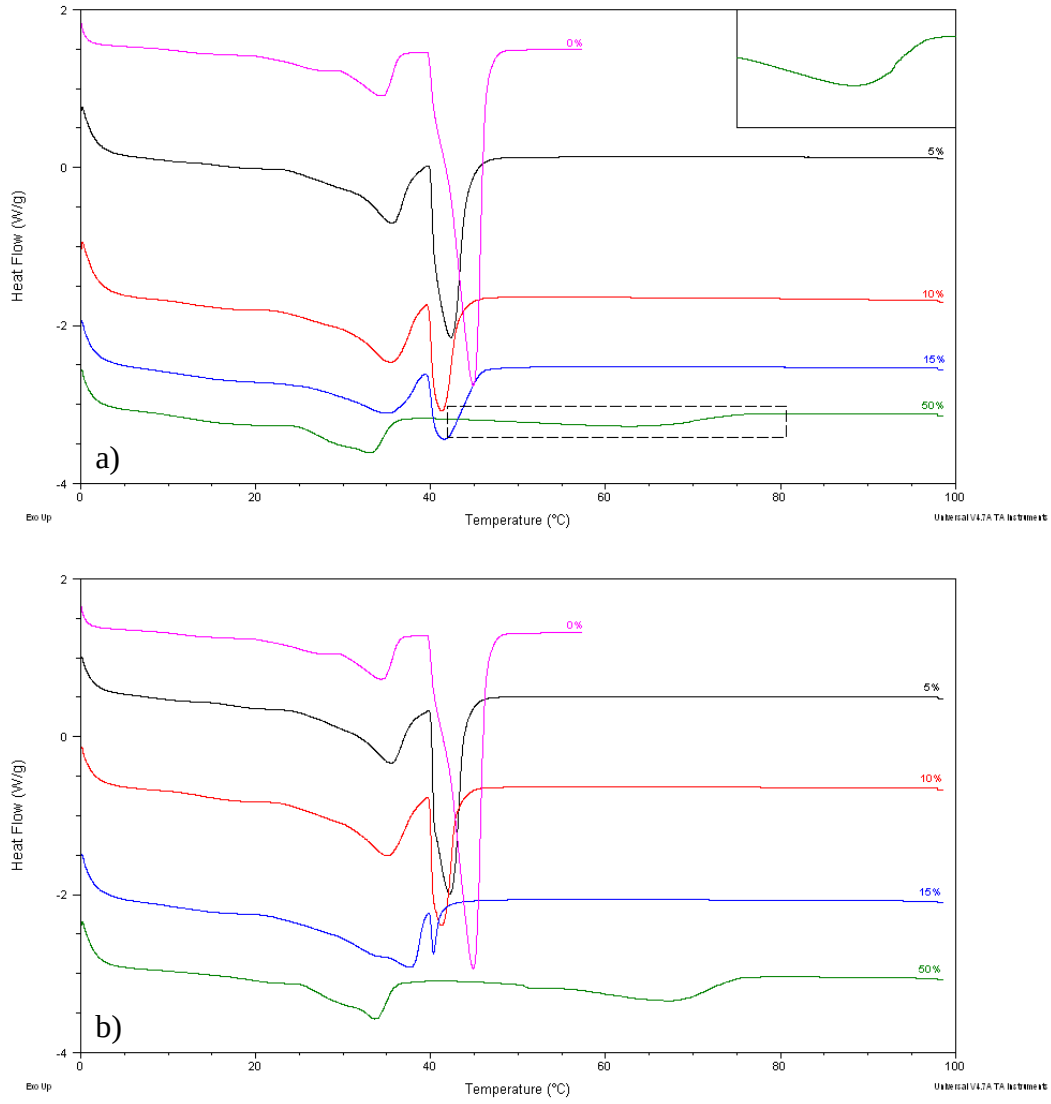

Figure 4.4 *Heat flow against temperature signal on heating at 10°C/minute of ibuprofen and Gelucire 44/14 a) SSD(20) and b) SSD(4) – First melt.*

No detectable ibuprofen melt was observed in the 5, 10 or 15% w/w SSD(20) systems. This was also observed by Chambin et al (2004), and in combination with XRD studies, they concluded that the SSD system existed as a solid solution. In this case the data suggested either the presence of a solid solution, with the ibuprofen completely dissolving into the lipid during formulation, or that any remaining crystalline drug dissolved during analysis at the slow heating rate, as suggested by Qi et al (2010b) and demonstrated by the physical mix study. This was investigated in more detail using HSM and Hyper DSC later in the Chapter. At this point however it indicated, when compared to the physical mix analysis (with the exception of the 5% system which did not demonstrate a drug melt), that a degree of ibuprofen solubilisation into Gelucire 44/14 occurred during formulation. If this had not been the case, an ibuprofen melt transition would have been detected.

An ibuprofen melting transition was observed at 50% w/w in both the SSD(20) and SSD(4) systems, occurring at $Tm_{(onset)}$ 42.8^{o}C ± 1.3 and $Tm_{(max)}$ 64.0^{o}C ± 1.0; $Tm_{(onset)}$ 56.2^{o}C ± 6.5 and $Tm_{(max)}$ 68.2^{o}C ± 2.4 respectively. This was significantly broader and lower in temperature than that seen for the drug alone, which displayed a sharp peak at $Tm_{(onset)}$ 74.8^{o}C and $Tm_{(max)}$ 76.4°C. This broad peak may be a combination of melting of the Gelucire 44/14 higher melting point fractions, and also that of ibuprofen. It must be considered that, once the Gelucire 44/14 lower melting point fractions become molten, the solid higher melting fractions begin to melt, as well as the crystalline ibuprofen in the formulation beginning to dissolve, with these two processes possibly occurring simultaneously. The endothermic peak may therefore represent both events. At this high drug loading, lipid dissolution into the drug may also be occurring, which may account for the changes seen in the Gelucire

44/14 melt transition. In the SSD(4) system, a larger ibuprofen melting endotherm was detected with an ΔH of 29.2 J/g ± 2.5 in relation to that of 17.5 J/g ± 3.4 for 50% SSD(20). This suggests the presence of a greater concentration of crystalline ibuprofen which may be affected by rate of cooling of the formulation.

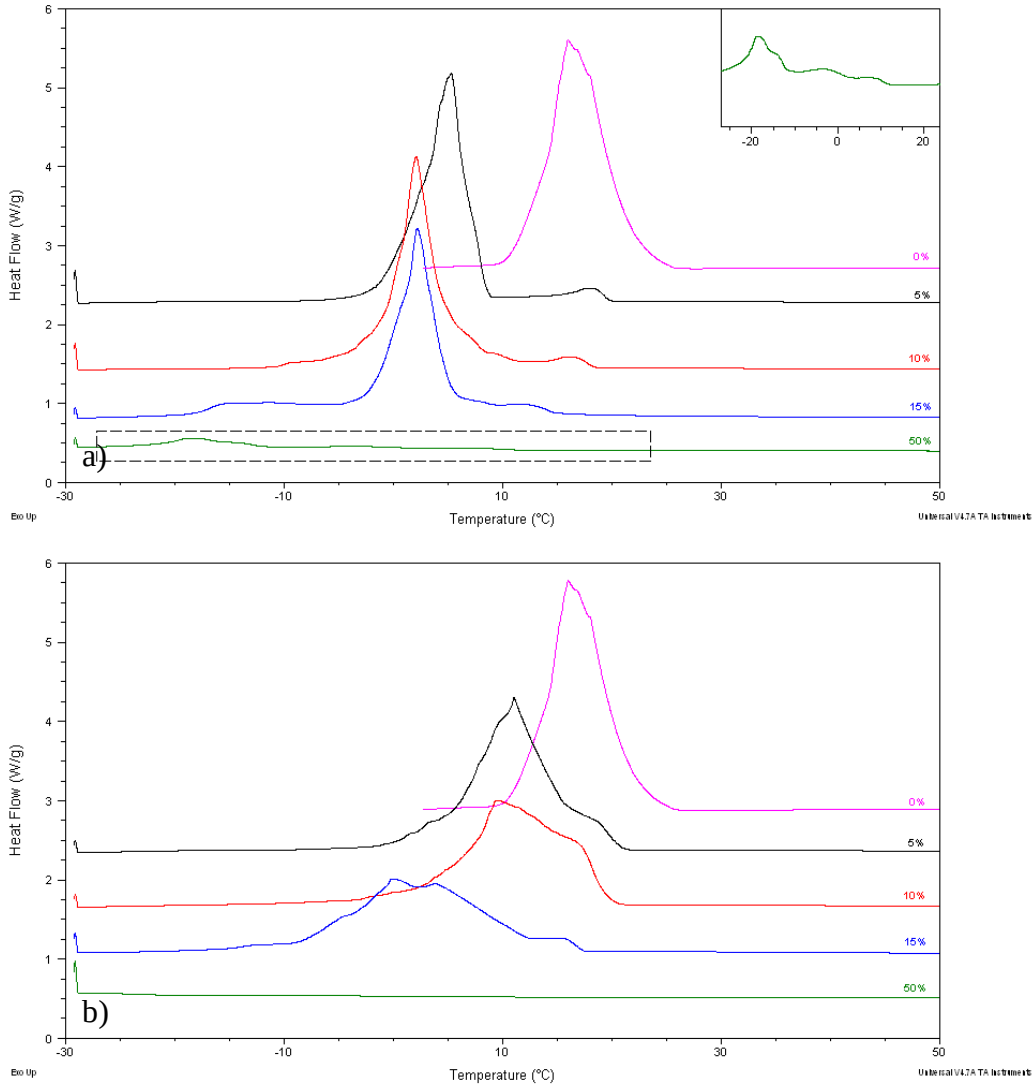

Figure 4.5 *Heat flow against temperature signal on heating at 10°C/minute of ibuprofen and Gelucire 44/14 a) SSD(20) and b) SSD(4) – Crystallisation.*

Crystallisation was seen to occur upon cooling and representative plots are displayed in Figure 4.5. The crystallisation transition in all cases was found to vary in shape

between repeated samples of each system, however the $Tc_{(onset)}$ and $Tc_{(end)}$ of the transitions were comparable. This was likely to be due to the complex nature of the process and also the complexity of the lipid-drug system itself. In the main, however, the 5, 10 and 15% w/w samples demonstrated similar peak shapes, a main peak with a leading shoulder which decreased in size and temperature with increasing drug loading. The different peak shapes observed during crystallisation illustrated the presence of different crystal formations, created via interaction between Gelucire 44/14 and molecularly dispersed ibuprofen.

In comparison of the SSD(20) and SSD(4) systems, the crystallisation ΔH values of each drug loading corresponded closely with each other, however there were significant differences in the shape of the exotherm. The faster cooled systems demonstrated much broader peaks than those of the slower cooled systems, therefore losing resolution between the primary peak and the leading shoulder. Both however could still be well defined. This suggested that crystal growth was a slower process, occurring to the same extent but over a wider temperature range.

The temperature of the leading shoulder appeared to correspond well with crystallisation of Gelucire 44/14 alone (Figure 4.5, 0%). Lloyd et al (1997) suggested that a bimodal crystallisation peak observed in PEG 4000 was attributable to the formation of two different crystalline forms. Taking this into account it may be possible that, in this case, the observed primary crystallisation peak may be due to a new crystal entity. This exotherm, and also its decrease in $Tc_{(max)}$, which can be seen to further decrease in temperature with increasing drug, may be due to dissolved drug acting as a diluent and subsequently reducing nuclei concentration, thereby

decreasing crystallinity of the sample (Long et al. 1995). Following this, at 50% w/w, there is little to no obvious crystallisation occurring, particularly for the SSD(4) system. An additional peak began to appear at approximately -10°C in the SSD(20) systems which increased in size with increasing drug loading; most prominent in the 15 and 50% w/w systems. This also suggested the formation of an additional crystal species.

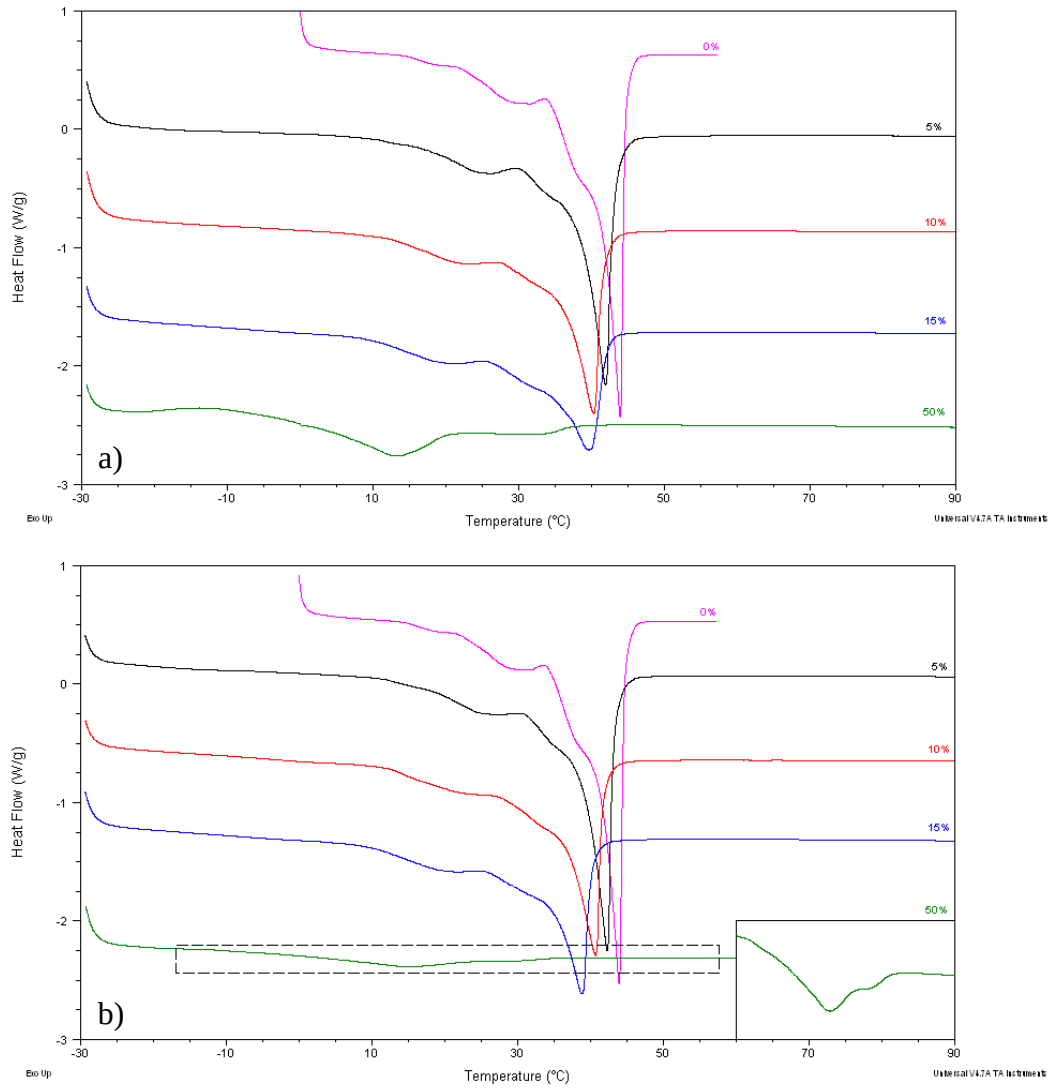

Figure 4.6 *Heat flow against temperature signal on heating at 10°C/minute of ibuprofen and Gelucire 44/14 a) SSD(20) and b) SSD(4) – Second melt.*

Upon re-melting, none of the SSD systems demonstrated an ibuprofen melting peak (Figure 4.6). This suggested that by this point the drug was either completely dissolved within the Gelucire 44/14 (which may have been the case with the 5 to 15% w/w systems), or that the remaining crystalline drug, seen to melt on first heating at 50% w/w, may now be present in the amorphous form. The glass transition of ibuprofen is known to be approximately -45^{o}C (Domanska et al. 2009) and would therefore not have been detected.

The Gelucire 44/14 melting endotherm no longer existed as two distinct peaks but as one larger peak with a leading shoulder. The lower and higher melting fractions could however still be defined, similar to that observed for the lipid alone (Figure 4.6, 0%). The changes observed in the lipid melting peak may possibly therefore be attributed to both the immediate cooling and re-melting of the sample, in addition to dissolution of the crystalline drug into the lipid and their subsequent interaction.

The overall endotherm shape corresponded closely with that of Gelucire 44/14 alone however the $Tm_{(onset)}$ and $Tm_{(max)}$ could be seen to reduce in temperature with increasing drug concentration which may be due to further lipid-drug interaction. The high crystalline drug content at 50% w/w, as highlighted by Qi et al (2010b), may also bring about dissolution, to an unknown extent, of the SSD carrier Gelucire 44/14 into the drug. The small melting endotherm detected at 50% does however suggest that there was a small degree of crystallisation which was difficult to detect on cooling at 10^{o}C/minute, particularly for the SSD(4) systems.

4.3.2 Assessment of Thermal Properties using Hyper (Fast Speed) Differential Scanning Calorimetry

4.3.2.1 Analysis of Raw Materials

The raw components of the SSD systems were first analysed at 500^{o}C/minute in order to investigate their response to the fast heating rate. The characteristic double melting endotherm of Gelucire 44/14 was observed (Figure 4.7). The resolution or separation of the primary and secondary peaks was reduced however due to the speed of melting, so for this reason the peak ΔH was measured as a whole. The peak was found to display an $Tm_{(onset)}$ of 33.5^{o}C ± 5.1, a $Tm_{(max)}$ of 56.0^{o}C ± 2.2 with an ΔH of 97.3J/g ± 8.3. In comparison to that at 10^{o}C/minute, the $Tm_{(onset)}$ increased in temperature, as did the primary $Tm_{(max)}$. The increase in $Tm_{(onset)}$ will be due to integration of the peak as a whole, instead of the two peaks individually, with the increase in $Tm_{(max)}$ being attributable to the fast heating rate broadening the transition.

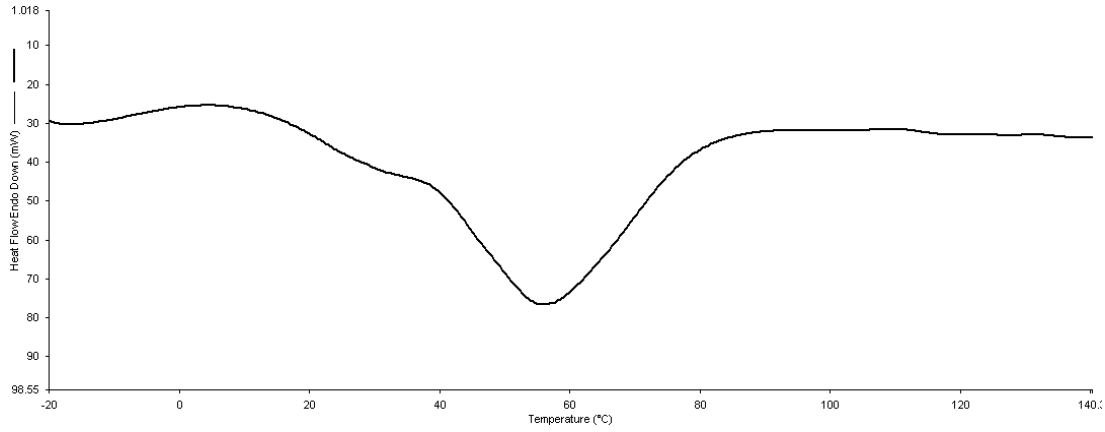

Figure 4.7 *Heat flow against temperature signal of the Gelucire 44/14 melting endotherm on heating at 500^{o}C/minute.*

The ibuprofen melting endotherm was significantly broader than that observed at slower rates due to thermal lag making the $Tm_{(max)}$ fall at a temperature approximately 7°C higher at 83.9°C ± 2.0 (Figure 4.8). The $Tm_{(onset)}$, however, was found to correspond closely at 75.5°C ± 0.6 compared to 74.8°C ± 0.05 as should be the case with thermodynamic events such as melting.

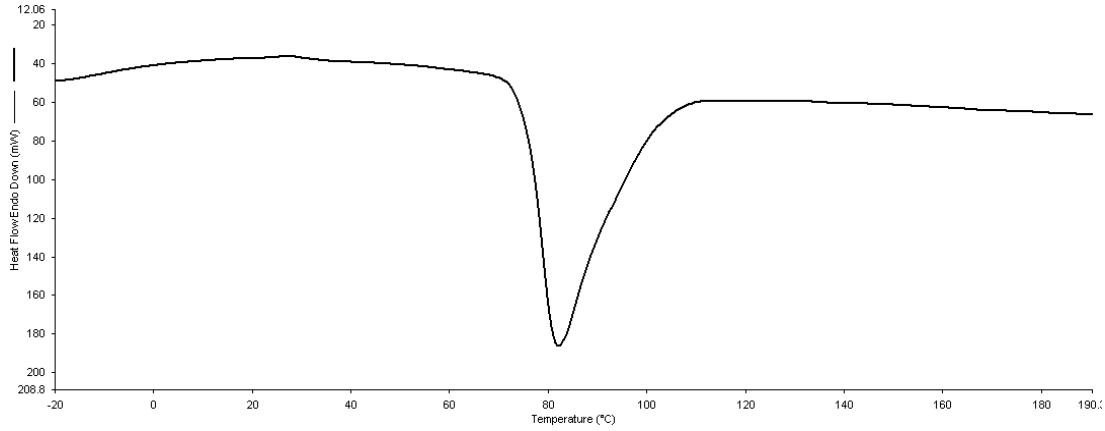

Figure 4.8 *Heat flow against temperature signal of the ibuprofen melting endotherm on heating at 500°C/minute.*

4.3.2.2 Analysis of Physical Mixes

When heated at a rate of 500°C/minute, the shape of the Gelucire 44/14 melting endotherm was observed to change with increasing drug loading (Figure 4.9). The peaks, unlike those at 10°C/minute, were integrated as a whole due to reduced resolution and therefore reduced separation of the two peaks. Maximum of the lipid secondary melting peak appeared to maintain at approximately 25°C in all samples. The higher melting temperature primary peak was however observed to reduce in size with increasing ibuprofen loading as observed at 10°C/minute. This may be

caused by reduction in mass of the lipid in the mix and also broadening of the peak due to heating at such a fast rate, bringing about reduced resolution of the peak from the melting endotherm of ibuprofen.

Ibuprofen melting endotherms were detected as low as 10% w/w, the ΔH values of which increased with loading. At higher drug loadings, reproducibility of peak ΔH was found to decline, however the $Tm_{(max)}$ could be observed to fall reproducibly at 79.7°C ± 0.8. Variability was also observed to be an issue in other studies such as McGregor and Bines (2008). Onset temperature of the ibuprofen melting endotherm reduced by approximately 1°C with each increase in drug loading concentration which may be an effect of the peak merging with that of the primary Gelucire 44/14 melting endotherm as suggested above.

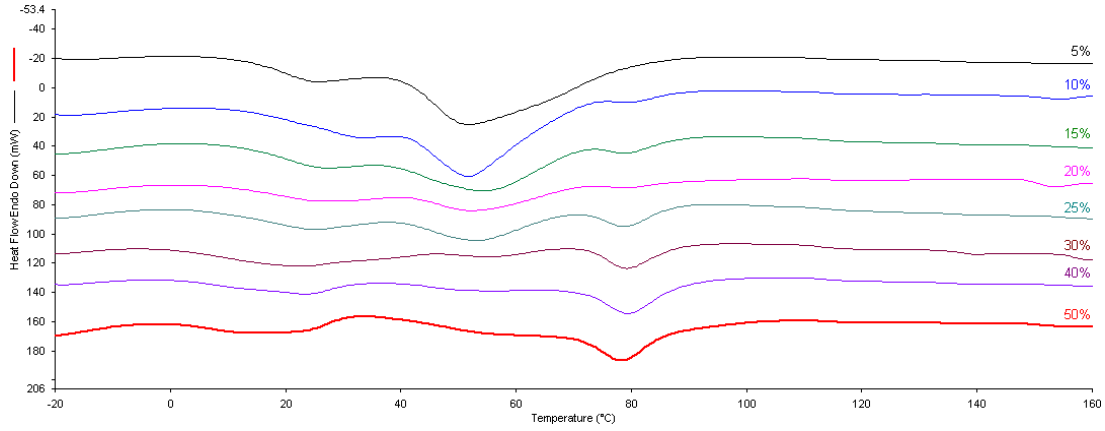

Figure 4.9 *Heat flow against temperature signal of ibuprofen and Gelucire 44/14 physical mixes on heating at 500°C/minute.*

4.3.2.3 Analysis of Semi-Solid Dispersion Systems

Analysis of the Gelucire 44/14 and ibuprofen SSD systems at a heating rate of 500^{o}C/minute demonstrated disappearance of the Gelucire 44/14 primary melting endotherm, with a depression in the $Tm_{(max)}$ of the secondary peak, in both the slow cooled (SSD(20)) and fast cooled (SSD(4)) formulations. The complete disappearance of the primary lipid melting endotherm implies some level of interaction of these crystals with the drug, brought about by solubilisation of drug into Gelucire 44/14 when in the molten state, as suggested by Chambin et al (2004).

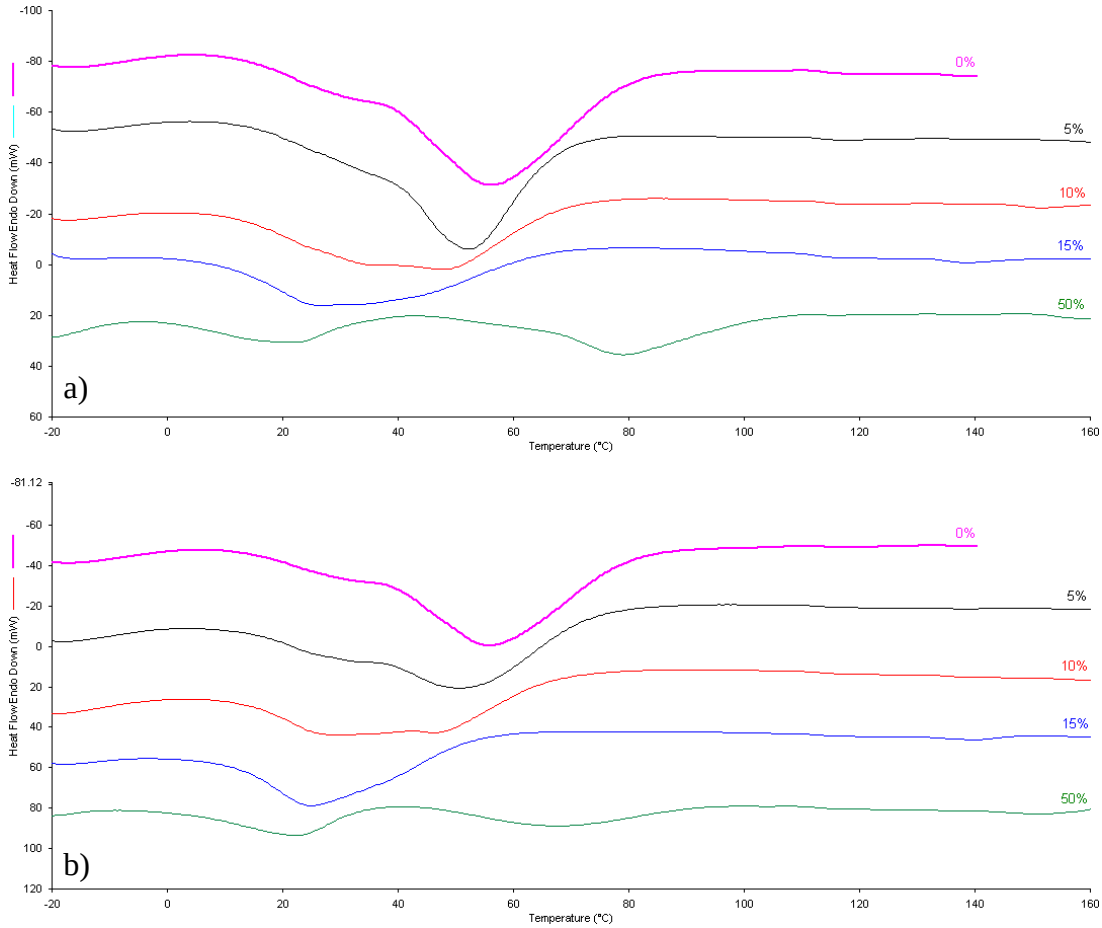

Figure 4.10 *Heat flow against temperature signal of ibuprofen and Gelucire 44/14 a) SSD(20) and b) SSD(4) on heating at 500^{o}C/minute.*

An ibuprofen melting endotherm could be detected for the 50% w/w systems only, in both cases. In ΔH, the peaks were found to be similar in both the SSD(20) and SSD(4) systems, however the peak $Tm_{(onset)}$ was approximately 20°C lower in the SSD(4) formulation than that of SSD(20), 45.4°C ± 0.6 and 65.7°C ± 1.1 respectively. There was also a significant difference in the $Tm_{(max)}$ at 68.0 ± 1.0 for SSD(4) and 82.3°C ± 4.0 for SSD(20). This may be due to varying levels of interaction between the primary melting fractions of the lipid with the drug during cooling.

4.3.3 Comparison of Conventional and Hyper Differential Scanning Calorimetry Data

As outlined previously, the assumption of a solid solution should not be made on the basis of the absence of a drug melting endotherm using DSC analysis at slow heating rates (10°C/minute) due to dissolution of drug into the lipid carrier during analysis. The use of fast heating rates (500°C/minute) has highlighted the possibility of reduction, but not complete elimination, of these dissolution effects seen at slower rates.

In theory, analysis of physical mixes of lipid and drug should illustrate melting endotherms of both components, independent of each other. In reality, this has been shown not to be the case i.e. the disappearance of a drug melting peak at 5% w/w. This phenomenon will therefore impact the assumptions made regarding the physical state of the final formulated SSD system. Qi et al (2010b) proposed that the ΔH value of the drug melting peaks measured represents not only melting but also the energy

of its dissolution into the carrier lipid. In order to determine the extent of molecular dispersion into Gelucire 44/14 during formulation, minus dissolution during analysis, physical mix analysis was used as a calibration plot.

All physical mix systems were analysed for ibuprofen melt ΔH values which were plotted against the initial crystalline ibuprofen concentration. For those systems subjected to heating at 10°C/minute, a linear relationship was not observed, as predicted by the Qi model (Figure 4.11). Similarly, the ΔH values for 25, 30 and 40% w/w systems were larger than expected compared to pure drug, probably due to dissolution effects contributing to the measured value.

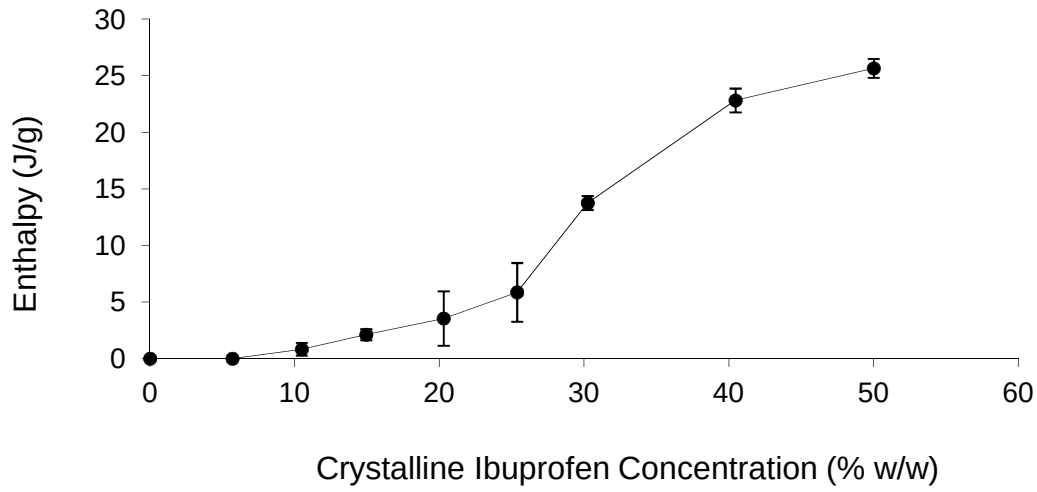

Figure 4.11 *Crystalline ibuprofen content in the physical mix against the measured ibuprofen melt enthalpy analysed on heating at 10°C/minute.*

The ΔH values for physical mixes analysed at 500°C/minute also appeared to follow the Qi model, however the point at which lipid dissolution into the drug became the dominant process did not appear to have been reached, suggesting that Gelucire 44/14 solubility in ibuprofen is less than 50% w/w (Figure 4.12). This also suggested

that faster heating rates reduce, but do not eliminate, the dissolution effects seen at 10°C/minute. The disappearance or reduction of the drug melting ΔH does not therefore necessarily signify the presence of a solid solution since no drug dissolution could have occurred prior to analysis for these physical mixes.

Given the above, it was decided to use the 500°C/minute physical mix data as a calibration standard in that, by comparing the SSD ibuprofen ΔH values to the physical mixes, a more reliable method of ascertaining solid crystalline drug content may be derived. The physical mix plot was not linear but demonstrated two of the three phases outlined by Qi et al (2010b).

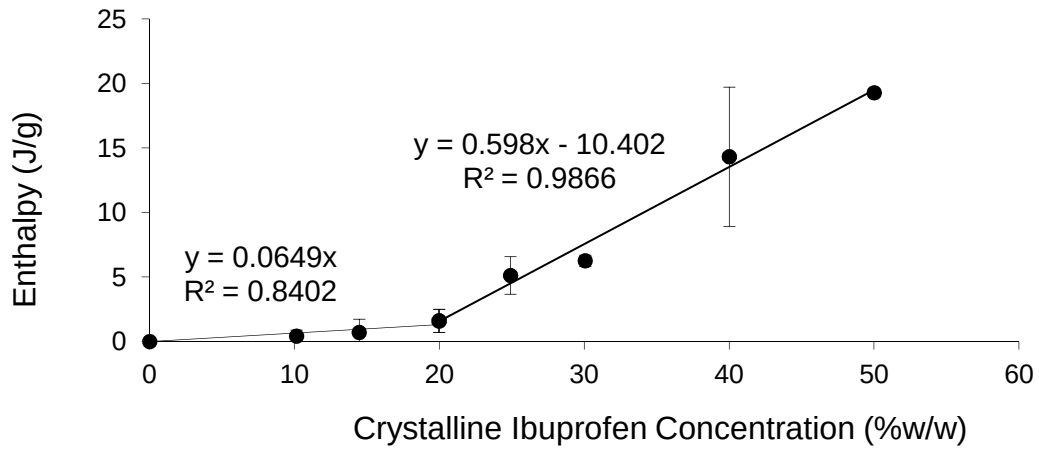

Figure 4.12 *Crystalline ibuprofen content in the physical mix against the measured ibuprofen melt enthalpy analysed on heating at 500°C/minute.*

Using this approach it was possible to estimate the solid drug content of the SSD systems using the equation from the appropriate region of the calibration plot (Table 4.1). For both SSD systems, ibuprofen melting peaks were detected only at 50% w/w when analysed at either 10 or 500°C/minute. On the whole the data indicated that the

drug was present as crystalline particles and also, to a small extent, a molecular dispersion within the Gelucire 44/14.

Table 4.1 *Calculated crystalline (Cryst.) and molecular (Mol.) ibuprofen content of SSD systems.*

System	Heating Rate (°C/min)	Ibup Conc (%w/w)	Enthalpy (J/g)	Cryst. Ibup Dispersion (%w/w)	Mol. Ibup Dispersion (%w/w)
SSD(20)	10	50	17.5 ± 3.4	46.6	3.4
	500	50	16.6 ± 1.4	45.1	4.9
SSD(4)	10	50	29.2 ± 2.5	66.1	0
	500	50	16.9 ± 2.6	45.7	4.3

Ibuprofen melt ΔH values were found to be similar, if not slightly lower, when analysed at 500^{o}C/minute, which was unexpected. If the fast speed was preventing further dissolution of the drug into the lipid during analysis, peak ΔH values should be greater thus corresponding with a more accurate estimation of drug concentration as a molecular dispersion after formulation into an SSD system. This however was not the case. As mentioned above, data obtained using the hyper DSC method was found to be lacking in reproducibility which will impact on the final calculated crystalline and molecular dispersion concentration values. It was however observed, with the exception of 10% SSD(4), that despite the rate of heating, the calculated concentration of molecular dispersion in the SSD system was circa 4% w/w. Unfortunately the data did not show, with any great certainty, the benefits of using fast heating rates and more research is required to this effect. It did however give an

indication that ibuprofen solubility in Gelucire 44/14 may fall at approximately 20% w/w.

4.3.4 Crystallisation Analysis using Quasi-Isothermal Modulated Temperature Differential Scanning Calorimetry

Quasi-Isothermal MTDSC was used to further characterise the crystallisation transition of the formulated SSD systems containing ibuprofen with the lipidic carrier Gelucire 44/14. The technique allows isolation of the true crystallisation temperature, independent of the kinetic effects of heating rate. This can then be compared with that of the lipid alone in order to establish the effect of drug presence on the transition. All SSD systems were analysed with an isothermal period of 20 minutes and an increment of -1^{o}C, reducing stepwise throughout the crystallisation temperature range. The reversing heat capacity time plot for representative samples of the SSD systems can be seen in Figure 4.13.

The crystallisation temperatures of the formulations cooled slowly (SSD(20)) and quickly (SSD(4)) appeared to correspond relatively closely with each other. In general, the crystallisation temperature of the lipid was decreased from 31^{o}C for the lipid alone, to 25^{o}C and below in the presence of ibuprofen, with the crystallisation temperature decreasing with increasing drug loading. At 50% w/w, no obvious crystallisation was observed. As suggested by Long et al (1995), the decrease in crystallisation temperature may be brought about by the drug acting as a diluent and subsequently reducing the concentration and number of nuclei able to bring about the process of crystallisation.

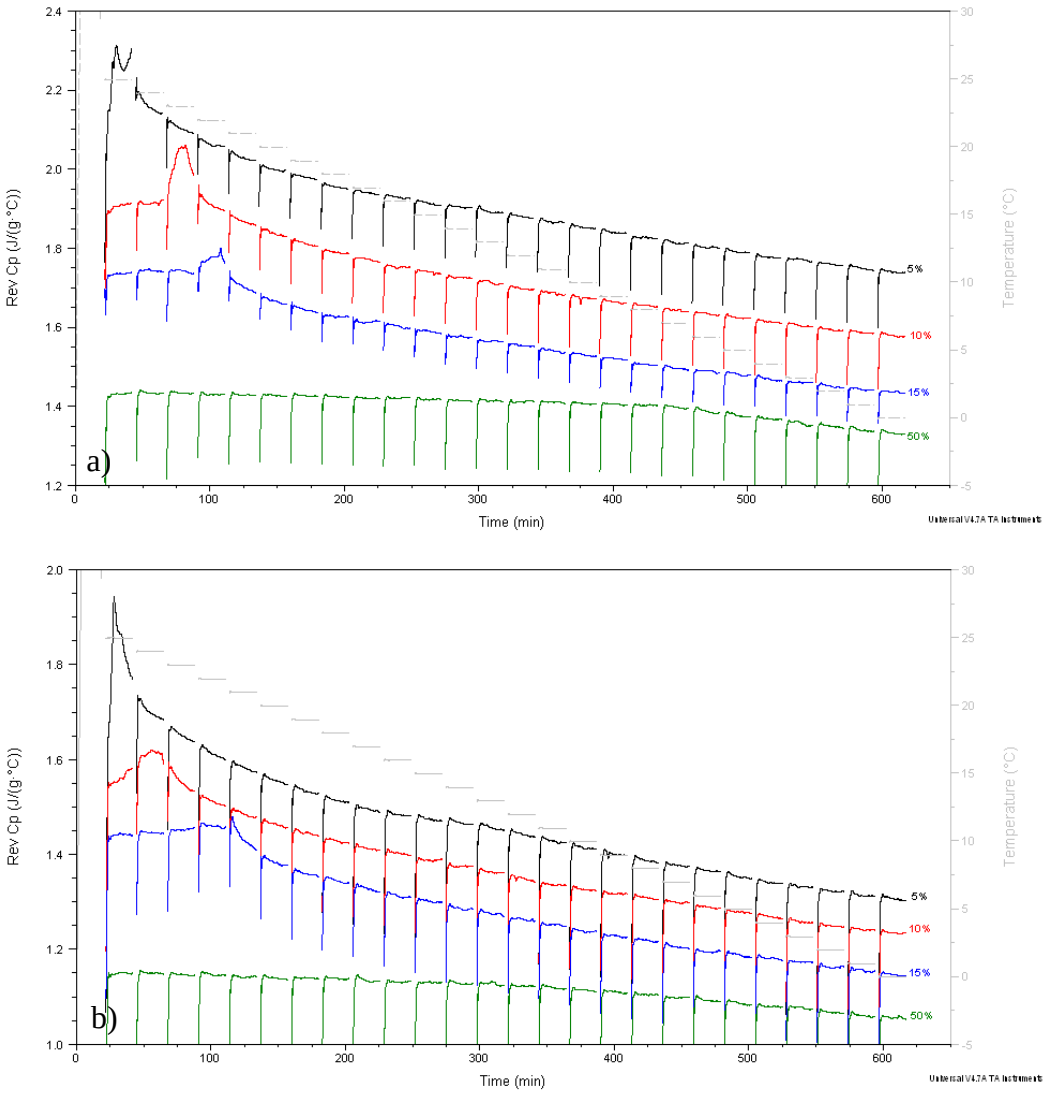

Figure 4.13 *Reversing heat capacity versus time signal for ibuprofen and Gelucire 44/14 a) SSD(20) and b) SSD(4) QIMTDSC 20 minute isotherm on cooling with 1°C increments.*

In all cases, after the event of crystallisation, the reversing heat capacity continued to decrease over time. This phenomenon was observed for Gelucire 44/14 alone in Chapter Three and was thought to be brought about by an initial or primary energetic crystallisation, followed by a secondary slower, more extended period of crystallisation which continued to much lower temperatures than previously expected.

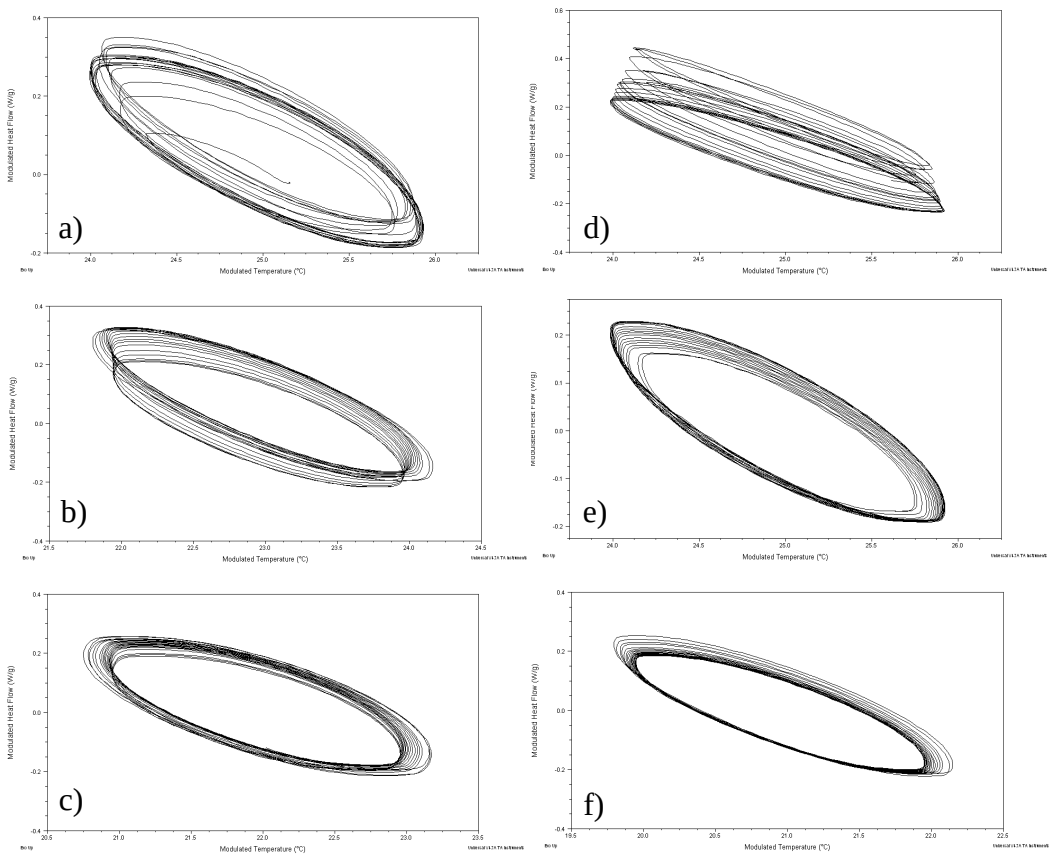

Figure 4.14 *Lissajous figures of the sine wave heat flow modulations (crystallisation) of ibuprofen and Gelucire 44/14 SSD systems; SSD(20) a) 5% b) 10% c) 15% and SSD(4) d) 5% e) 10% f) 15%.*

Lissajous figures were isolated for each temperature increment by plotting the modulated heat flow against modulated temperature to observe any deviation from the steady state thus indicating the occurrence of crystallisation. Representative samples can be seen in Figure 4.14. The Lissajous analyses were found, on the whole, to support the crystallisation temperatures observed from the reversing heat capacity time plots above. Isolation of each QIMTDSC temperature increment for the 50% w/w samples showed no obvious sine wave deviation, as suggested by the reversing heat capacity time plot above, therefore this data is not presented.

The major slope of the Lissajous analysis is known to give an indication of the heat capacity of the sample. In all samples, the axis was found to reduce from the start to the conclusion of the experiment, suggesting a subsequent decline in heat capacity. This agrees with the observation from the reversing heat capacity time plot above (and also that of Gelucire 44/14 alone in Chapter Three) of an extended period of secondary crystallisation after that of the primary energetic phase.

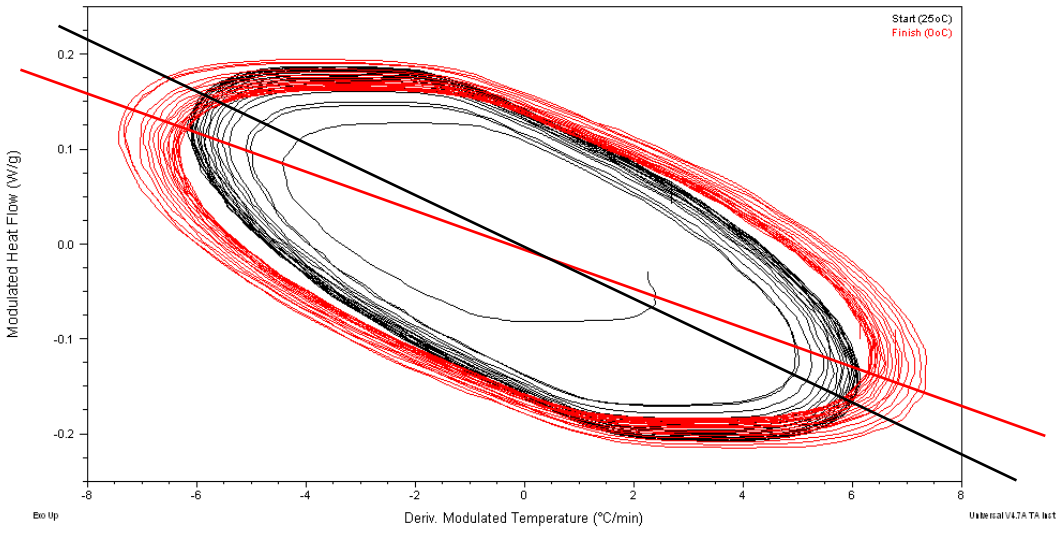

Figure 4.15 *Lissajous figures of the sine wave heat flow modulations of ibuprofen and Gelucire 44/14 SSD(20) 10% w/w systems at the start (25°C, black) and finish (0°C, red) of the cooling experiment showing the major slope of each plot.*

Of the repeated sample analyses carried out for each formulation, reproducibility of the detected crystallisation temperatures was found to be poor, with the transition being found to occur over two temperature increments in one of the three repeats (see Table 4.2). This may be brought about by nucleation occurring at varying rates, and also the growth of different crystal formations. It may also be due to crystallisation of

the lower and higher melting point fractions of Gelucire 44/14 crystallising over two different temperatures.

Table 4.2 *Measured crystallisation temperatures for ibuprofen and Gelucire 44/14 SSD systems using QIMTDSC reversing heat capacity versus time and Lissajous analysis.*

System	Ibuprofen Loading (%w/w)	Crystallisation Temp: Reversing Cp (^{o}C)	Crystallisation Temp: Lissajous (^{o}C)
SSD(20)	5	24.8^{o}C ± 0.2	24.8^{o}C ± 0.2
	10	21.7 ± 3.2	21.8 ± 3.4
	15	21.7 ± 0.6	21.7 ± 0.6
	50	None	None
SSD(4)	5	24.7 ± 0.6	24.8 ± 0.3
	10	22.7 ± 2.3	23.2 ± 2.8
	15	21.3 ± 0.6	21.3 ± 0.4
	50	None	None

4.3.5 Observation of Thermal Transitions by Hot Stage Microscopy

On visualisation of the 5% w/w SSD(20) systems there appeared to be a small number of ibuprofen crystallites, which dissolve rapidly during and after melting of Gelucire 44/14 (Figure 4.16 b). This confirmed that complete ibuprofen dissolution, at this drug loading, did not occur during formulation as suggested by thermal analysis at slow and also higher rates, and that an amount of dissolution occurs during formulation into the Gelucire 44/14 since the crystallites have sufficient time

to dissolve prior to their melting temperature. At 5% w/w SSD(4) however, there is no indication of any crystalline ibuprofen (Figure 4.16 d). This may suggest that complete dissolution does occur during formulation however, the slower cooling rate of the SSD(20) systems allows formation of small ibuprofen crystallites before complete solidification.

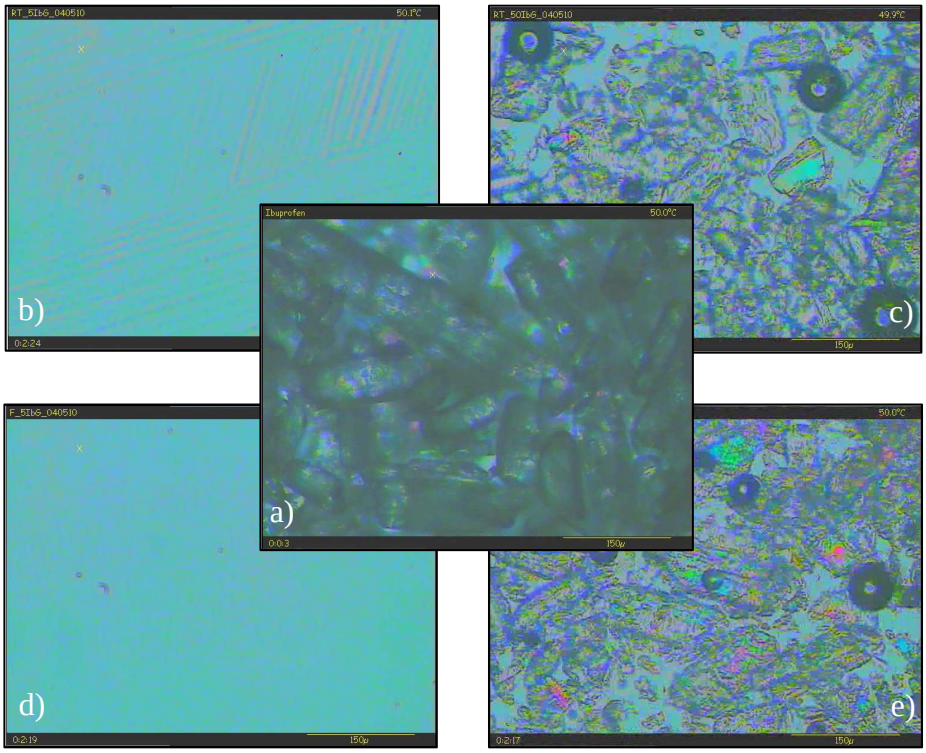

Figure 4.16 *HSM images of a) ibuprofen, b) SSD(20) 5%, c) SSD(20) 50%, d) SSD(4) 5% and e) SSD(4) 50% at 50°C in order to visualise only crystalline ibuprofen.*

At 50% w/w a significant number of ibuprofen crystals could be observed in both formulations (Figure 4.16 c and e). These crystals were larger in size than those seen at 5% SSD(20), however, with the exception of a small number, were smaller in size than crystalline ibuprofen alone (Figure 4.16 a). These crystals began to reduce in size immediately post Gelucire 44/14 melting, initially due to dissolution into the

molten lipid, and then melting with increasing temperature, having completely disappeared before 70^{o}C. This indicated melting point depression, as demonstrated by conventional DSC, as crystalline ibuprofen alone can be seen to begin melting just after 70^{o}C, being molten by 80^{o}C.

It should be noted at this point that HSM and DSC measurements cannot be compared directly with any absolute certainty due to differences in measurement method. Data obtained from HSM gives an indication as to the behaviour of a small number of individual crystals; however DSC averages the melting of all the crystal species at a similar temperature as a whole. It should also be considered that the heat flux experienced by a sample enclosed in an aluminium pan will not be the same as that experienced by a sample exposed to the atmosphere (Sutananta et al. 1994b).

4.3.6 Summary of Ibuprofen and Gelucire 44/14 Semi-Solid Dispersion System Characterisation Studies

The characterisation of SSD systems composed of ibuprofen and Gelucire 44/14 has produced some interesting findings into the existence of drug within the formulation and also to the interpretation of data. The DSC physical mix data at 10 and 500°C/minute showed a similar trend in that a drug melting peak was absent at 5% w/w. This could be taken to suggest that the crystalline ibuprofen present is dissolving during analysis or that the mass falls below the instrument limit of detection. So at first glance there is no difference and also little benefit of the faster heating rate in this case. Analysis using fast heating rates may be best suited to linear models. On plotting the crystalline ibuprofen melt ΔH values against the initial

crystalline ibuprofen content, it became apparent that the faster heating rate followed, to some extent, the model put forward by Qi et al (2010b), highlighting the processes of drug dissolution into the lipid at low drug loadings, lipid dissolution into the drug at high drug loadings and both occurring in between. The use of the corresponding sections of the plot to calculate the crystalline ibuprofen content of the SSD systems suggested that those systems with a measurable drug melt ΔH (50% w/w at both 10°C/min and 500°C/min) also, on the whole, contained molecularly dispersed drug of circa 4% w/w. Conventional DSC along with Quasi-isothermal MTDSC showed the decrease of lipid crystallisation temperature with increasing drug loading, thought to be due to dilution of nuclei by the molecularly dispersed drug (Long et al. 1995).

4.4 INDOMETACIN AND GELUCIRE 44/14 SEMI-SOLID DISPERSION SYSTEMS

In this section, formulations of the lipidic carrier Gelucire 44/14 with the model drug indometacin, a BSC Class II drug, were investigated.

4.4.1 Assessment of Thermal Properties using Conventional Differential Scanning Calorimetry

4.4.1.1 Analysis of Raw Materials

The melting endotherm observed upon heating of crystalline indometacin presents as a sharp peak occurring reproducibly at $Tm_{(onset)}$ 159.6°C ± 0.04 and $Tm_{(max)}$ 160.7°C ± 0.09 (Figure 4.17).

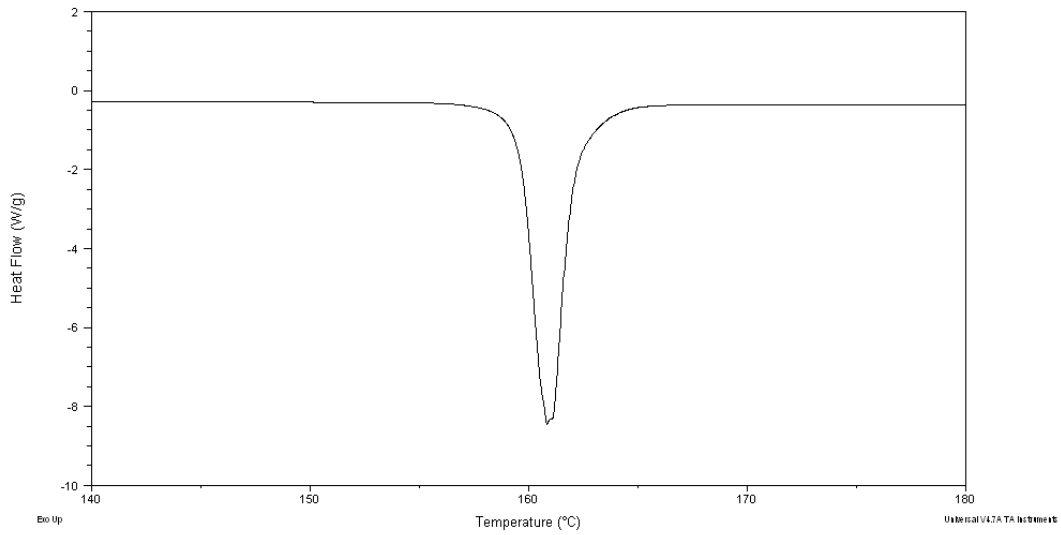

Figure 4.17 *Heat flow against temperature signal of the indometacin melting endotherm on heating at 10°C/minute.*

4.4.1.2 Analysis of Physical Mixes

Upon analysis of indometacin and Gelucire 44/14 physical mixes using conventional DSC, the characteristic Gelucire 44/14 double endotherm was observed in all cases (Figure 4.18). The $Tm_{(onset)}$ and $Tm_{(max)}$ values of both the primary and secondary endotherms occurred reproducibly at 40.0°C ± 0.1 and 44.9°C ± 0.1, and 27.2°C ± 0.4 and 34.3°C ± 0.2 respectively, corresponding well with those of the lipid alone. This confirmed the absence of any previous interaction between the two components prior to analysis. The ΔH values for both peaks could however be observed to decrease with increasing indometacin loading attributable to the decreasing mass of lipid in the binary mix.

The baseline at the point of indometacin melting was found, in most cases, to be very noisy. At least six repeats were therefore carried out in order to achieve a minimum of three measurable and usable results for further analysis. Measurable melting endotherms were detected at 15% w/w indometacin and above. In general, the $Tm_{(onset)}$ and $Tm_{(max)}$ values appeared to increase with increasing drug loading in the range 122 to 146°C and 136 to 151°C, both of which were significantly lower than those observed for the crystalline drug alone ($Tm_{(onset)}$ 159.6°C, $Tm_{(max)}$ 160.7°C). Both this and the increased broadness of the peaks suggested an interaction with the molten lipid during analysis. As outlined earlier, peak broadness is thought to be attributed to the melting and dissolution of the drug over a wide range of temperatures. The measured ΔH values were also observed to increase.

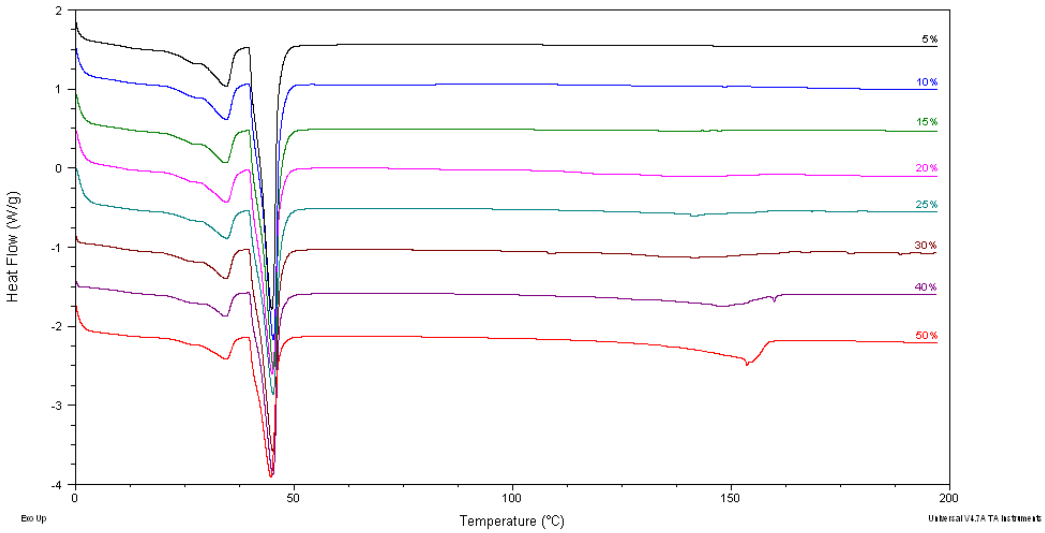

Figure 4.18 *Heat flow against temperature signal of indometacin and Gelucire 44/14 physical mixes on heating at 10°C/minute.*

As with the ibuprofen physical mixes, the absence of a drug melting peak at 5% w/w suggests one of two things. That the crystalline indometacin present is completely dissolving into the Gelucire 44/14 during analysis, or that the indometacin melting peak is undetectable due to its small mass in the mix, which is certainly much less likely with the 10% systems. The crystalline indometacin seen to melt at the higher drug concentrations may thus only be accountable for that remaining after a standard amount of dissolution into the lipid given time to occur during the slow heating rate. The ΔH values may also be attributable, in some part, to the energy of dissolution of indometacin into the molten Gelucire 44/14 during analysis, as discussed previously.

4.4.1.3 Analysis of Semi-Solid Dispersion Systems

Upon melting of the formulated SSD systems, the Gelucire 44/14 double melting endotherm could be observed to occur reproducibly at $Tm_{(onset)}$ 39^{o}C and $Tm_{(max)}$ 35^{o}C (Figure 4.19). In comparison with the lipid alone, both peaks corresponded well however a slight decrease in the primary $Tm_{(max)}$, in the range of 3^{o}C, could be observed. This melting point depression of the higher melting point fraction of the lipid may suggest solubilisation of indometacin into the molten Gelucire 44/14 either during formulation or analysis, or a combination of the two. The ΔH values of the lipid melting endotherms in both systems did not demonstrate any particular pattern of change with increasing drug. At 50%, however, the ΔH value decreased considerably, possibly owing to the reduced lipid mass in the mix.

An indometacin melting endotherm could be detected only for the 50% w/w formulations of both the SSD(20) and SSD(4) systems. The $Tm_{(onset)}$ and $Tm_{(max)}$ values of the peaks, in both cases, were reduced in comparison to those of the crystalline drug alone, again suggesting interaction with the lipidic carrier during manufacture and analysis, the extent to which is attributable to analysis cannot be defined at this stage. The indometacin molecule is known to consist of four hydrogen bond acceptor groups and one hydrogen bond donor group. It is reasonable to assume that the indometacin molecule may therefore be capable of forming hydrogen bonds with the many components of Gelucire 44/14 which express both hydrogen acceptor and donor groups. The interaction observed between indometacin and Gelucire 44/14 may be stronger in nature that that seen with ibuprofen due to the larger number of groups capable of bonding.

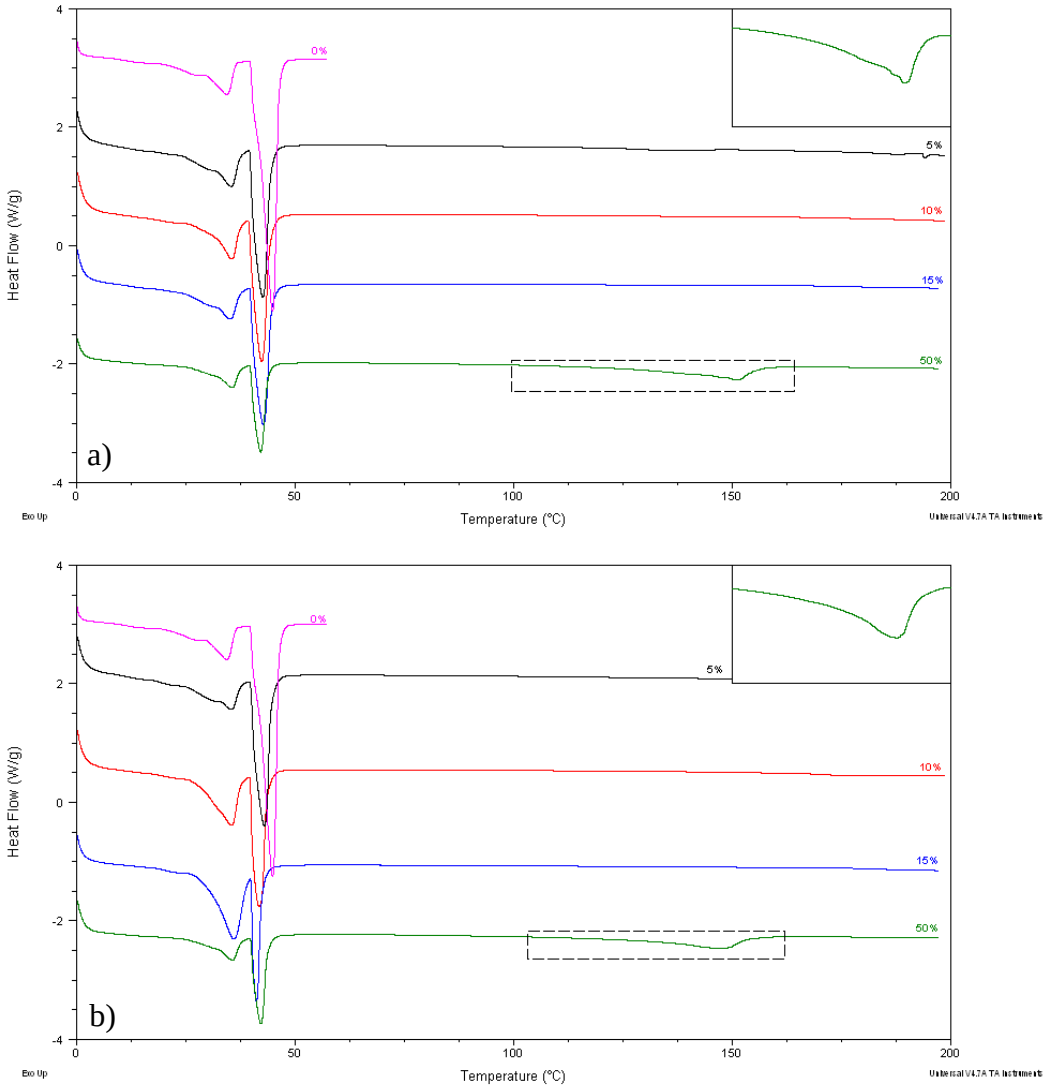

Figure 4.19 *Heat flow against temperature signal on heating at 10°C/minute of indometacin and Gelucire 44/14 a) SSD(20) and b) SSD(4) – First melt.*

Crystallisation upon cooling of the SSD systems is shown in Figure 4.20. The temperature of crystallisation was reduced significantly when compared to that of Gelucire 44/14 alone. It could also be observed to decrease further with increasing indometacin loading. This may be attributable to dissolved drug acting as a diluent and subsequently reducing nuclei concentration, thereby decreasing crystallinity of the sample (Long et al. 1995), as observed with the ibuprofen SSD systems. The shape of the crystallisation exotherm varied between formulations due to the

complex nature of the process and of the lipid-drug system itself. The different peaks observed possibly representing different crystal formations due to hydrogen bonding between the molten lipid and molecularly dispersed drug (Lloyd et al 1997).

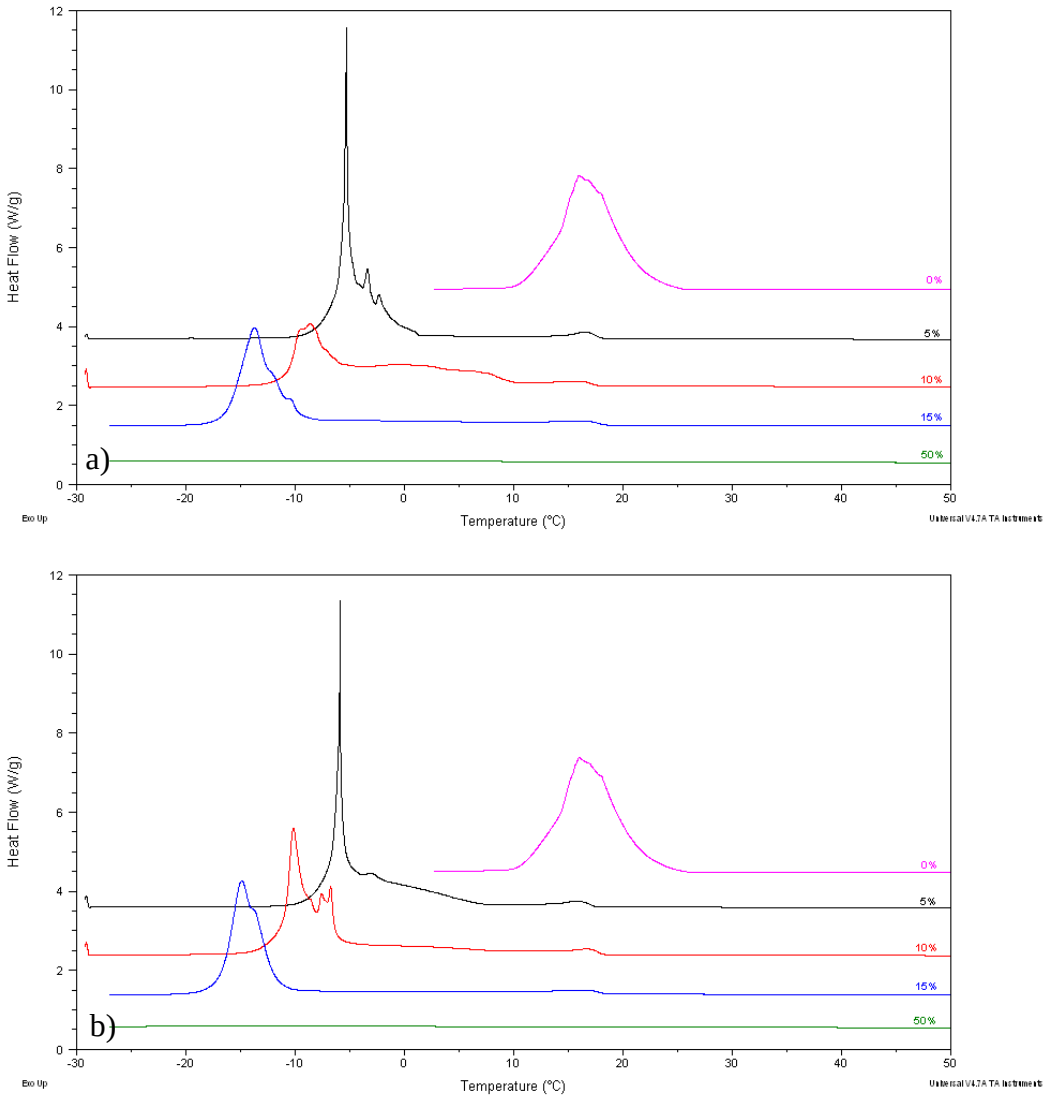

Figure 4.20 *Heat flow against temperature signal on heating at 10°C/minute of indometacin and Gelucire 44/14 a) SSD(20) and b) SSD(4) – Crystallisation.*

The 5 to 15% w/w formulations demonstrated a leading shoulder at approximately 15°C which appeared to correspond well with crystallisation of Gelucire 44/14 alone. As noted previously, Lloyd et al (1997) suggested that the appearance of a bimodal

crystallisation peak may indicate the presence of two different crystal forms. In this case, the observed leading shoulder may be attributable to the formation of a proportion of the original lipid crystal configuration, with the majority constituting the formation of a new crystal entity or entities. The crystallisation peaks appeared to be uncharacteristically sharp in nature, since in general the lipid demonstrated a broader transition in relation to the complexity of the process. No obvious crystallisation was observed to occur upon cooling of the 50% w/w formulations of either SSD system, suggesting complete inhibition of crystallisation of lipid over the temperature range observed in the presence of a large concentration of molten drug, with the systems remaining, on the whole, liquid in nature.

The second heating of both SSD systems demonstrated changes to the Gelucire 44/14 melting endotherm from those observed upon first heating (Figure 4.21). There was reduced separation between the primary and secondary peaks, which could also be observed for the lipid alone, with the $Tm_{(max)}$ values in both cases decreasing with increasing indometacin loading, probably due to interaction with the drug. Despite no obvious sign of crystallisation on cooling of the 50% w/w systems, a small endothermic peak was detected upon reheating. It should be considered that, at this large drug concentration, not only will dissolution of drug be occurring into the lipid but vice versa and also a combination of the two. No measurable indometacin melting peaks could be detected in all cases suggesting that it may be present as a molecular dispersion or exist in the amorphous form.

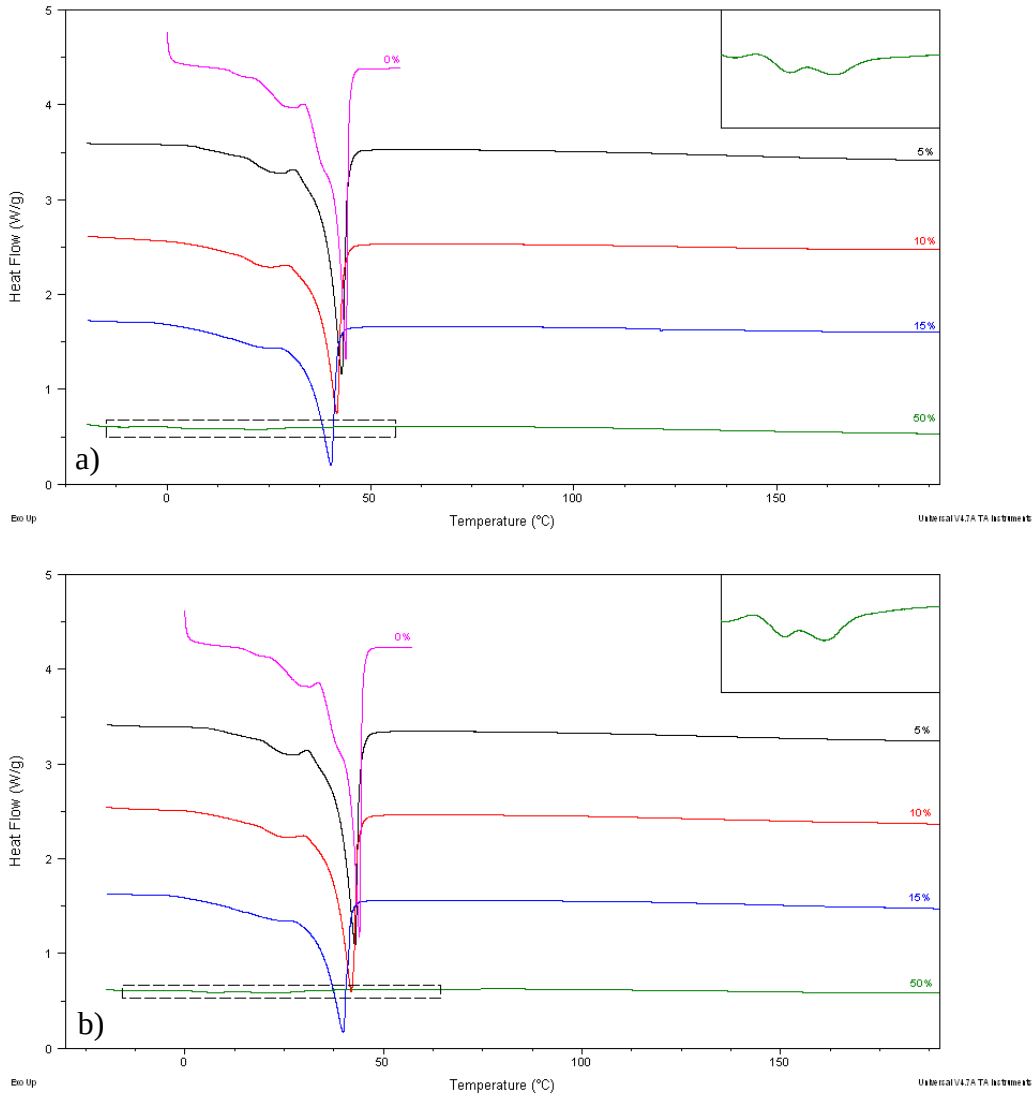

Figure 4.21 *Heat flow against temperature signal on heating at 10°C/minute of indometacin and Gelucire 44/14 a) SSD(20) and b) SSD(4) – Second melt.*

4.4.2 Assessment of Thermal Properties using Hyper (Fast Speed) Differential Scanning Calorimetry

4.4.2.1 Analysis of Raw Materials

Upon analysis at fast heating rates, crystalline indometacin displayed a sharp endotherm at $Tm_{(onset)}$ 158.7°C ±1.0 and $Tm_{(max)}$ 165.5°C ± 0.8. These values increased in comparison with those measured using conventional DSC.

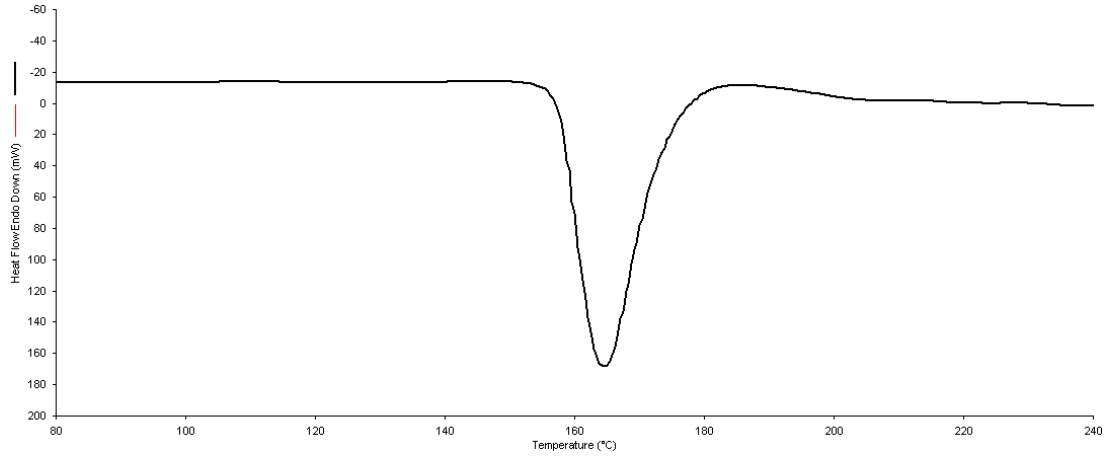

Figure 4.22 *Heat flow against temperature signal of the indometacin melting endotherm on heating at 500°C/minute.*

4.4.2.2 Analysis of Physical Mixes

Analysis of indometacin and Gelucire 44/14 physical mixes allowed distinction of the characteristic lipid melting endotherm in all cases. The peak $Tm_{(onset)}$ and $Tm_{(max)}$ values displayed no particular pattern of change with increasing drug loading, occurring at 35.0°C ± 4.7 and 53.4°C ± 1.2 respectively. These values differed from

those of the lipid alone probably due to limited reproducibility of the technique however it did still suggest no prior interaction between the two components.

Indometacin melting endotherms could be measured in all samples, from 5% w/w and above, occurring reproducibly at $Tm_{(onset)}$ 154.8°C ± 0.6 and $Tm_{(max)}$ 161.5°C ± 0.8, both of which were slightly reduced in comparison with those of the drug alone. This may be as a result of possible hydrogen bonding with the molten lipid during analysis. This effect should be reduced due to the fast heating rate, however will not be completely eliminated.

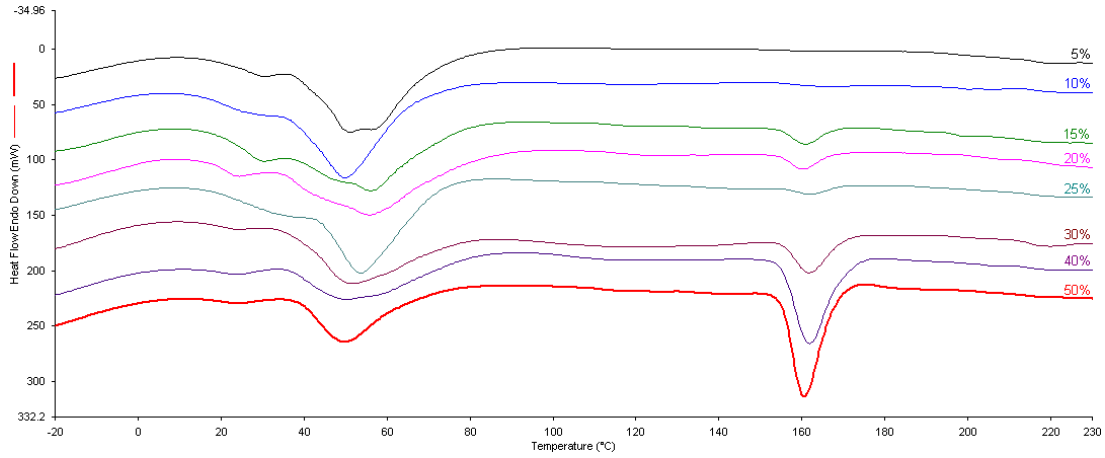

Figure 4.23 *Heat flow against temperature signal of indometacin and Gelucire 44/14 physical mixes on heating at 500°C/minute.*

4.4.2.3 Analysis of Semi-Solid Dispersion Systems

Analysis of indometacin and Gelucire 44/14 SSD systems at 500°C/minute heating rate can be observed in Figure 4.24. The $Tm_{(onset)}$ and $Tm_{(max)}$ values of the lipidic melting endotherm appeared to vary between repeated samples as observed

previously using this technique. In all cases, the measured $Tm_{(onset)}$ values were greater in temperature compared to that of the lipid alone, being most prominent at 50% w/w. The $Tm_{(max)}$ of the melting peaks however were found to be lower, suggesting that the peak is narrower. This shifting of the transition as a whole may suggest possible hydrogen bonding interaction with the drug.

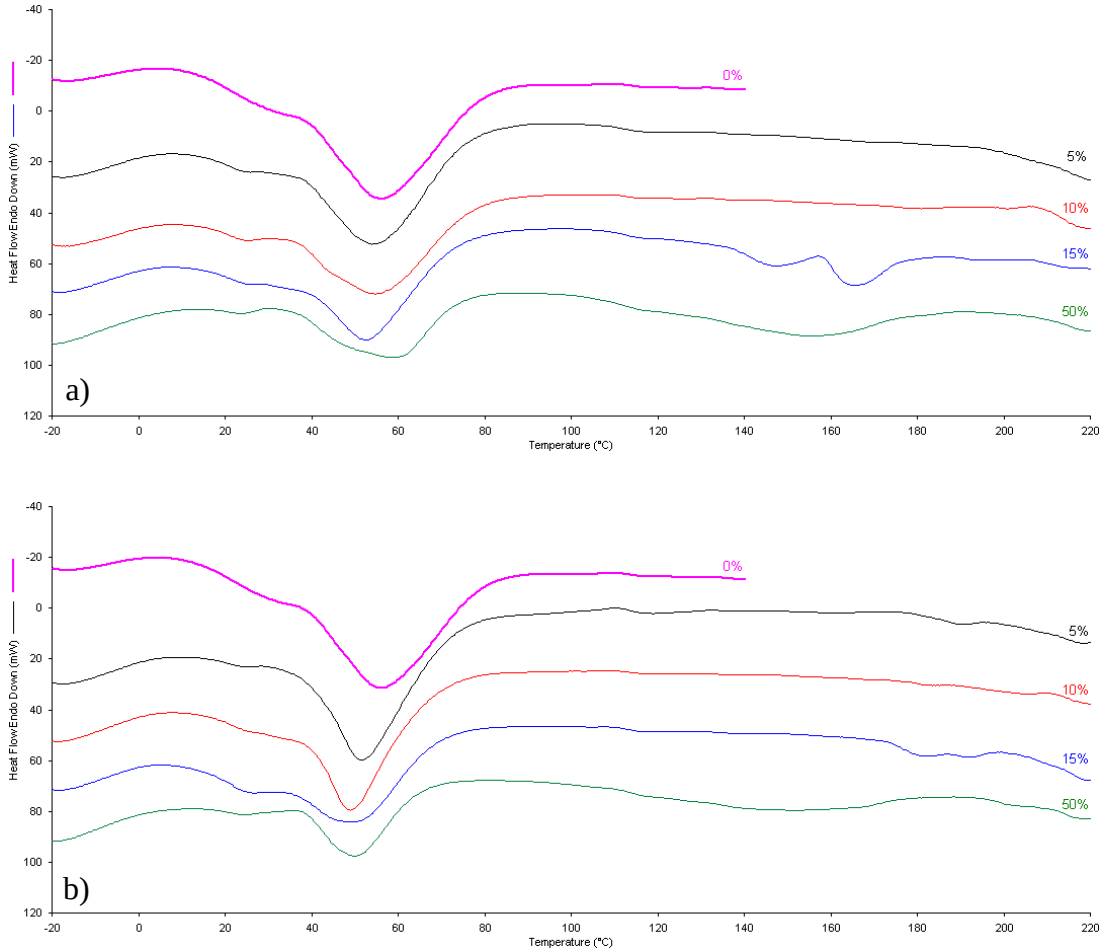

Figure 4.24 *Heat flow against temperature signal of indometacin and Gelucire 44/14 a) SSD(20) and b) SSD(4) on heating at 500°C/minute.*

Distinct and measurable indometacin melting endotherms could be distinguished at 15 and 50% for SSD(20) and 10 to 50% w/w for the SSD(4) systems. These peaks, however, demonstrated poor reproducibility. At 15%, the indometacin melting

endotherm was observed to consist of two peaks, this event however was not observed in all repeated samples.

4.4.3 Comparison of Conventional and Hyper Differential Scanning Calorimetry Data

All conventional DSC data was analysed for indometacin melt ΔH values. Physical mix ΔH data was plotted against the initial crystalline indometacin concentration. As discussed previously, Qi et al (2010b) proposed that the measured ΔH value represents not only melting of the drug but also the energy of its dissolution into the carrier lipid. The ΔH against crystalline indometacin plot for physical mixes analysed at 10°C/minute demonstrated a comparatively linear relationship, excluding 20% w/w whose value was larger than expected compared to pure drug, possibly due to dissolution effects contributing to the measured value (Figure 4.25).

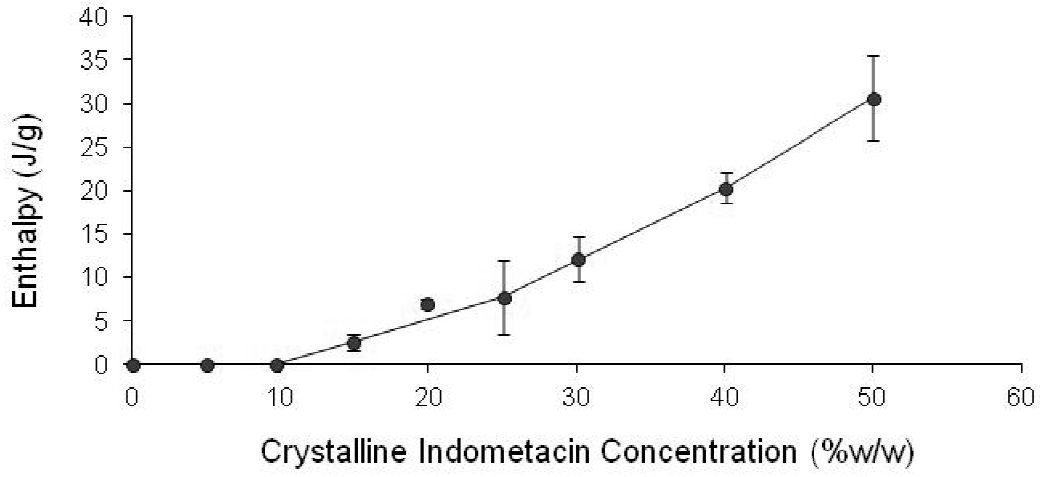

Figure 4.25 *Crystalline indometacin content in the physical mix against the measured indometacin melt enthalpy analysed on heating at 10°C/minute.*

At 500°C/minute, the measured indometacin ΔH valuess appeared to follow the Qi model in that it was triphasic in nature (Figure 4.26). The values obtained for 15 and 20% w/w were higher than expected, again possibly due to dissolution effects, however this should be reduced in comparison to that seen for conventional DSC. This plot was therefore used as a calibration standard against which to determine the solid crystalline indometacin content of the formulated SSD systems (Table 4.3). It could also be determined from this plot that indometacin solubility in Gelucire 44/14 appears to be 25% w/w, with Gelucire 44/14 solubility within molten indometacin being 60% w/w.

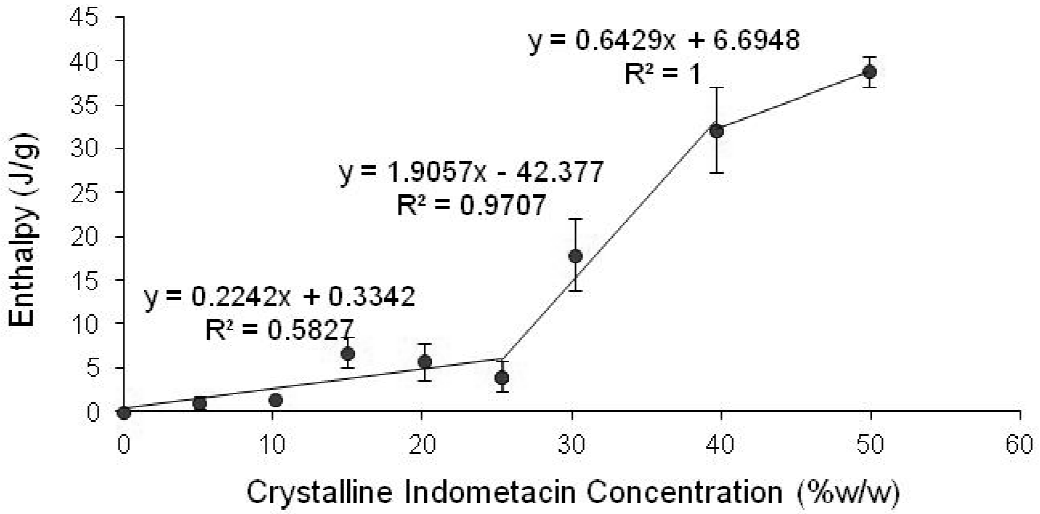

Figure 4.26 *Crystalline indometacin content in the physical mix against the measured indometacin melt enthalpy analysed on heating at 500°C/minute.*

Indometacin peaks were detected only at 50% w/w for those SSD systems analysed at 10°C/minute; however at a heating rate of 500°C/minute, crystalline melting endotherms could be measured as low as 15% for SSD(20) and 10% for the SSD(4) systems. Firstly this highlights that heating at slower rates allows dissolution of crystalline drug into the molten lipid during analysis, thus preventing detection and

measurement of drug melting and therefore the incorrect assumption of a solid solution created purely from the formulation process. And secondly, by increasing the rate at which the sample is heated, the extent to which the crystalline drug dissolves during analysis can be reduced though not completely prevented. At 500^{o}C/minute, the SSD(4) system demonstrated a drug melt at a lower drug concentration than that seen for SSD(20), and therefore a larger concentration of crystalline drug after formulation. It may be a possibility that any remaining crystalline drug may continue to dissolve in the molten lipid whilst cooling at a slow rate to room temperature.

The measured crystalline indometacin melt ΔH values at 500^{o}C/minute were found to be similar to those at the slower heating rate, subsequently giving comparable calculated values of crystalline indometacin in the final SSD systems. It would be expected that heating at faster rates would demonstrate larger indometacin melt ΔH values. It should however be considered that there are a great number of factors which can affect the data obtained, such as instrument error, calibration and baseline error, sample and reference pan variation etc. The measured ΔH values of the repeat samples were significantly variable in value, as can be seen by the standard deviation, which will give a false indication as to the true concentration.

Table 4.3 *Calculated crystalline (Cryst.) and molecular (Mol.) indometacin content of SSD systems.*

System	Heating Rate (°C/min)	Indo Conc (%w/w)	Enthalpy (J/g)	Cryst. Indo Dispersion (%w/w)	Mol. Indo Dispersion (%w/w)
SSD(20)	10	10	–	–	–
		15	–	–	–
		50	29.7 ± 2.0	37.8	12.2
	500	10	–	–	–
		15	23.7 ± 11.1	34.6	0
		50	24.6 ± 6.9	35.2	14.8
SSD(4)	10	10	–	–	–
		15	–	–	–
		50	31.3 ± 2.2	36.6	13.4
	500	10	1.8 ± 0.5	6.6	3.4
		15	2.7 ± 1.7	10.7	4.3
		50	19.6 ± 2.3	32.5	17.5

The molecular dispersion concentration values increased with increasing indometacin loading into the SSD formulation. This may suggest that the system was unable to reach indometacin saturation into the molten Gelucire 44/14 during the time allowed for mixing during manufacture. At 50% w/w, the calculated concentrations of molecularly dispersed indometacin were similar in value, ranging from 12.2 to 17.5% w/w which may suggest that it is at this point that saturation is achieved.

4.4.4 Crystallisation Analysis using Quasi-Isothermal Modulated Temperature Differential Scanning Calorimetry

Quasi-Isothermal MTDSC was utilised as a tool to identify the true crystallisation temperature of the formulated SSD systems, and also to investigate the effect of drug presence on the lipidic carrier. The reversing heat capacity time plot for representative samples of the SSD systems are demonstrated in Figure 4.27.

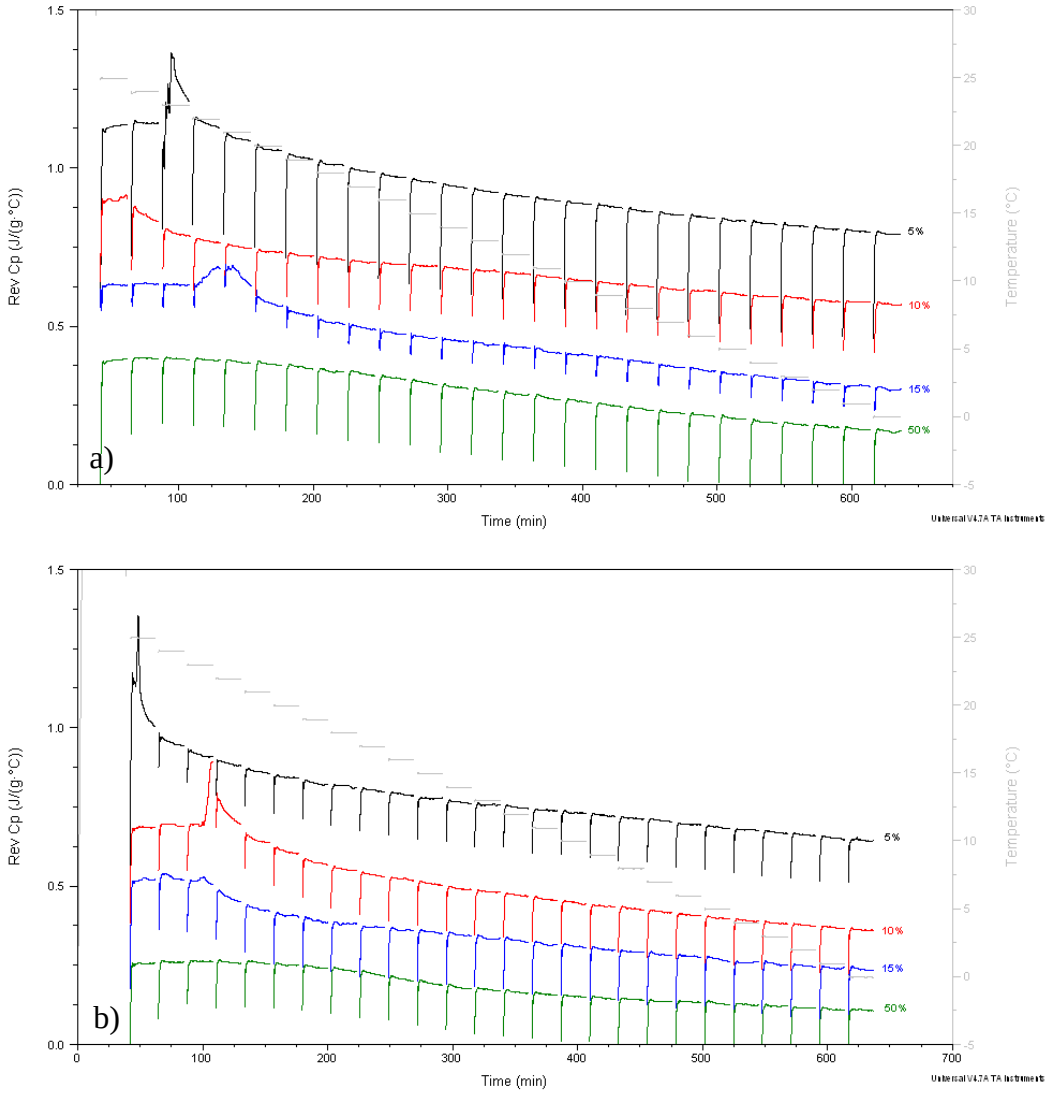

Figure 4.27 *Reversing heat capacity versus time signal for indometacin and Gelucire 44/14 a) SSD(20) and b) SSD(4) QIMTDSC 20 minute isotherm on cooling with 1°C increments.*

Overall, crystallisation of Gelucire 44/14 was significantly reduced in temperature from 31°C to 25°C and below due to interaction, possibly hydrogen bond related, with indometacin, as also demonstrated with ibuprofen. This effect may have been caused by molten indometacin acting as a diluent, reducing the number of nuclei and subsequently delaying crystallisation (Long et al. 1995). The reversing heat capacity of all systems could be observed to decrease over time, even after the main energetic crystallisation had taken place, suggesting a secondary process ongoing over a longer time and to much lower temperatures. No energetic crystallisation process was detected for the 50% w/w formulations of either SSD system, the reversing heat capacity did however still decrease over time.

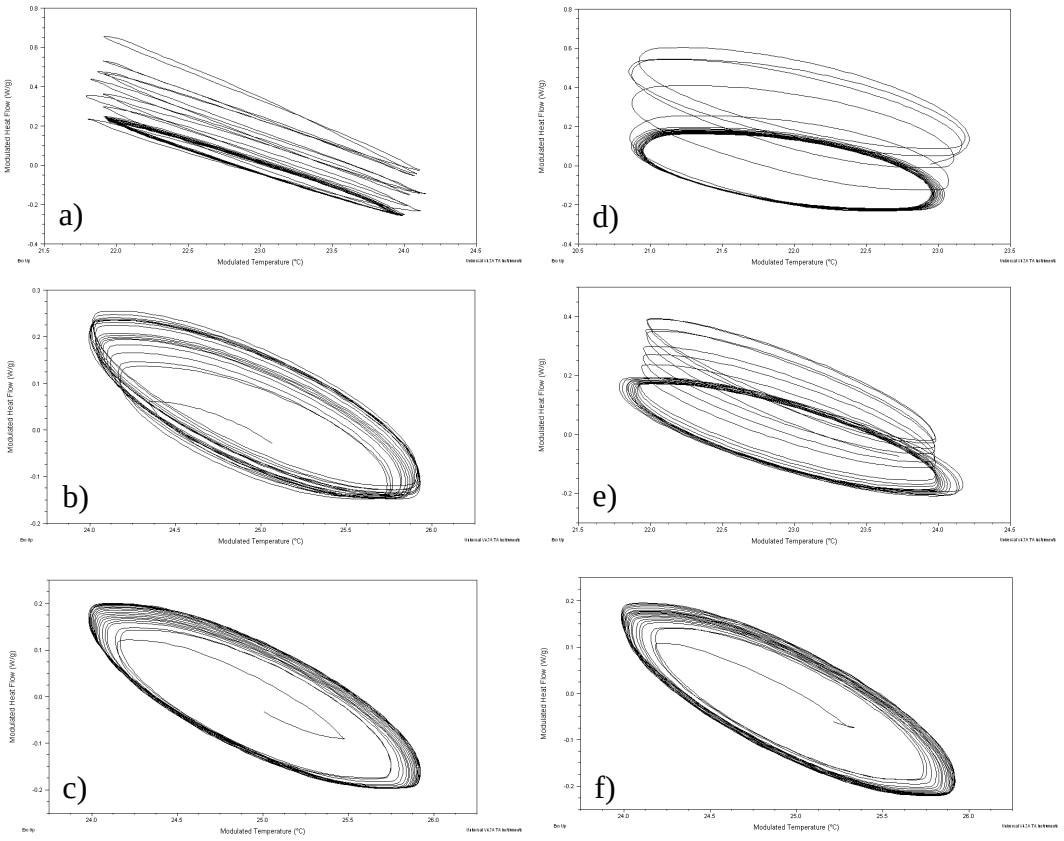

Figure 4.28 *Lissajous figures of the sine wave heat flow modulations (crystallisation) of indometacin and Gelucire 44/14 SSD systems; SSD(20) a) 5% b) 10% c) 15% and SSD(4) d) 5% e) 10% f) 15%.*

Deviation of the sine wave modulations was observed using Lissajous analyses, indicating the occurrence of crystallisation (Figure 4.28). The extent to which the sine wave ellipses deviated from the steady state of the liquid or solid form varied between SSD systems and even between samples. On the whole however, the crystallisation temperature indicated by modulation of the Lissajous analyses coincided with the equivalent reversing heat capacity time plot. Following the absence of crystallisation in all 50% w/w formulations in the reversing heat capacity time plots, isolation of each temperature increment as a Lissajous figure demonstrated no sine wave deviation, and therefore no crystallisation. This data is not shown.

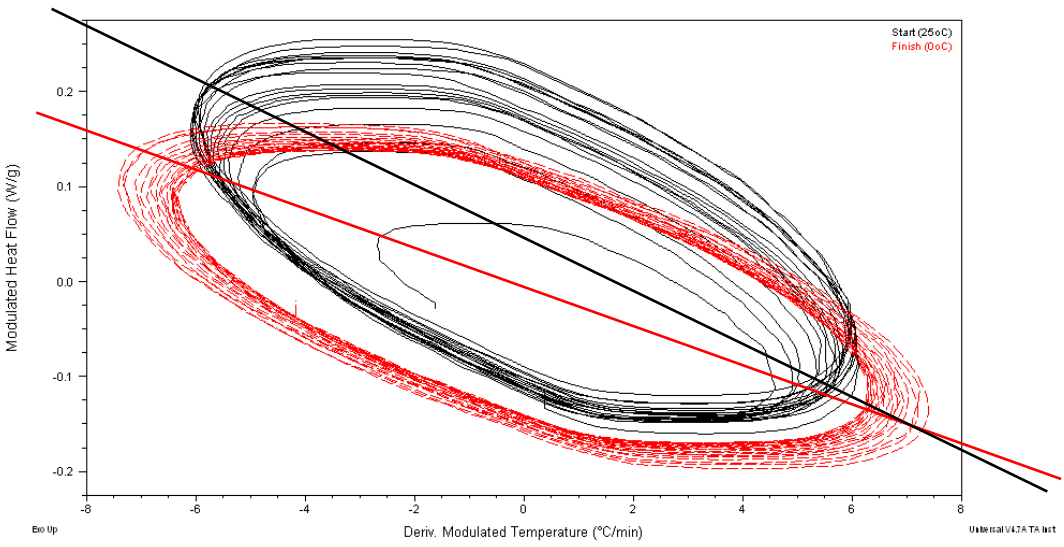

Figure 4.29 *Lissajous figures of the sine wave heat flow modulations of indometacin and Gelucire 44/14 SSD(20) 10% w/w systems at the start (25^{o}C, black) and finish (0^{o}C, red) of the cooling experiment showing the major slope of each plot.*

The major slope of the sine waves could be observed to change between samples, thus suggesting that the extent to which the samples were loaded with drug, and also

the rate at which the SSD systems were cooled during manufacture, affected the heat capacity of the final formulation. The slope was also found to reduce from start to finish of each experiment, in all cases, confirming that the heat capacity of each sample reduced over the course of the experiment. This provides further evidence of an extended period of secondary crystallisation (Figure 4.29). The width of the ellipses were also observed to increase which can suggest that there is a change in the phase lag, probably brought about by the sample undergoing crystallisation. The interpretation of phase lag should be done with care as a change can also be caused by factors such as asymmetry of the reference and sample pan placement and uneven purge gas.

Table 4.4 *Measured crystallisation temperatures for indometacin and Gelucire 44/14 SSD systems using QIMTDSC reversing heat capacity versus time and Lissajous analysis.*

System	Indometacin Loading (%w/w)	Crystallisation Temp: Reversing Cp (^{o}C)	Crystallisation Temp: Lissajous (^{o}C)
SSD(20)	5	21.3 ± 1.5	21.3 ± 1.5
	10	24.6 ± 0.6	24.8 ± 0.3
	15	22.3 ± 2.4	22.3 ± 2.4
	50	None	None
SSD(4)	5	21 ± 4.6	21 ± 4.6
	10	22.2 ± 2.8	22.2 ± 2.8
	15	24.3 ± 0.6	24.0
	50	None	None

Reproducibility of the detected crystallisation temperatures for formulations of the SSD(20) and SSD(4) systems was found to be poor, occurring at a different temperature for each of the repeated samples (Table 4.4). On the whole, however, the crystallisation temperature was reduced, from that observed for Gelucire 44/14 alone (31^{o}C), most significantly by the 5% w/w formulation. The 10 and 15% systems demonstrated a reduction in crystallisation temperature to a lesser extent.

4.4.5 Observation of Thermal Transitions by Hot Stage Microscopy

Observation of the SSD systems using HSM demonstrated that at 5% w/w no crystalline indometacin was present (Figure 4.30 b and d). It should be noted that the dark areas observed in these images were not indometacin crystals. They did not melt at the indometacin melting temperature, and were most probably dirt on the slide or lens and therefore should be discounted. The absence of visible indometacin crystals confirmed that dissolution during analysis did not contribute to the absence of a drug melting endotherm in both conventional and hyper DSC data, and that the solubility of indometacin in Gelucire 44/14 is greater than 5% w/w.

At 50% w/w, indometacin crystals were very dense in the formulation (Figure 4.30 c and e), however these crystals began to dissolve into the molten Gelucire 44/14 well below their own melting temperature of 160^{o}C, thus confirming the presence of dissolution effects caused by slow heating rates. Dissolution of the crystals appeared to be complete by approximately 150^{o}C in both systems i.e. melting point depression as observed using thermal analysis.

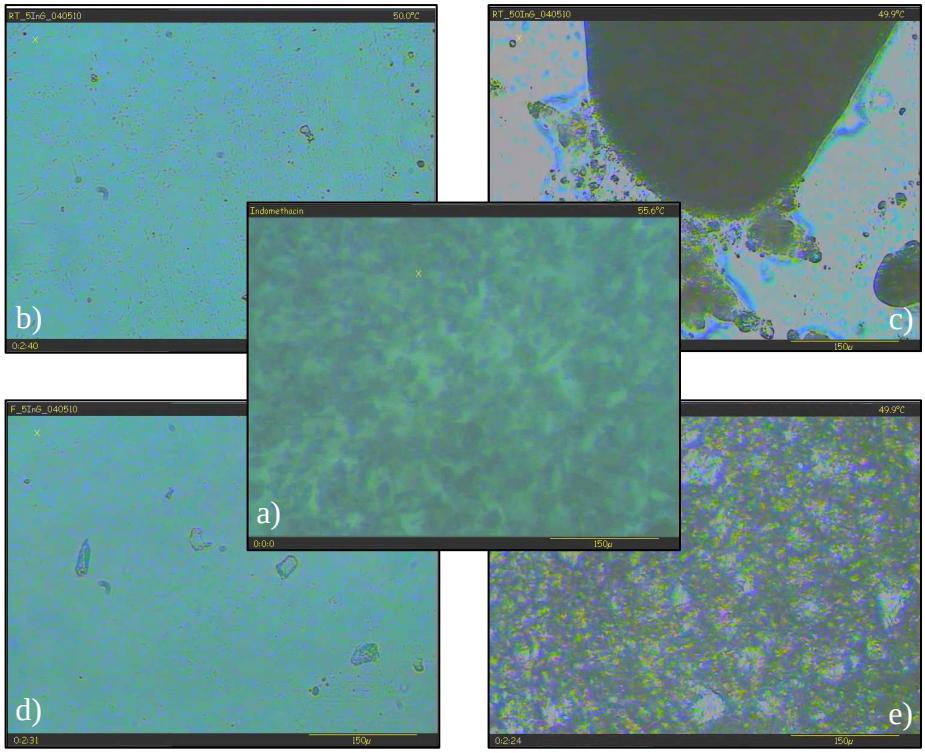

Figure 4.30 *HSM images of a) indometacin, b) SSD(20) 5%, c) SSD(20) 50%, d) SSD(4) 5% and e) SSD(4) 50% at 50°C in order to visualise only crystalline indometacin.*

4.4.6 Summary of Indometacin and Gelucire 44/14 Semi-Solid Dispersion System Characterisation Studies

Characterisation of indometacin and Gelucire 44/14 SSD systems using thermal analysis techniques has given an insight into the physical state of the incorporated constituents. When investigated at slower heating rates using conventional DSC, dissolution effects during analysis of physical mixes brought about the absence of indometacin melting endotherms at 5 and 10% w/w. At higher drug loading, changes could be observed to the melting endotherm suggesting interaction with Gelucire 44/14 occurring during analysis, possibly due to potential hydrogen bonding between

the two components. Solid dispersions demonstrated indometacin melting endotherms only at 50% w/w however the presence of a solid solution at lower drug loadings could not be attributed to either dissolution into the lipid during analysis or during formulation at this point. Analysis using hyper DSC confirmed that the absence of indometacin melting peaks at the lower drug loadings were contributed to by dissolution effects during analysis by demonstrating peaks at 10 and 15% w/w. The crystalline indometacin concentration versus the indometacin melting ΔH plot closely followed the model proposed by Qi et al (2010b) however subsequent calculation of SSD indometacin molecular dispersion content of 50% formulations showed a value in the range of 12 to 17% w/w suggesting a the dissolution of a standard amount of indometacin in all cases. The solubility of indometacin in Gelucire 44/14 was also calculated to be 25% w/w, just above the molecular dispersion value, with Gelucire 44/14 solubility in molten indometacin being 60% w/w. QIMTDSC data confirmed the decrease in temperature of the Gelucire 44/14 crystallisation transition as observed for ibuprofen.

4.5 PIROXICAM AND GELUCIRE 44/14 SEMI-SOLID DISPERSION SYSTEMS

In this section, formulations of the lipidic carrier Gelucire 44/14 with the model drug piroxicam, a BSC Class II drug, were investigated.

4.5.1 Assessment of Thermal Properties using Conventional Differential Scanning Calorimetry

4.5.1.1 Analysis of Raw Materials

Upon heating, crystalline piroxicam displayed a sharp melting endotherm at $Tm_{(onset)}$ 201.8°C ± 0.2, $Tm_{(max)}$ 202.3°C ± 0.06 and ΔH 108.3 J/g ± 1.6. This data will act as a comparison on which to base any observed changes to the melt as part of a physical mix or SSD.

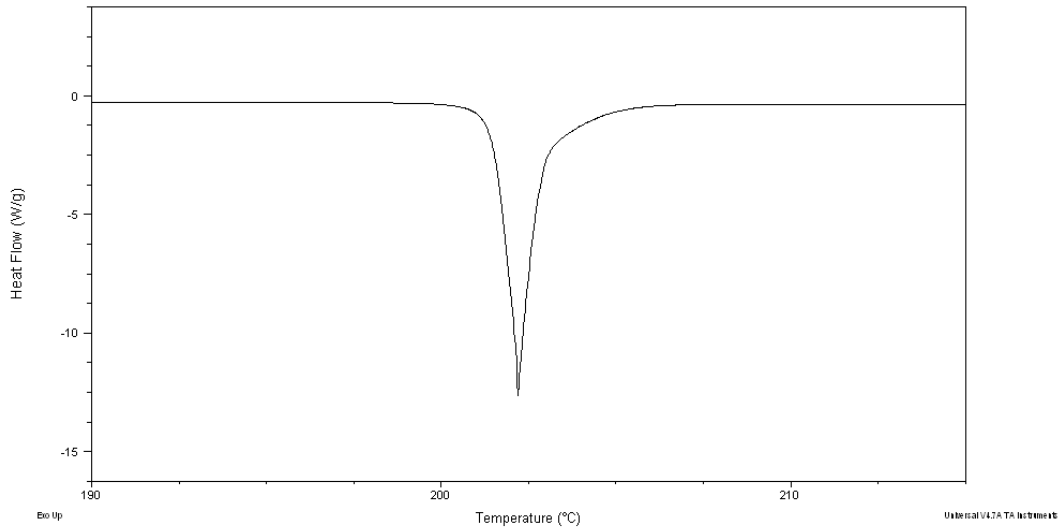

Figure 4.31 *Heat flow against temperature signal of the piroxicam melting endotherm on heating at 10°C/minute.*

4.5.1.2 Analysis of Physical Mixes

Representative samples of piroxicam and Gelucire 44/14 physical mixes, analysed using conventional DSC, are demonstrated in Figure 4.32. The $Tm_{(onset)}$ and $Tm_{(max)}$ values of the Gelucire 44/14 double melting endotherms remained stable over the increasing piroxicam concentrations. These values also corresponded well with those of the lipid alone, thus confirming the absence of any interaction between the two components prior to analysis.

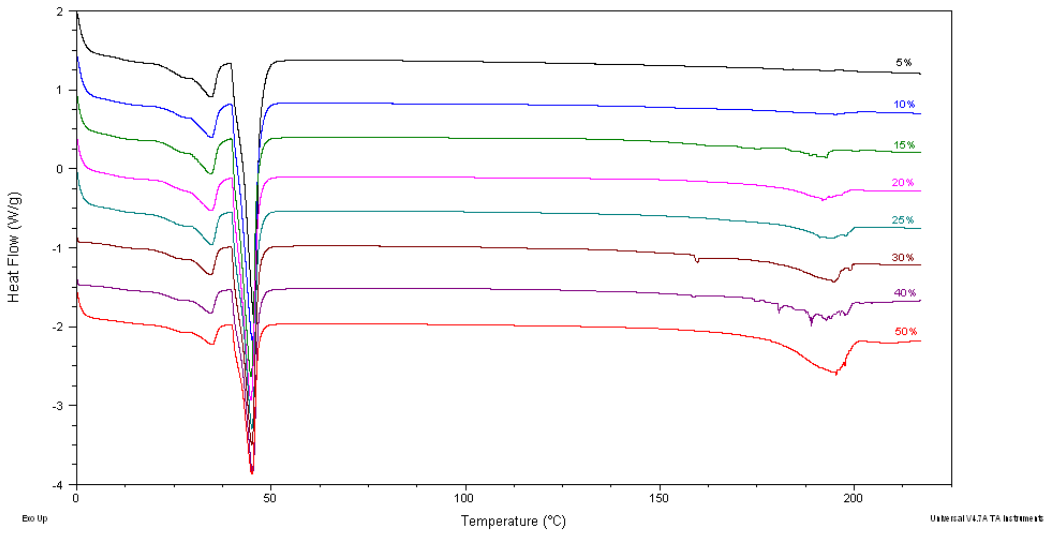

Figure 4.32 *Heat flow against temperature signal of piroxicam and Gelucire 44/14 physical mixes on heating at 10°C/minute.*

Piroxicam melting endotherms could be detected from 10% w/w and above. The baseline around this peak tended to be noisy however it was still possible to measure usable ΔH values. These values increased with increasing piroxicam concentration. No particular pattern of change was noted for the $Tm_{(onset)}$ and $Tm_{(max)}$ values which remained in the region of 183 and 190°C, both of which are well below those of the

crystalline drug alone, thus suggesting interaction with the molten lipid during analysis.

The absence of a piroxicam melting endotherm at 5% w/w suggests either the complete dissolution of the crystalline drug during analysis, or the limit of detection of the instrument lies above the mass of the drug in the mix. If the former is the case, then it is reasonable to assume that the measured ΔH values for the drug melting endotherms of the higher loading mixes may be contributed to by an unknown extent of dissolution into the lipid during analysis, as suggested by the Qi model.

4.5.1.3 Analysis of Semi-Solid Dispersion Systems

SSD formulations of piroxicam and Gelucire 44/14, upon heating, demonstrated the characteristic lipid melting endotherm (Figure 4.33). With increasing drug concentration, the $Tm_{(onset)}$ and $Tm_{(max)}$ remained consistent at 29.1°C ± 0.7 and 35.3°C ± 0.3, 40.1°C ± 0.1 and 43.5°C ± 0.2; and 28.9°C ± 1.1 and 34.9°C ± 0.9, 40.1°C ± 0.05 and 43.4°C ± 0.1 for SSD(20) and SSD(4) respectively. These values corresponded very closely with those of the lipid alone. The lipid double melting endotherm appeared to remain unchanged by formulation into an SSD with crystalline piroxicam, possibly due to low compatibility between the two components.

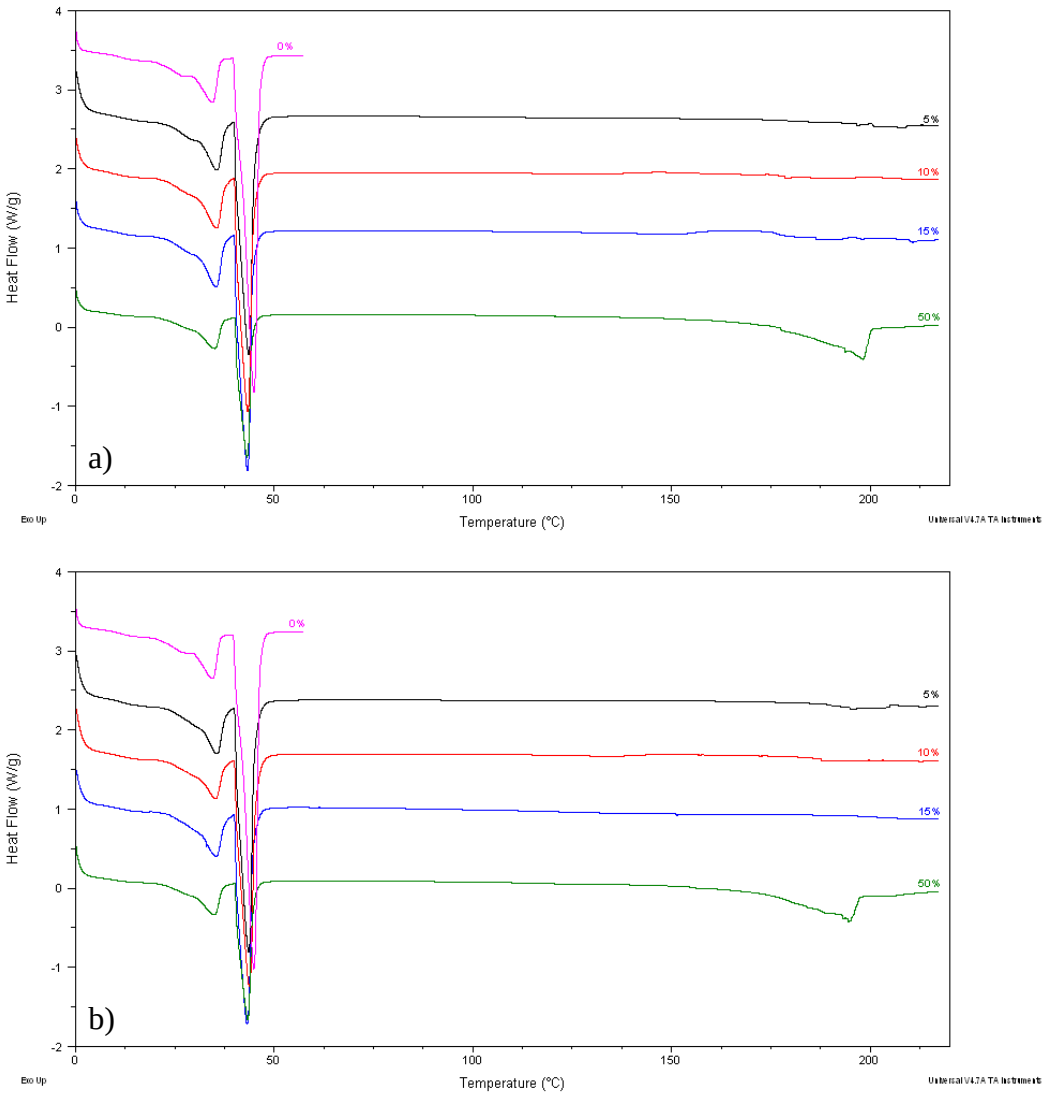

Figure 4.33 *Heat flow against temperature signal on heating at 10°C/minute of piroxicam and Gelucire 44/14 a) SSD(20) and b) SSD(4) – First melt.*

Measurable crystalline piroxicam melting peaks, with a $Tm_{(max)}$ between 185 and 202°C, were detected in all cases, increasing in ΔH with increasing drug concentration. In general, the baseline around the crystalline piroxicam melting peak was found to exhibit a degree of noise making confident measurement more difficult.

At 10 and 15% w/w, in addition to a piroxicam melting peak at the lower temperature of circa 187°C, another endotherm was observed, occurring in the region

of 110°C at 10% and 124°C at 15% w/w (Figure 4.34). These additional endotherms, despite the integration values of which being variable in nature, were found to occur in all repeat samples for these formulations. It is known that piroxicam can display polymorphism and it is unknown how many different forms exist (Vrečer et al. 1991). It may be possible that, during formulation, conversion to an alternative polymorphic form may have been induced by the kinetic energy of the process. Another possibility may be that piroxicam present as a molecular dispersion may have crystallised during cooling into a metastable form.

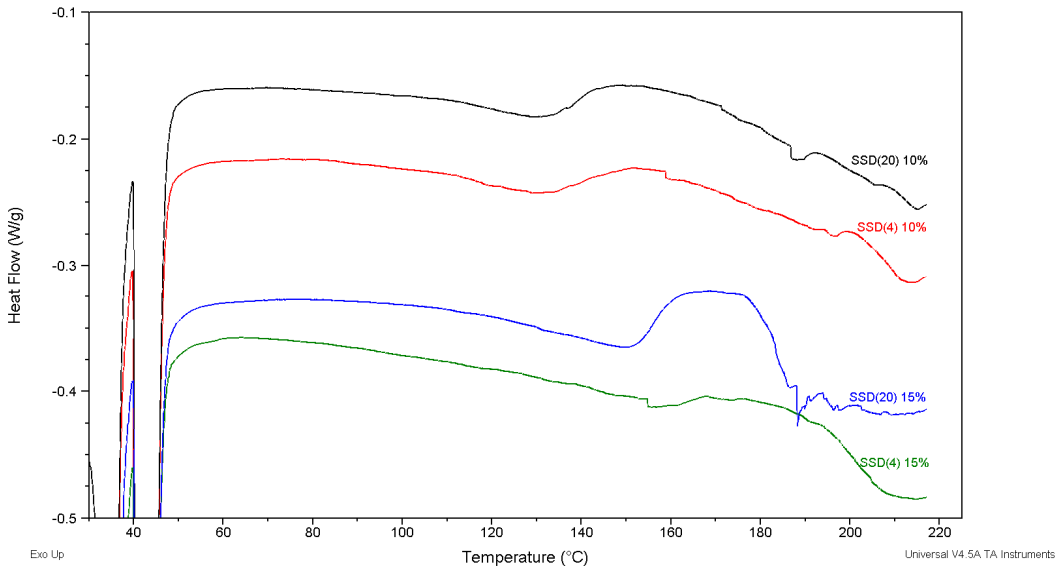

Figure 4.34 *Heat flow against temperature signal on heating at 10°C/minute of piroxicam and Gelucire 44/14 SSD – First piroxicam melt at 10 and 15% w/w magnified.*

An endothermic peak was also observed in similar formulations of piroxicam and Gelucire 44/14 by Karataş et al (2005) who suggested it may be attributable to an interaction between the benzothiazine ring -OH group of piroxicam with the fatty acid esters of the lipid, initiated by applied heat during the formulation process.

At 50% w/w, the broad piroxicam melting endotherm was found to occur at approximately 196^{o}C $Tm_{(max)}$ for both SSD systems. This reduced temperature may be attributable to melting point depression brought about by interaction of the piroxicam with Gelucire 44/14. It could also be due to the creation of an alternative polymorphic crystalline formation with a melting point of 195^{o}C as noted by Vrečer et al (1991).

Upon cooling of the molten SSD systems, the 50% w/w formulations of both the SSD(20) and SSD(4) systems demonstrated no obvious crystallisation. At 5 to 15%, both the $Tm_{(onset)}$ and $Tm_{(max)}$ of the transition were found to decrease, in comparison with Gelucire 44/14 alone, with increasing piroxicam concentration (Figure 4.35). As suggested previously in this Chapter, this effect may be due to the molten drug acting as a diluent, thereby reducing the nuclei concentration and decreasing crystallinity of the system (Long et al. 1995). In all cases, with the exception of 50%, a leading peak was present at a temperature corresponding with the $Tc_{(max)}$ of crystallisation of the lipid alone suggesting formation of the original Gelucire 44/14 crystal arrangement (Lloyd et al 1997). In addition to this, the formulations appeared to form another crystal entity, indicated by the shoulder of the main peak. This peak became less prominent and lower in temperature with increasing drug loading, being completely absent by 15%. It should also be noted that again, as seen for indometacin systems, the crystallisation peaks were uncharacteristically sharp in nature.

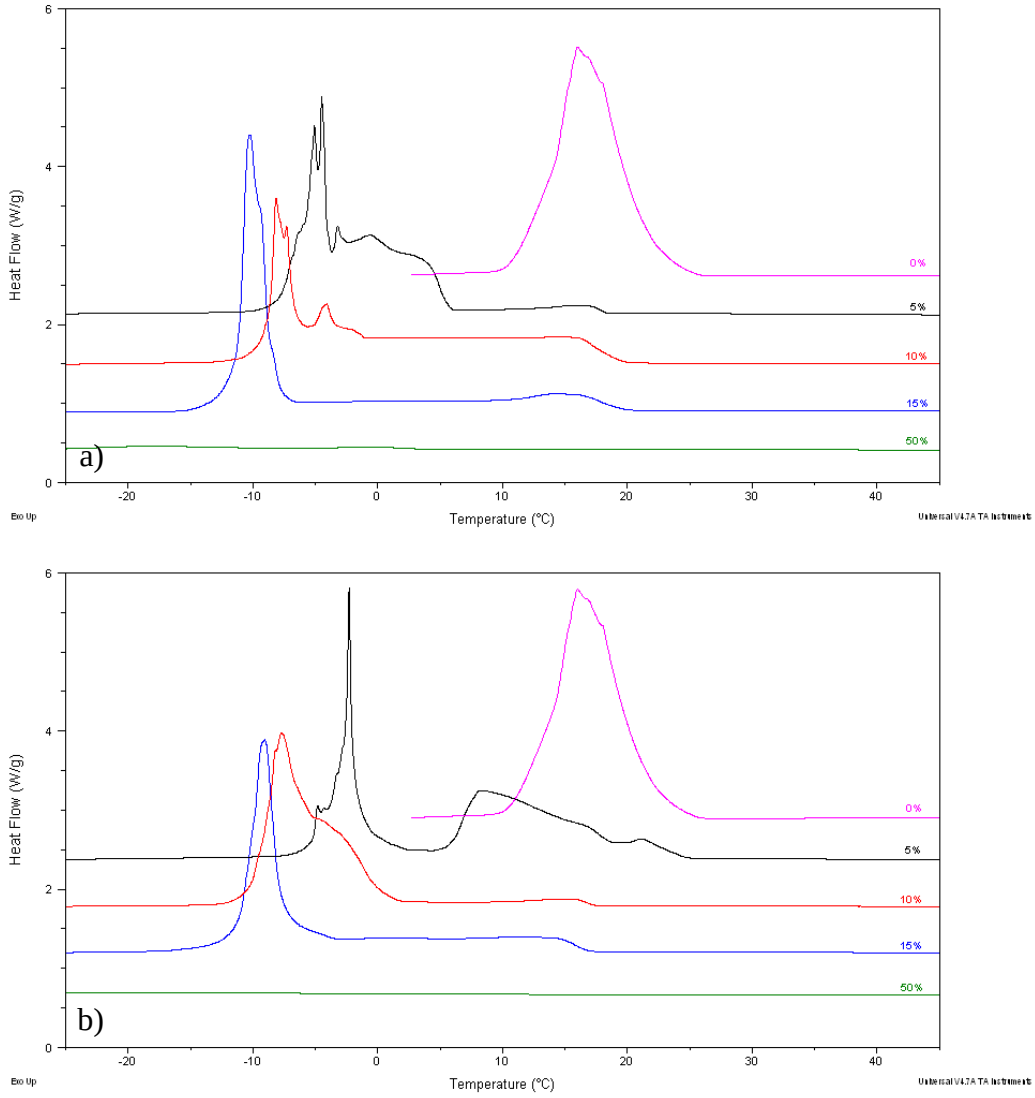

Figure 4.35 *Heat flow against temperature signal on heating at 10°C/minute of piroxicam and Gelucire 44/14 a) SSD(20) and b) SSD(4) – Crystallisation.*

Re-heating of the SSD systems demonstrated an endothermic transition in the region of 20 to 50°C in all cases, most likely attributable to melting of re-crystallised Gelucire 44/14 (Figure 4.36). At 5% w/w, the endotherm was unchanged from that of Gelucire 44/14 alone, confirming its presence and crystal formation in the system, and also the lack of interaction with piroxicam. At 10%, the secondary peak became more prominent, with the primary peak being completely absent at 15%. The ΔH was found to decrease with increasing drug loading. This may suggest a closer proximity

between the piroxicam and Gelucire 44/14 on a molecular level than the complete lack of interaction observed upon initial melting, promoted by melting both components together. The interaction appeared to occur with the higher melting point fractions of the lipid, suggested by the disappearance of the primary melting endotherm, with the effect becoming more prominent with increasing drug loading.

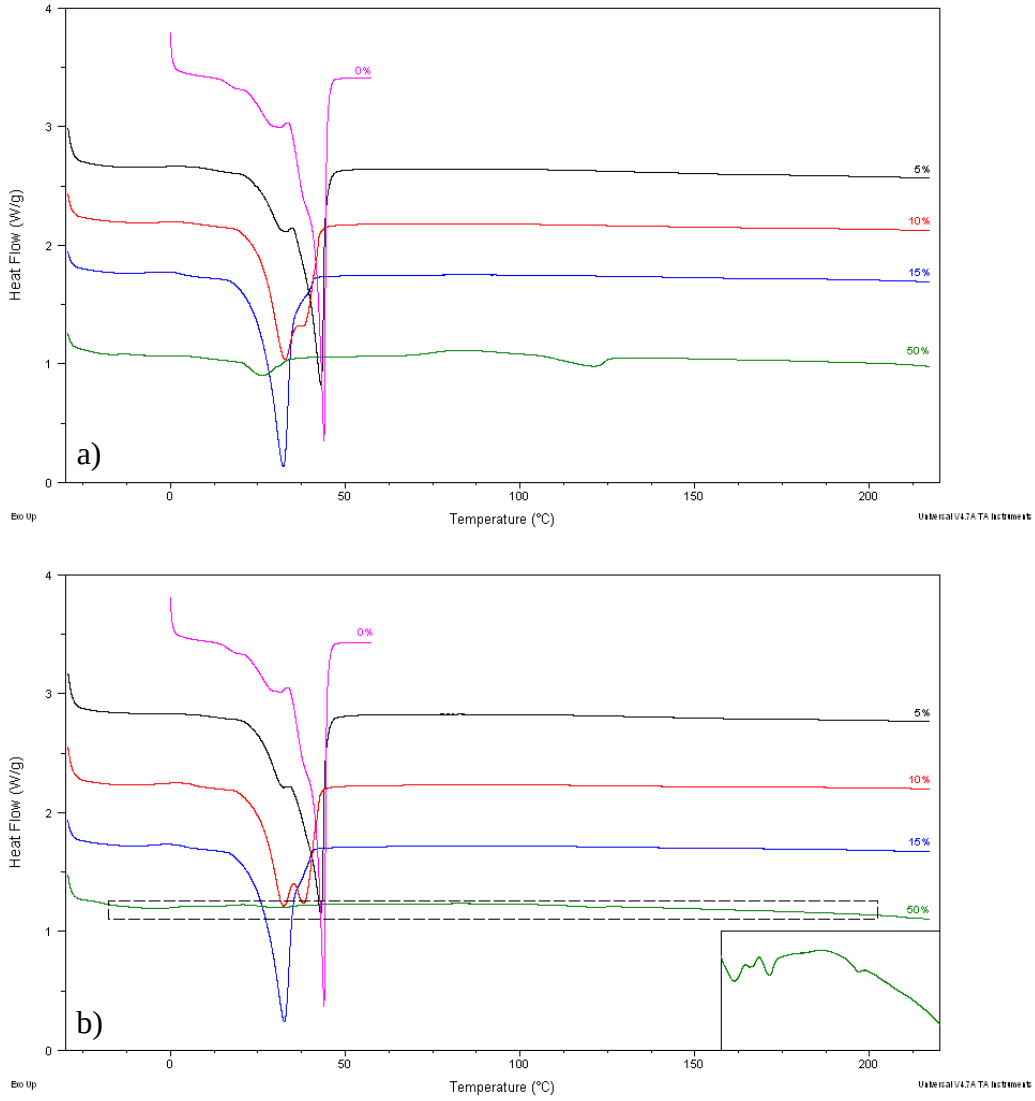

Figure 4.36 *Heat flow against temperature signal on heating at 10°C/minute of piroxicam and Gelucire 44/14 a) SSD(20) and b) SSD(4) – Second Melt.*

The 15% w/w formulation of the SSD(20) system and the 5 to 15% formulations of the SSD(4) systems demonstrated a small endothermic peak at approximately 157^{o}C and all of similar ΔH which may be attributable to the melting of a new piroxicam polymorph created after melting and cooling.

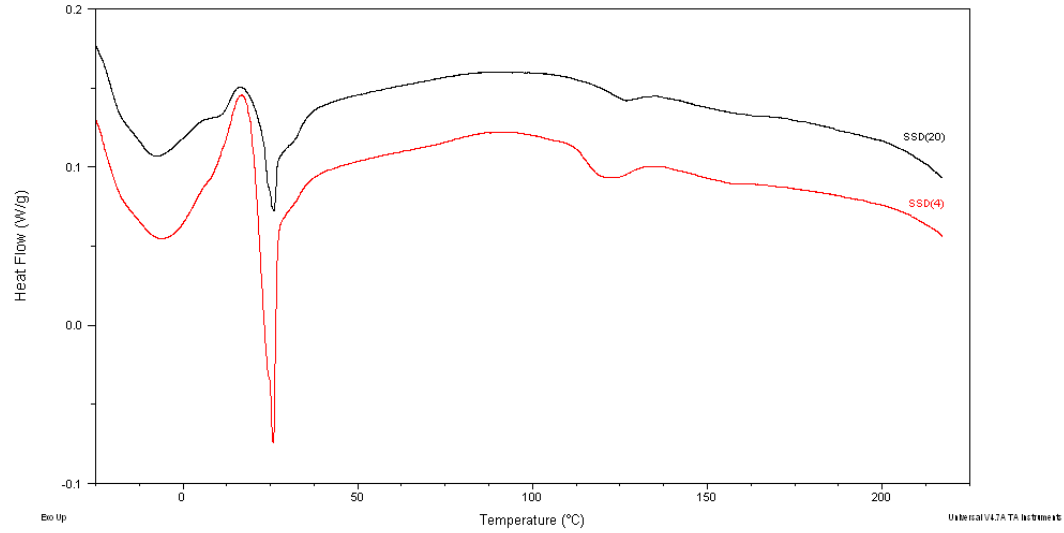

Figure 4.37 *Heat flow against temperature signal of piroxicam and Gelucire 44/14 50% SSD systems – Second Melt magnified.*

At 50% piroxicam loading, no crystallisation peak was detected upon cooling however a possible melting peak, at $Tm_{(max)}$ 17^{o}C, was present during re-heating in the region of Gelucire 44/14 melting (Figure 4.37). The $Tm_{(max)}$ was found to occur at 26.1^{o}C ± 0.3 and 27.6^{o}C ± 2.7 for SSD(20) and SSD(4) respectively. In addition to this lipidic melting peak, a small peak was detected at 123.3^{o}C ± 3.0 for SSD(20) and 119.7^{o}C ± 0.6 for SSD(4) systems, with an ΔH larger in that of the SSD(20) formulations at 2.7 J/g ± 3.2 in comparison with 0.5 J/g ± 0.5 for SSD(4). This additional peak may be attributable to a new polymorph of piroxicam, crystallising from the amorphous form. It is possible that the formation of microcrystals occurred upon cooling which was undetectable using thermal analysis in this case, the melting

of which was able to overcome the instrument detection limit and therefore demonstrating an endotherm on the DSC plot.

4.5.2 Assessment of Thermal Properties using Hyper (Fast Speed) Differential Scanning Calorimetry

4.5.2.1 Analysis of Raw Materials

Under analysis at fast heating rates, crystalline piroxicam demonstrated a melting endotherm on heating, occurring at $Tm_{(onset)}$ 198.9^{o}C ± 0.6 and $Tm_{(max)}$ 206.1^{o}C ± 1.3. The $Tm_{(onset)}$ value corresponded closely to that of the drug at slower heating rates, as described above, falling within a couple of degrees. The ΔH of the endotherm was also found to be comparable, at 102.3 J/g ± 0.6. The peak was however much broader, increasing the $Tm_{(max)}$ by approximately 4^{o}C.

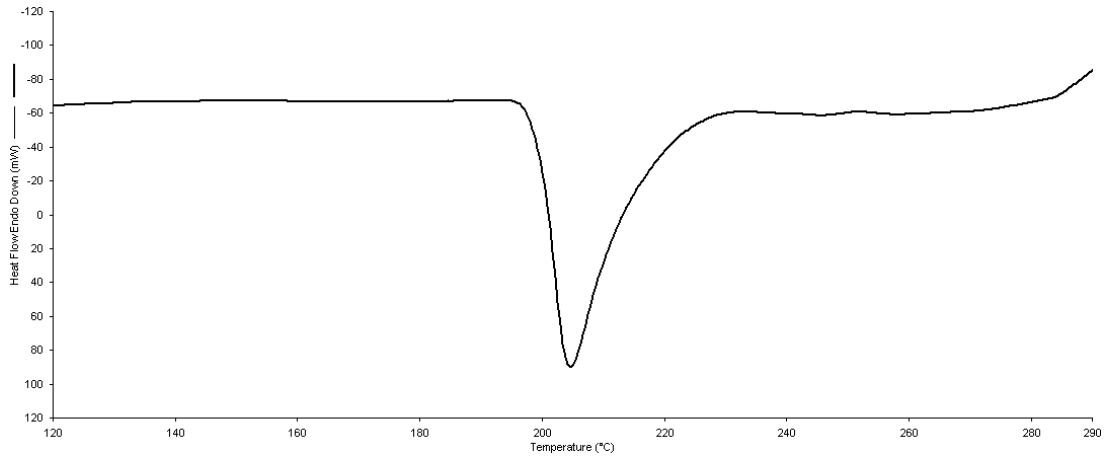

Figure 4.38 *Heat flow against temperature signal of the piroxicam melting endotherm on heating at 500^{o}C/minute.*

4.5.2.2 Analysis of Physical Mixes

Overall, on heating, the Gelucire 44/14 melting endotherm remained generally unchanged for the physical mixes, with an $Tm_{(onset)}$ of 37.5°C ± 1.7 and $Tm_{(max)}$ of 55.5°C ± 1.1, comparable to that of the lipid alone. This indicated the absence of any prior interaction with piroxicam. Peak ΔH was found to decrease with increasing piroxicam concentration. A piroxicam melting endotherm could be detected in all cases, being reproducible between repeated samples and also with increasing loading ($Tm_{(onset)}$ 197.3°C ± 1.2; $Tm_{(max)}$ 204.6°C ± 1.8), thus also confirming that no interaction had taken place between the two components. The ΔH of these peaks increased with piroxicam concentration.

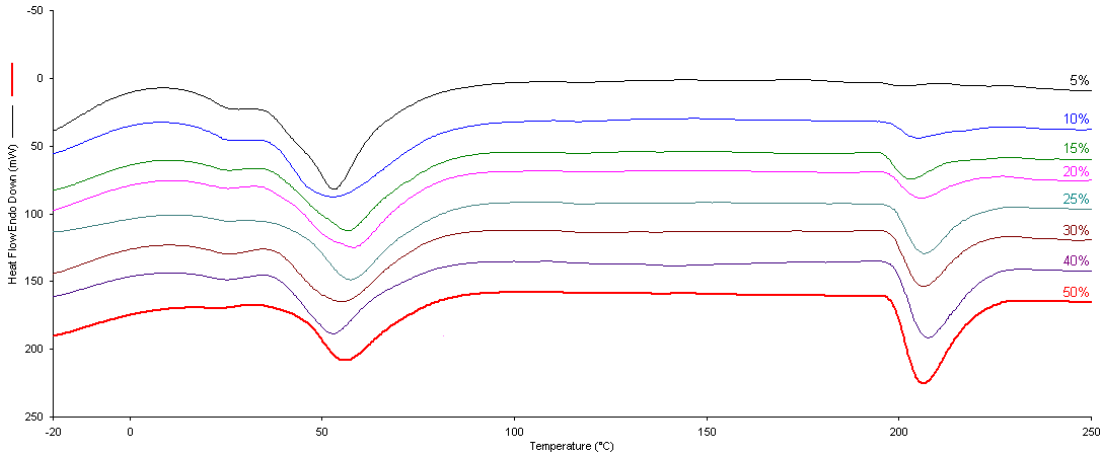

Figure 4.39 *Heat flow against temperature signal of piroxicam and Gelucire 44/14 physical mixes on heating at 500°C/minute.*

4.5.2.3 Analysis of Semi-Solid Dispersion Systems

Analysis of Gelucire 44/14 and piroxicam SSD systems at 500°C/minute demonstrated that the lipid melting endotherm remained a similar shape to that of the lipid alone, as the drug concentration increased. However, despite the $Tm_{(onset)}$ being increased from 33.5°C for the lipid alone to 39.3°C ± 0.9 and 38.5°C ± 1.0 for the SSD(20) and SSD(4) systems respectively, the $Tm_{(max)}$ was comparable in both cases for all formulations.

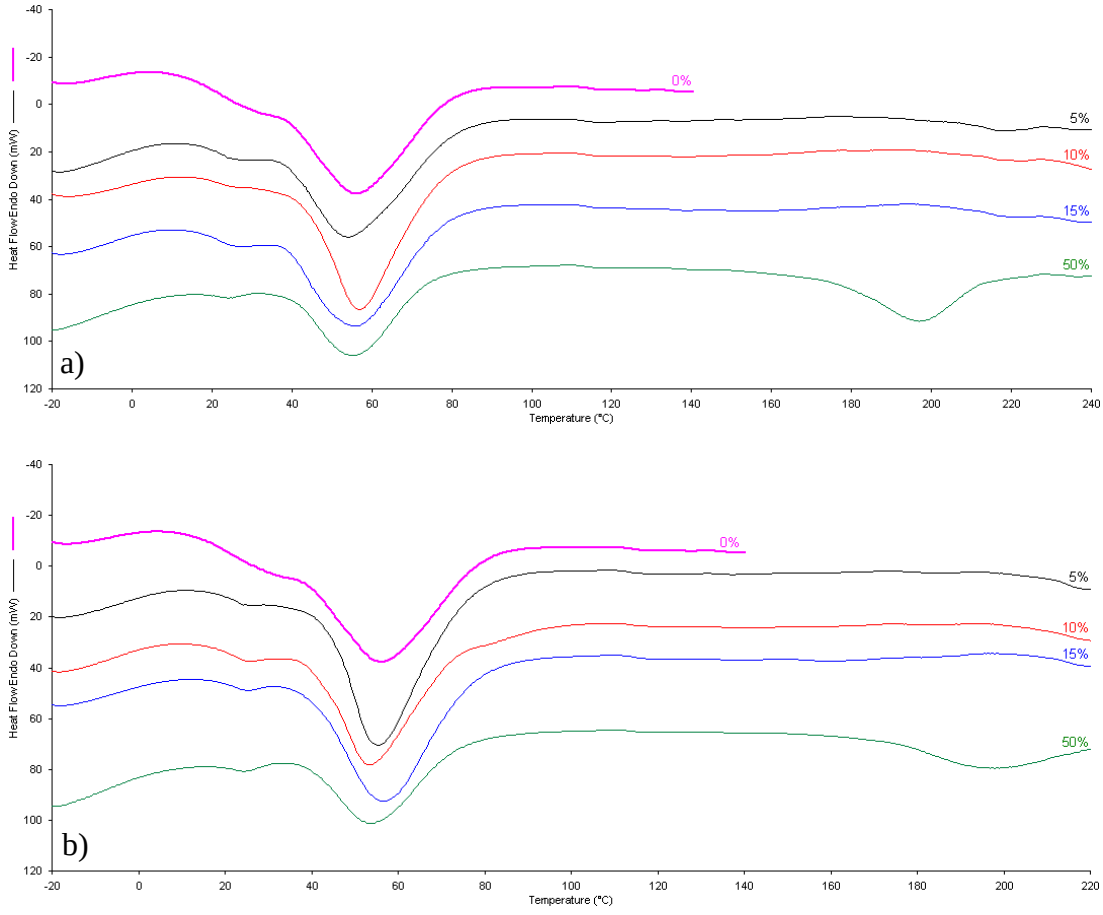

Figure 4.40 *Heat flow against temperature signal of piroxicam and Gelucire 44/14 a) SSD(20) and b) SSD(4) on heating at 500°C/minute.*

A piroxicam melting endotherm could be detected at all drug concentrations. At 5 to 15% w/w drug concentration, the peak was found to occur at a $Tm_{(onset)}$ and $Tm_{(max)}$ significantly higher that observed for the drug alone ($Tm_{(onset)}$ 198.9^{o}C; $Tm_{(max)}$ 206.1^{o}C). The values corresponded closely between formulations at $Tm_{(onset)}$ approximately 210^{o}C and $Tm_{(max)}$ approximately 218^{o}C for the SSD(20) systems, as did those for SSD(4) at $Tm_{(onset)}$ approximately 211^{o}C and $Tm_{(max)}$ approximately 219, with the exception of 15% $Tm_{(onset)}$ at 213^{o}C. It should be considered that this increased piroxicam melt (particularly the $Tm_{(onset)}$, as the $Tm_{(max)}$ would increase due to peak broadness at fast heating rates) may be attributable to a different polymorphic form, the conversion to which was brought about during manufacture. This was not, however, observed at slower heating rates suggesting that any conversion taking place does not occur during manufacture but during analysis. In theory however any change occurring in the sample should be reduced the faster the analysis takes place. The measured ΔH values were found to be equally small for 5 to 15% formulations with no particular pattern of change. Again, the values obtained using this technique were found to be variable.

At 50% w/w, the piroxicam melting endotherm was observed to occur at a lower temperature than that of the lower drug loaded formulations and also of the drug alone at an $Tm_{(onset)}$ of approximately 175^{o}C and a $Tm_{(max)}$ of approximately 197^{o}C. Such a melting point depression was also noted for the SSD systems analysed using conventional DSC and attributed to possible interaction with the molten lipid during analysis.

4.5.3 Comparison of Conventional and Hyper Differential Scanning Calorimetry Data

Upon examination of the piroxicam and Gelucire 44/14 physical mixes using conventional and hyper DSC (Figures 4.41 and 4.42), it was apparent that the measured drug melt ΔH values again followed the model proposed by Qi et al (2010b).

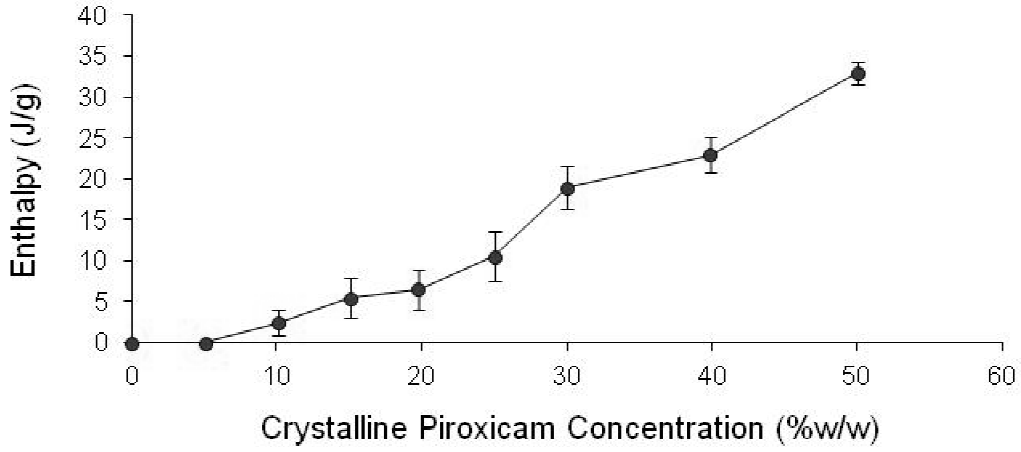

Figure 4.41 *Crystalline piroxicam content in the physical mix against the measured piroxicam melt enthalpy analysed on heating at 10°C/minute.*

At 500°C/minute, the melt ΔH versus crystalline concentration plot demonstrated two of the three phases suggested by the model indicating that the point of Gelucire 44/14 solubility in piroxicam had not been reached, therefore being lower than 50% w/w. This was not unexpected as the DSC data did suggest low compatibility of the two components. Piroxicam solubility in Gelucire 44/14 could however be estimated as 10% w/w. This plot was used for the purposes of determining the crystalline piroxicam concentration in the formulated SSD systems, and subsequently the

amount, if any, present as a solid solution or molecular dispersion. It was assumed that this data represented a more accurate estimation of the true physical state of drug in the SSD system since the fast heating rate reduced, but not eliminated, dissolution into the molten lipid during analysis.

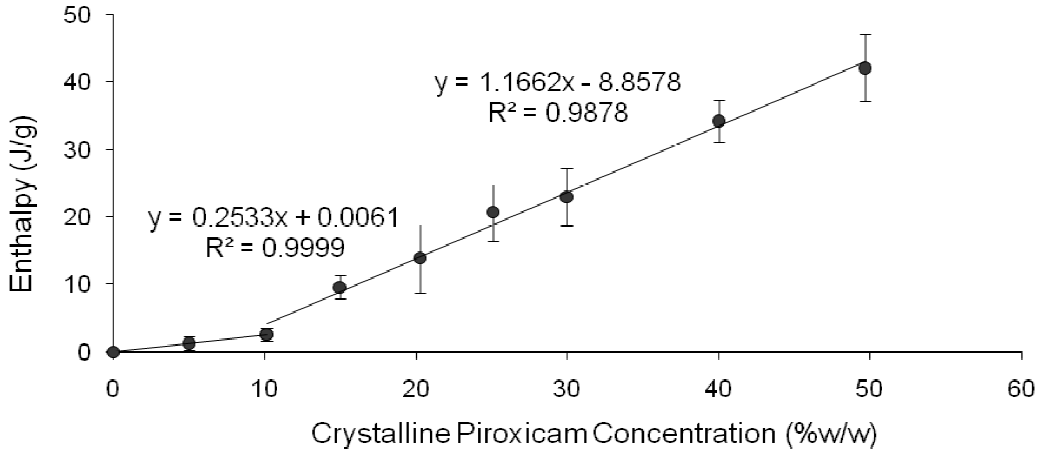

Figure 4.42 *Crystalline piroxicam content in the physical mix against the measured piroxicam melt enthalpy analysed on heating at 500°C/minute.*

All SSD systems, at both 10 and 500°C/minute, demonstrated a piroxicam melt endotherm, from 5 to 50% w/w. Table 4.5 does however highlight that, in all cases, the drug melt ΔH, and subsequently the crystalline concentration, was reduced when analysed at 500°C/minute in comparison with those measured at 10°C/minute which was unexpected. If the fast heating rate was reducing drug dissolution into the lipid during analysis, the crystalline melt ΔH should have been greater. This again demonstrateed that speeds greater than those employed in this study may be required in order to overcome drug dissolution effect into the carrier material during analysis.

Table 4.5 *Calculated crystalline (Cryst.) and molecular (Mol.) piroxicam content of SSD systems.*

System	Heating Rate (°C/min)	Pirox Conc (%w/w)	Enthalpy (J/g)	Cryst. Pirox Dispersion (%w/w)	Mol. Pirox Dispersion (%w/w)
SSD(20)	10	5	3.2 ± 0.6	10.3	0
		10	1.9 ± 1.7	7.3	2.7
		15	3.6 ± 2.3	10.7	4.3
		50	32.2 ± 2.8	38.6	11.4
	500	5	1.3 ± 0.8	5.2	0
		10	3.3 ± 3.8	10.4	0
		15	2.1 ± 2.0	8.3	6.7
		50	24.3 ± 4.5	29.9	20.1
SSD(4)	10	5	2.8 ± 1.8	10.0	0
		10	4.1 ± 1.3	11.1	0
		15	3.7 ± 1.1	10.8	4.2
		50	28.4 ± 2.9	34.4	15.6
	500	5	1.9 ± 1.6	7.5	0
		10	1.4 ± 0.2	5.4	4.6
		15	0.4 ± 0.05	1.4	13.6
		50	23.5 ± 9.1	29.0	21.0

The extent to which piroxicam was molecularly dispersed within Gelucire 44/14 was found to increase with increasing piroxicam loading into the SSD formulation. Piroxicam demonstrated a lower solubility of 10% w/w in the lipid when in comparison with ibuprofen (20% w/w) and indometacin (25% w/w). Reaching a

value of 21% molecular dispersion within Gelucire 44/14 would therefore be unexpected, especially since at low piroxicam concentrations there appeared to be no molecular dispersion. As discussed previously, it is likely that the drug melting endotherm observed upon heating of the SSD systems may be attributable to not only melting of the crystalline drug alone, but its dissolution into the carrier excipient. It may also be possible that the endotherm ΔH is contributed to by dissolution of the lipid into the high concentration of molten drug. This would bring about an increase in the measured ΔH value and a therefore a subsequent increase in the calculated content of what was assumed to be solely molecularly dispersed piroxicam making interpretation of this value incorrect.

4.5.4 Crystallisation Analysis using Quasi-Isothermal Modulated Temperature Differential Scanning Calorimetry

The piroxicam and Gelucire 44/14 SSD systems were analysed using QIMTDSC in order to further characterise the effect of drug on crystallisation of the lipidic carrier. As with the other two model drugs, piroxicam was also found to significantly reduce the measured crystallisation temperature of Gelucire 44/14, independent of heating rate, to 25^{o}C and below. The reversing heat capacity time plot also demonstrated the noted energetic primary crystallisation followed by a slower more extended period of secondary crystallisation continuing to much lower temperatures, as observed for the lipid alone (Figure 4.43).

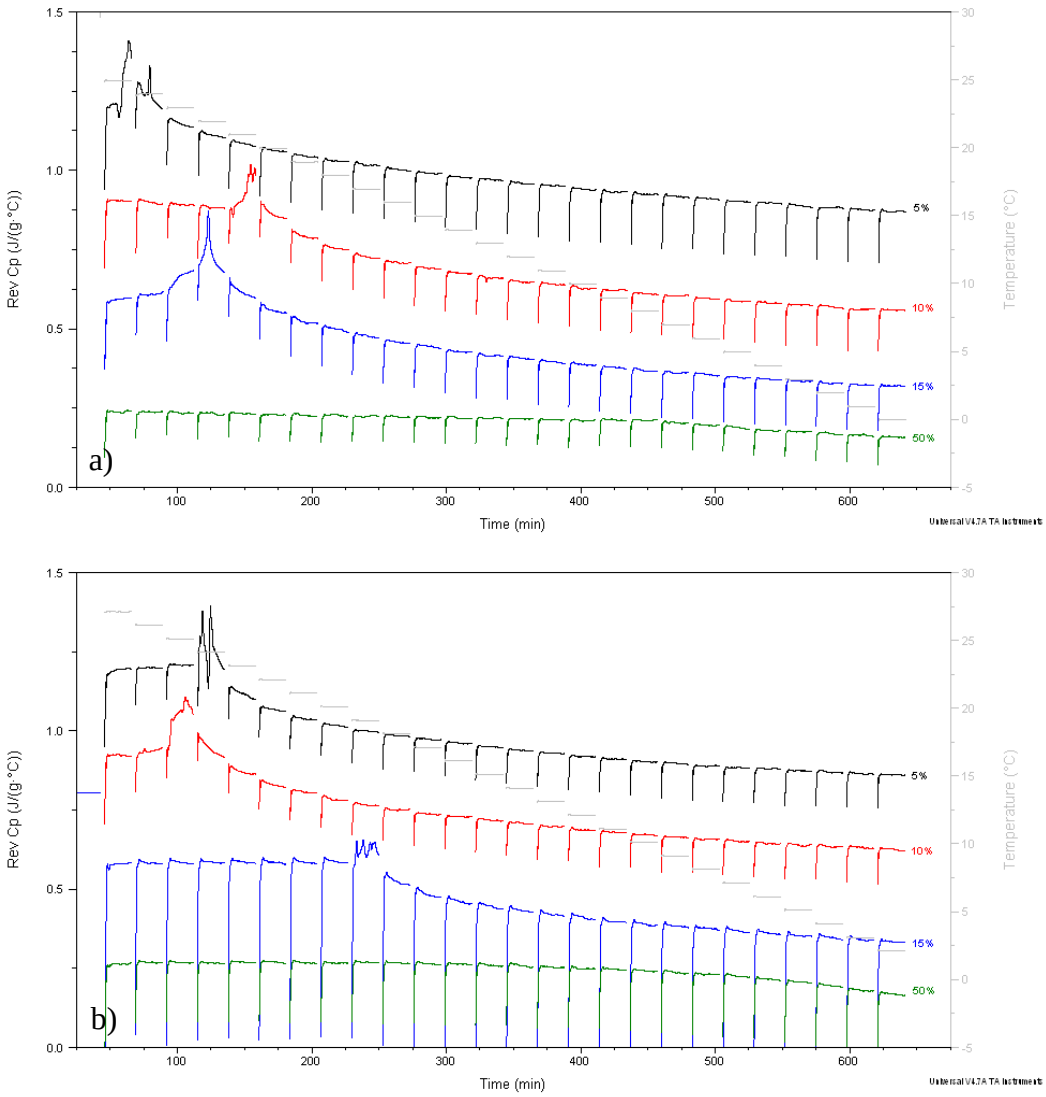

Figure 4.43 *Reversing heat capacity versus time signal for piroxicam and Gelucire 44/14 a) SSD(20) and b) SSD(4) QIMTDSC 20 minute isotherm on cooling with 1°C increments.*

Isolation of the Lissajous figures allowed the sine wave modulations to be monitored for any deviation from the equilibrium or steady state. Representative samples can be seen in Figure 4.44. On the whole, the detected crystallisation temperatures corresponded well with those observed from the reversing heat capacity time plots. Reproducibility between repeated samples was however found to be poor (Table 4.46).

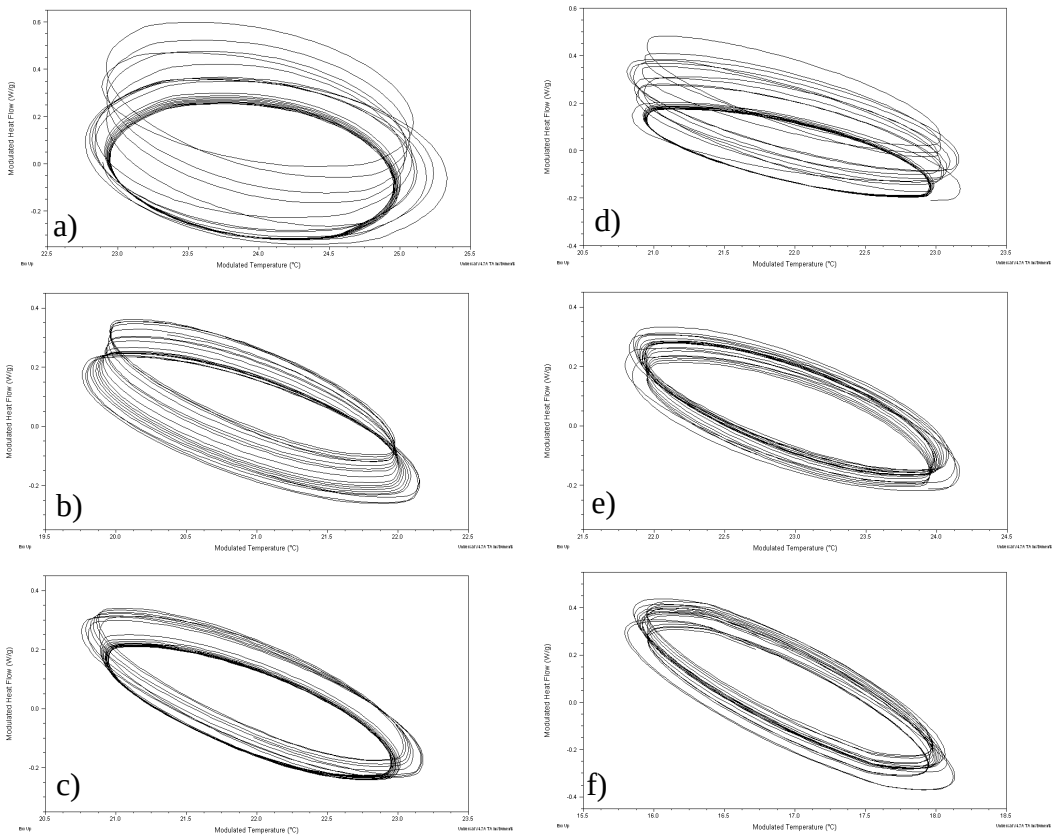

Figure 4.44 *Lissajous figures of the sine wave heat flow modulations (crystallisation) of piroxicam and Gelucire 44/14 SSD systems; SSD(20) a) 5% b) 10% c) 15% and SSD(4) d) 5% e) 10% f) 15%.*

In all samples, the major slope was found to reduce from the start to the conclusion of the experiment, suggesting a subsequent decline in heat capacity. This provided further weight to the argument of a slower, extended period of secondary crystallisation taking place after the initial energetic crystallisation as observed in the reversing heat capacity time plot above.

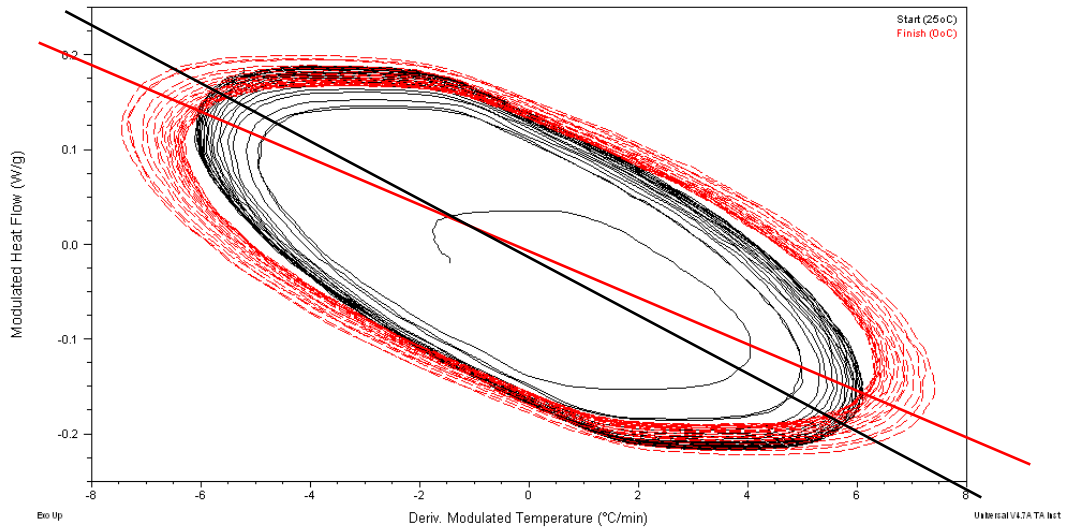

Figure 4.45 *Lissajous figures of the sine wave heat flow modulations of piroxicam and Gelucire 44/14 SSD(20) 10% w/w systems at the start (25°C, black) and finish (0°C, red) of the cooling experiment showing the major slope of each plot.*

Table 4.6 *Measured crystallisation temperatures for piroxicam and Gelucire 44/14 SSD systems using QIMTDSC reversing heat capacity versus time and Lissajous analysis.*

System	Piroxicam Loading (%w/w)	Crystallisation Temp: Reversing Cp (°C)	Crystallisation Temp: Lissajous (°C)
SSD(20)	5	24.0 ± 1.0	23.8 ± 0.8
	10	19.7 ± 2.3	19.7 ± 2.3
	15	22.7 ± 0.6	23.2 ± 1.1
	50	None	None
SSD(4)	5	21.3 ± 3.1	21.3 ± 3.1
	10	21.7 ± 3.2	21.7 ± 3.2
	15	18.3 ± 4.2	20.0 ± 4.2
	50	None	None

4.5.5 Observation of Thermal Transitions by Hot Stage Microscopy

HSM of the formulated piroxicam and Gelucire 44/14 SSD systems allowed visualisation of the physical state of the drug. At 5% w/w a large number of piroxicam crystals were present in both the SSD(20) and SSD(4) systems. These crystals began to dissolve immediately post Gelucire 44/14 melting, with the process being complete by approximately 120^{o}C in both cases.

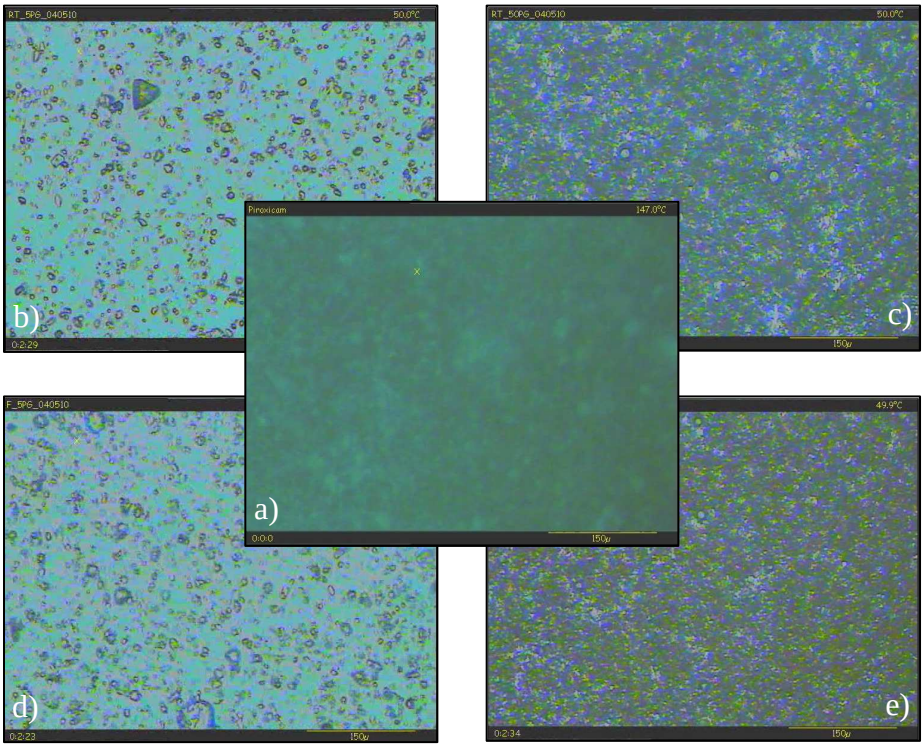

Figure 4.46 *HSM images of a) piroxicam, b) SSD(20) 5%, c) SSD(20) 50%, d) SSD(4) 5% and e) SSD(4) 50% at 50^{o}C in order to visualise only crystalline piroxicam.*

This temperature was lower than that expected in comparison with that measured for conventional DSC This effect highlighted the process by which crystalline drug can dissolve into the molten lipid during DSC analysis at slow heating rates. At 50%

w/w, the drug crystals appeared very dense in the formulation. Again these crystals began to dissolve once in molten lipid, with all signs of solid drug gone by 188 and 194^{o}C for the SSD(20) and SSD(4) systems respectively.

4.5.7 Summary of Piroxicam and Gelucire 44/14 Semi-Solid Dispersion System Characterisation Studies

Considering the DSC data, limited alterations to the thermal properties of either the piroxicam or Gelucire 44/14 were detected. Even after formulation into SSD systems, at low piroxicam concentration, and at slow heating rates, it was possible to detect measurable drug melting endotherms. This suggested that the compatibility between the two components was limited. Analysis of physical mix data at 500^{o}C/minute, to some extent, followed the Qi model in that it demonstrated the first two proposed phases. From this, piroxicam solubility in Gelucire 44/14 could be estimated as 10% w/w. It was however noted that, in general, this fast heating rate gave lower piroxicam melt ΔH values which was unexpected. This subsequently suggested that dissolution effects known to occur during thermal analysis were occurring to a greater extent at the faster heating rate. The hyper DSC data was however found to exhibit poor reproducibility which may contribute to this effect. QIMTDSC data also further confirmed the inhibition of Gelucire 44/14 crystallisation by the presence of molten piroxicam.

4.6 CONCLUSIONS

All the investigated model drug SSD systems with Gelucire 44/14 were found to follow the Qi model to some extent. This therefore does suggest that using faster heating rates does give a more accurate estimation of the actual crystalline content of the SSD systems. However, in the systems studied in this project, the measured ΔH values of the crystalline drug melt at 500^{o}C/minute were found to be similar, if not less, than those measured at 10^{o}C/minute. Despite heating at speeds of 500^{o}C/minute, it proved insufficient to overcome the dissolution effect of drug into the lipidic carrier during analysis since many of the components of Gelucire 44/14 such as PEG, when in the molten state, are good drug solubilisers. A rate of up to 1500^{o}C/minute is most likely required, for systems with this complexity, before a reliable effect can be seen. Nonetheless the model drug solubilities in the lipidic carrier Gelucire 44/14 were approximated to be 20%, 25% and 10% w/w for ibuprofen, indometacin and piroxicam respectively, with Gelucire 44/14 solubility in indometacin being 60% w/w. An estimation of Gelucire 44/14 in ibuprofen and piroxicam could not be speculated since the third phase of the Qi model was not achieved below 50% w/w drug loading (up to which was tested), thus suggesting that in both cases the solubility is less than 50% w/w. HSM proved useful in confirming the presence, or not, of drug crystals in the lower drug loaded systems, thus confirming the presence of dissolution effects at slower heating rates. Cooling of the molten systems during analysis using conventional DSC demonstrated the reduction in temperature, and almost complete inhibition at 50% w/w, of the lipidic crystallisation process. This data coincided with that obtained from QIMTDSC in all cases; however it was found to demonstrate poor reproducibility.

CHAPTER FIVE

IN VITRO RELEASE CHARACTERISTICS OF SEMI-SOLID DISPERSION SYSTEMS

5.1 INTRODUCTION

Gelucire 44/14 is well established as an effective excipient known for improving the dissolution properties of poorly soluble drugs and consequently increasing their bioavailability. This effect has been demonstrated with a number of different drug SSD systems, including halofantrine (Abdul-Fattah and Bhargava 2002), rofecoxib (Ahuja et al. 2007) and glibenclamide (Tashtoush et al. 2004). The process by which this dissolution enhancement occurs is not completely understood however there are many suggestions in the literature. Gelucire 44/14 is known to spontaneously emulsify on contact with aqueous media which in turn has been shown to increase drug wettability and dispersibility, protecting the particles from aggregation agglomeration and precipitation (Tashtoush et al. 2004). The incorporation of drug into the hydration layer of the lipid after self-emulsification has also been noted (Barker et al. 2003). Alongside this, other authors have suggested a decrease in interfacial tension between the drug and water by microemulsion (Ahuja et al. 2007) and decrease in drug particle size (Abdul-Fattah and Bhargava 2002).

Upon in vitro dissolution of drug and lipid SSD systems, the first minutes are occupied with disintegration of the hard gelatin capsule surrounding the formulation. Dissolution of the drug from the SSD then occurs once in contact with the aqueous media. Drug release from swellable matrices can be controlled by one or more of a number of processes:

1. Water diffusion into the matrix.
2. Swelling of the matrix due to hydration or relaxation of the polymer chains ("Case II Transport"), i.e. structural polymer changes brought about by the penetration of water, causing the polymer to swell.
3. Drug diffusion through the swollen matrix and existing pores if present.
4. Matrix erosion or dissolution (Sutananta et al. 1995a).

The mechanism by which drug is released from the formulation can be determined via the application of a mathematical model to the dissolution data collected.

The Higuchi model is the most well known method used to describe the rate of release of drug from a matrix system, however it only applies when pure diffusion is the controlling mechanism (Gao 2011; Higuchi 1961):

$$\frac{M_t}{M_\infty} = k\sqrt{t} \qquad \textbf{\textit{Equation 5.1}}$$

Where M_t/M_∞ is the fraction of drug released at time t and k is a constant which takes into account the design variables of the system. This equation therefore demonstrates that the fraction of drug released is proportional to the square root of time. In order to apply this model, a number of assumptions have to be made, these include the fine state of suspended particles, negligible swelling or dissolution of the matrix, and one-dimensional diffusion of the formulation, among others, which for SSD systems are not suitable or applicable (Siepmann and Peppas 2001).

However, the semi-empirical power-law model, developed by Korsmeyer and co-workers has been found to best describe the drug release kinetics from these kinds of systems (Ahuja et al. 2007).

The power-law model is demonstrated as follows (Korsmeyer et al. 1986a; Korsmeyer et al. 1986b):

$$\frac{M_t}{M_\infty} = kt^n \qquad \textit{Equation 5.2}$$

Where M_t/M_∞ is the fraction of drug released at time t as previously, k is the release constant and n is the release exponent. The n value is a dimensionless number which is suggestive of the dominating mechanism of drug release from the formulation. For n = 0.5, Fickian diffusion of drug through the matrix controls release, n = 1 indicates Case II Transport or non-Fickian transport, and any value between ($0.5 < n < 1$) indicates anomalous transport i.e. a combination of the two processes (Qi et al. 2008). Values of *n* below 0.5 are also thought to suggest anomalous transport, however in this case a combination of diffusion and fast release brought about by disintegration is thought to be responsible (Gao 2011). It should be noted however that these values are valid only for formulations with a slab geometry, for cylindrical or spherical systems, the values are replaced with 0.45 to 0.89 and 0.43 to 0.85 respectively. The model has been found to hold true for the first 70% of drug released (Sutananta et al. 1995a).

The mechanisms by which drugs are released from Gelucires are dependent upon the composition of the base. The fast rate of drug release from pharmaceutical glycerides

with high HLB values, such as Gelucire 44/14, is thought to involve both dissolution and erosion processes. These Gelucires may also swell when in contact with aqueous media (Sutananta et al. 1995a). Furthermore, a study conducted by Ahuja et al (2007) also found that Gelucire 44/14 SSD systems containing rofecoxib demonstrated slightly non-Fickian release behaviour.

In addition to determining if drug release from SSD systems is controlled by diffusion or case II transport, another method of defining this release is presented in a review by Craig (2002). The model attempts to explain the behaviour of drug particles during dissolution by suggesting dissolution may be controlled either by the drug or the carrier material. In carrier-controlled systems the rate of drug release is equivalent to that of the polymer alone, and in general, the drug is required to be present as the minor component. The ratio of carrier to drug at which dominance of control of dissolution changes can be presented using Equation 3

$$\frac{N_A}{N_B} = \frac{D_A C_{SA}}{D_B C_{SB}} \qquad \textit{Equation 5.3}$$

where N represents the proportion of carrier (A) and drug (B), D is the diffusion coefficient and C_S the solubility of each component in the investigated media. The ratio at which the change in control of dissolution occurs is dependent upon the solubility of the drug in relation to the carrier. If the drug demonstrates a low solubility compared to that of the carrier then the ratio at which carrier-controlled release will dominate also be low, and vice versa. If the carrier is known to control dissolution, it has been argued that the drug physical form should therefore have no effect on the rate of release (Lloyd et al 1999). Dissolution of SSD systems may also

be controlled by the properties of the drug if the concentration is high enough i.e. the dissolution properties are similar to those of the drug alone due to the formation of an drug rich layer exposed to the dissolution media.

The model proposed by Craig (2002) is illustrated by the following schematic (Figure 5.1). It makes the assumption that there is a polymer-rich layer at the surface which becomes hydrated when in contact with aqueous media.

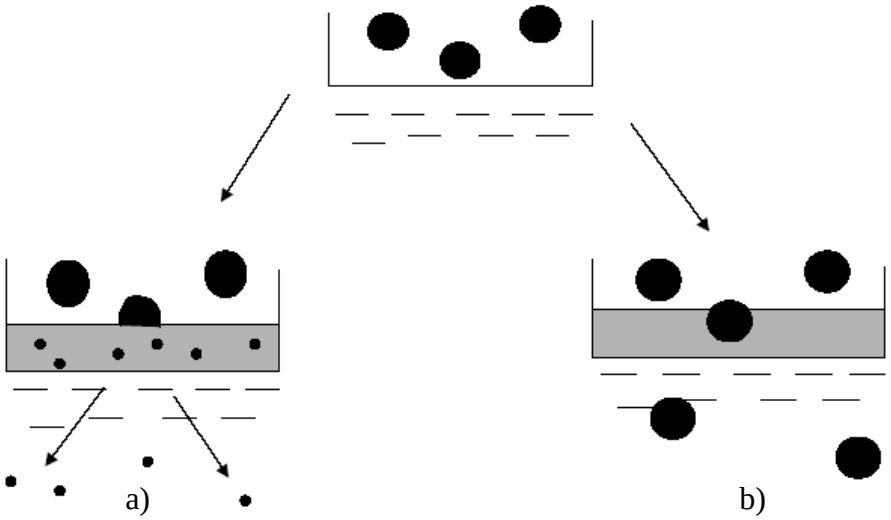

Figure 5.1 *A schematic diagram showing the fate of drug particles during the dissolution process; (a) carrier-controlled dissolution (b) drug-controlled dissolution, where large spheres represent undissolved drug particles, small spheres partially dissolved drug particles and shaded regions hydrated material.*

Carrier-controlled dissolution (a), involves the rapid molecular dispersion of drug particles in the carrier-rich diffusion layer, and therefore the rate limiting step to dissolution is the release of the carrier. This method of drug release is largely dependent upon drug solubility in the carrier. Drug-controlled dissolution (b)

however involves slow molecular dispersion of drug into the carrier-rich diffusion layer and the subsequent release of intact drug particles into the aqueous media. This process is therefore determined by drug properties such as physical form and particle size (Craig 2002).

In this chapter, in vitro dissolution studies have been used to establish any enhancement of the aqueous dissolution properties of the poorly soluble model drugs investigated, and also to analyse the release characteristics of drug from the formulated Gelucire 44/14 SSD systems.

5.2 METHODOLOGY

Prior to data collection, a calibration plot was produced for each of the three model drugs by either dissolving an amount of the appropriate 5% w/w SSD(20) for ibuprofen and indometacin or equal parts piroxicam and Gelucire 44/14, in 500ml distilled water on shaking and heating. The addition of Gelucire 44/14 was chosen in an attempt to reduce the solubility issues associated with the crystalline drugs alone which are known to be highly water insoluble, and obtain at least a small amount of drug in aqueous solution for detection. A series of dilutions were made, the absorbances of which were measured using a UV spectrometer at a wavelength of 220nm for ibuprofen, 320nm for indometacin and 356nm for piroxicam (Figure 5.2 a, b and c).

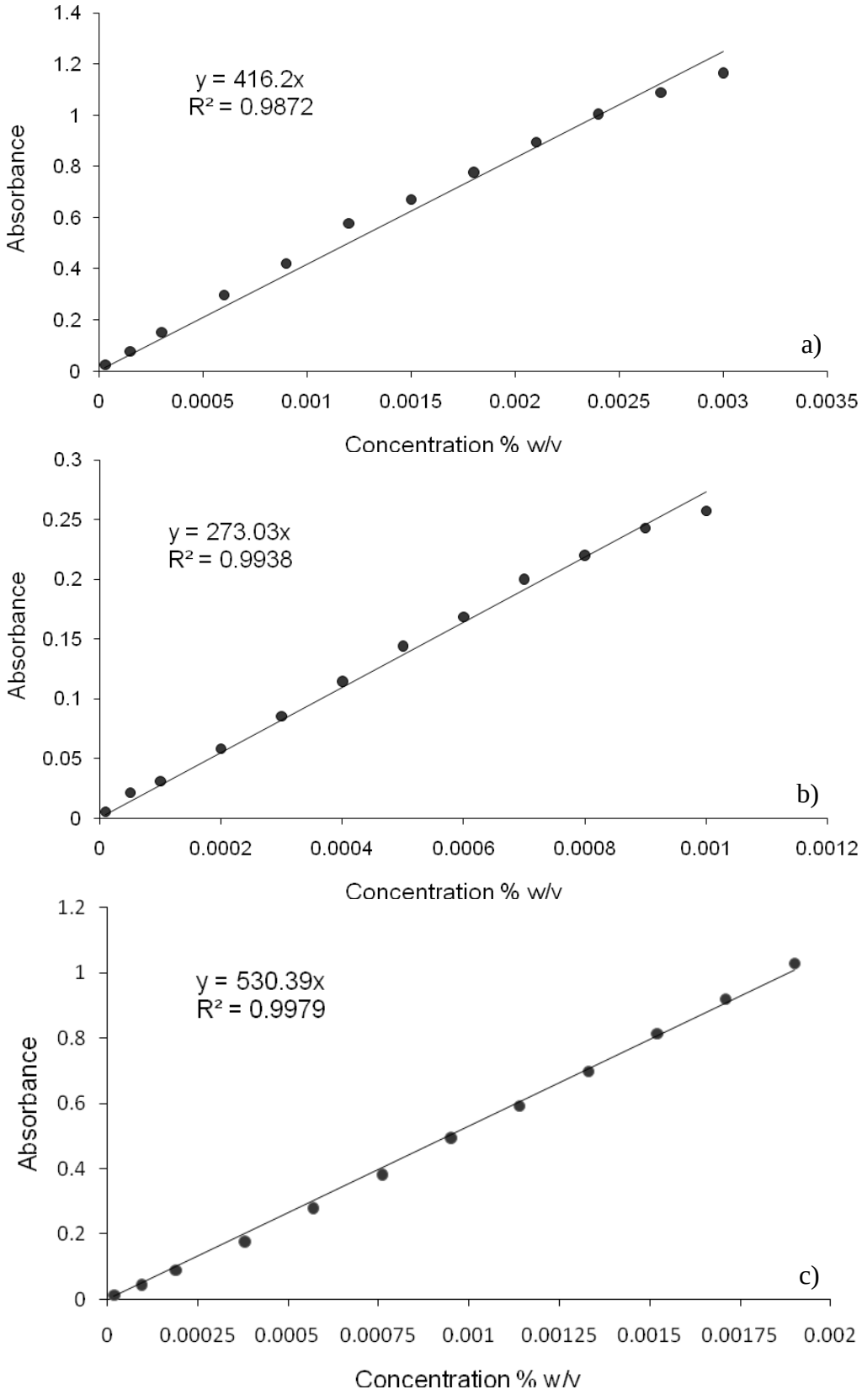

Figure 5.2 *Calibration plot of UV absorbance against drug concentration for a) ibuprofen, b) indometacin and c) piroxicam.*

Samples for analysis were formulated and prepared into capsules as outlined in Chapter Two. The drug content in each capsule was equivalent to 25mg ibuprofen, 25mg indometacin and 10mg piroxicam. The quantities of indometacin and piroxicam were chosen to match the lowest strength oral formulations currently on the market. Since marketed formulations of ibuprofen contain a minimum of 200mg, a reduced ibuprofen content was chosen for this study i.e. 25mg. The insoluble nature of the drugs, and also the equipment available, made it impracticable to obtain sink conditions in all cases. It did however allow the comparison of drug release from the formulated SSD systems with that of the drugs alone. Dissolution studies were carried out, in triplicate, in 900ml distilled water at 37^{o}C over 45 minutes. Samples, 10ml in volume, were withdrawn periodically and replaced with an equivalent volume of dissolution medium at the same temperature. The samples were filtered through a 0.45µm filter, the UV absorbances of which were recorded in triplicate.

5.3 IN VITRO RELEASE PROFILE OF IBUPROFEN AND GELUCIRE 44/14 SEMI-SOLID DISPERSION SYSTEMS

5.3.1 In Vitro Release Studies of Ibuprofen and Gelucire 44/14 Semi-Solid Dispersion Systems

Upon in vitro dissolution analysis of ibuprofen and Gelucire 44/14 SSD systems in water at 37^{o}C, the dissolution properties of ibuprofen were observed to be greatly improved in comparison to that of the crystalline drug alone (Figure 5.3). In the cases of 5, 10 and 15% w/w, ibuprofen was released to its greatest extent. The mean dissolution time for ibuprofen release up to 50% indicated that all lower ibuprofen loaded systems demonstrated a fast release of similar time ranging from 4 to 8 minutes (Table 5.1). For both SSD(20) and SSD(4) the 50% w/w systems were observed to release ibuprofen at the slowest rate, as expected due to the probable formation of a crystalline drug rich surface layer hindering dissolution. The extent to which ibuprofen was released from the 50% w/w systems was however still observed to be greater than that of the drug alone.

In an attempt to determine the mechanism of drug release from the formulated SSD systems, the power-law mathematical model was used to fit the dissolution data. The data was found, in most cases, to fit this law relatively poorly. It should be noted at this point that Gelucire 44/14 is an amphiphilic excipient known to spontaneously emulsify on contact with aqueous media and therefore care should be taken when attempting to categorise the mechanism of drug release from these systems. The n values obtained did however give an indication as to the method of drug release. All n values calculated were found to be lower than 0.5 which is outside the limits of the

power-law in this case. This suggested that the mechanisms of drug release were controlled by both diffusion and fast release by disintegration. No trend in the values appeared to be present.

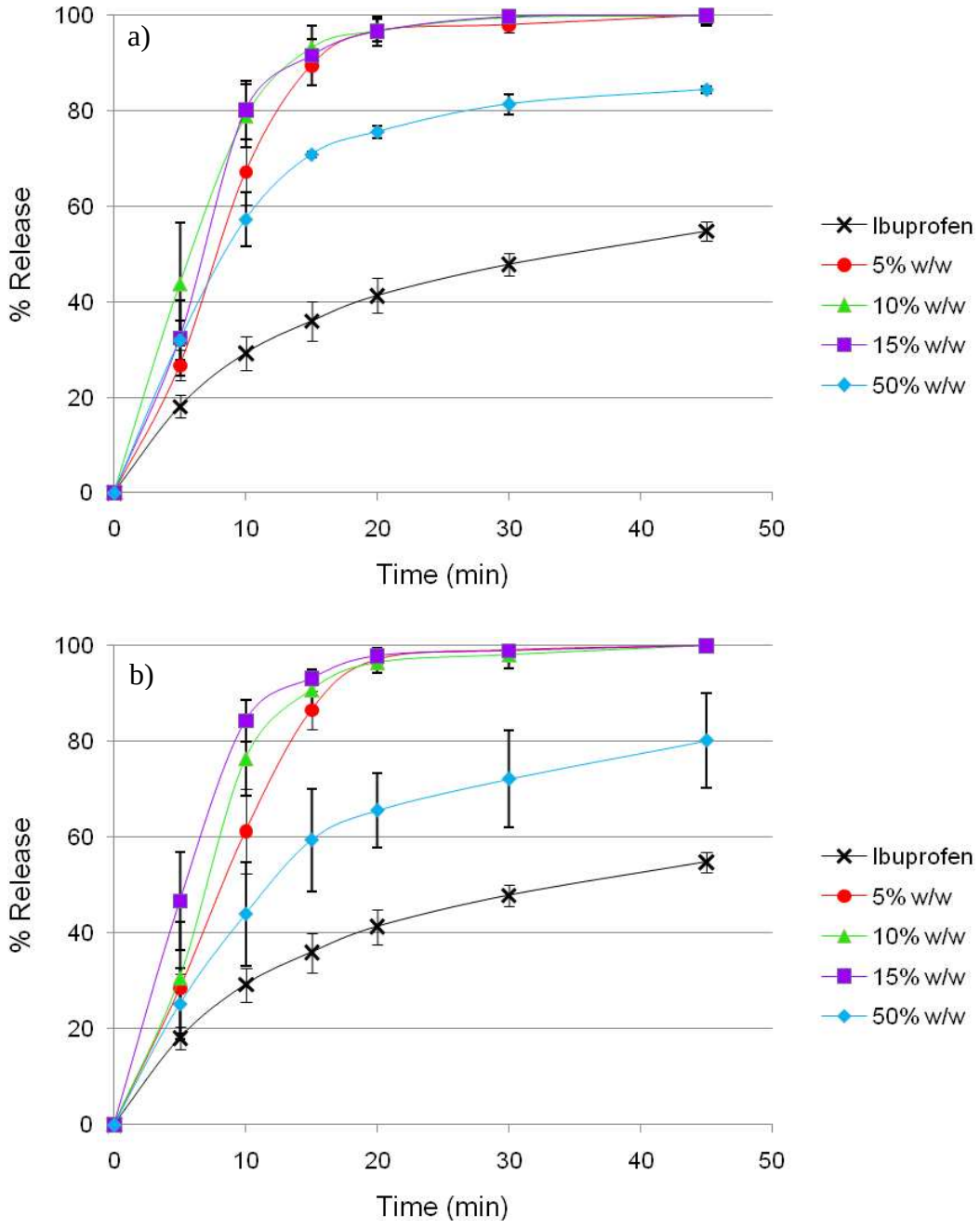

Figure 5.3 *Percentage release of ibuprofen over time from a) SSD(20) and b) SSD(4) systems in water at 37°C.*

Table 5.1 *Mean dissolution time for ibuprofen release up to 50% (MDT-50%) and the calculated release exponent n using the Power-Law.*

Formulation		MDT-50% (min)	Power-Law Model *n*	R^2
Ibuprofen Alone		34.8	0.45	0.989
SSD(20)	5%	7.5	0.37	0.862
	10%	4.9	0.27	0.913
	15%	6.4	0.32	0.864
	50%	8.6	0.34	0.940
SSD(4)	5%	8.1	0.39	0.880
	10%	6.3	0.33	0.865
	15%	4.7	0.24	0.913
	50%	11.8	0.43	0.961

Thermal characterisation of these systems detailed in Chapter Four suggested that ibuprofen, in lower concentrations, was present in the form of a molecular dispersion. This was highlighted by the absence of an ibuprofen melting endotherm, even at high heating rates. It would be reasonably assumed, in the case of molecular dispersion, that drug release would be controlled purely by those mechanisms thought to be attributable to the lipid carrier alone i.e. the anomalous transport of a combination of dissolution, erosion and swelling, demonstrating an n value of between 0.5 and 1. Alteration to the Gelucire 44/14 melting endotherm upon heating of the SSD systems however suggested some degree of interaction, potentially hydrogen bonding, between ibuprofen and the lipid which may have an effect on the mechanism by which the drug was released. Values lower than 0.5 were calculated,

indicating that the mechanism of release had changed to not only diffusion but fast release of drug due to disintegration. This is in line with the mechanism of release for the pure drug alone.

5.3.2 Summary of Ibuprofen and Gelucire 44/14 Semi-Solid Dispersion System In Vitro Release Studies

Dissolution properties of ibuprofen were found to be drastically enhanced by formulation into SSD systems with the lipid Gelucire 44/14. All formulations, with the exception of the highest loading of 50% w/w, were found to release ibuprofen up to 100%. Overall, the mechanism of ibuprofen release was found to be anomalous, consisting of both diffusion and disintegration despite the presence of a suspected molecular dispersion in the lower loaded systems.

5.4 IN VITRO RELEASE PROFILE OF INDOMETACIN AND GELUCIRE 44/14 SEMI-SOLID DISPERSION SYSTEMS

5.4.1 In Vitro Release Studies of Indometacin and Gelucire 44/14 Semi-Solid Dispersion Systems

Formulation of crystalline indometacin with the lipid Gelucire 44/14 into SSD systems demonstrated an improvement in dissolution compared with crystalline indometacin alone, however complete dissolution was not achieved (Figure 5.4). Both the 5 and 10% w/w systems were found to release indometacin to the largest extent, with the two being comparable. It would be expected however that the release of indometacin would continue to increase over the course of the experiment rather than reach equilibrium at just below 60%. This suggests that the dissolution media may have become saturated due to non-sink conditions. An increase in the extent of indometacin after formulation into an SSD with Gelucire 44/14 could be observed nonetheless.

The mean dissolution time for indometacin release up to 50% i.e. rate of release, was found to be similar if not slightly faster for 10% w/w (Table 5.2). The 15 and 50% w/w systems, along with indometacin alone, were found not to reach 50% drug release over the 45 minute course of the experiment.

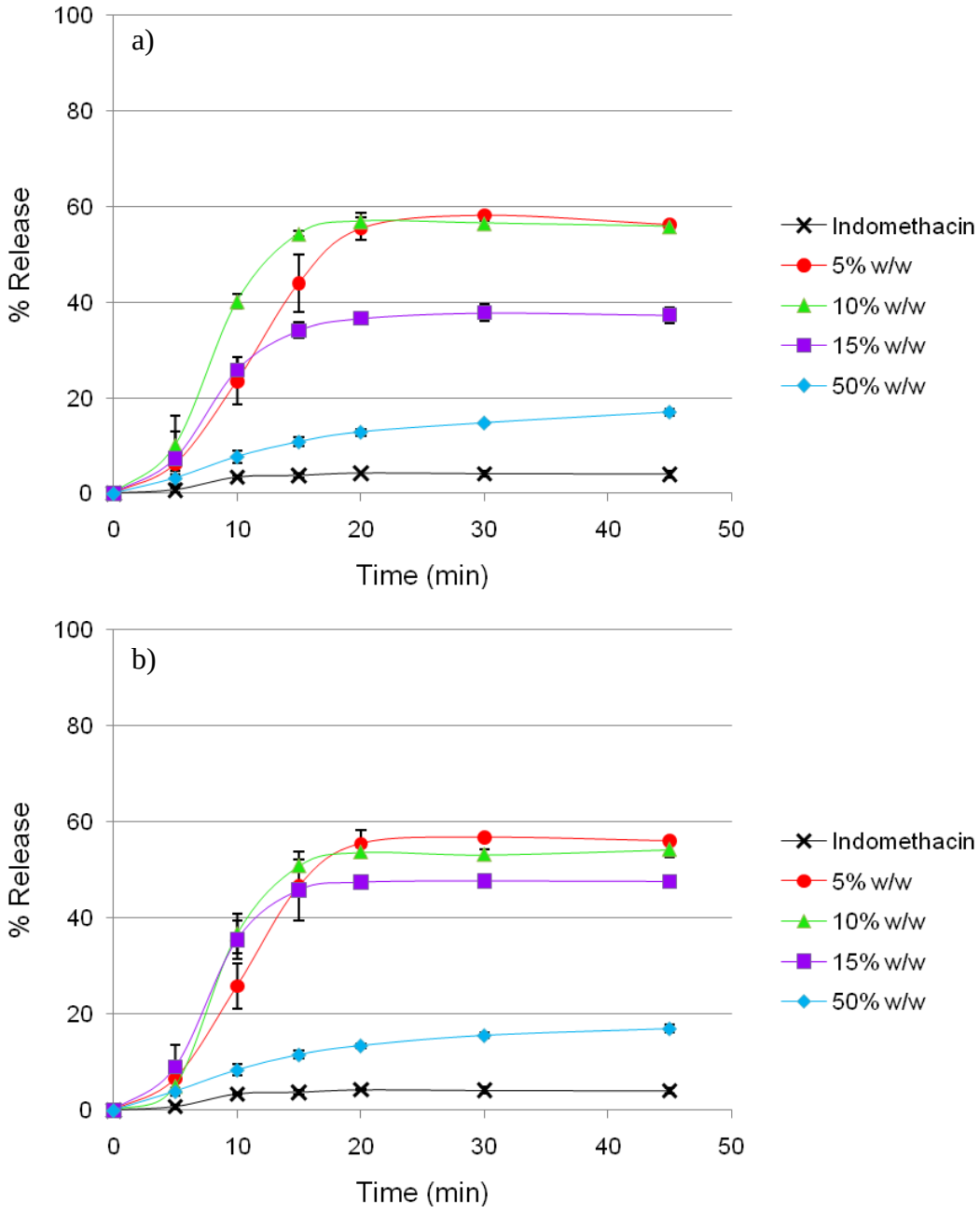

Figure 5.4 *Percentage release of indometacin over time from a) SSD(20) and b) SSD(4) systems in water at 37°C.*

Modelling of the dissolution data using the power-law equation gave an indication of the process by which indometacin was released from the formulation, however due to the nature of the emulsifying properties of Gelucire 44/14, the data again did not fit well. Crystalline indometacin alone demonstrated an n value of 0.34 suggesting that

it was controlled by diffusion and disintegration. At 5% w/w SSD indometacin loading, an n value of slightly greater than 0.5 was achieved in both cases, indicating anomalous transport, being controlled by diffusion as well as swelling/erosion processes. This was also true for the 50% w/w loaded formulations. However, at 10 and 15% w/w, low values of *n* were calculated indicating that indometacin release is controlled again by diffusion and disintegration as for indometacin alone. It should be considered that the value of *n* also depends upon the geometry of the system and the particle size distribution. Qi et al (2008) noted that for microsphere systems, particle sizes of below 180µm demonstrated an *n* value of below 0.5 which was assigned to accelerated drug transport and dissolution of the small particle size. Particle sizes of 180 to 250µm showed values close to 0.5.

Table 5.2 *Mean dissolution time for indometacin release up to 50% (MDT-50%) and the calculated release exponent n using the Power-Law.*

Formulation		MDT-50% (min)	Power-Law Model *n*	R^2
Indometacin Alone		> 45	0.34	0.759
SSD(20)	5%	17.7	0.54	0.813
	10%	13.3	0.38	0.780
	15%	> 45	0.40	0.819
	50%	> 45	0.56	0.956
SSD(4)	5%	16.6	0.51	0.808
	10%	14.8	0.43	0.759
	15%	> 45	0.37	0.788
	50%	> 45	0.51	0.952

At 5% w/w, thermal characterisation outlined in Chapter Four suggested that indometacin may be molecularly dispersed throughout Gelucire 44/14. The *n* value of slightly greater than 0.5, indicating diffusion along with swelling/erosion, is known to occur with this lipid. At 10 and 15% w/w, solid crystalline indometacin particles were thought to be present in the system. Formulation into SSD systems with Gelucire 44/14 is known to reduce the particle size of the dispersed drug, thus improving wetting properties and encouraging micellar solubilisation. The *n* value, being lower than 0.5, may be influenced by the particle size of these crystals as in the Qi et al (2008) study. At 50% w/w, a large proportion of crystalline indometacin particles were found to be present. The *n* value, calculated to be slightly greater than 0.5, may therefore be influenced by the larger particle size in combination with the lipid.

5.4.2 Summary of Indometacin and Gelucire 44/14 Semi-Solid Dispersion System In Vitro Release Studies

The dissolution properties of indometacin were found to improve with formulation into SSD systems with the lipid Gelucire 44/14. Lower drug concentrations were found to be optimum, with 5 and 10% w/w achieving the largest extent of release. In all cases however, no greater than 56% indometacin release was achieved in water at 37^{o}C, most likely due to non-sink conditions. The mechanism of release was found to vary with indometacin loading, possibly being influenced by particle size of the crystalline drug distributed throughout the lipid SSD system.

5.5 IN VITRO RELEASE PROFILE OF PIROXICAM AND GELUCIRE 44/14 SEMI-SOLID DISPERSION SYSTEMS

5.5.1 In Vitro Release Studies of Piroxicam and Gelucire 44/14 Semi-Solid Dispersion Systems

The formulation of piroxicam into SSD systems with Gelucire 44/14 was observed to greatly increase the extent of dissolution in water at 37^{o}C (Figure 5.5). At 5% w/w piroxicam loading, on completion of the experiment, dissolution to the extent of 95% was achieved. As the piroxicam content was increased, the extent of dissolution was found to decrease.

Considering the mean dissolution time for piroxicam release up to 50% (Table 5.3), the 5 and 10% w/w SSD(20) systems demonstrated a rate of release of approximately 11 minutes, with that of 15% being slightly slower at 15 minutes. The SSD(4) systems showed similar release rates for 5, 10 and 15% w/w formulations, being 12 to 13 minutes. The lower piroxicam loaded systems all demonstrated similar release rates, despite being released to varying extents. The 50% piroxicam loaded systems were found to release the drug at a much slower rate, with 50% of the drug being released after 39 minutes for SSD(20) formulations or over 45 minutes for SSD(4). This was similar to piroxicam alone which did not reach 50% drug release over the course of the 45 minute experiment.

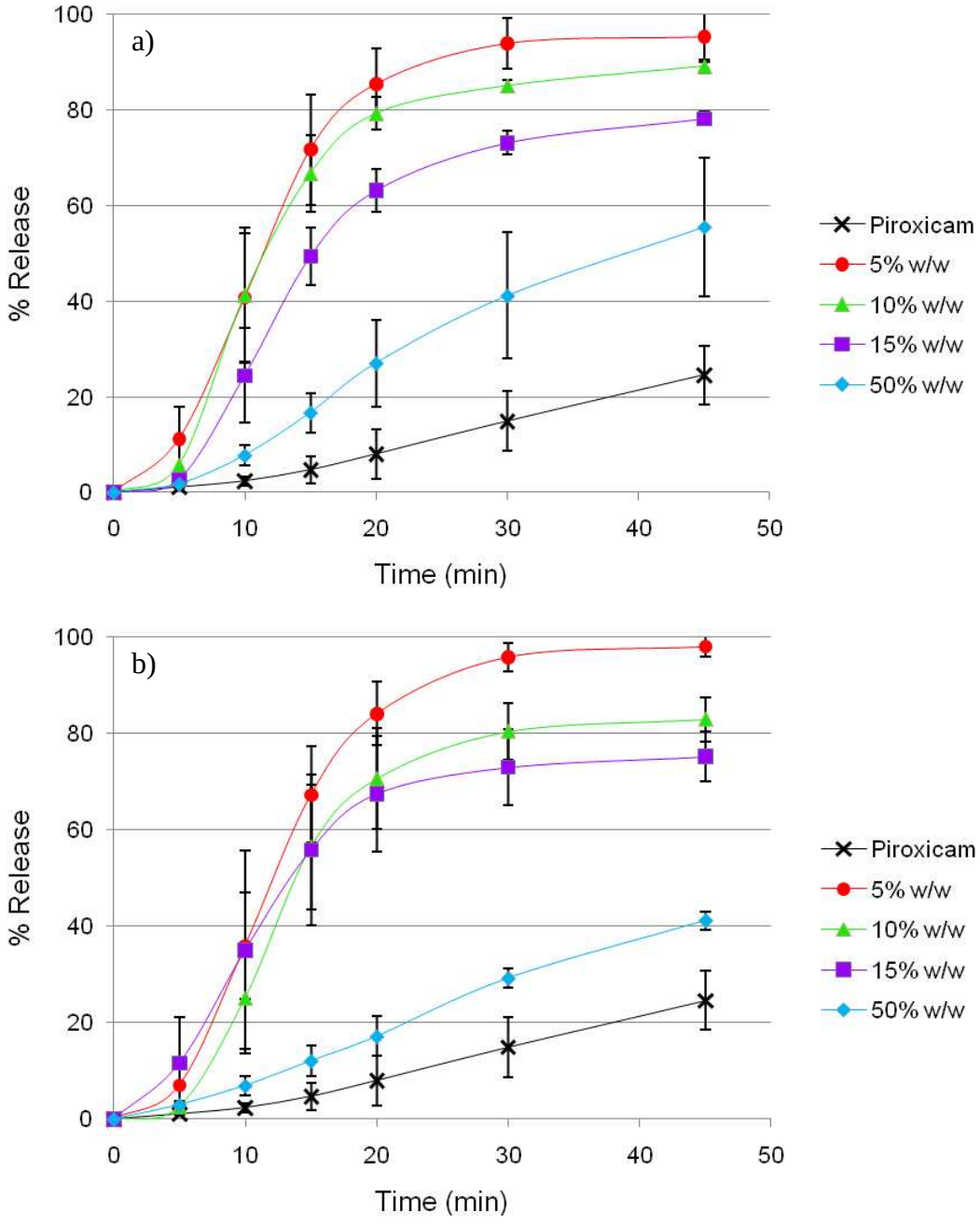

Figure 5.5 *Percentage release of piroxicam over time from a) SSD(20) and b) SSD(4) systems in water at 37°C.*

The n values calculated by modelling the collected dissolution data using the power-law equation are shown in Table 5.3. As expected for Gelucire 44/14 SSD systems, the data did not fit well, however an *n* value of 1 was obtained for piroxicam alone and 50% w/w systems for both SSD(20) and SSD(4), thus confirming zero order

release kinetics. It suggested that drug release was controlled by case II transport (erosion/swelling). The lower piroxicam loaded systems all demonstrated similar *n* values (*n* = 0.53 to 0.68) suggesting that with increasing Gelucire 44/14 content and decreasing drug loading, drug release was controlled mainly by Fickian diffusion, with an element of swelling/erosion which follows the observations made by Sutananta et al (1995a) and Ahuja et al (2007) outlined in the introduction of this chapter.

Table 5.3 *Mean dissolution time for piroxicam release up to 50% (MDT-50%) and the calculated release exponent n using the Power-Law.*

Formulation		**MDT-50% (min)**	**Power-Law Model *n***	**R^2**
Piroxicam Alone		> 45	1	-0.500
SSD(20)	5%	11.3	0.55	0.857
	10%	11.5	0.56	0.842
	15%	15.1	0.68	0.870
	50%	39.2	1	0.678
SSD(4)	5%	12.3	0.62	0.861
	10%	13.8	0.66	0.840
	15%	13.5	0.53	0.877
	50%	> 45	1	0.632

Thermal characterisation of the piroxicam and Gelucire 44/14 SSD systems outlined in Chapter Four suggested low compatibility between the two components indicated by crystalline melting endotherms in all systems. This was found to result in the

major proportion of piroxicam being dispersed in the lipid as crystalline particles, with only a small amount being molecularly dispersed. Dissolution of piroxicam present as crystalline particles, upon spontaneous emulsification of Gelucire 44/14 in contact with water, may be brought about by emulsification and micellar solubilisation and therefore improved wetting characteristics (Karatas et al. 2005).

A study carried out by Karatas et al (2005) investigated the combination of piroxicam with Gelucire 44/14 as a solid dispersion. They also found the dissolution properties of piroxicam to be increased, from approximately 40% alone to 75.6% in water at 37^{o}C for 5% w/w loaded dispersions. They noted that piroxicam release was pH dependent, with 100% in buffer 6.8 and 71.6% in 4.5. The extent of release was found to improve upon the addition of labrasol, a liquid surfactant with an HLB also of 14. In this present study however, piroxicam dissolution in water at 37^{o}C was discovered to be almost optimum, reaching 95 and 98% for the 5% w/w SSD(20) and SSD(4) systems respectively. Karatas et al also observed that in simulated gastric fluid without pepsin (pH 1.2) at 37^{o}C, 5% w/w piroxicam SSD release was complete within 45 minutes, giving an indication that these types of systems may allow total piroxicam release in vivo, although it is difficult to make this correlation with any certainty. The authors attributed this enhanced dissolution to partial molecular dispersion, solubilising effects of the carriers, and also an improvement in wettability of the piroxicam.

5.5.2 Summary of Piroxicam and Gelucire 44/14 Semi-Solid Dispersion System In Vitro Release Studies

SSD formulation of piroxicam with Gelucire 44/14 was found to notably improve the dissolution profile of the drug in aqueous media. Of all the drug loadings, a piroxicam content of 5% was found to be optimum in terms of drug release, being almost 100%. At low piroxicam loadings, release was found to be controlled by both diffusion and case II transport and demonstrated first order release kinetics.

5.6 CONCLUSIONS

Overall, SSD formulations of poorly soluble drugs in combination with the lipid Gelucire 44/14 appear to consistently increase the rate and extent of drug dissolution in aqueous media, whether by molecular dispersion of drug or increased wetting or micellar solubilisation of solid drug particles, as demonstrated by this study and also many examples in the literature. This dissolution enhancement may correspond to a subsequent improvement in the in vivo bioavailability however this correlation is difficult to establish. The power-law mathematical model is a useful tool to predict the mechanism of drug release from the formulation, although care should be taken when relating these data to systems composed of Gelucire 44/14 due to its ability to spontaneously emulsify on contact with aqueous media.

CHAPTER SIX

HYDRATION STUDIES OF SEMI-SOLID DISPERSION SYSTEMS

6.1 INTRODUCTION

The hydration properties of the lipid Gelucire 44/14 have been outlined previously in this thesis, in terms of the literature detailed in Chapter One and dynamic vapour sorption analysis in Chapter Three. This analysis was useful in giving an indication as to temperature and humidity parameters below which the lipidic carrier alone would remain stable. These studies suggested that the capacity of Gelucire 44/14 to absorb atmospheric moisture increased at high temperatures and relative humidities attributable to its many components, in particular the presence of PEG which serves to facilitate hydrogen bond interactions with water molecules (Barakat 2006). Below 30^{o}C and 40% RH, the moisture content of the lipid remained below the European Pharmacopeia limit of 1% weight increase and at ambient temperatures only limited moisture was absorbed below 70% RH. These properties will inevitably be altered by the incorporation of insoluble drug as an SSD. In this case however, any solid drug present in the formulation is likely to be present in the insoluble crystalline form and not the more soluble amorphous energy state, as is the case in the vast majority of SSD systems. This will therefore have an impact upon the affinity for atmospheric water demonstrated and it is accepted that the association of water with components, drugs in particular, at relatively low levels can and will affect the physicochemical properties of the formulation for example chemical degradation and dissolution rate (Ahlneck and Zografi 1990).

The analysis presented in this Chapter hopes to provide an insight into the changes in the hydration process of the lipid in combination with drug to assist in the

anticipation of SSD behaviour, which will in turn facilitate prediction of the behaviour of the final product during storage.

6.2 METHODOLOGY

6.2.1 Dynamic Vapour Sorption

Samples to be analysed gravimetrically using DVS were formulated using the method outlined in Chapter Two and prepared into quartz crucibles against an empty reference. All samples were dried at 25^{o}C and 0% RH for 60 minutes before being held isothermally at 75% RH and either 35, 45 or 55^{o}C for 60 minutes. Desorption and absorption of water was measured as weight loss or gain. Samples were analysed in triplicate.

6.3 HYDRATION BEHAVIOUR OF IBUPROFEN AND GELUCIRE 44/14 SEMI-SOLID DISPERSION SYSTEMS

Upon holding at isothermal temperatures at 75% RH, the SSD(20) systems demonstrated properties on the whole that were different to those of the lipid alone (Figure 6.1). At 35^{o}C, Gelucire 44/14 absorbed the smallest proportion of atmospheric moisture; however the presence of 5% w/w ibuprofen allowed the uptake of a much greater weight percent of moisture (Figure 6.1 a).

At 5% w/w, the analysis shown in Chapter Four suggested that the majority of ibuprofen present in these systems existed as a molecular dispersion in Gelucire 44/14, attributable to its reasonable solubility in the lipid. The ordered molecular arrangement of crystalline solids is known to be altered by defects and imperfections, and it is not unreasonable to assume that a molecular dispersion of drug within Gelucire 44/14 will demonstrate a similar effect on the crystalline lipid (Figure 6.2). This effect is recognized to bring about regions of local molecular disorder with enhanced chemical reactivity due to increased molecular movement and the exposure of a greater number of reactive chemical groups (Ahlneck and Zografi 1990). This suggests therefore that, since at this temperature the lipid would on the whole be in the solid state, the potential increased chemical reactivity of the crystalline Gelucire 44/14 may encourage the uptake of atmospheric moisture to a greater extent than observed for the lipid alone.

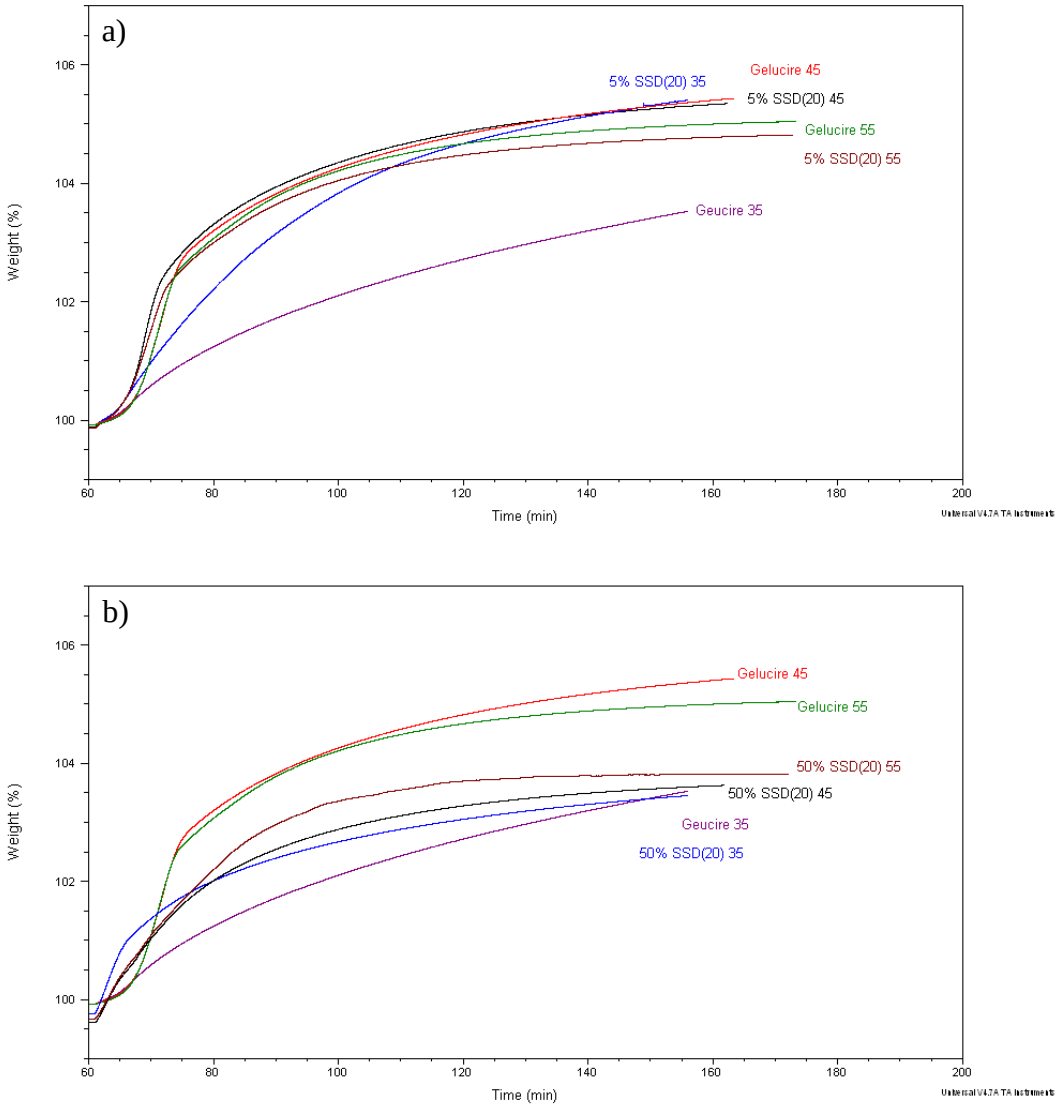

Figure 6.1 *Weight percent versus time signal for ibuprofen and Gelucire 44/14 SSD(20) a) 5% w/w and b) 50% w/w compared to that of Gelucire 44/14 alone at 75% RH isothermal at 35, 45 and 55°C.*

At temperatures above 35^{o}C, the SSD(20) systems showed similar moisture uptake to that of the lipid alone. Once in the liquid state, the SSD(20) with ibuprofen molecularly dispersed within it and the lipid alone are disordered to equal extents, therefore demonstrating comparable atmospheric moisture absorption profiles.

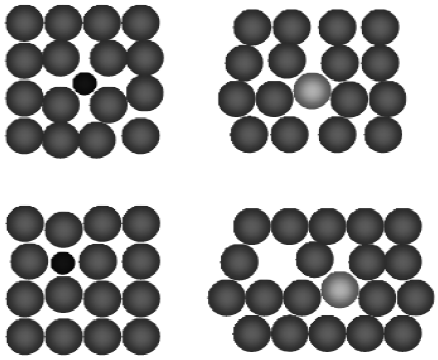

Figure 6.2 *Schematic of potential defects in the ordered structure of a crystalline particle (adapted from Kopeliovich (2009)).*

At all equivalent temperatures, the shape of the plots remained similar. At 35^{o}C, weight gain appeared to demonstrate a steady increase over the course of the experiment. However at 45 and 55^{o}C, water uptake appeared to be fast over the initial stages of the process up to a weight increase of 2.5%. The rate and extent of moisture uptake then began to slow for the remainder of the experiment.

At 50% w/w ibuprofen (Figure 6.1 b), all SSD(20) systems increased in weight equivalent to the extent of atmospheric moisture absorbed to similar degrees, which was close in value to that of Gelucire 44/14 at 35^{o}C. At 35^{o}C the shape of the SSD(20) plot suggested a more rapid rate of absorption than that of the lipid alone, it did however slow over the course of the experiment, giving a final total weight increase similar in value. The SSD(20) formulations demonstrated a lower affinity for atmospheric water than the lipid alone once in the liquid state at 45 and 55^{o}C. This effect will be attributable to the large proportion of insoluble drug present in the system in combination with a reduced mass, by half, of Gelucire 44/14. Even when molten at 55^{o}C, the ibuprofen would exist, in the majority, as insoluble crystalline

solid particles. Crystalline ibuprofen is known to have the capacity to adsorb water up to two molecular layers at high RH, however since Gelucire 44/14 is water soluble, the moisture uptake would most likely entirely be associated with Gelucire 44/14 (Nokhodchi 2005). The presence of these particles and the subsequent reduction in mass of Gelucire 44/14 would thus limit the extent of water uptake achieved.

Table 6.1 *Moisture uptake as percentage weight gain by ibuprofen and Gelucire 44/14 SSD systems in comparison with Gelucire 44/14 alone under isothermal temperature conditions at 75% RH.*

Isothermal Temperature (^{o}C)	Formulation	Weight Gain (%)	Standard Deviation
35	Gelucire 44/14	3.8	1.4
	5% SSD(20)	5.2	1.8
	50% SSD(20)	3.8	1.0
45	Gelucire 44/14	5.7	1.8
	5% SSD(20)	5.4	1.8
	50% SSD(20)	3.7	1.0
55	Gelucire 44/14	5.2	1.6
	5% SSD(20)	5.0	1.7
	50% SSD(20)	3.9	1.2

Overall, the collected DVS data was relatively reproducible (Table 6.1), with the variation of the weight gain values most likely being attributable to a number of factors including the mass of sample in the crucible, the initial moisture content after drying for 60 minutes and also instrument effects.

6.4 HYDRATION BEHAVIOUR OF INDOMETACIN AND GELUCIRE 44/14 SEMI-SOLID DISPERSION SYSTEMS

Upon analysis by DVS, indometacin and Gelucire 44/14 SSD(20) systems demonstrated properties similar to those observed for the ibuprofen formulations. At 35^{o}C, the 5% w/w systems were found to absorb atmospheric moisture to a much greater extent than the lipid alone (Figure 6.3 a). It did however show a similar curve shape suggesting that moisture absorption steadily increased over time. The DSC analysis presented in Chapter Four suggested that at 5% w/w the indometacin was present as a molecular dispersion, completely dissolved within Gelucire 44/14. The increased affinity of SSD(20) for atmospheric moisture at this temperature, as detailed above, may therefore be explained by the disordered nature of the lipid crystalline structure due to the incorporation of molecular indometacin disrupting the crystal formation and packing, and thus increasing its chemical reactivity in localised regions.

At higher temperatures (45 and 55^{o}C) both the SSD(20) systems and Gelucire 44/14 displayed similar weight increases. The shapes of the curves were also similar, appearing to undergo a rapid moisture intake up to weight gain of 2.5 to 3.5% which then slowed for the remainder of the experiment. It suggested that once in the molten state, the addition of indometacin at low concentrations did not significantly affect the absorption properties of the lipid. This would be attributable to the equal state of molecular disorder experienced by the samples in the liquid state.

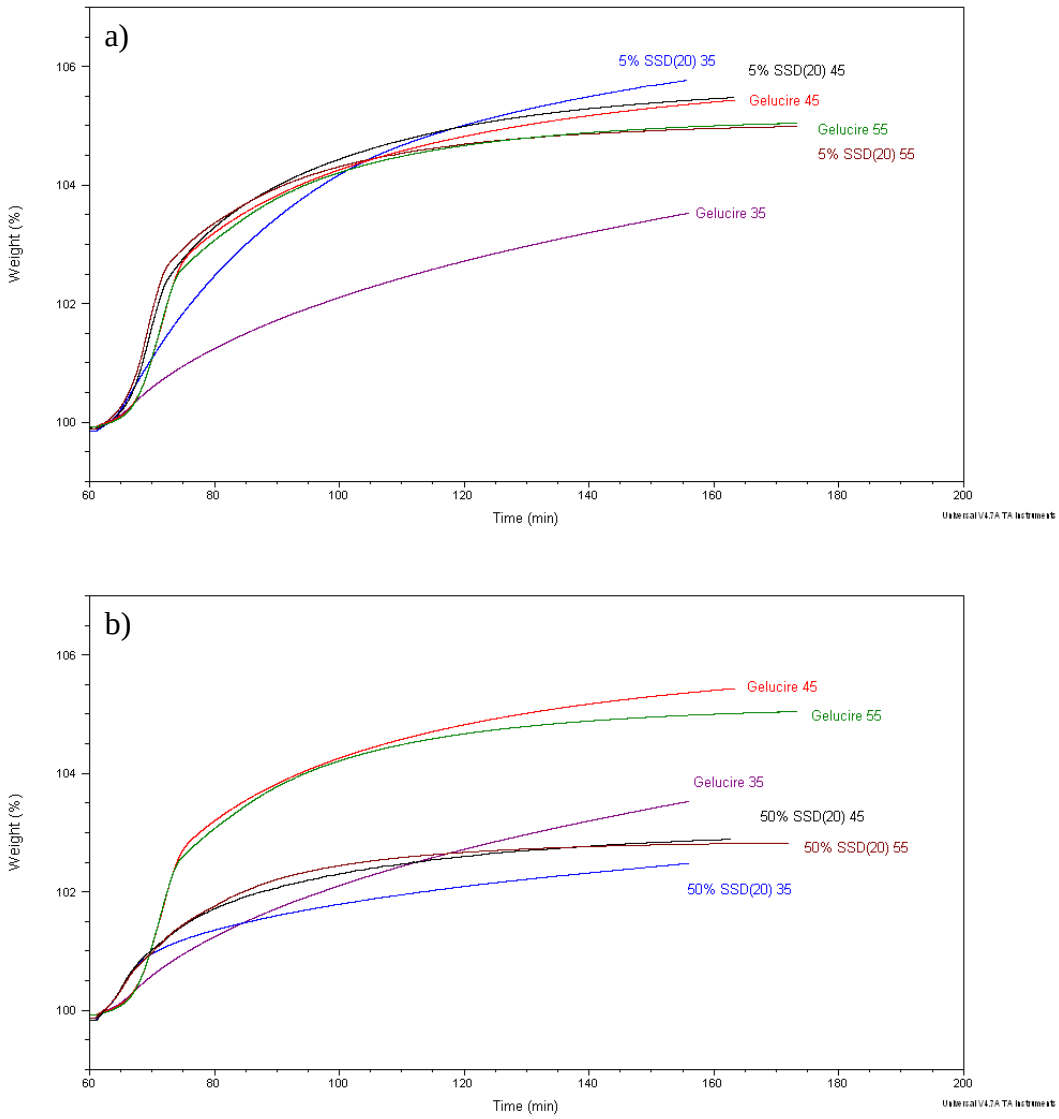

Figure 6.3 *Weight percent versus time signal for indometacin and Gelucire 44/14 SSD(20) a) 5% w/w and b) 50% w/w compared to that of Gelucire 44/14 alone at 75% RH isothermal at 35, 45 and 55°C.*

At 50% w/w (Figure 6.3 b), the SSD(20) systems were observed to absorb less moisture than Gelucire 44/14 at all temperatures. At 35^{o}C however, the shape of the SSD(20) plot appeared to be closer to that of the samples analysed at higher temperatures, with a rapid water uptake initially which began to slow over time, unlike that of the lipid alone at this temperature which absorbed moisture at a steady rate over the course of the experiment.

Table 6.2 *Moisture uptake as percentage weight gain by indometacin and Gelucire 44/14 SSD systems in comparison with Gelucire 44/14 alone under isothermal temperature conditions at 75% RH.*

Isothermal Temperature (°C)	Formulation	Weight Gain (%)	Standard Deviation
35	Gelucire 44/14	3.8	1.4
	5% SSD(20)	5.9	1.6
	50% SSD(20)	2.8	0.7
45	Gelucire 44/14	5.7	1.8
	5% SSD(20)	5.3	2.0
	50% SSD(20)	3.0	0.7
55	Gelucire 44/14	5.2	1.6
	5% SSD(20)	4.9	1.7
	50% SSD(20)	2.7	0.7

At this high concentration, the drug constitutes a major component of the SSD system, and it was shown in Chapter Four that of the solid crystalline indometacin that was formulated into the system, approximately 35% w/w remained in the crystalline state. It would be reasonable to assume that whether the lipid be in the solid or liquid state, the presence of a large proportion of insoluble crystalline drug particles would retard the water absorption capability and capacity of the formulation. It should also be noted that Gelucire 44/14 would only constitute 50% w/w of the system and therefore, in terms of mass in the crucible, would be significantly less than that of the lipid alone.

6.5 HYDRATION BEHAVIOUR OF PIROXICAM AND GELUCIRE 44/14 SEMI-SOLID DISPERSION SYSTEMS

The piroxicam and Gelucire 44/14 SSD(20) systems demonstrated a similar hydration profile as that observed for both ibuprofen and indometacin. At 35^{o}C low piroxicam concentrations (5% w/w) were seen to have a greater affinity for atmospheric moisture than that of the lipid alone (Figure 6.4 a). Data outlined in Chapter Four however suggested unexpectedly that, at 5% w/w, there was no molecular dispersion of piroxicam possibly due to low miscibility between the lipid and drug, and subsequently therefore that the piroxicam existed in the formulation as solid crystalline particles. Despite this, this hydration data may give an indication that there could possibly be a small extent of molecular piroxicam dispersion, enough to create sufficient lipid crystalline molecular disorder to allow an increased level of water uptake when in comparison with the lipid alone.

The SSD(20) systems at 45 and 55^{o}C absorbed moisture at a similar rate and to a similar extent as the lipid alone due to the molten state of the systems creating complete molecular disorder to equal extents in both the SSD(20) and Gelucire 44/14 samples alike.

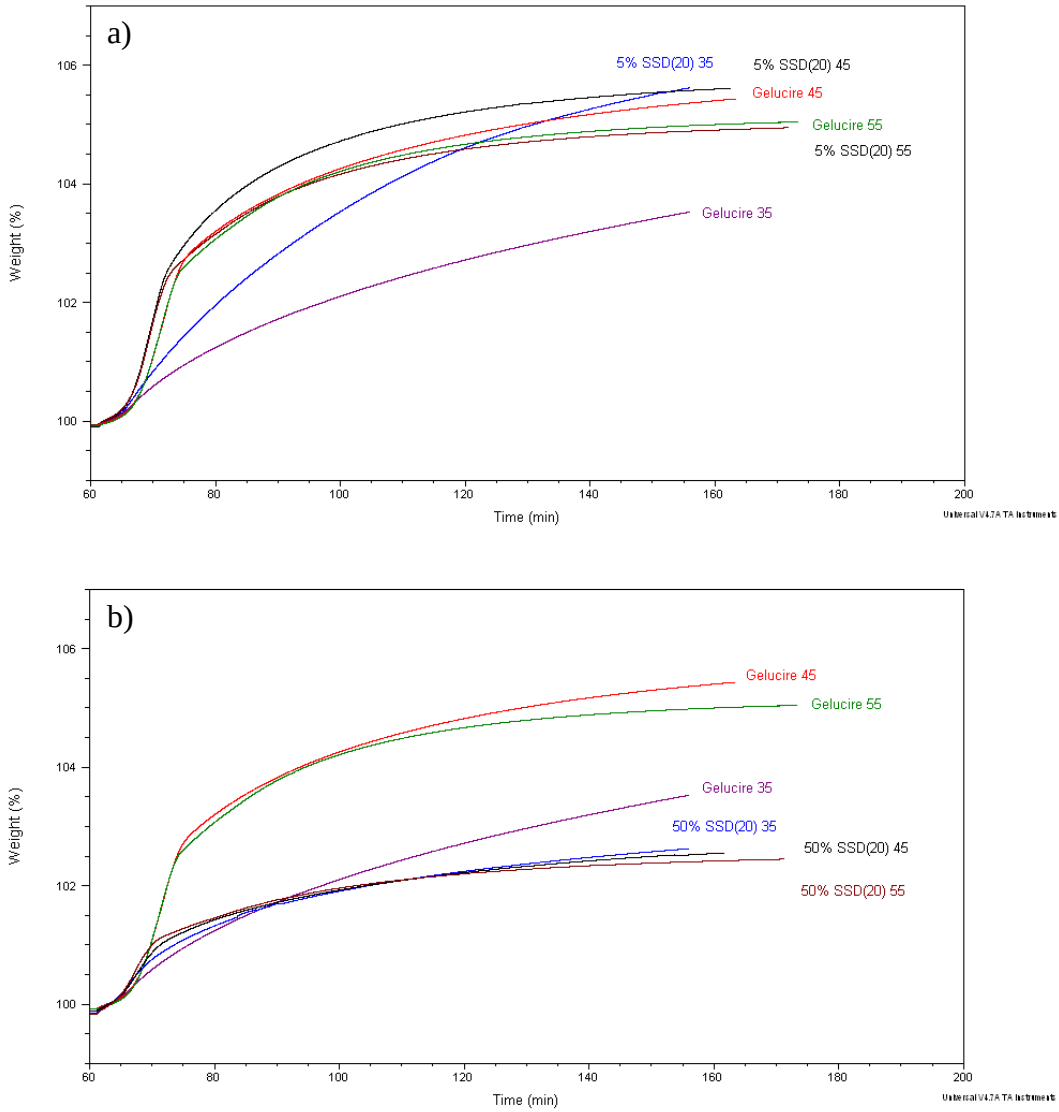

Figure 6.4 *Weight percent versus time signal for piroxicam and Gelucire 44/14 SSD(20) a) 5% w/w and b) 50% w/w compared to that of Gelucire 44/14 alone at 75% RH isothermal at 35, 45 and 55°C.*

At a piroxicam loading concentration of 50% w/w, the SSD(20) systems showed a consensus of reduced water affinity compared to that of the lipid alone at all temperatures (Figure 6.4 b). This was as expected due to the likelihood of the large proportion of solid insoluble crystalline piroxicam still present in the system during analysis retarding the water uptake capability of the SSD(20) systems along with a reduced mass of Gelucire 44/14.

Table 6.3 *Moisture uptake as percentage weight gain by piroxicam and Gelucire 44/14 SSD systems in comparison with Gelucire 44/14 alone under isothermal temperature conditions at 75% RH.*

Isothermal Temperature (^{o}C)	Formulation	Weight Gain (%)	Standard Deviation
35	Gelucire 44/14	3.8	1.4
	5% SSD(20)	5.9	1.4
	50% SSD(20)	2.6	0.6
45	Gelucire 44/14	5.7	1.8
	5% SSD(20)	5.5	1.7
	50% SSD(20)	2.7	0.8
55	Gelucire 44/14	5.2	1.6
	5% SSD(20)	4.9	1.7
	50% SSD(20)	2.5	0.7

6.6 CONCLUSIONS

Overall, the DVS analysis of the three insoluble model drug SSD systems demonstrated very similar results. The most interesting point to note is that at low drug SSD loading and at the lowest temperature investigated, 35^{o}C (which is not unattainable during storage), the affinity for water of the formulation increased noticeably. Despite this experiment being conducted at 75% RH, it gave a good indication of the samples response to humidity, and it should be considered that under ambient conditions the RH will fluctuate, potentially reaching a maximum of 60%. This effect of low drug concentration will have an impact on the effect of

storage on the formulation and should therefore be taken into consideration. At high drug concentrations, the effect of temperature appeared to have little effect upon the water affinity of the SSD systems, with all absorbing moisture to similar extents. It therefore seems reasonable that not only should the enhancement of dissolution properties be taken into account (which decreases with increasing drug) but also the effect on the affinity for atmospheric moisture (which decreases with increasing drug) when selecting suitable drug loadings for formulated drug SSD systems.

CHAPTER SEVEN

EFFECT OF AGING ON SEMI-SOLID DISPERSION SYSTEMS

7.1 INTRODUCTION

Aging of formulations upon storage and subsequent alteration of their physical properties is a major issue governing the success of prospective dosage forms. These changes must therefore be fully investigated and characterised, determining the effect on the biopharmaceutic parameters and thereby allowing establishment of product stability and optimum conditions for storage over its intended shelf life. Gelucires, being composed of varying amounts of glycerides and PEG esters, and their formulations are known to exhibit physical instability upon aging thereby causing modification to the in vitro and in vivo release of drug from the dosage form. The glyceride and PEG ester components of Gelucires are known to display different physical properties and limited solubility within one another meaning that, after aging, extensive segregation of these components into different melting fractions in microscopic regions has been noted in the literature. These changes have also been correlated with alterations in tensile strength of the sample (San Vincente et al. 2000; Sutananta et al. 1994a). It should also be considered that Gelucires, being lipidic in nature, have the capacity to spontaneously react with oxygen bringing about subsequent degradation of the excipient (San Vincente et al. 2000).

Gelucires have been found to demonstrate increased melting temperatures after storage however this effect could not be correlated with drug release (Dennis 1988). Thermal history has also been shown to impact the crystal structure and dissolution properties of PEGs which are found in large proportions in many grades of Gelucires (Craig and Newton 1991). There have however been studies which noted no change

in the dissolution properties of SSD systems of Gelucire 44/14 after storage over 3 months (Dordunoo et al. 1991).

Khan and Craig (2004) noted that upon storage of Gelucire 50/13 and caffeine or paracetamol SSD systems, significant changes in the surface morphology were found to take place in the form of microcracks (due to contraction of the matrix) and also blooming which, in relation to fat systems, is associated with the migration of lipid to the surface of the formulation rather than polymorphic changes, most likely to occur in soft, low melting point lipid systems like those of Gelucire 44/14. These gross surface alterations were attributed to supramolecular or microscopic changes in the SSD integrity which were undetectable using DSC.

These factors are investigated in this chapter with aged SSD formulations being characterised using conventional differential scanning calorimetry and hot stage microscopy, and the release properties of the model drugs from the formulations being observed using in vitro dissolution testing.

7.2 METHODOLOGY

7.2.1 Conventional Differential Scanning Calorimetry

Conventional DSC experiments were performed under a nitrogen environment, with a purge rate of 50ml/minute. Calibration of the instrument was conducted, prior to experimentation which involved cell resistance and capacitance (baseline) calibrations with an empty cell and sapphire disks (Tzero calibration), cell constant calibrations using indium standard (melting point 156.6°C, heat of fusion 28.6J/g),

and finally temperature calibrations using benzoic acid (melting point 122.4°C) and n-octadecane (melting point 28.2°C). Temperature calibrations were carried out at the same rate as intended for sample analysis. Samples were formulated into SSD systems as outlined in Chapter Two, prepared and crimped into Tzero aluminium pans and analysed at time zero and also after being stored at room temperature and humidity, protected from light, for 12 months.

Experiments were conducted at 10^{o}C/minute, heating throughout the melting transition to 100^{o}C for ibuprofen formulations, 200^{o}C for indometacin, and 220^{o}C for piroxicam. Samples were then cooled to -30^{o}C. Experiments were repeated four times.

7.2.2 Hot Stage Microscopy

Samples for analysis were formulated into SSD systems as outlined in Chapter Two and stored at room temperature and humidity, protected from light, for 12 months prior to analysis. Samples were applied to glass microscope slides, enclosed with a glass cover slip and heated from room temperature through the melt transitions of both the lipidic carrier and the model drug at 10^{o}C/minute. Capture was terminated on visualisation of complete melting. Images were captured at x20 magnification under polarised light.

7.2.3 In Vitro Release

Samples for analysis were formulated and prepared into capsules as outlined in Chapter Two. Capsules were stored at ambient temperature and either ambient humidity or 0% relative humidity achieved under a phosphorous pentoxide environment, protected from light, for 2 months. Dissolution studies were carried out, in triplicate, in 900ml distilled water at 37^{o}C over 45 minutes. Samples, 10ml in volume, were withdrawn periodically and replaced with an equivalent volume of dissolution medium at the same temperature. The samples were filtered through a 0.45µm filter, the UV absorbances of which were recorded in triplicate. Full details of calibration data can be found in Chapter Five, Section 5.2.

7.3 AGED IBUPROFEN AND GELUCIRE 44/14 SEMI-SOLID DISPERSION SYSTEMS

7.3.1 Assessment of Thermal Properties using Conventional Differential Scanning Calorimetry

Differential scanning calorimetric analysis of the first melting transition of SSD samples at time zero and after storage under ambient conditions for 12 months is shown in Figure 7.1. For 5% w/w systems, the melting endotherm of the lower melting point fractions of Gelucire 44/14 displayed an increase in $Tm_{(onset)}$ and $Tm_{(max)}$ for the SSD(20) formulations, also noted by Dennis (1988), with only a higher $Tm_{(onset)}$ for SSD(4). In both cases, a small increase in ΔH of the peaks was measured. Damian (2002) made a similar observation and attributed it to a reorganisation of the Gelucire 44/14 structure. Following on from this however, the primary melting endotherm corresponding to the higher melting point fractions was found to occur at a lower $Tm_{(max)}$ with a significantly reduced ΔH value in both cases i.e. from 44.7 J/g ± 1.8 to 15.5 J/g ± 5.5 for SSD(20) and 40.4 J/g ± 1.6 to 24.6 J/g ± 1.4 for SSD(4) also possibly attributable to a structural reorganisation. The aged samples did not demonstrate an ibuprofen melting endotherm, comparable with the fresh samples, which suggests that a molecular dispersion of the drug still existed and therefore no phase separation occurred during storage.

There are many different opinions with regards aging of Gelucires presented in the literature. A study carried out by Sutananta et al (1994a) noted that Gelucire 50/13, known to contain both glycerides and PEG esters, like 44/14, which display varying physical properties, separated into its constituent parts or melting fractions upon

aging. This segregation was more prominent for those samples that had been cooled slowly from the melt due to increased opportunity for segregation. It was also observed that the solubility between glycerides and PEG esters was limited which would also promote separation. This effect was not necessarily observed in the data collected in this present study, however changes in DSC traces after storage were found to be associated with the recombination or segregation of the numerous components into different regions on a microscopic scale. Further to this, it was observed by San Vicente et al (2000) that the mechanism behind the aging effects seen in Gelucires may in part be attributed to the conversion of triglycerides into more stable polymorphic forms, however they did not observe any noteworthy changes in the DSC trace after 12 months storage. This effect was most prominent in fast release lipidic systems (as is Gelucire 44/14) due to the low melting point and the subsequent possibility of a proportion of the lipid being liquid in nature at ambient temperature which may recrystallise on storage.

At 50% w/w, as described in Chapter 4, the primary melting endotherm was completely absent suggesting interaction between the higher melting point fractions with the ibuprofen. This was not detected at lower drug concentrations. This was also confirmed by the broadening of the ibuprofen melting peak with a subsequent depression in the melting point from 76^{o}C for ibuprofen alone to 68^{o}C. This effect was also seen in the aged samples. For the SSD(20) systems, the ibuprofen melt endotherm was found to increase significantly in $Tm_{(onset)}$ and ΔH, in the range of 11^{o}C and 14 J/g respectively, suggesting recrystallisation of the molecularly dispersed ibuprofen over time. The SSD(4) however only demonstrated a slight increase in the $Tm_{(onset)}$, with the $Tm_{(max)}$ and ΔH being similar in value. In both cases

the lipid secondary peak was smaller and sharper, with an increased $Tm_{(onset)}$ and reduced $Tm_{(max)}$. The ΔH of the peaks was significantly reduced from 28.1 J/g ± 1.9 to 2.7 J/g ± 0.7 for SSD(20) and 25.1 ± 1.1 to 4.1 J/g ± 1.2 for SSD(4). The changes in the DSC traces again suggested that upon aging, reorganisation of the Gelucire 44/14 structure may have taken place, involving the recombination or segregation of components into different microscopic regions.

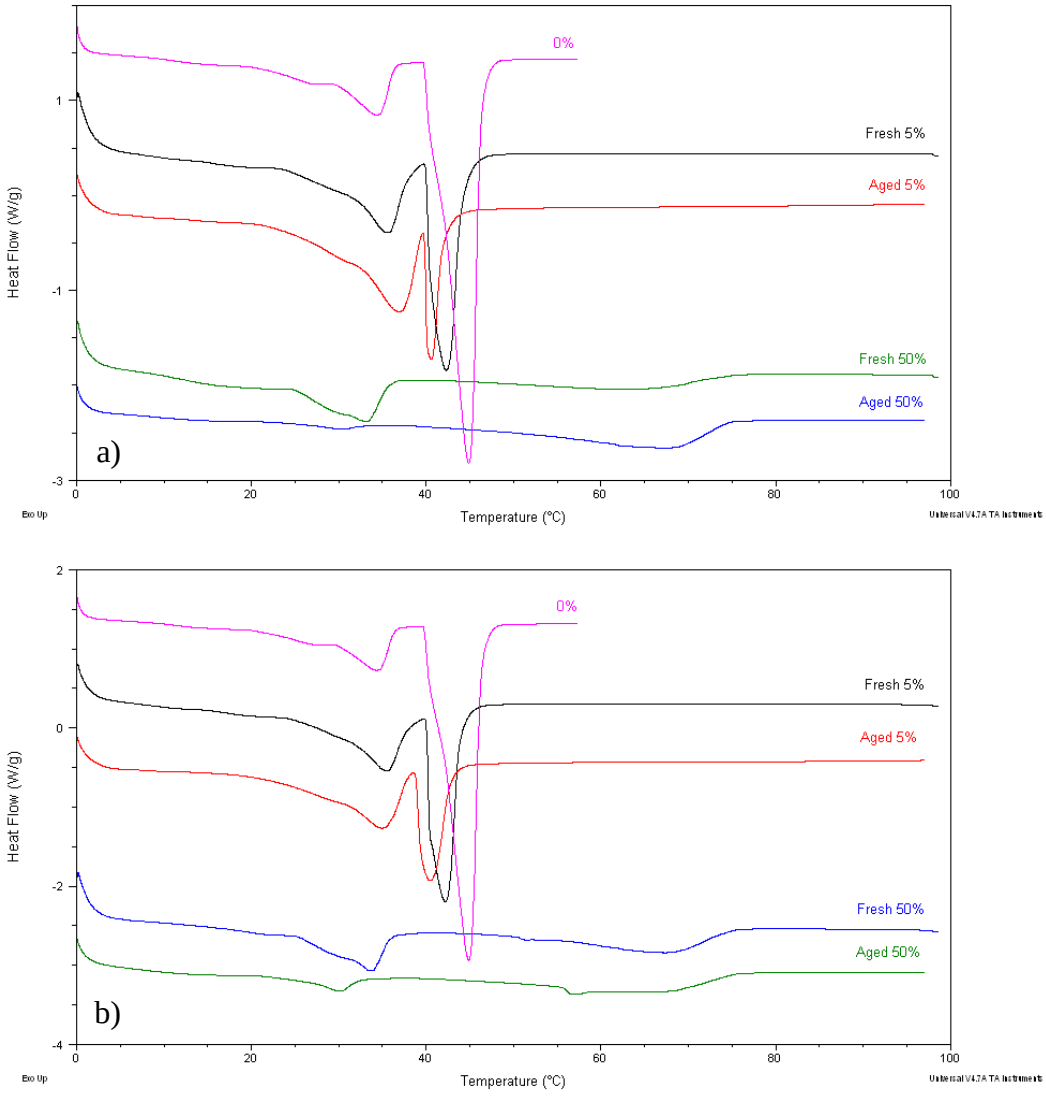

Figure 7.1 *Heat flow against temperature signal on heating at 10°C/minute of aged ibuprofen and Gelucire 44/14 a) SSD(20) and b) SSD(4) – First melt.*

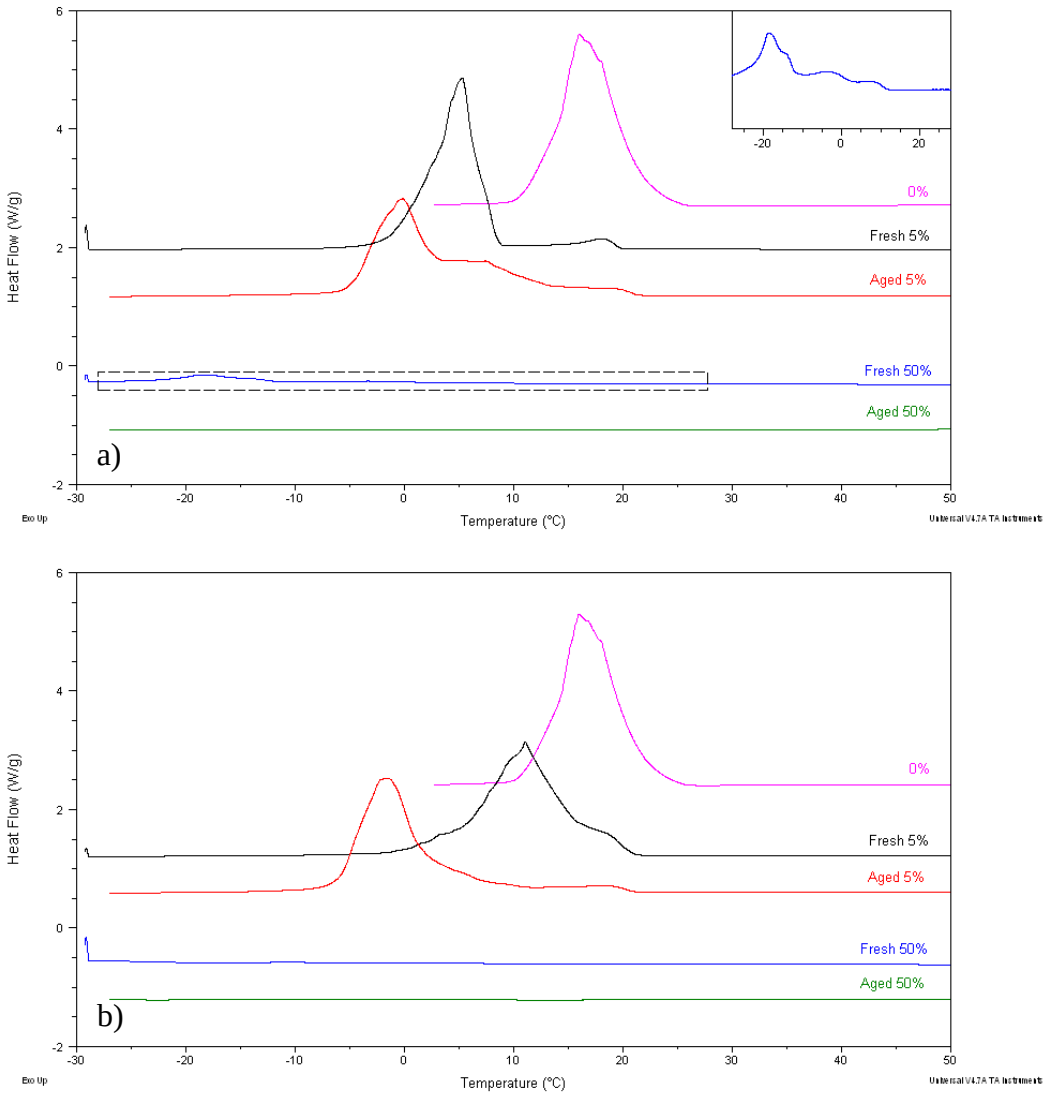

Figure 7.2 *Heat flow against temperature signal on heating at 10°C/minute of aged ibuprofen and Gelucire 44/14 a) SSD(20) and b) SSD(4) – Crystallisation.*

Upon cooling of the 5% w/w aged systems, in both cases, the shape of the crystallisation exotherm demonstrated changes in relation to that prior to aging (Figure 7.2). A leading shoulder was still observed, which appeared to correspond with the original Gelucire 44/14 crystal formation at approximately 20°C, however the main crystallisation peak reduced in temperature to below 0°C. In the aged SSD(20) formulations, an additional shoulder was present, which appeared to

correlate with that of the main crystallisation peak of the freshly prepared formulations.

After heating however, both the lipid and drug were in the molten state and therefore isotropic in nature, and theoretically identical to that of the fresh samples. One possible explanation for the changes observed in the crystallisation transition may be that Gelucire 44/14 underwent auto-oxidation during storage bringing about degradation of the lipid (San Vincente et al. 2000).

7.3.2 Observation of Thermal Transitions by Hot Stage Microscopy

HSM images were captured of SSD formulations after aging. At 5% w/w, the fresh and aged samples were observed to be much the same in appearance, with the complete absence of ibuprofen crystal particles. This was attributable to the dissolution of ibuprofen during formulation creating a molecular dispersion, and it therefore suggests the absence of phase separation of the ibuprofen from the lipid during storage, in line with conventional DSC.

At 50% w/w however, as expected, crystalline ibuprofen was present. The crystals present in the freshly formulated sample were visibly smaller in size and great in number. After aging however the ibuprofen crystals were much larger and more structured in shape. It should be considered that the position of the microscope over the sample may be a factor. It is also possible however that during formulation the molten Gelucire 44/14 became supersaturated with molecularly dispersed ibuprofen, which then proceeded to recrystallise out of the lipid during storage causing growth

of the pre-existing crystals. DSC was able to lend weight to this conclusion by demonstrating an increased ΔH of the ibuprofen melt for the aged SSD(20) systems, however this was not the case for the SSD(4) systems.

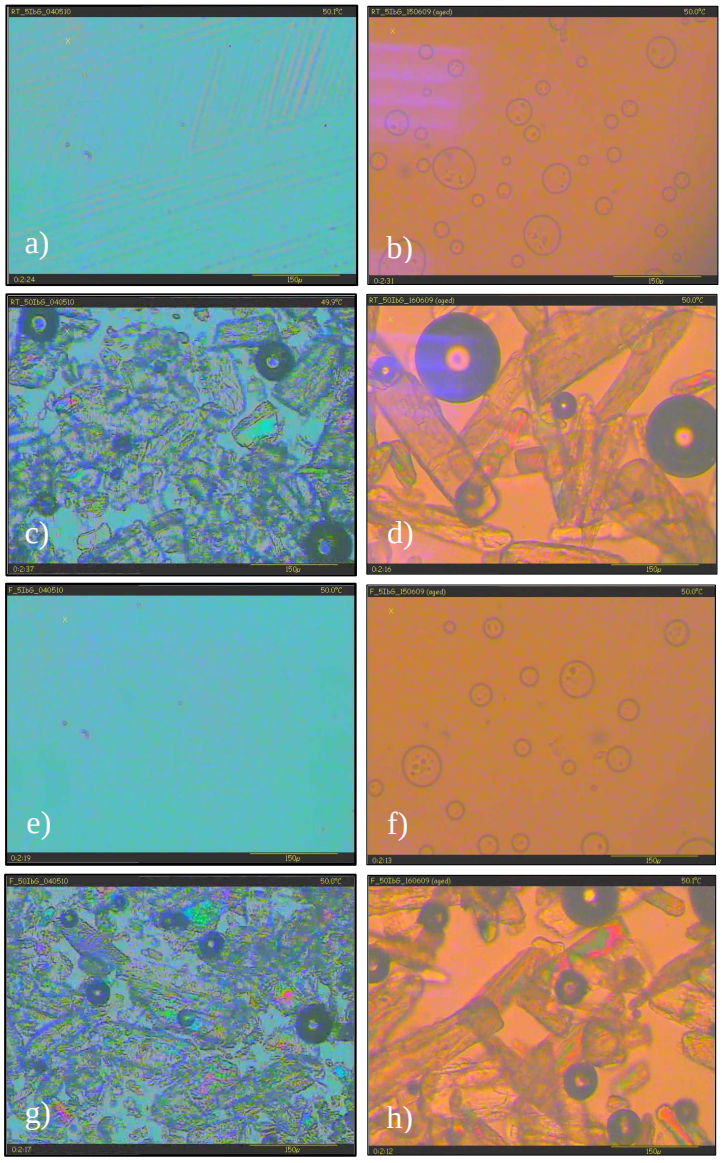

Figure 7.3 *HSM images of ibuprofen and Gelucire 44/14 SSD(20) a) 5% fresh; b) 5% aged; c) 50% fresh; d) 50% aged; and SSD(4) e) 5% fresh; f) 5% aged; g) 50% fresh; h) 50% aged at 50°C in order to visualise only crystalline ibuprofen.*

7.3.3 In Vitro Release Profile

In the literature it is apparent that many studies have found it difficult to correlate changes observed in the physicochemical properties of the aged SSD systems with those subsequent changes seen in the dissolution profile (Sutananta et al. 1995b; Sutananta et al. 1996).

In this study, upon in vitro dissolution of ibuprofen and Gelucire 44/14 SSD systems in water at 37^{o}C after aging under ambient conditions, no noteworthy changes in the release profile were observed. At 5% both aged formulations achieved a total ibuprofen release of 100%, comparable to that of the fresh samples. The MDT-50% values were also similar. At 50% w/w again there were no significant changes observed in the release profile or MDT-50%, with both the aged and fresh formulations releasing ibuprofen to approximately 80%.

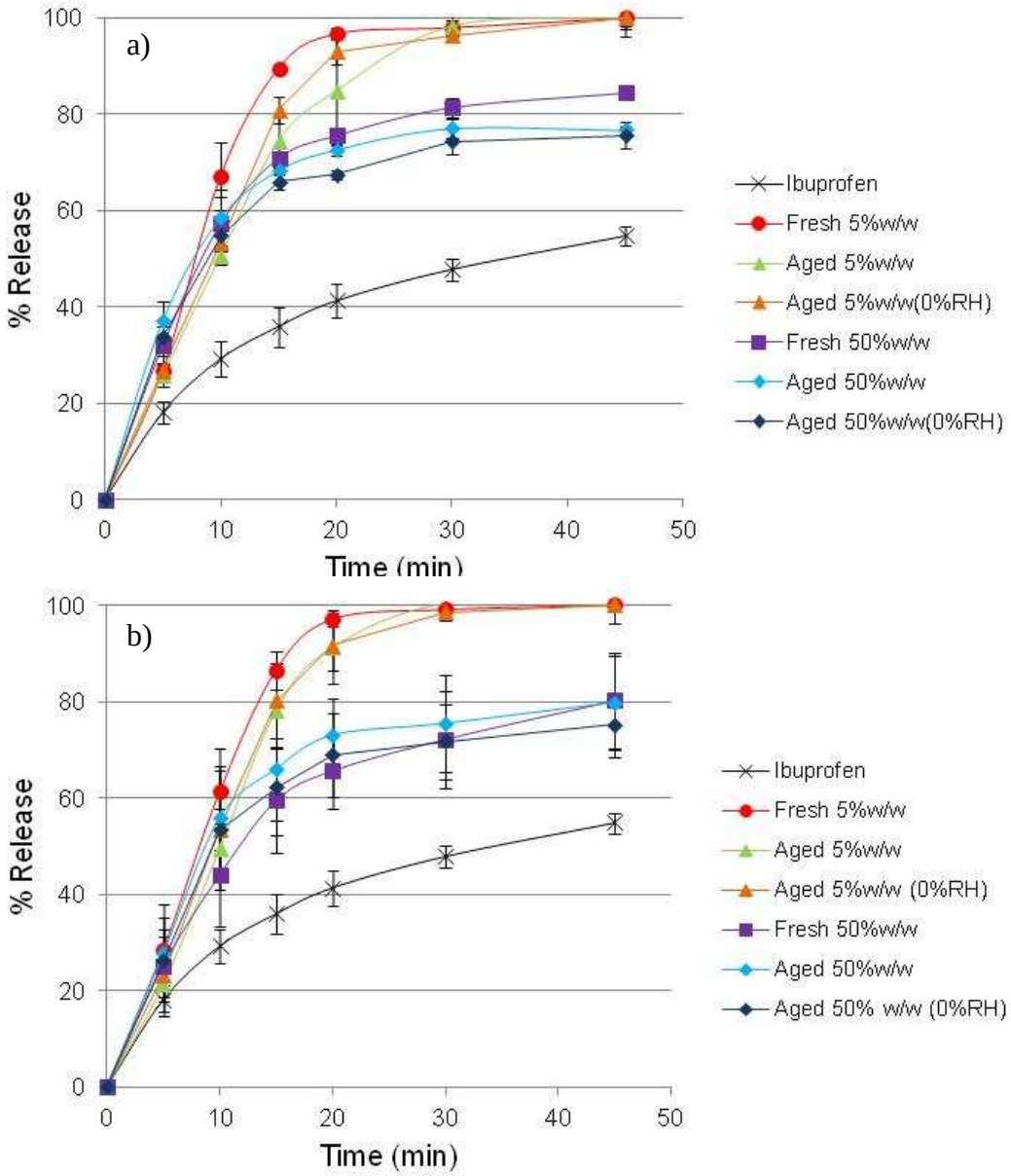

Figure 7.4 *Release of ibuprofen from a) SSD(20) and b) SSD(4) systems over time in water at 37°C either freshly prepared or after storage at ambient and 0% RH.*

Table 7.1 *Mean dissolution time for ibuprofen release up to 50% (MDT-50%) and the calculated release exponent n using the Power-Law.*

Formulation		Storage Humidity	MDT-50% (min)	Power-Law Model *n*
Ibuprofen Alone			34.8	0.45
SSD(20)	5%	Fresh	7.5	0.37
		Aged Ambient	8.6	0.96
		Aged 0% RH	9.1	1
	50%	Fresh	8.6	0.34
		Aged Ambient	8.2	0.45
		Aged 0% RH	9.1	0.38
SSD(4)	5%	Fresh	8.1	0.39
		Aged Ambient	8.8	1
		Aged 0% RH	9.3	1
	50%	Fresh	11.8	0.43
		Aged Ambient	8.9	0.61
		Aged 0% RH	9.3	0.44

In studies carried out by Khan and Craig (2004) however, an increased release rate and extent of release were observed. This increase was backed up by SEM data which indicated that supramolecular changes in the Gelucire 50/13 SSD matrix had occurred during storage, compromising its integrity with a subsequent increase in erosion of the matrix and therefore drug release rate. In this case, minor changes to the thermal properties were noted using conventional DSC suggesting physicochemical alteration on storage to some extent, possibly due to degradation of

the lipid by auto-oxidation; however these changes do not appear to have impacted the release of ibuprofen from the formulations.

The power-law mathematical model was used to give an indication as to the mechanism of drug release from the aged SSD systems, which was used as a comparison with the fresh samples. It is essential to bear in mind at this point that care must be taken in the interpretation of the modelling data. These systems are known to self emulsify upon contact with aqueous media due to the nature of Gelucire 44/14 and therefore the mechanisms of drug release cannot be easily categorised. It is however interesting to note how the data fits the model. The calculated values, *n*, are presented in Table 7.1. In all cases, changes in the values and therefore the mechanism of drug release were observed. At 5% w/w, *n* was found to take a value of 1 or close to, in comparison with a value of less than 0.5 for the fresh samples. This suggests that after storage under ambient conditions, drug release from the SSD systems changed from anomalous transport, diffusion and disintegration controlled, to a release controlled by case II transport (erosion/swelling) with zero order kinetics. It is not possible to speculate as to the exact mechanism by which the release of ibuprofen has been altered, however it is reasonable to suggest that the possible reorganisation of the lipid components into different microscopic regions during storage, as demonstrated by thermal analysis, may be a contributing factor. At 50% w/w however *n* was found to be closer in value to that of the fresh samples. For the SSD(20) systems, the mechanism of ibuprofen release remained controlled by diffusion although the SSD(4) formulations demonstrated anomalous drug transport i.e. a combination between both processes.

San Vicente et al (2000) found the *n* value of all investigated Gelucires not to change significantly upon aging, suggesting that despite physical changes occurring during storage, with subsequent dissolution changes, the mechanism was found to be maintained.

Again, after storage at 0% RH, the fresh and aged 5% w/w samples demonstrated comparable ibuprofen release profiles, with similar extent of release and MDT-50% values (Figure 7.4 and Table 7.1). In both cases the 50% w/w systems were also found to display a dissolution profile similar to that of the fresh and aged at ambient formulations. This suggests that since the majority of the drug present in the system was in the stable crystalline form, that storage and even ambient humidity, which can reach levels as high as 60%, had little effect on the formulation.

After modelling of the dissolution data using the power-law equation (Table 7.1), it was observed that at 5% w/w, after aging at 0% RH, the mechanism of release was similar to if not the same as the aged at ambient systems. Again this showed that before aging and storage, drug release was controlled by Fickian diffusion and disintegration, which is found to change to non-Fickian case II transport, again possibly due to the reorganisation or segregation of the lipid components over time. At 50% w/w however, those systems aged at 0% humidity were found to display *n* values comparable with those of the fresh samples i.e. diffusion and disintegration controlled release, which lends weight to the assumption that the large proportion of stable crystalline ibuprofen, alongside the crystalline lipid did not promote physicochemical changes over time.

Literature has suggested that the effect of storage humidity on the physicochemical properties of Gelucires, and therefore the rate of drug release from their SSD formulations, may be determined by the mechanism by which drug is released from the system. In the case of Gelucire 50/02, drug release from SSD formulations is controlled by diffusion and after aging under high RH, the dissolution rate was observed to decrease. Drug release from systems composed of Gelucire 50/13, however, is known to be controlled by erosion (case II transport) and formulations of this lipid were found to demonstrate an increase in drug release after storage at high RH. This may be due to the presence of a high proportion of PEG stearates which can hydrogen bond with atmospheric moisture and bring about significant changes in the lipid structure (Sutananta et al. 1996). In this case however, despite Gelucire 44/14 being known to contain up to 72% PEG esters, no change in the ibuprofen release was observed after aging, either at ambient or 0% RH suggesting that the formulations were very stable on storage.

7.3.4 Summary of Aged Ibuprofen and Gelucire 44/14 Semi-Solid Dispersion System Characterisation Studies

Characterisation of the ibuprofen and Gelucire 44/14 SSD systems over time has demonstrated a number of changes to the physicochemical properties of the formulations. DSC analysis of these systems suggested that in all cases a reorganisation of the lipid components into different microscopic regions may have taken place during storage bringing about alterations in the observed melting endotherm. The formulations with a higher ibuprofen content also suggested that there may have been further crystallisation of the molecularly dispersed drug upon

aging. The HSM images showed no change to the 5% w/w systems in the absence of crystalline ibuprofen particles, however at 50% w/w the crystals appeared to be larger in size, which backed up the observation from the DSC data of further crystallisation at this drug concentration.

Despite these changes, a subsequent alteration to the in vitro ibuprofen release profile from the SSD systems was not observed after storage at either ambient or 0% RH. The mechanism of drug release from the low concentration systems was seen to change after aging from diffusion and disintegration controlled to solely case II transport. The mechanism of ibuprofen release from the high concentration formulations did not change, possibly attributable to the large proportion of stable ibuprofen crystals. The formulations therefore demonstrated good stability in terms of in vivo ibuprofen release after aging.

7.4 AGED INDOMETACIN AND GELUCIRE 44/14 SEMI-SOLID DISPERSION SYSTEMS

7.4.1 Assessment of Thermal Properties using Conventional Differential Scanning Calorimetry

After aging of indometacin and Gelucire 44/14 SSD formulations under ambient conditions the characteristic lipid melting endotherm could be observed (Figure 7.5 a and b). At 5% w/w the secondary melting peak of the lipid lower melting point fractions was found to occur at a slightly lower $Tm_{(onset)}$ and $Tm_{(max)}$, however the measured ΔH values were comparable to those of the fresh samples. The lipid primary melting endotherm corresponding to the most prominent peak of the higher melting point fractions was observed to show similar $Tm_{(onset)}$ and $Tm_{(max)}$ to the fresh samples however were measured to have greater ΔH values i.e. from 52.8 J/g ± 1.8 to 65.9 J/g ± 2.9 for SSD(20) and 51.6 J/g ± 0.9 to 64.1 J/g ± 1.2 for SSD(4).

This change in transition ΔH may be attributable to a reorganisation of the lipid structure brought about by recombination or segregation of the many components into different microscopic regions (Damian 2002; Sutananta et al. 1994a). As with the fresh samples, the aged systems did not display indometacin melting endotherms suggesting that, even after storage, a molecular dispersion of indometacin was still present despite alterations within the lipid.

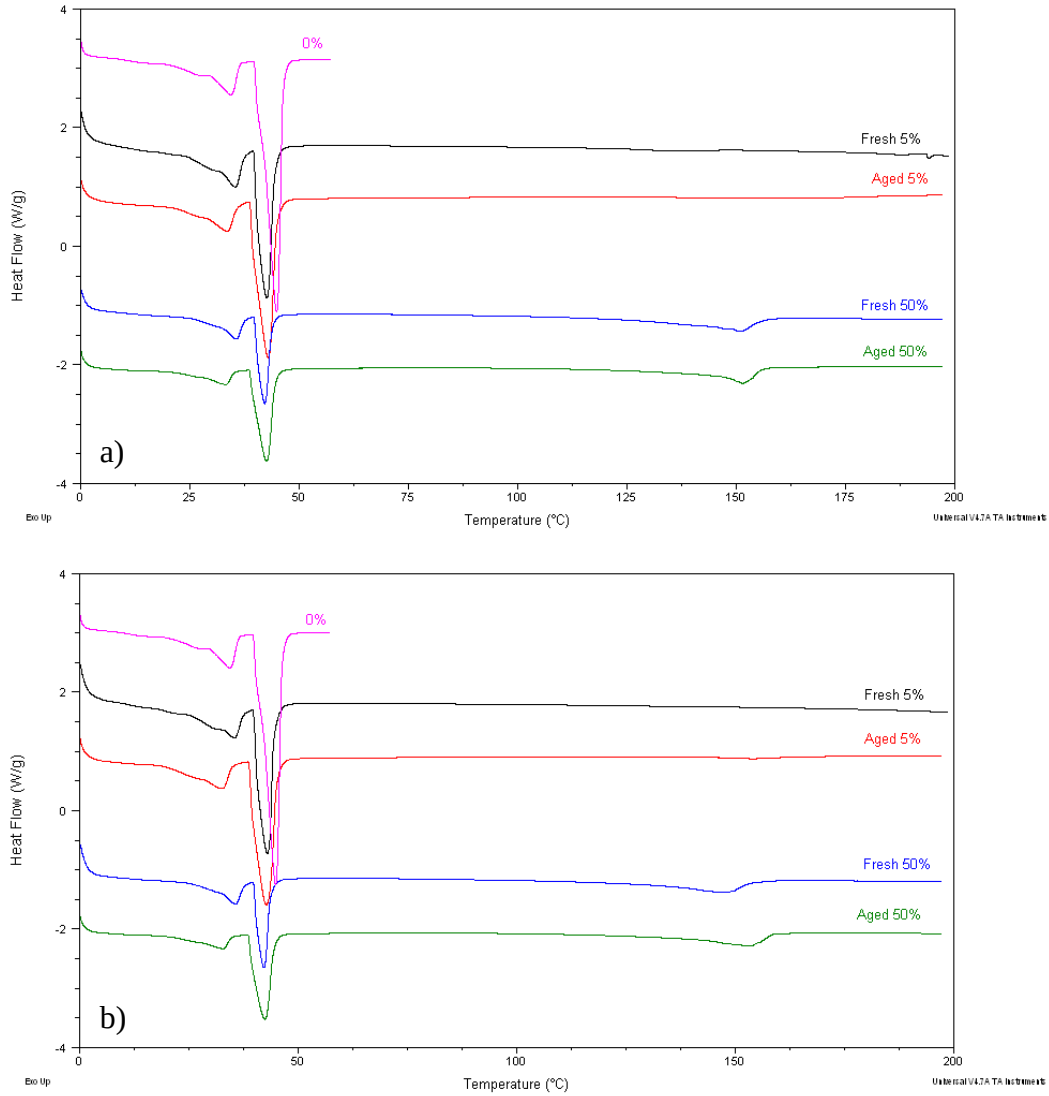

Figure 7.5 *Heat flow against temperature signal on heating at 10°C/minute of aged indometacin and Gelucire 44/14 a) SSD(20) and b) SSD(4) – First melt.*

At 50% w/w, the secondary melting endotherm was observed to shift to a slightly lower $Tm_{(onset)}$ and $Tm_{(max)}$ than that of the fresh samples. The melt ΔH was also observed to decrease in the range of 2 to 3J/g. The temperatures of the primary melting transition were found not to have changed after aging, however the ΔH increased by 10J/g in both cases, again possibly due to lipid segregation or reorganisation. On average, the indometacin melting endotherm, after aging of the SSD(20) systems was observed to shift to a higher $Tm_{(onset)}$ and $Tm_{(max)}$ by 10°C in

each case, with a reduced ΔH in the region of 7J/g in comparison with the freshly analysed samples. The drug melt of the SSD(4) formulations however were comparable with those of the fresh samples.

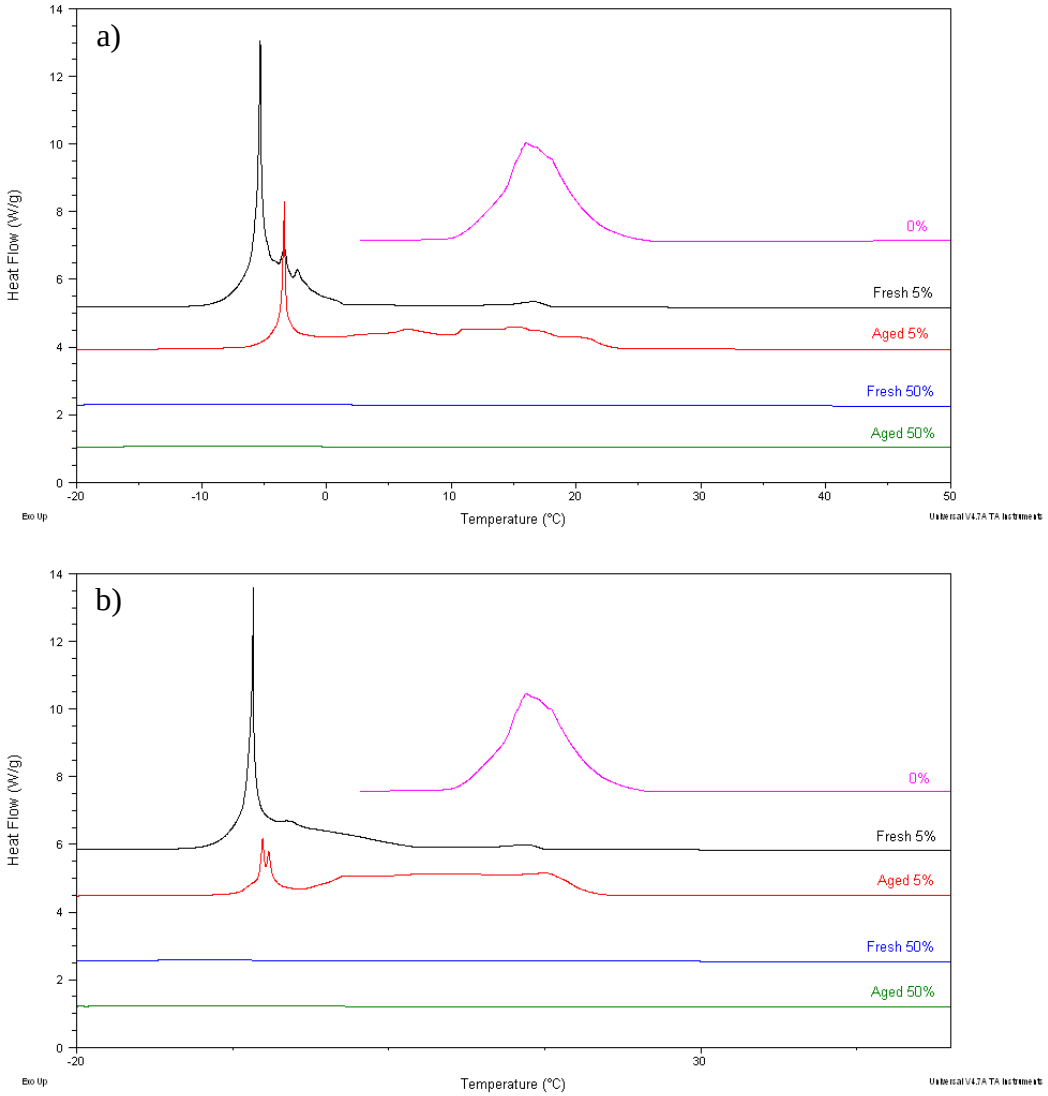

Figure 7.6 *Heat flow against temperature signal on heating at 10°C/minute of aged indometacin and Gelucire 44/14 a) SSD(20) and b) SSD(4) – Crystallisation.*

Upon cooling of the 5% w/w SSD systems, in both cases, the main crystallisation peak was observed to visually decrease in size (Figure 7.6 a and b). The $Tc_{(onset)}$ was found to remain the same at -3°C after aging. In terms of peak ΔH, this was

comparable for the SSD(4) systems however it was observed to decrease from 89.6 J/g ± 2.7 to 67.2 J/g ± 3.4 for the SSD(20) formulations. The shapes of the crystallisation transition demonstrated obvious differences however. The fresh samples displayed a small leading shoulder to the crystallisation exotherm which appeared to correspond well with that of the Gelucire 44/14 alone. In the aged samples, this shoulder appeared to be more prominent suggesting more extensive conversion of the lipid to its original crystalline formation. It should be noted that the crystallisation peaks for both the fresh and aged samples were uncharacteristically sharp for lipids which tend to be broad in nature due to their complex characteristics. The observed changes may have been attributable to lipid degradation brought about by auto-oxidation as suggested earlier in the Chapter. At 50% w/w, again no crystallisation transition could be observed for the aged samples as was observed with those analysed at time zero.

7.4.2 Observation of Thermal Transitions by Hot Stage Microscopy

In all cases, there were no obvious differences in the HSM images of the aged SSD systems in comparison with the fresh samples. Crystalline indometacin particles were completely absent from the 5% w/w systems confirming the presence of a molecular drug dispersion in the lipid. As expected, a large number of indometacin crystals were observed at 50% w/w which was comparable between the fresh and aged samples.

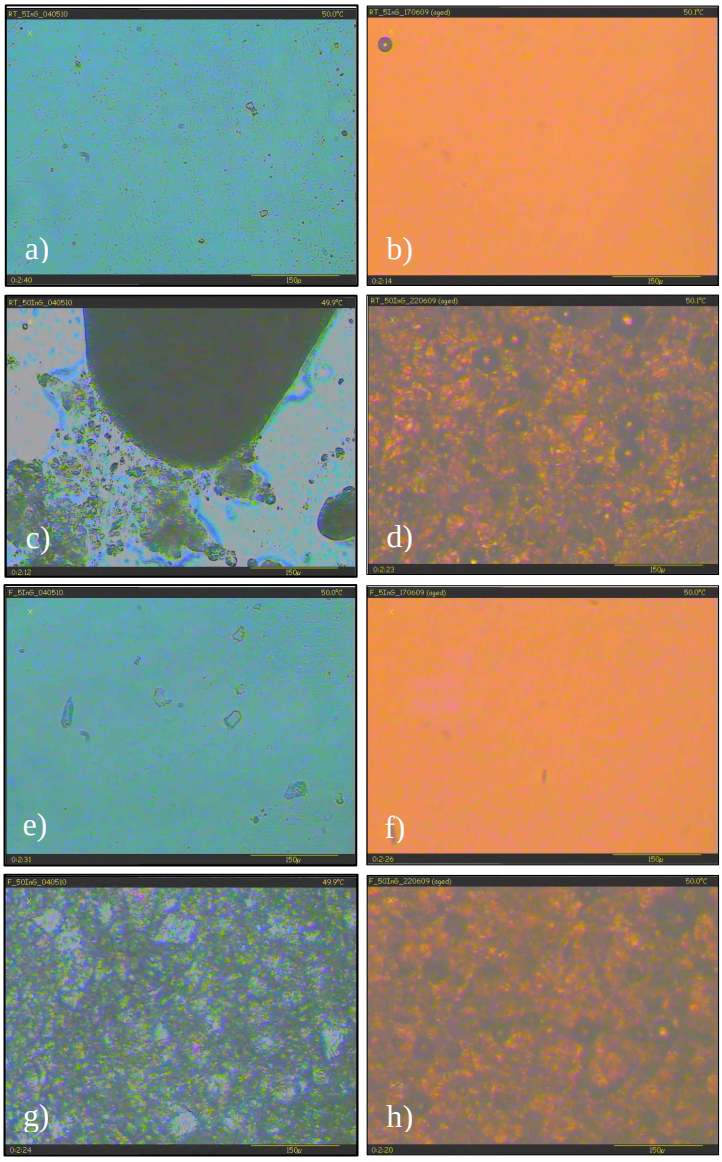

Figure 7.7 *HSM images of indometacin and Gelucire 44/14 SSD(20) a) 5% fresh; b) 5% aged; c) 50% fresh; d) 50% aged; and SSD(4) e) 5% fresh; f) 5% aged; g) 50% fresh; h) 50% aged at 50°C in order to visualise only crystalline indometacin.*

7.4.3 In Vitro Release Profile

The dissolution profile of indometacin and Gelucire 44/14 SSD systems, aged under ambient conditions protected from light, were investigated in water at 37^{o}C over 45 minutes (Figure 7.8). The 5% w/w systems released indometacin to the same extent, slightly less than 60%. This is likely to be attributable to non-sink conditions of the experiment. After aging however indometacin was released at a slower rate than that of the fresh samples, with the MDT-50% increasing from 17.7 to 25.8 minutes for SSD(20) and 16.6 to 31.1 minutes for SSD(4). The changes observed in the DSC traces of the aged samples suggested a reorganisation or segregation of the Gelucire 44/14 components which may have an effect on the rate at which the indometacin was released. The DSC data demonstrated that at 5%, the indometacin was still present as a molecular dispersion after aging suggesting that the extent to which it was released over the course of the experiment would be comparable. However it was suggested by Remunan et al (1992) that changes in the dissolution profile of Gelucire 53/10 SSD systems may be attributable to the formation of microcrystals which were undetectable using DSC which may be a possibility in this case. At 50% w/w, the SSD systems demonstrated equivalent dissolution profiles suggesting little change in the SSD physicochemical properties over time, most likely attributable to the large proportion of stable crystalline indometacin present in the formulation.

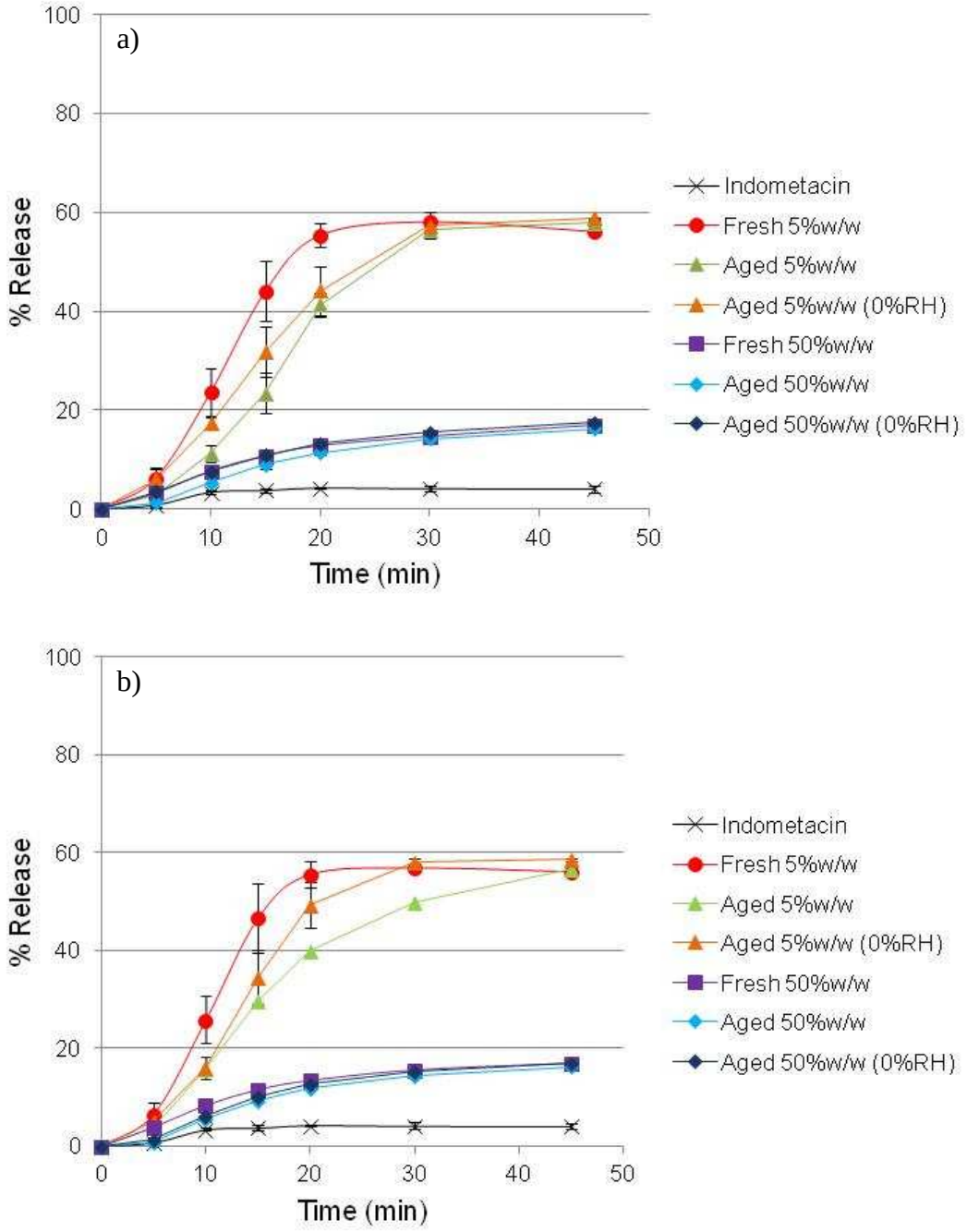

Figure 7.8 *Release of indometacin from a) SSD(20) and b) SSD(4) systems over time in water at 37°C either freshly prepared or after storage at ambient and 0% RH.*

Table 7.2 *Mean dissolution time for indometacin release up to 50% (MDT-50%) and the calculated release exponent n using the Power-Law.*

Formulation		Storage Humidity	MDT-50% (min)	Power-Law Model *n*
Indometacin Alone			>45	0.34
SSD(20)	5%	Fresh	17.7	0.54
		Aged Ambient	25.8	1
		Aged 0% RH	24.4	1
	50%	Fresh	> 45	0.56
		Aged Ambient	> 45	0.71
		Aged 0% RH	> 45	0.73
SSD(4)	5%	Fresh	16.6	0.51
		Aged Ambient	31.1	1
		Aged 0% RH	21.1	1
	50%	Fresh	> 45	0.51
		Aged Ambient	> 45	1
		Aged 0% RH	> 45	1

After modelling using the power-law equation, the *n* value obtained gave an indication of the mechanism by which drug was released from the formulation (Table 7.2). Again however, care should be taken in interpretation of these data due to the self-emulsifying nature of Gelucire 44/14. After aging under ambient conditions, the release of drug from the 5% w/w SSD systems in both cases shifted from anomalous transport to that entirely dominated by case II transport. At 50% w/w, the SSD(20) systems were found still to demonstrate anomalous drug release i.e. a combination of

diffusion and case II transport (erosion / swelling). The indometacin release from SSD(4) formulations was however found to be controlled solely by case II transport. As was the case with ibuprofen and also demonstrated by the thermal analysis of the indometacin systems, the possible recombination or segregation of the Gelucire 44/14 components over time may be a contributing factor to the changes in drug release mechanism observed.

Aging under conditions with 0% RH did not demonstrate noteworthy differences to those SSD systems which were exposed to a greater RH over time during storage (Figure 7.8). In both cases, the 5% w/w systems were found to release indometacin to equal extents, demonstrating similar release profiles (note the error bars for SSD(4) aged in Figure 7.8). The 50% w/w systems were also observed to demonstrate dissolution profiles with similar properties suggesting again that there was little change to the formulation over time.

The *n* values of the SSD systems aged at 0% RH, calculated by modelling of the dissolution data using the power-law equation, were found to demonstrate values very close to if not equal to those obtained for those samples aged under ambient conditions (Table 7.2). This suggests that the absence of atmospheric moisture in this case did not have any advantageous effect in comparison to those formulations stored under ambient conditions.

7.4.4 Summary of Aged Indometacin and Gelucire 44/14 Semi-Solid Dispersion System Characterisation Studies

A reorganisation or segregation of the Gelucire 44/14 components was suggested by the DSC data collected for the indometacin and Gelucire 44/14 SSD systems after aging. The 5% w/w formulations still however suggested that the indometacin existed as a molecular dispersion within the lipid. Similar changes were observed in the 50% w/w systems. The HSM images did not demonstrate any alterations to the physical state of the indometacin in the samples after aging, with crystalline drug particles being completely absent at 5% w/w and in great abundance at 50% w/w. A decrease in indometacin rate of release was observed after aging of the 5% w/w systems under ambient conditions which may possibly be due to the formation of insoluble microcrystals, undetectable using DSC. These changes also led to subsequent changes in the mechanism of drug release. Few changes were noted in the 50% w/w formulations.

7.5 AGED PIROXICAM AND GELUCIRE 44/14 SEMI-SOLID DISPERSION SYSTEMS

7.5.1 Assessment of Thermal Properties using Conventional Differential Scanning Calorimetry

After aging under ambient conditions, the heating profiles of the aged piroxicam and Gelucire 44/14 SSD systems are demonstrated in comparison with the fresh samples in Figure 7.9. Upon calculation of the transition properties for the 5% w/w systems, the secondary peak corresponding to the lower melting point fractions of the lipid was observed to decrease in $Tm_{(onset)}$ and $Tm_{(max)}$ in both cases after aging, in the range of 2 to 6^{o}C, however the ΔH was comparable in value. The main primary lipid melt peak was observed to be comparable in all properties with the exception of the SSD(4) formulations which were found to increase in ΔH from 62.9 J/g ± 0.7 to 71.8 J/g ± 2.2.

Unlike these other model drug systems, due to the low solubility of piroxicam in Gelucire 44/14, a drug melting endotherm could be measured as low as 5% w/w. As observed in Chapter Four, the melting endotherm of crystalline piroxicam present in the SSD systems demonstrated poor reproducibility with large standard deviation values. However on average, the piroxicam melt of the aged samples was found to occur at a lower $Tm_{(onset)}$ and $Tm_{(max)}$, with ΔHs similar to those calculated at time zero. Taking this into account, the changes observed in the lipid melting endotherm were less noteworthy than those observed for the other model drug systems presented above suggesting limited aging effects occurring during storage possibly due to the poor compatibility with the drug and therefore limited interaction between the two.

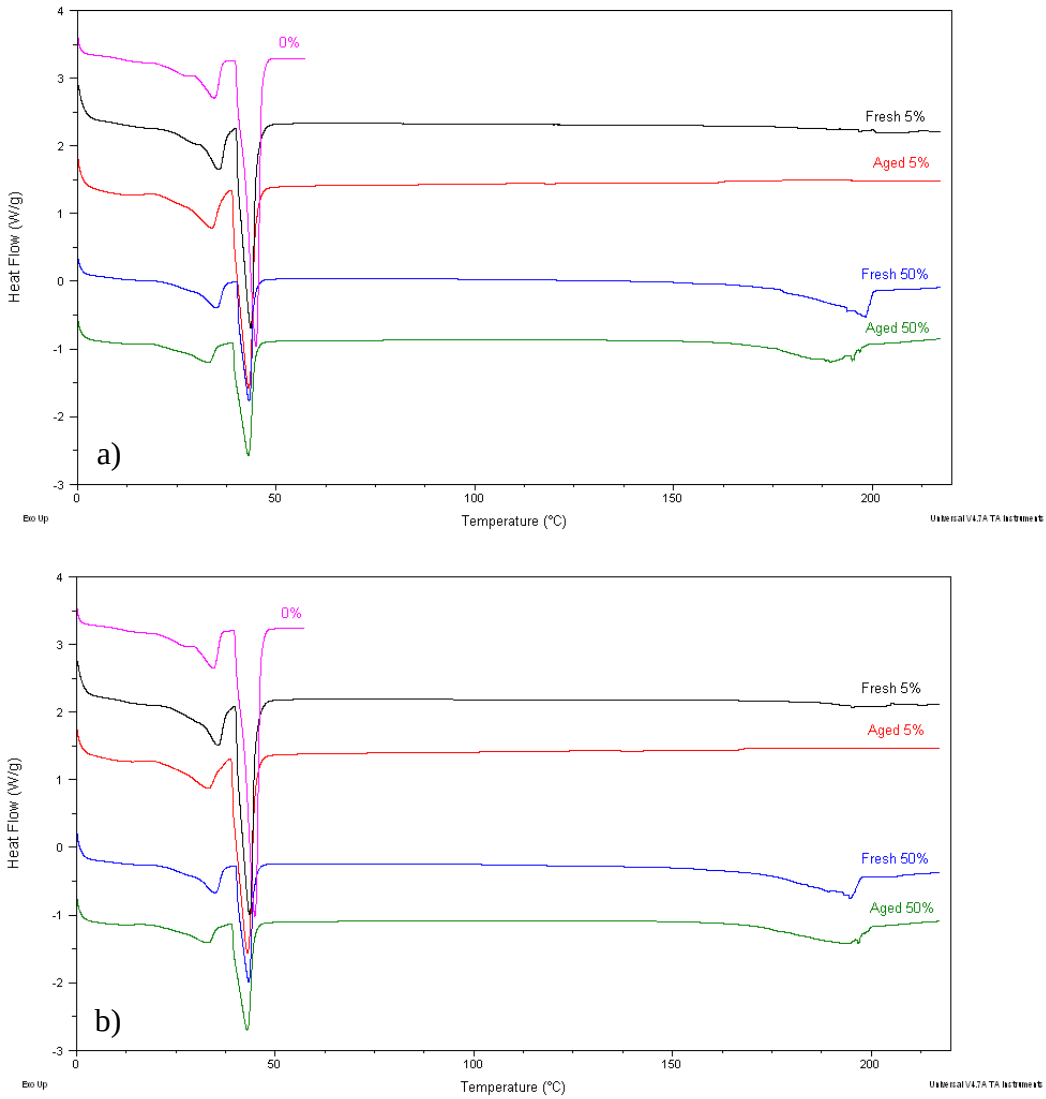

Figure 7.9 *Heat flow against temperature signal on heating at 10°C/minute of aged piroxicam and Gelucire 44/14 a) SSD(20) and b) SSD(4) – First melt.*

At 50% w/w, the SSD(20) systems after aging demonstrated no obvious differences to the fresh samples in terms of the Gelucire 44/14 melting transition. The measured piroxicam peak however was seen to broaden after storage, with a reduced $Tm_{(onset)}$ and increased $Tm_{(max)}$. The ΔH values were found to be comparable. The secondary Gelucire 44/14 melting peak of the SSD(4) formulations was observed to decrease in $Tm_{(onset)}$, and also in ΔH by approximately 12J/g. The primary lipid melting peak did not change greatly. In terms of the piroxicam melting, the endotherm was seen to

shift to a slightly lower $Tm_{(onset)}$. This may not however suggest a definitive change in the melting endotherm as differentiation of the peak from the baseline was difficult due to its noisy nature. The measured ΔH values remained similar.

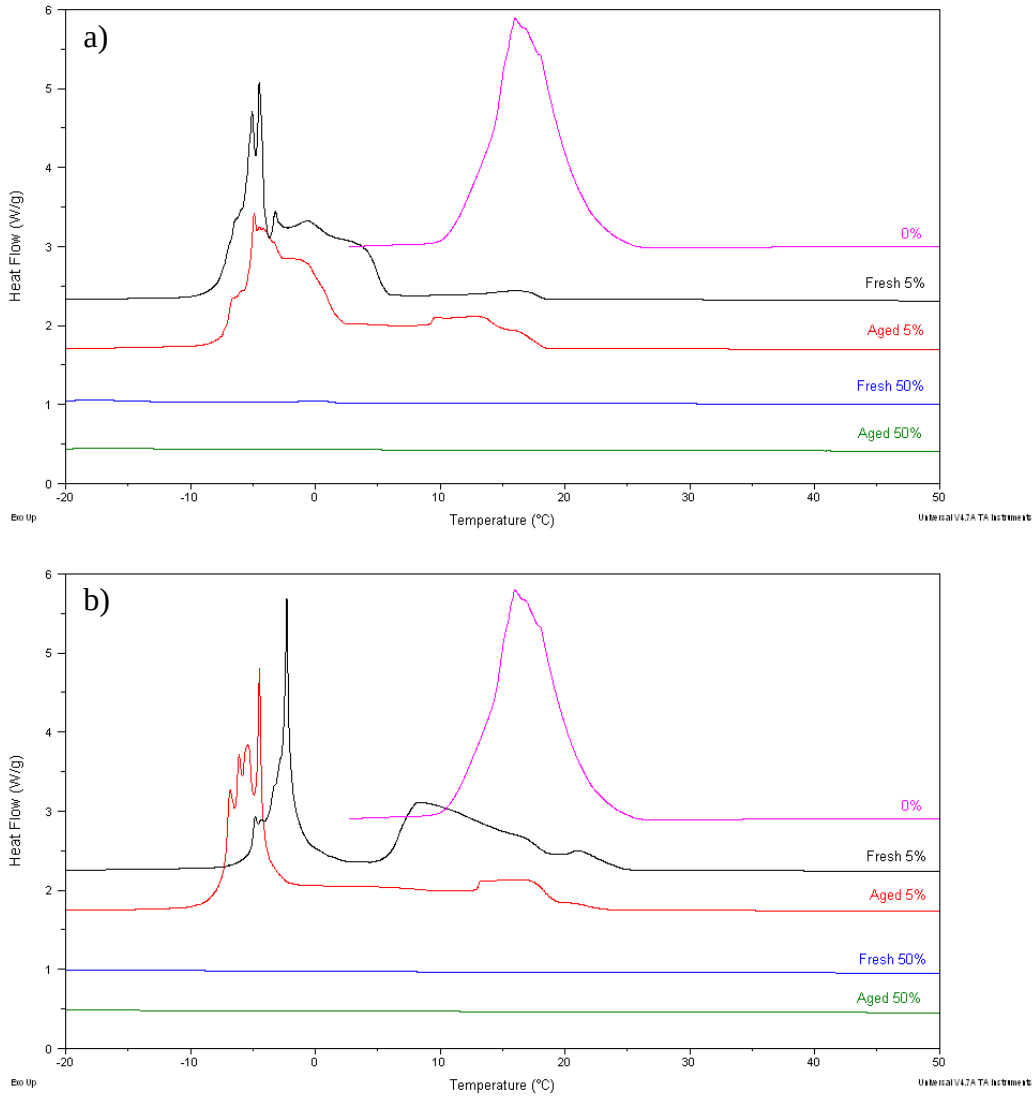

Figure 7.10 *Heat flow against temperature signal on heating at 10°C/minute of aged piroxicam and Gelucire 44/14 a) SSD(20) and b) SSD(4) – Crystallisation.*

The 5% w/w formulations demonstrated similar crystallisation peak pattern after aging to those seen for the fresh samples. In terms of calculated peak properties, the peaks were comparable i.e. $Tc_{(onset)}$, $Tc_{(max)}$ and ΔH, however there appeared to be a

redistribution of crystalline formations. The leading shoulder which appeared to correspond with the crystallisation of Gelucire 44/14 alone was more prominent in the SSD(20) aged samples. In the SSD(4) systems however, the main peak had shifted to a lower temperature and the leading lipid peak appeared to be less prominent than the fresh formulations. Again, as noted for the indometacin formulations, the crystallisation peaks appeared to be uncharacteristically sharp. As discussed previously, the changes observed in the crystallisation transition may be attributable to oxidative degradation of the lipid during storage. As at time zero in both cases, a crystallisation transition in the aged 50% w/w systems was not visible.

7.5.2 Observation of Thermal Transitions by Hot Stage Microscopy

The presence of piroxicam crystalline particles and the extent to which they existed in the SSD systems were comparable between the fresh and aged samples in all cases due to the relatively immiscible nature of the piroxicam with Gelucire 44/14. The 5% w/w formulations were observed to contain crystals which appeared to be evenly dispersed. At 50% w/w the piroxicam were much more abundant as expected. There did not appear to have been any significant change in the appearance i.e. shape and size of the piroxicam crystalline particle after aging.

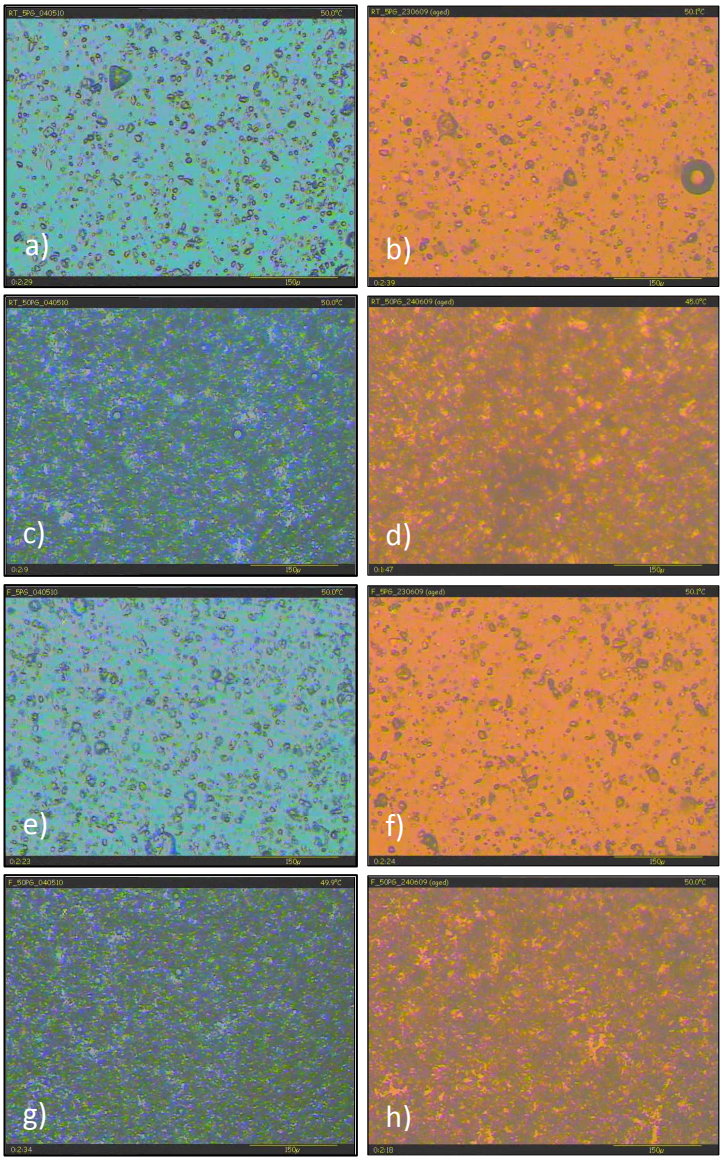

Figure 7.11 *HSM images of piroxicam and Gelucire 44/14 SSD(20) a) 5% fresh; b) 5% aged; c) 50% fresh; d) 50% aged; and SSD(4) e) 5% fresh; f) 5% aged; g) 50% fresh; h) 50% aged at 50^{o}C in order to visualise only crystalline piroxicam.*

7.5.3 In Vitro Release Profile

The dissolution profiles of the Gelucire 44/14 and piroxicam SSD systems upon aging, protected from light under ambient conditions, can be observed in Figure 7.12. At 5% w/w, the rate of piroxicam release and also the extent to which it was released over the course of the experiment was significantly reduced after aging. The overall drug release was less by approximately 20%, with the MDT-50% being increased in the region of 4 to 6 minutes. In Chapter Four it was suggested that at 5% w/w, piroxicam exists solely in the crystalline form. This may suggest that since there was little possibility of the reduced dissolution rate being attributable to changes in the physicochemical properties of the drug, it must therefore be due to alterations occurring in the lipid. These alterations, as detailed above, have been noted previously however only minor changes were detected in the DSC data of the aged samples. At 50% w/w there was little change in the drug release over time in both cases with regards rate and extent of release suggesting no significant changes in the SSD physicochemical properties over time.

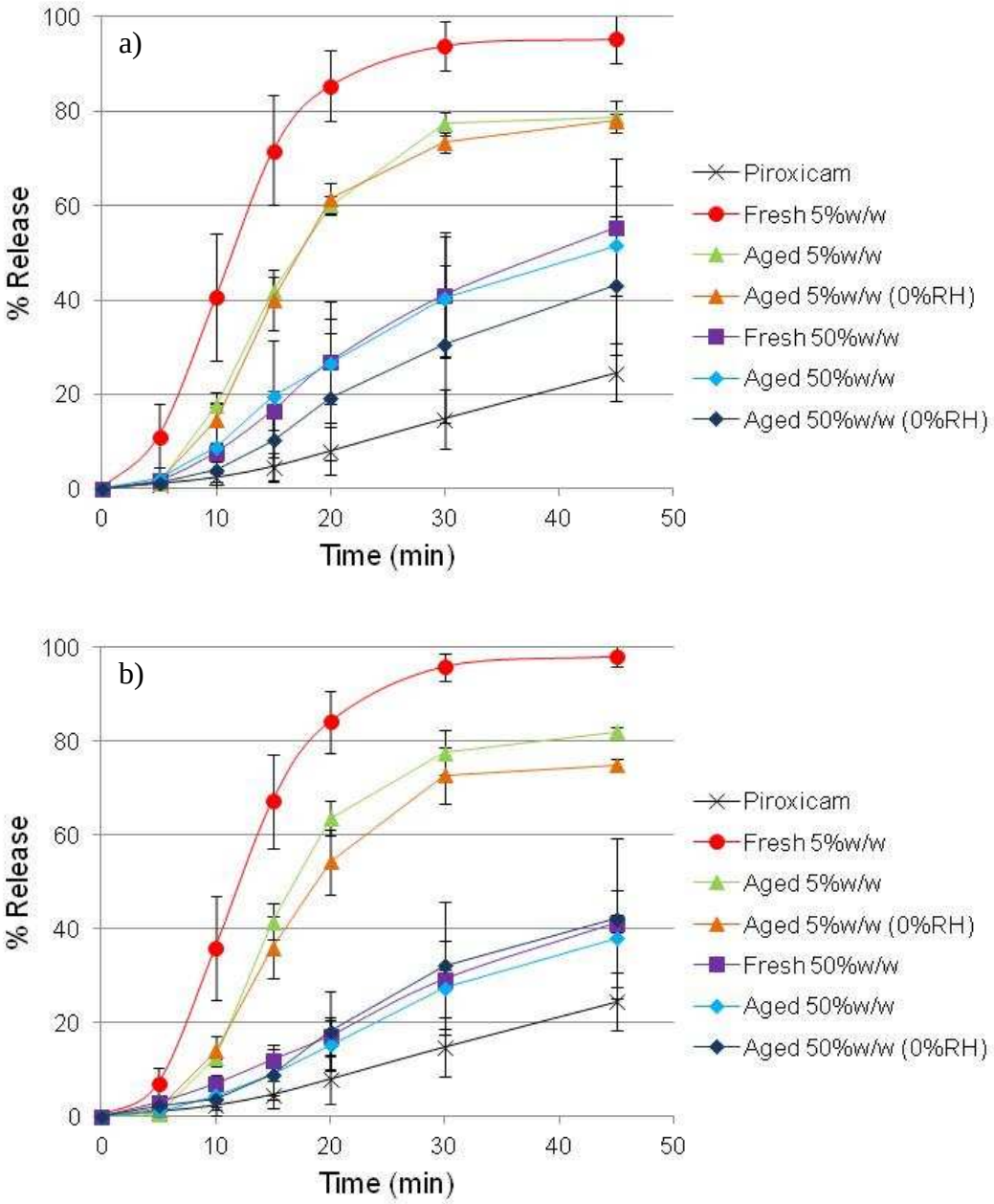

Figure 7.12 *Release of piroxicam from a) SSD(20) and b) SSD(4) systems over time in water at 37°C either freshly prepared or after storage at ambient and 0% RH.*

Table 7.3 *Mean dissolution time for piroxicam release up to 50% (MDT-50%) and the calculated release exponent n using the Power-Law.*

Formulation		Storage Humidity	MDT-50% (min)	Power-Law Model *n*
Piroxicam Alone			> 45	1
SSD(20)	5%	Fresh	11.3	0.55
		Aged Ambient	17.2	1
		Aged 0% RH	17.3	1
	50%	Fresh	39.2	1
		Aged Ambient	43.1	0.98
		Aged 0% RH	> 45	1
SSD(4)	5%	Fresh	12.3	0.62
		Aged Ambient	16.8	1
		Aged 0% RH	18.5	1
	50%	Fresh	> 45	1
		Aged Ambient	> 45	1
		Aged 0% RH	> 45	1

The *n* value calculated by applying the power-law model to the dissolution data is detailed in Table 7.3. The freshly prepared 5% w/w systems demonstrated a drug release mechanism consisting of anomalous transport with a value between 0.5 and 1. After aging under ambient conditions however, drug release became controlled solely by case II transport (erosion / swelling). The changes noted, as suggested earlier, are most likely attributable to the lipid in the SSD system. Limited aging effects were noted upon heating of the formulations, however alterations to the

crystallisation transition could possibly be caused by oxidative degradation of the samples over time, which could potentially have a subsequent impact upon the drug release. The 50% w/w formulations showed no change in drug release mechanism, being controlled by case II transport both before and after aging and suggesting that the release mechanism is maintained during storage. This follows the DSC and dissolution profile data which also imply little alteration to the formulation. It should be noted that fitting of these data to the power-law model should be considered with care due to the self-emulsifying nature of these systems imparted by the lipid Gelucire 44/14.

The Gelucire 44/14 and piroxicam SSD systems were also stored under dry conditions (0% RH, ambient temperature) before in vitro dissolution analysis (Figure 7.12). In this case the 5% w/w SSD(20) systems showed little change from those aged under ambient conditions, however the SSD(4) formulations demonstrated a greater difference in the extent of piroxicam release. Those samples stored under ambient conditions were observed to release the drug to a greater extent than those aged at 0% RH, however it should be noted that the error bars coincide for a number of data points. This effect was also observed by Sutananta et al (1996). They suggested that since slow cooling from the melt appeared to result in an increase in dissolution rate in comparison with ambiently cooled samples (not noted in this study), that the increase in dissolution rate observed for the formulations stored under high humidity may be attributable with the presence of atmospheric moisture producing a similar structure to that of the fresh slow cooled systems. The 50% w/w systems in both cases demonstrated similar profiles with relatively large error bars suggesting poor reproducibility.

The power-law *n* values of the SSD systems aged at 0% RH were found, in all cases, to be the same as those calculated for the samples stored under ambient conditions, suggesting that the release mechanism of the formulations was not altered by the RH (Table 7.3). In relation to those of the fresh samples only the 5% w/w systems demonstrated a change from anomalous transport to case II transport (erosion / swelling) alone, again potentially attributable to auto-oxidation of the Gelucire 44/14 during storage.

7.5.4 Summary of Aged Piroxicam and Gelucire 44/14 Semi-Solid Dispersion System Characterisation Studies

As detailed in Chapter Four, piroxicam was calculated to have a lower solubility with Gelucire 44/14 than the other model drugs and therefore limited if not no interaction between the two components. For this reason the formulated SSD systems demonstrated little change in the DSC melting profile after aging. The HSM images were comparable before and after aging which followed the DSC data. Upon dissolution of the SSD systems aged under ambient conditions, a decrease in drug release was demonstrated. It is most likely that these changes are attributable to aging effects of the lipid, possibly degradation suggested by DSC crystallisation, since initial characterisation suggested the absence of any molecular dispersion of piroxicam and its almost complete existence in the crystalline form. The mechanism of release (*n*) was found to change from anomalous transport to case II transport (erosion / swelling) on storage. The 50% w/w systems did not demonstrate any significant change in drug release over time and the mechanism by which drug is released was maintained as case II transport over the course of the experiment.

After aging under dry conditions only minor changes were observed for the 50% w/w systems although the reproducibility of the data was poor. There was also no obvious change to the dissolution at 5% for the SSD(20) formulations however piroxicam dissolution from the SSD(4) systems was found to decrease compared to that of the ambiently stored samples, possibly do to moisture effects also seen by Sutananta et al (1996). The mechanism of release in all cases was comparable to that of the samples stored under ambient conditions.

7.6 CONCLUSIONS

Overall, the data demonstrated that Gelucire 44/14 can exhibit aging effects during storage possibly attributable to reorganisation of the lipid components and also auto-oxidative degradation. Aging of SSD formulations of Gelucire 44/14 with model poorly soluble drugs appeared to depend upon the compatability and also the extent of interaction between the two components. As the solubility of the drug in the lipid increased, as did the tendency to age over time, as determined by DSC and HSM. The effects of storage appeared to be more extensive in those systems containing ibuprofen and indometacin, in comparison with those of piroxicam which demonstrated limited solubility in the lipid and therefore limited changes upon aging. The aging effects seen using DSC and HSM did not however translate to the in vitro dissolution profiles of the formulations. The ibuprofen and indometacin SSD systems, which demonstrated more significant physicochemical changes using DSC and HSM, did not demonstrate a subsequent change in the in vitro release characteristics. The extent of drug released from the low loaded piroxicam and Gelucire 44/14 SSD systems was however found to reduce after aging without

corresponding changes to the DSC and HSM data. In this case the two components demonstrated little interaction after formulation. This could possibly make the Gelucire 44/14 more prone to oxidative degradation, as with the lipid alone. In the case of the indometacin and ibuprofen SSD systems, the aging effect seen using thermal analysis techniques are most likely due to segregation of the lipid components, possibly encouraged by the disruption of the lipid crystalline structure by molecularly dispersed drug. This segregation may not necessarily bring about a reduction in the activity of the lipid to enhance the dissolution properties. The dissolution effect of aging appears to be difficult to predict, not always correlating well with DSC analysis. The aging of lipidic SSD systems, particularly with Gelucires appears to be dependent upon numerous factors and is therefore unpredictable.

CHAPTER EIGHT

CONCLUDING REMARKS AND FUTURE WORK

8.1 CONCLUDING REMARKS

This project has attempted to enhance the current knowledge surrounding lipid based semi-solid dispersion systems in the hope of bringing the industry a small step closer to taking full advantage of this promising technology. The work in this project has focussed around the surface active lipidic carrier excipient, Gelucire 44/14, the poorly soluble model drugs, ibuprofen, indometacin and piroxicam, their physicochemical characterisation alone and also in combination as an SSD. The ultimate goal was to successfully enhance the in vitro dissolution profile which in turn may lead to an increase in in vivo bioavailability. Gelucire 44/14 is capable of self-emulsifying upon contact with aqueous media allowing solubilisation of the poorly soluble drug particles, increasing their contact angle, reducing their surface tension and thus preventing aggregation and agglomeration. Gelucire 44/14 does however have a very complex multi-component structure which subsequently imparts complex physicochemical and behavioural properties upon the SSD systems into which it is incorporated. This complex nature means that a multi-instrumental approach is essential in order to establish a full characterisation profile. The aim of this study was therefore to provide a thorough characterisation of the structure, behaviour and performance of Gelucire 44/14 SSD formulations, in particular developing a range of analytical methods, so that the associations between these factors could be identified.

Chapter Three presented physicochemical characterisation of the selected surface active lipidic carrier materials, Gelucire 44/14 and TPGS, upon heating and cooling. The key points to note from these data were found to be:

1. Complex properties occurred during melting and temperature cycling of both lipids, for example a double melting endotherm consisting of low and high melting point fractions of Gelucire 44/14 and a double T_m for TPGS possibly attributable to the presence of both mono- and di-substituted PEG chains.
2. The rate at which the lipids are cooled appears to greatly impact the physical state at ambient temperature. Cooling at slower rates was found to promote a more complete crystallisation by ambient temperature unlike faster rates which were observed to create larger and broader crystallisation exotherms being complete by much lower temperatures.
3. Crystallisation of both lipids, independent of cooling rate, was found to continue to much lower temperatures than originally expected, the transition being composed of an initial primary energetic crystallisation followed by a much slower extended crystallisation.

Chapter Four began to characterise the physicochemical properties of binary physical mixes and SSD formulations of Gelucire 44/14 and the model drugs, ibuprofen, indometacin and piroxicam, using thermal analysis techniques. The key findings presented can be summarised by:

1. Conventional DSC demonstrated dissolution effects of the model drug into the carrier during analysis. This was suggested by the disappearance of the drug melting endotherm. Melting point depression of the lipid and drug was noted for both the ibuprofen and indometacin SSD systems suggesting interaction between the two components; however this was not the case for the piroxicam formulations due to poor miscibility.

2. Fast heating rates appeared to reduce these dissolution effects however not to a significant extent, suggesting that rates greater than 500^{o}C are required due to the complexity of the systems. Analysis of the drug crystalline melt endotherms did however appear to follow the model proposed by Qi et al (2010b) for all drug systems suggesting that a more accurate estimation of drug solubility in the carrier and also therefore the crystalline drug content in the formulated SSD could be calculated.
3. Drug solubilities in Gelucire 44/14 were calculated to be 20%, 25% and 10% w/w for ibuprofen, indometacin and piroxicam respectively, with Gelucire 44/14 solubility in indometacin being 60% w/w.
4. The presence of drug solid crystalline particles at low drug loading was confirmed using HSM for piroxicam however no evidence of solid drug crystals was noted for ibuprofen or indometacin systems, suggesting the presence of a molecular dispersion or solid solution.
5. Upon cooling of the molten SSD systems, the presence of drug was found to reduce the Gelucire 44/14 Tc to the extent that at 50% w/w, crystallisation was completely inhibited in all cases. Quasi-isothermal MTDSC confirmed this finding however the extended period of slow crystallisation was still apparent despite not being visible using conventional DSC methods.

Chapter Five demonstrated the drug release profile from the formulated SSD systems in water at 37^{o}C. The main points to note are as follows:

1. In all cases the dissolution properties of the poorly soluble model drugs were greatly enhanced by the formulation of SSD systems with Gelucire 44/14

consistently when compared with the crystalline drug alone. Overall a lower drug concentration with a greater lipid fraction was found to be optimum, demonstrating a higher extent of release. As the drug load increased the extent of release decreased due to the larger proportion of solid crystalline drug.

2. Dissolution enhancement may correspond to subsequent improvement in in vivo bioavailability however correlation is difficult to establish.
3. The power-law mathematical model proved a useful tool in the prediction of the mechanism of drug release from the SSD formulations however the data should be considered with care due to the complex nature of the lipid and also its ability to self emulsify upon contact with aqueous media.

Chapter Six outlined the hydration properties of the formulated SSD systems upon exposure to varying temperatures at high RH. The key points were found to be:

1. All model drug systems demonstrated similar hydration properties.
2. The affinity for water was found to increase considerably at 35^{o}C at low drug loading. This may have a significant effect on the formulation upon storage and should therefore be taken into consideration. This effect may be attributable to the molecular incorporation of drug into the lipid crystalline structure, disrupting the crystal formation and packing and therefore increasing its chemical reactivity in localised regions allowing hydrogen bonding with atmospheric moisture.

Chapter Seven outlined the effect of aging on the formulated SSD systems using thermal analysis methods along with in vitro drug release. These data suggested that:

1. Gelucire 44/14 exhibits aging effects upon storage possibly due to auto-oxidative degradation and also reorganisation of the lipid components.
2. The solubility of the drug within the lipid and therefore the miscibility of the two components appeared to affect the extent of lipid aging demonstrated by the SSD formulations. As the compatibility of the drug and lipid increased, as seen with ibuprofen and indometacin, the aging effects became more prominent. However, limited drug solubility and therefore poor miscibility with the lipid, as demonstrated by piroxicam, exhibited greater stability over time due to both components being present in the stable crystalline form.
3. The effect of aging on drug release from the SSD formulations was difficult to predict. A greater change was noted in the case of piroxicam which demonstrated limited miscibility with Gelucire 44/14. In the case of increased drug solubility, the changes observed using thermal analysis techniques did not correspond with the in vitro dissolution profile which demonstrated little change.

Table 8.1 *Parameters of the model drug compounds.*

Parameter	Ibuprofen	Indometacin	Piroxicam
Aqueous Solubility	0.01 mg/ml	0.003 mg/ml	0.02 mg/ml
Sol. in Gelucire 44/14	20 % w/w	25% w/w	10% w/w
pKa	4.91	4.5	6.3
logP	3.6	3.4	3.0

Table 8.2 *Key parameters of the formulated SSD systems using the model drugs ibuprofen, indometacin and piroxicam.*

Parameter	**Ibuprofen SSD**	**Indometacin SSD**	**Piroxicam SSD**
Drug Sol. In Gelucire 44/14	20 % w/w	25% w/w	10% w/w
Change in Gelucire 44/14 melt (10^{o}C/min)	Yes	Slight	No
Drug melt detected at concentration (10^{o}C/min)	50% w/w	50% w/w	5, 10, 15 and 50% w/w
Change in Gelucire 44/14 melt (500^{o}C/min)	Yes	Yes	No
Drug melt detected at concentration (500^{o}C/min)	50% w/w	10, 15 and 50% w/w	5, 10, 15 and 50% w/w
Effect of ↑ heating rate on adherence with Qi model	Low	High	Low
↓ Lipid Tc (QIMTDSC)	Yes	Yes	Yes
Maximum drug release	100%	60%	95%
Maximum drug released at concentration	5, 10 and 15% w/w	5 and 10% w/w	5% w/w
Affinity for moisture	High	High	High
Tendency to age	High	High	Low

Solubility of the drug compound in Gelucire 44/14 determined using the Qi model appeared to be proportional to the logP value and inversely proportional to the aqueous solubility and pKa value of the drug (Table 8.1). The affinity of the drug for the lipid Gelucire 44/14 therefore increased as the drug lipophilicity increased. Drug solubility in Gelucire 44/14 and therefore interaction between the two components was suggested by subsequent alteration of the Gelucire 44/14 melting endotherm upon heating which was less significant in the case of piroxicam which demonstrated the lowest lipid solubility.

The processing variable, cooling rate, unexpectedly did not impart any great fundamental difference to the behaviour or physicochemical properties of the SSD dosage form, with the formulations cooled slowly at 20^{o}C and quickly at 4^{o}C being comparable in almost all situations. The physical state of Gelucire 44/14 alone at ambient temperature was greatly dependent upon the rate of cooling from the molten state, with slower cooling encouraging a more complete crystallisation. This was however found not to be of great consequence. The novel technique QIMTDSC was further developed as a means of determining a more accurate estimation of the true crystallisation temperature, independent of cooling rate. Crystallisation of the lipid was found to be significantly hindered by the presence of drug, with complete crystallisation inhibition at 50% w/w drug loading, thought to be due to the molten drug acting as a diluent and subsequently reducing nuclei concentration.

Dissolution of the drug into Gelucire 44/14 during analysis, known to be affected by the rate of heating, appeared of little consequence to the adherence of ibuprofen and piroxicam systems to the Qi model i.e. both calibration plots of crystalline drug

concentration against crystalline drug melt enthalpy of physical mixes were comparable, with drug melt endotherms detected only at 50% w/w for ibuprofen or for all drug loading concentrations for piroxicam. Indometacin systems appeared to be greatly influenced by the heating rate, attributable to the increased solubility within Gelucire 44/14 and therefore a greater capacity for any remaining crystalline drug to dissolve during analysis. In terms of the quantity of molecularly dispersed drug present in each SSD system, estimated using the Qi model calibration plot, ibuprofen appeared to remain stable at circa 4% w/w in those systems in which a drug melt could be detected. In the case of indometacin and piroxicam SSD systems, the quantity of molecularly dispersed drug increased with increasing drug loading. For indometacin this may suggest that the saturation concentration of the drug had not yet been reached. However in the case of piroxicam it is possible that the calculated molecular dispersion values may have been influenced by the enthalpy of Gelucire 44/14 dissolution into the drug.

Both ibuprofen and piroxicam SSD systems released drug to the greatest extent. Indometacin however did not reach 100% release but reached a plateau at approximately 60%, probably due to non-sink conditions of the experiment impeding indometacin release. All low drug loading SSD systems appeared to be most successful in enhancing drug release to the greatest extent, most likely due to the existence of molecularly dispersed drug present in the formulation. At 50% w/w the extent of drug release decreased in all cases due to a large presence of solid crystalline drug particles, however it remained markedly greater than that of the solid crystalline drug alone suggesting that the lipid successfully increased the wettability

and dispersibility of the crystalline particles allowing for a greater dissolution into the aqueous media.

All 5% w/w drug loaded SSD systems demonstrated a greatly increased affinity for atmospheric moisture in comparison with Gelucire 44/14 alone at 35^{o}C. This increase may be attributable to the molecularly dispersed drug causing local molecular disorder of the crystalline lipid, resulting in increased chemical reactivity. This effect had the potential to bring about extensive aging effects over time with a subsequent decrease in drug release. This however was not the case. The drug concentration within the SSD formulations, and also the miscibility between the two components played a vital role in determining the physical state of the drug in the final dosage form and therefore also its behaviour at time zero as well as after aging. Low drug/carrier affinity and therefore the presence of a large proportion (if not solely) crystalline particles appeared to limit aging effects within the lipid as noted by thermal analysis however a reduction in drug release was demonstrated, possibly due to degradation of the lipid. Higher drug/carrier compatibility, allowing for the presence of a molecular dispersion or solid solution, left the formulation more susceptible to changes in the physicochemical properties however the dissolution properties remained similar over time. This may be attributable to the limited effect of segregation of the lipid components. The effect of aging on the prediction of in vitro drug release remains difficult.

Overall, therefore, this study has developed a range of characterisation techniques that has led to new insights into not merely the structure but also the behaviour of Gelucire 44/14 SSD formulations in terms of solidification, water uptake and ageing.

This information has in turn been related to the drug release properties of the corresponding SSD systems. The behaviour of the final SSD formulations has ultimately been found to be related to the aqueous solubility of the incorporated drug which in turn determines the solubility within the lipid carrier excipient. The less aqueous soluble the drug compound, the more soluble it is likely to be in the lipid. The more soluble the drug in the lipid, the more the drug was found to exist as a molecular dispersion within the SSD system. The formulation of SSD systems using Gelucire 44/14 was successful in all cases of enhancing the extent to which the poorly aqueous soluble drug was released into aqueous media at 37^{o}C. Generally, however, lower drug loadings demonstrated greater release which corresponded well with a greater proportion of molecular dispersion in the formulation. The presence of molecularly dispersed drug did however bring about a significantly increased capacity of the lipid to uptake atmospheric moisture, thought to be due to the disruption of the ordered lipid crystalline structure and the subsequent increased reactivity. This increase in affinity for moisture did not relate to increased aging effects as expected. The increased presence of molecular dispersion did however appear to bring about more extensive physicochemical aging effects which did not correspond with decrease in vitro drug release.

The theme running through these data appears to be that the existence or non-existence of poorly soluble drug as a molecular dispersion within the lipid carrier excipient of the formulated SSD system, determined by the solubility of the drug within the lipid, is a determining factor of the subsequent behaviour and stability of the final SSD system.

8.2 FUTURE WORK

The data collected during this project, as with any research, has highlighted areas requiring more in depth investigation which falls outside the scope of this study. In relation to the characterisation of the lipids alone, infrared spectroscopy may be useful to gain a greater insight into the chemical composition; however the usefulness of this technique may be diminished by the complexity of the sample.

In terms of further characterisation of the SSD systems, these other techniques and experiments may useful:

1. X-ray diffraction to confirm the presence of crystallinity in the SSD sample which can be utilised as an adjunct to thermal methods.
2. SEM to observe the sample in greater detail; however this may prove difficult due to the waxy nature of the carrier.
3. Infrared spectroscopy to further investigate interactions occurring between SSD components; however again the complex nature of the systems may make interpretation of the data difficult.
4. Dissolution studies in more realistic media, for example simulated gastric and intestinal fluid, in order to make more accurate assumptions regarding the in vitro / in vivo correlation. In vivo bioavailability testing in animals may also be useful in this regard.
5. Expansion of the DVS studies to include a more extensive hydration profile of each SSD system in order to allow more accurate prediction of the dosage form behaviour during storage and aging.

6. Expansion of the aging study to include a wider range of storage temperatures and humidities which can be linked to the DVS data.
7. It would also be beneficial to further develop the method of QIMTDSC for characterisation of the SSD crystallisation transition.

REFERENCES

Abdul-Fattah, A M and Bhargava, H N (2002). "Preparation and in vitro evaluation of solid dispersions of halofantrine." International Journal of Pharmaceutics **235**(1-2): 17-33.

Ahlneck, C and Zografi, G (1990). "The molecular basis of moisture effects on the physical and chemical stability of drugs in the solid state." International Journal of Pharmaceutics **62**: 87-95.

Ahuja, N, Katare, O P and Singh, B (2007). "Studies on dissolution enhancement and mathematical modeling of drug release of a poorly water-soluble drug using water-soluble carriers." European Journal of Pharmaceutics and Biopharmaceutics **65**(1): 26-38.

Amidon, G L, Lennernas, H, Shah, V P and Crison, J R (1995). "A theoretical basis for a biopharmaceutic drug classification: the correlation of in vitro drug product dissolution and in vivo bioavailability." Pharm Res **12**(3): 413-20.

Andronis, V and Zografi, G (2000). "Crystal nucleation and growth of indomethacin polymorphs from the amorphous state." Journal of Non-Crystalline Solids **271**(3): 236-248.

Avrami, M (1939). "Kinetics of Phase Change. 1* General Theory." Journal of Chemical Physics **7**: 1103-1112.

Bandi, N, Wei, W, Roberts, C B, Kotra, L P and Kompella, U B (2004). "Preparation of budesonide- and indomethacin-hydroxypropyl-β-cyclodextrin (HPBCD) complexes using a single step, organic-solvent free supercritical fluid process." European Journal of Pharmaceutical Sciences. **23**: 159-168.

Barakat, N S (2006). "Etodolac-liquid-filled dispersion into hard gelatin capsules: an approach to improve dissolution and stability of etodolac formulation." Drug Development and Industrial Pharmacy **32**(7): 865.

Barker, S A, Yap, S P, Yuen, K H, McCoy, C P, Murphy, J R and Craig, D Q M (2003). "An investigation into the structure and bioavailability of alpha-tocopherol dispersions in Gelucire 44/14." Journal of Control Release **91**(3): 477.

Bottom, R (1999). "The role of modulated temperature differential scanning calorimetry in the characterisation of a drug molecule exhibiting polymorphic and glass forming tendencies." International Journal of Pharmaceutics **192**(1): 47.

Bourlieu, C, Guillard, V, Ferreira, M, Powell, H, Vallès-Pàmies, B, Guilbert, S and Gontard, N (2010). "Effect of cooling rate on the structural and moisture barrier properties of high and low melting point fats." Journal of the American Oil Chemists' Society **87**: 133-145.

British Pharmacopoeia (2010). "Monograph for Ibuprofen."

British Pharmacopoeia (2010). "Monograph for Indometacin."

British Pharmacopoeia (2010). "Monograph for Piroxicam."

Broman, E (2001). "A comparison of alternative polymer excipients and processing methods for making solid dispersions of a poorly water soluble drug." International Journal of Pharmaceutics **222**(1): 139.

Chakraborty, S, Shukla, D, Mishra, B and Singh, S (2009). "Lipid - An emerging platform for oral delivery of drugs with poor bioavailability." European Journal of Pharmaceutics and Biopharmaceutics **73**: 1-15.

Chambin, O and Jannin, V (2005). "Interest of multifunctional lipid excipients: case of Gelucire 44/14." Drug Development and Industrial Pharmacy **31**(6): 527-34.

Chambin, O, Jannin, V, Champion, D, Chevalier, C, Rochat-Gonthier, M H and Pourcelot, Y (2004). "Influence of cryogenic grinding on properties of a self-emulsifying formulation." International Journal of Pharmaceutics **278**(1): 79-89.

Chen, M-L and Yu, L X (2009). "The use of drug metabolism for prediction of intestinal permeability." Molecular Pharmaceutics **6**: 74-81.

Chiou, W L and Riegelman, S (1971). "Pharmaceutical applications of solid dispersion systems." Journal of Pharmaceutical Sciences **60**(9): 1281-1302.

Coleman, N J and Craig, D Q M (1996). "Modulated temperature differential scanning calorimetry: A novel approach to pharmaceutical thermal analysis." International Journal of Pharmaceutics **135**(1-2): 13-29.

Collnot, E M, Baldes, C, Wempe, M F, Kappl, R, Huttermann, J, Hyatt, J A, Edgar, K J, Schaefer, U F and Lehr, C M (2007). "Mechanism of inhibition of P-glycoprotein mediated efflux by vitamin E TPGS: influence on ATPase activity and membrane fluidity." Molecular Pharmaceutics **4**(3): 465-74.

Craig, D Q (2002). "The mechanisms of drug release from solid dispersions in water-soluble polymers." Int J Pharm **231**(2): 131-44.

Craig, D Q M and Newton, J M (1991). "Characterisation of polyethylene glycols using differential scanning calorimetry." International Journal of Pharmaceutics **74**: 33-41.

Damian, F (2002). "Physical stability of solid dispersions of the antiviral agent UC-781 with PEG 6000, Gelucire 44/14 and PVP K30." International Journal of Pharmaceutics. **244**(1-2): 87-2)87-98.

Damian, F, Blaton, N, Naesens, L, Balzarini, J, Kinget, R, Augustijns, P and Van den Mooter, G (2000). "Physicochemical characterization of solid dispersions of the antiviral agent UC-781 with polyethylene glycol 6000 and Gelucire 44/14." Eurpean Journal of Pharmaceutical Sciences **10**(4): 311-22.

Dennis, A B (1988). Drug release from semi-solid capsule formulation. The Welsh School of Pharmacy. Cardiff. **PhD**.

Dintaman, J M and Silverman, J A (1999). "Inhibition of P-glycoprotein by D-alpha-tocopheryl polyethylene glycol 1000 succinate (TPGS)." Pharmaceutical Research **16**(10): 1550-6.

Dokoumetzidis, A and Macheras, P (2006). "A century of dissolution research: from Noyes and Whitney to the biopharmaceutics classification system." Int J Pharm **321**(1-2): 1-11.

Domanska, U, Pobudkowska, A, Pelczarska, A and Gierycz, P (2009). "pK(a) and Solubility of Drugs in Water, Ethanol, and 1-Octanol." Journal of Physical Chemistry B **113**(26): 8941-8947.

Dordunoo, S K, Ford, J L and Rubinstein, M H (1991). "Preformulation studies on solid dispersions containing triamterene or temazepam in polyethylene glycols or Gelucire 44/14 for liquid filling of hard gelatin capsules." Drug Development and Industrial Pharmacy **17**(12): 1685-1713.

Dressman, J B (1998). "Dissolution testing as a prognostic tool for oral drug absorption: Immediate release dosage forms." Pharmaceutical Research **15**(1): 11-22.

Eastman (2005). "Vitamin E TPGS NF: Applications and Properties." Product Information.

Edwards, G (2003). "Ivermectin: Does P-glycoprotein play a role in neurotoxicity?" Filaria Journal **2**(1).

El-Badry, M, Fetih, G and Fathy, M (2009). "Improvement of solubility and dissolution rate of indomethacin by solid dispersions in Gelucire 50/13 and PEG 4000." Saudi Pharmaceutical Journal **17**(3).

Gabbott, P (2008). Principles and applications of thermal analysis, Blackwell Publishing.

Gaisford, S (2008). "Fast-scan differential scanning calorimetry." European Pharmaceutical Review(4): 83-89.

Gao, Z (2011). "Mathematical modelling of variables involved in dissolution testing." Journal of Pharmaceutical Sciences.

Gattefossé (2007). "Gelucire 44/14: Immediate Release and Enhanced Bioavailability." Product Information.

Gramaglia, D (2005). "High speed DSC (hyper-DSC) as a tool to measure the solubility of a drug within a solid or semi-solid matrix." International Journal of Pharmaceutics(1-2): 5-2):.

Gursoy, R N and Benita, S (2004). "Self-emulsifying drug delivery systems (SEDDS) for improved oral delivery of lipophilic drugs." Biomed Pharmacother **58**(3): 173-82.

Hancock, B C and Zografi, G (1997). "Characteristics and significance of the amorphous state in pharmaceutical systems." J Pharm Sci **86**(1): 1-12.

Hauss, D J (2007). "Oral lipid-based formulations." Advanced Drug Delivery Reviews **59**(7): 667-676.

Higuchi, T (1961). "Rate of release of medicaments from ointment bases containing crugs in suspensions." Journal of Pharmaceutical Sciences **50**: 874-875.

Hill, V L, Craig, D Q M and Feely, L C (1998). "Characterisation of spray-dried lactose using modulated differential scanning calorimetry." International Journal of Pharmaceutics **161**: 95-107.

Horter, D and Dressman, J B (1997). "Influence of physicochemical properties on dissolution of drugs in the gastrointestinal tract." Advanced Drug Delivery Reviews. **25**: 3-14.

Hüttenrauch, R (1974). "Injection moulding of repository oral preparations." Pharmazie **29**(5): 297-302.

Ismailos, G, Reppas, C and Macheras, P (1994). "Enhancement of cyclosporin A solubility by d-alphatocopheryl-polyethylene-glycol-1000 succinate (TPGS)." European Journal of Pharmaceutical Sciences. **1**(5): 269-271.

Jannin, V, Musakhanian, J and Marchaud, D (2008). "Approaches for the development of solid and semi-solid lipid-based formulations." Advanced Drug Delivery Reviews **60**: 734-746.

Janssens, S and Van den Mooter, G (2009). "Review: Physical chemistry of solid dispersions." Journal of Pharmacy and Pharmacology **61**: 1571-1586.

Joshi, H N, Tejwani, R W, Davidovich, M, Sahasrabudhe, V P, Jemal, M, Bathala, M S, Varia, S A and Serajuddin, A T (2004). "Bioavailability enhancement of a poorly water-soluble drug by solid dispersion in polyethylene glycol-polysorbate 80 mixture." International Journal of Pharmaceutics **269**(1): 251-8.

Karatas, A, Yuksel, N and Baykara, T (2005). "Improved solubility and dissolution rate of piroxicam using gelucire 44/14 and labrasol." Farmaco. **60**(9): 777-782.

Kasim, N A, Whitehouse, M, Ramachandran, C, Bermejo, M, Lennernas, H, Hussain, A S, Junginger, H E, Stavchansky, S A, Midha, K K, Shah, V P and Amidon, G L (2003). "Molecular properties of WHO essential drugs and provisional biopharmaceutical classification." Molecular Pharmaceutics **1**(1): 85-96.

Kawakami, K (2004). "Solubilization behavior of poorly soluble drugs with combined use of Gelucire 44/14 and cosolvent." Journal of Pharmaceutical Sciences. **93**(6): 1471-1479.

Khan, N and Craig, D Q M (2004). "Role of blooming in determining the storage stability of lipid-based dosage forms." Journal of Pharmaceutical Sciences **93**(12): 2962-2971.

Khoo, S-M (2000). "The formulation of Halofantrine as either non-solubilising PEG 6000 or solubilising lipid based solid dispersions: Physical stability and absolute bioavailability assessment." International Journal of Pharmaceutics **205**(1-2): 65-2.

Knox, C, Law, V, Jewison, T, Liu, P, Ly, S, Frolkis, A, Pon, A, Banco, K, Mak, C, Nevau, V, Djoumbou, Y, Eisner, R, Guo, A C and Wishart, D S (2011). "DrugBank 3.0: A comprehensive resource for 'omics' research on drugs." Nucleic Acids Research **39 (Database Issue)**: D1035-1041.

Kopeliovich, D (2009). "Substech: Substances and Technologies." Retrieved 12th August, 2011.

Korsmeyer, R W, Lustig, S R and Peppas, N A (1986a). "Solute and penetrant diffusion in swellable polymers. I. Mathematical modelling." Journal of Polymer Science and Polymer Physics **24**: 395-408.

Korsmeyer, R W, von Meerwall, E and Peppas, N A (1986b). "Solute and penetrant diffusion in swellable polymers. II. Verification of theoretical models." Journal of Polymer Science and Polymer Physics **24**: 409-434.

Kumar, S (2009). Colloidal based drug delivery systems. Pharmainfo.net. **2011**.

Leuner, C and Dressman, J (2000). "Improving drug solubility for oral delivery using solid dispersions." European Journal of Pharmaceutics and Biopharmaceutics **50**(1): 47-60.

Lloyd, G R, Craig, D Q M and Smith, A (1997). "An investigation into the melting behavior of binary mixes and solid dispersions of paracetamol and PEG 4000." Journal of Pharmaceutical Sciences **86**(9): 991-996.

Long, Y, Shanks, R A and Stachurski, Z H (1995). "Kinetics of polymer crystallisation." Progress in Polymer Science **20**(4): 651-701.

Lorenzo, A T, Arnal, M L, Albuerne, J and Müller, A J (2007). "DSC isothermal polymer crystallisation kinetics measurements and the use of the Avrami equation to fit the data: Guidelines to avoid common problems." Polymer Testing **26**: 222-231.

Martinez, M N and Amidon, G L (2002). "A mechanistic approach to understanding the factors affecting drug absorption: A review of fundamentals." Journal of Clinical Pharmacology **42**: 620-643.

McGregor, C and Bines, E (2008). "The use of high-speed differential scanning calorimetry (Hyper-DSC (TM)) in the study of pharmaceutical polymorphs." International Journal of Pharmaceutics **350**(1-2): 48-52.

Meehan, E, Hammond, J and Moir, A (2007). Characterisation of surface active carriers used in pharmaceutical solid dispersions. AstraZeneca.

Metin, S and Hartel, R W (1998). "Thermal analysis of isothermal crystallisation kinetics in blends of cocoa butter with milk fat fractions." Journal of the American Oil Chemists' Society **75**(11): 1617-1624.

Metin, S and Hartel, R W (2005). Crystallisation of fats and oils. Bailey's industrial oil and fat products. F. Shahidi, John Wiley & Sons, Inc.

Moneghini, M (2008). "Microwave generated solid dispersions containing Ibuprofen." International Journal of Pharmaceutics **361**(1-2): 125-2.

Nokhodchi, A (2005). "An overview of the effect of moisture on compaction and compression." Pharmaceutical Technology: 47-66.

Okumura, T, Ishida, M, Takayama, K and Otsuka, M (2006). "Polymorphic transformation of indomethacin under high pressures." Journal of Pharmaceutical Sciences **95**(3): 689-700.

Otsuka, M, Kato, F and Matsuda, Y (2001). "Determination of indomethacin polymorphic contents by chemometric near-infrared spectroscopy and conventional powder X-ray diffractometry." Analyst **126**(9): 1578-1582.

Papas, K, Kalbfleisch, J and Mohon, R (2007). "Bioavailability of a novel, water-soluble vitamin E formulation in malabsorbing patients." Digestive Diseases and Sciences **52**(2): 347-52.

Pillay, V and Fassihi, R (1999). "A new method for dissolution studies of lipid-filled capsules employing nifedipine as a model drug." Pharmaceutical Research **16**(2): 333-7.

Potthast, H, Dressman, J B, Junginger, H E, Midha, K K, Oeser, H, Shah, V P, Vogelpoel, H and Barends, D M (2005). "Biowaver Monographs for Immediate Release Solid Oral Dosage Forms: Ibuprofen." Journal of Pharmaceutical Sciences **94**(10): 2121-2131.

Pouton, C W (2006). Formulation of poorly water-soluble drugs for oral administration: Physicochemical and physiological issues and the lipid formulation classification system. 3rd World Conference on Drug Absorption, Transport and Delivery, Barcelona, SPAIN.

Prabhu, S (2005). "Novel lipid-based formulations enhancing the in vitro dissolution and permeability characteristics of a poorly water-soluble model drug, piroxicam." International Journal of Pharmaceutics **301**(1-2): 209-2.

Qi, S, Belton, P, Nollenberger, K, Claydon, N, Reading, M and Craig, D Q M (2010b). "Characterisation and prediction of phase separation in hot-melt extruded solid dispersions: A thermal, microscopic and NMR relaxometry study." Pharmaceutical Research **27**: 1869-1883.

Qi, S, Deutsch, D and Craig, D Q M (2008). "An investigation into the mechanisms of drug release from taste-masking fatty acid microspheres." Journal of Pharmaceutical Sciences **97**(9): 3842-3854.

Qi, S, Marchaud, D and Craig, D Q M (2010a). "An investigation into the mechanism of dissolution rate enhancement of poorly water-soluble drugs from spray chilled Gelucire 50/13 microspheres." Journal of Pharmaceutical Sciences **99**(1).

Reading, M and Craig, D Q M (2007). Principles of Differential Scanning Calorimetry. Thermal Analysis of Pharmaceuticals. D. Q. M. Craig and M. Reading, CRC Press.

Reading, M, Craig, D Q M, Murphy, J R and Kett, V L (2007). Modulated temperature differential scanning calorimetry. Thermal Analysis of Pharmaceuticals. D. Q. M. Craig and M. Reading, CRC Press**:** 140-144.

Rege, B D, Kao, J P and Polli, J E (2002). "Effects of nonionic surfactants on membrane transporters in Caco-2 cell monolayers." Eurpean Journal of Pharmaceutical Sciences **16**(4-5): 237-46.

Remuñán, C, Bretal, M J, Nunez, A and Jato, J L V (1992). "Accelerated stability study of sustained-release nifedipine tablets prepared with Gelucire." International Journal of Pharmaceutics **80**(2-3): 151-159.

Romero, A J, Savastano, L and Rhodes, C T (1993). "Monitoring crystal modifications in systems containing ibuprofen." International Journal of Pharmaceutics **99**(2-3): 125-134.

Sachs-Barrable, K, Thamboo, A, Lee, S D and Wasan, K M (2007). "Lipid Excipients Peceol and Gelucire 44/14 decrease P-glycoprotein mediated efflux of Rhodamine 123 partially due to modifying P-glycoprotein protein expression within Caco-2 Cells." Journal of Pharmacy and Pharmaceutical Sciences **10**(3): 319-331.

San Vincente, A, Hernández, R M, Gascón, A R, Calvo, M B and Pedraz, J L (2000). "Effect of aging on the release of salbutamol sulfate from lipid matrices." International Journal of Pharmaceutics **208**: 13-21.

Saunders, M (2008). Thermal Analysis of Pharmaceuticals. Principles and Applications of Thermal Analysis. P. Gabbott, Blackwell Publishing.

Saville, D J (2001). "Influence of storage on in-vitro release of ibuprofen from sugar coated tablets." International Journal of Pharmaceutics **224**(1-2): 39-49.

Schamp, K, Schreder, S A and Dressman, J (2006). "Development of an in vitro/in vivo correlation for lipid formulations of EMD 50733, a poorly soluble, lipophilic drug substance." European Journal of Pharmaceutics and Biopharmaceutics **62**(3): 227-34.

Sekiguchi, K and Obi, N (1961). "Studies on absorption of eutectic mixture. 1. Comparison of behaviour of eutectic mixture of sulfathiazole and that of ordinary sulfathiazole in man." Chemical & Pharmaceutical Bulletin **9**(11): 866-872.

Serajuddin, A T (1999). "Solid dispersion of poorly water-soluble drugs: early promises, subsequent problems, and recent breakthroughs." Journal of Pharmaceutical Sciences **88**(10): 1058-66.

Serajuddin, A T M, Sheen, P C, Mufson, D, Bernstein, D F and Augustine, M A (1988). "Effect of vehicle amphiphilicity on the dissolution and bioavailability of a poorly water-soluble drug from solid dispersions." Journal of Pharmaceutical Sciences **77**(5): 414-417.

Sheen, P C, Khetarpal, V K, Cariola, C M and Rowlings, C E (1995). "Formulation studies of a poorly water-soluble drug in solid dispersions to improve bioavailability." International Journal of Pharmaceutics **118**(2): 221-227.

Shin, S C and Kim, J (2003). "Physicochemical characterization of solid dispersion of furosemide with TPGS." International Journal of Pharmaceutics **251**(1-2): 79-84.

Siepmann, J and Peppas, N A (2001). "Modelling of drug release from delivery systems based on hydroxypropyl methylcellulose (HPMC)." Advanced Drug Delivery Reviews **48**: 139-157.

Sokol, R J, Johnson, K E, Karrer, F M, Narkewicz, M R, Smith, D and Kam, I (1991). "Improvement of cyclosporin absorption in children after liver transplantation by means of water-soluble vitamin E." Lancet **338**(8761): 212-4.

Strickley, R J (2007). Currently marketed oral lipid-based dosage forms: Drug products and excipients. Oral lipid-based formulations: Enhancing the bioavailability of poorly water soluble drugs. D. J. Hauss. New York, Informa Healthcare, Inc.

Sutananta, W, Craig, D Q M and Newton, J M (1994a). "The effect of aging on the thermal behaviour and mechanical properties of pharmaceutical glycerides." International Journal of Pharmaceutics **111**(1): 51-62.

Sutananta, W, Craig, D Q M and Newton, J M (1994b). "An investigation into the effect of preparation conditions on the structure and mechanical-properties of pharmaceutical glyceride bases." International Journal of Pharmaceutics **110**(1): 75-91.

Sutananta, W, Craig, D Q M and Newton, J M (1995a). "An evaluation of the mechanisms of drug release from glyceride bases." Journal of Pharmacy and Pharmacology **47**: 182-187.

Sutananta, W, Craig, D Q M and Newton, J M (1995b). "An investigation into the effects of preparation conditions and storage on the rate of drug release from pharmaceutical glyceride bases." Journal of Pharmacy and Pharmacology **47**: 355-359.

Sutananta, W, Craig, D Q M and Newton, J M (1996). "The use of dielectric analysis as a means of characterising the effects of moisture uptake by pharmaceutical glyceride bases." International Journal of Pharmaceutics **132**(1-2): 1-8.

Svensson, A, Neves, C and Cabane, B (2004). "Hydration of an amphiphilic excipient, Gelucire 44/14." International Journal of Pharmaceutics **281**(1-2): 107-18.

TA Instruments (2010). "Q2000 Product Brochure."

TA Instruments (2010). "Q5000 SA Product Brochure."

Tachiban, T and Nakamura, A (1965). "A method for preparing an aqueous colloidal dispersion of organic materials by using water-soluble polymers: Dispersion of beta-carotene by polyvinylpyrrolidone." Kolloid-Zeitschrift and Zeitschrift Fur Polymere **203**(2): 130-133.

Tashtoush, B M, Al-Qashi, Z S and Najib, N M (2004). "In vitro and in vivo evaluation of glibenclamide in solid dispersion systems." Drug Development and Industrial Pharmacy **30**(6): 601-7.

Traber, M G, Thellman, C A, Rindler, M J and Kayden, H J (1988). "Uptake of intact TPGS (d-alpha-tocopheryl polyethylene glycol 1000 succinate) a water-miscible form of vitamin E by human cells in vitro." American Journal of Clinical Nutrition **48**(3): 605-11.

Varma, M V and Panchagnula, R (2005). "Enhanced oral paclitaxel absorption with vitamin E-TPGS: effect on solubility and permeability in vitro, in situ and in vivo." Eurpean Journal of Pharmaceutical Sciences **25**(4-5): 445-53.

Vippagunta, S R, Brittain, H G and Grant, D J (2001). "Crystalline solids." Adv Drug Deliv Rev **48**(1): 3-26.

Vitez, I M, Newman, A W, Davidovich, M and Kiesnowski, C (1998). "The evolution of hot-stage microscopy to aid solid-state characterizations of pharmaceutical solids." Thermochimica Acta **324**: 187-196.

Vrečer, F, Srčič, S and Šmid-Korbar, J (1991). "Investigation of prioxicam polymorphism." International Journal of Pharmaceutics **68**.

Weuts, I, Van Dycke, F, Voorspoels, J, De Cort, S, StokBroekx, S, Leemans, R, Brewster, M E, Xu, D, Segmuller, B, Turner, Y A, Roberts, C J, Davies, M C, Qi, S, Craig, D Q M and Reading, M (2010). "Physicochemical properties of the amorphous drug, cast films, and spray dried powders to predict formulation probablilty of success for solid dispersions: Etravirine." Pharmaceutical Technology **100**(1): 260-274.

Wu, C Y and Benet, L Z (2005). "Predicting drug disposition via application of BCS: Transport/absorption/elimination interplay and development of a biopharmaceutics drug disposition classification system." Pharmaceutical Research **22**(1): 11-23.

Wunderlich, B (2003). "Reversible crystallization and the rigid-amorphous phase in semicrystalline macromolecules." Progress in Polymer Science **28**(3): 383-450.

York, P (2002). The design of doseage forms. Pharmaceutics: The science of doseage form design. M. E. Aulton, Churchill Livingstone.

Yu, L, Bridgers, A, Polli, J, Vickers, A, Long, S, Roy, A, Winnike, R and Coffin, M (1999). "Vitamin E-TPGS increases absorption flux of an HIV protease inhibitor by enhancing its solubility and permeability." Pharmaceutical Research **16**(12): 1812-7.

Yuksel, N (2003). "Enhanced bioavailability of piroxicam using Gelucire 44/14 and labrasol: in vitro and in vivo evaluation." European Journal of Pharmaceutics and Biopharmaceutics **56**(3): 453-9.

Zhang, G G, Law, D, Schmitt, E A and Qiu, Y (2004). "Phase transformation considerations during process development and manufacture of solid oral dosage forms." Adv Drug Deliv Rev **56**(3): 371-90.

CONFERENCE PROCEEDINGS

British Pharmaceutical Conference, Manchester, UK, September 2008.

The use of quasi-isothermal modulated temperature DSC as a means of characterising the re-crystallisation of Gelucire 44/14. Otun S.O, Meehan E., Qi S. and Craig D.Q.M. Journal of Pharmacy and Pharmacology, **60**, A41-A42.

Objectives: *To use standard and quasi-isothermal modulated DSC methods to characterise the re-crystallisation process of Gelucire 44/14 in order to determine the effect of cooling rate.*

Methods: *Samples of Gelucire 44/14 in the weight range 2-2.5mg were prepared in standard aluminium crimped pans and run using standard DSC, melting and cooling at 0.5, 2,10 and 20^{o}C/min. The solid fat content of Gelucire 44/14 was calculated as a function of temperature using the area under the re-crystallisation traces at various temperature points and expressed as percentages of the total on complete re-crystallisation. Samples of Gelucire 44/14, prepared in the same manner as above, after complete melting at 60^{o}C for 10 minutes, were run using quasi-isothermal modulated temperature DSC with an amplitude of ± 1^{o}C and a period of 60 seconds, cooling at 1^{o}C increments from 35-5^{o}C with an isotherm of 10 and 40 minutes at each increment.*

Results: *Using standard DSC, re-crystallisation of Gelucire 44/14 occurred at decreasing temperatures with increasing cooling rate. Profile measurements were repeated four times each with excellent reproducibility throughout. The solid fat content technique allowed the visual simplification of the re-crystallisation process. By plotting the percentage solid against the temperature, for each individual cooling rate, it is possible to identify the amount of Gelucire 44/14 present in the solid state at any temperature point during the re-crystallisation process. The quasi-isothermal modulated temperature DSC method allowed the isolation of the temperature at which Gelucire 44/14 re-crystallisation occurred by holding the molten sample at each temperature increment for an extended period. This was detected by the use of Lissajous figures, whereby the modulated heat flow is plotted against modulated temperature. This in turn allows observation of the reproducibility of the sine wave heat flow modulations within a single isothermal period. The re-crystallisation could be observed in real time by noting the deviation of the sine wave curves from the steady state through the course of the crystallisation process, thereby providing a novel means of deconvoluting the heat flow processes associated with the thermal event as a function of time. It was noted that the re-crystallisation temperature of Gelucire 44/14 was 32-31^{o}C with an isotherm of 40 minutes, and 30^{o}C with an isotherm of 10 minutes.*

Conclusions: *Quasi-isothermal MTDSC appears to be a very promising new tool in the investigation of the Gelucire 44/14 re-crystallisation process. By holding the sample at each temperature increment*

for an extended period, it is possible to isolate the re-crystallisation process. This in turn leads to the possibility of mathematically modelling the associated kinetics; work is ongoing to this effect.

British Pharmaceutical Conference, Manchester, UK, September 2009.

Overcoming Dissolution Effects: The use of hyper differential scanning calorimetry to detect drug melting in solid dispersion systems. Otun S.O, Blade H., Meehan E., Qi S. and Craig D.Q.M.

Objectives: *To investigate the potential advantages of hyper DSC over standard to determine the presence of crystalline indometacin in solid dispersions using the polymer Gelucire 44/14. At slow heating rates, crystalline drug dispersed in a solid dispersion can further dissolve into the molten carrier, therefore eliminating the drug melting peak (Lloyd et al 1997). This may be interpreted incorrectly as the solid dispersion actually being a solid solution of drug in the carrier. This effect could potentially be overcome by increasing the rate of heating as this is known to inhibit kinetically controlled events such as dissolution (Gramaglia et al 2005).*

Methods: *Physical mixes at concentrations of 5, 10, 15, 20 and 25% w/w indometacin in Gelucire 44/14 were formulated in the DSC pan by weighing indometacin on top of Gelucire 44/14. This allowed mixing of the solid indometacin with molten Gelucire 44/14 during analysis. Solid dispersions at concentrations of 5, 10 and 50% w/w were formulated by adding indometacin to molten Gelucire 44/14 with continuous stirring, then cooling at room temperature for 48 hours. Samples were run at 10^{o}C/min using a TA Q1000 DSC in aluminium standard crimped pans, and 500^{o}C/min using a Perkin Elmer Diamond DSC in aluminium pin-hole pans.*

Results: A) *Physical Mixes: Crystalline indometacin melt enthalpies could be obtained for all physical mixes when heated at 500^{o}C/min. These enthalpies (x) were plotted against physical mix initial crystalline indometacin concentration (y) and extrapolated back to zero; the relationship y = 1.468x + 3.3125 was derived. This therefore allows us to calculate the % crystallinity in the solid dispersion systems. The 5 and 15% w/w physical mixes analysed at 10^{o}C/min did not display melting peaks. An endothermic transition was present on the 25% w/w physical mix DSC trace, however the peak max was found to be 139.70^{o}C, approximately 20^{o}C lower than that expected for indometacin.* ***B)*** *Solid Dispersions: Solid dispersions at concentrations of 5, 10, and 50% w/w were heated at 500^{o}C/min and analysed for crystalline indometacin melt enthalpies. These enthalpies were used to calculate the concentration of crystalline indometacin remaining in the formulation by applying the physical mix calibration plot equation (above). The 5, 10 and 50% w/w solid dispersions were calculated to contain 3.9%, 6.9% and 32.5% crystalline indometacin respectively. The study has therefore provided a new method of estimating crystalline drug concentration in polymers.*

Conclusions: *The fast heating rates employed by Hyper DSC appears to be a useful tool in determining a more accurate value for the true indometacin solubility by significantly reducing its further dissolution in the polymer Gelucire 44/14 during analysis. The data obtained at slower rates*

has the disadvantage of giving misleading conclusions due to the elimination of crystalline drug melting peaks.

References: 1) *Lloyd, G. R., Craig, D. Q. M., Smith, A. (1997) Int. J. Pharm.* ***158****: 39-46* ***2)*** *Gramaglia, D., Conway, B. R., Kett, V. L., Malcolm, K. R., Batchelor, H. K. (2005) Int. J. Pharm.* ***301****: 1-5*

American Association of Pharmaceutical Scientists Conference, Los Angeles, USA, November 2009.

Overcoming Dissolution Effects: The use of hyper differential scanning calorimetry to detect drug melting in solid dispersion systems. Otun S.O, Blade H., Meehan E., Qi S. and Craig D.Q.M. Journal of Pharmacy and Pharmacology, **61**, A48-A49.

Purpose: *To investigate the potential advantages of hyper over standard DSC to overcome dissolution effects and determine the presence of crystalline indometacin in solid dispersions containing the polymer Gelucire 44/14.*

Methods: *Indometacin and Gelucire 44/14 were formulated into physical mixes directly in the DSC pans at concentrations from 5 to 25% w/w. Solid dispersions, at concentrations of 5 to 50% w/w, were prepared via the melt method and held at 20°C or 4°C to cool for 48 hours prior to DSC measurements. Samples were analysed at 10°C/min and 500°C/min.*

Results: *In order to understand the miscibility of indometacin crystals in Gelucire 44/14 on heating, physical mixes were studied using hyper DSC. Crystalline indometacin melt enthalpies (x) were obtained at 500°C/min for all physical mixes and plotted against initial crystalline indometacin concentration (y). A linear relationship y = 1.468x + 3.3125 was derived. Solid dispersions were heated at 500°C/min and analysed for crystalline indometacin melt enthalpies. The crystalline indometacin (% w/w) in the formulation was calculated using the physical mix calibration plot obtained above. The 20°C cooled 5, 10, 15 and 50% w/w solid dispersions were calculated to contain 3.9, 6.9, 3.3 and 32.5% w/w crystalline indometacin respectively. The equivalent 4°C cooled solid dispersions contained 5.3, 4.4, 6.2 and 31.4% w/w crystalline indometacin. The increased rate of cooling showed no significant effect on the crystalline indometacin contents in the solid dispersions. Solid dispersions at concentrations of 5, 10 and 15% w/w, heated at 10°C/min, demonstrated no obvious indometacin melting peaks, indicating further dissolution of indometacin in Gelucire 44/14 during heating. Therefore, the fast heating rate showed potential in minimising the dissolution of model drug in the polymer matrix in solid dispersions during heating.*

Conclusions: *The fast heating rates employed by Hyper DSC appears to be a useful tool in providing more accurate estimation of crystalline drug concentration in polymeric solid dispersions compared to standard DSC by significantly reducing dissolution effects of the model drug in the polymer during analysis.*

Academy of Pharmaceutical Scientists, Nottingham, UK, September 2010.

The characterisation of slow crystallisation of lipidic solid dispersion systems using Quasi-isothermal MTDSC. Otun S.O, Meehan E., Qi S. and Craig D.Q.M. Journal of Pharmacy and Pharmacology, **62** (10) 1352-1353.

Introduction: *Quasi-isothermal modulated temperature DSC is a technique by which the sample material is subjected to modulations about a constant temperature for a prolonged period of time. This temperature is incrementally increased or decreased through a thermal transition, minimising the kinetic effects of the heating programme and meaning that the isothermal data sequence obtained illustrates the true transition temperature of the sample (Manduva et al 2008). In this study this method has been used to investigate the crystallisation process of lipid-based solid dispersion systems. In particular, it is recognized that slow or incomplete crystallisation is a significant manufacturing issue, but very little information is available on this phenomenon. Here we suggest a novel means by which it may be quantitatively monitored.*

Materials and Methods: *Samples of Gelucire 44/14 and the formulated solid dispersion systems, in the weight range 1.97 to 2.25mg, were prepared into aluminium Tzero pans and analysed using a TA Q2000 DSC. After complete melting at 60°C for Gelucire alone and a maximum of 220°C for the model drug systems to allow for any crystalline drug melting, the samples were run using Quasi-Isothermal MTDSC, cooling at 1°C increments from 35 to 5°C for Gelucire 44/14 alone and 25 to 0° for solid dispersions, with an isotherm of 20 minutes at each increment, an amplitude of ± 1°C and a period of 60 seconds.*

Results and Discussion: *Quasi-Isothermal MTDSC Lissajous analysis of the polymer Gelucire 44/14 illustrates obvious crystallisation on cooling at 31°C. Observation of the reversing heat capacity as a function of time, however, demonstrates crystallisation onset during the 33°C modulation, continuing until the conclusion of the experiment at 5°C, thus suggesting incomplete crystallisation. Solid dispersion formulation of Gelucire 44/14 with the selected model drugs appears to significantly reduce the polymer crystallisation temperature. Those systems containing 5% w/w ibuprofen reduced the crystallisation temperature to 25°C, with increasing drug loading reducing the temperature further still. At 50% w/w ibuprofen no obvious crystallisation occurred, however in all cases the reversing heat capacity steadily decreased over time suggesting that equilibrium was not reached and crystallisation was therefore incomplete. Indometacin and piroxicam solid dispersions with Gelucire 44/14 were also found to have a much reduced crystallisation onset at 21, 25 and 21 for indometacin 24, 21 and 25°C for piroxicam 5, 10 and 15% w/w drug loadings respectively. Again the 50% w/w systems for both model drugs did not demonstrate an obvious crystallisation peak however, as with all cases there was a steady decrease in heat capacity over time, becoming more pronounced at 7°C in the case of piroxicam. We believe the model drugs present in the solid dispersions to be crystalline, as a melt transition can be seen for the higher drug loadings on heating. Typically one would expect drugs to either promote crystallization (via nucleation) or to have no effect, hence the counterintuitive observation of retardation is of interest and practical significance. The presence of un-dissolved drug*

particles is known to affect the overall crystal growth rate of the polymer (Long et al 1995). In the present case, however, we suggest that dissolved drug may be suppressing either nucleation or growth. Solid dispersions of Gelucire 44/14 with the model crystalline drugs ibuprofen, indomethacin and piroxicam were prepared via the melt method at 60°C and allowed to cool at 20°C for 48 hours prior to analysis.

Conclusions: *Quasi-isothermal MTDSC appears to be a promising tool in the investigation of the crystallisation process. The combination of drug with polymer in solid dispersion systems appears to reduce the crystallisation temperature quite significantly if not eradicating it altogether. It is imperative to have an understanding of this process in order to predict its impact on the physicochemical properties of the final product. We would like to acknowledge AstraZeneca for the funding of this project.*

References: 1) *R. Manduva, V. L. Kett, S. R. Banks, J. Wood, M. Reading and D. Q. M. Craig, J. Pharm. Sci, 97 (2008) 1285 – 1300.* ***2)*** *Y. Long, R. A. Shanks and Z. H. Stachurski, Prog. Polym. Sci, 20 (1995) 651 – 701.*

American Association of Pharmaceutical Scientists Conference, New Orleans, USA, November 2010.

The use of quasi-isothermal MTDSC to characterise slow crystallisation of lipidic solid dispersion systems. Otun S.O, Meehan E., Qi S. and Craig D.Q.M.

Purpose: *To investigate the crystallisation process of lipid based solid dispersion systems using Quasi-Isothermal MTDSC. Here we suggest a novel means by which slow crystallization may be quantitatively monitored.*

Methods: *Samples of Gelucire 44/14 and the formulated solid dispersion systems were prepared into aluminium Tzero pans and, after complete melting, were run using Quasi-Isothermal MTDSC. The samples were cooled at 1°C increments from 35 to 5°C for Gelucire 44/14 alone and 25 to 0°C for solid dispersions, with an isotherm of 20 minutes at each increment, an amplitude of ± 1°C and a period of 60 seconds. Solid dispersions of Gelucire 44/14 with the model drugs ibuprofen, indometacin and piroxicam were prepared via the melt.*

Results: *Quasi-Isothermal MTDSC Lissajous analysis of the polymer Gelucire 44/14 illustrates obvious crystallisation on cooling at 31°C. Observation of the reversing heat capacity as a function of time, however, demonstrates crystallisation onset during the 33°C modulation, continuing until the conclusion of the experiment at 5°C, thus suggesting incomplete crystallisation. Solid dispersion formulation of Gelucire 44/14 with the selected model drugs appears to significantly reduce the polymer crystallisation temperature. For example, those systems containing 5% w/w ibuprofen reduced the crystallisation temperature to 25°C, with increasing drug loading reducing the temperature further still. Indometacin and piroxicam solid dispersions with Gelucire 44/14 were also found to have a much reduced crystallisation onset temperature. Typically one would expect drugs to either promote crystallization (via nucleation) or to have no effect, hence the counterintuitive*

observation of retardation is of interest and practical significance. The presence of un-dissolved drug particles is known to affect the overall crystal growth rate (Long et al 1995). In the present case, however, we suggest that dissolved drug may be suppressing either nucleation or growth.

Conclusions: *Quasi-isothermal MTDSC appears to be a promising tool in the investigation of the crystallisation process. The combination of drug with polymer in solid dispersion systems appears to reduce the crystallisation temperature significantly.* *We would like to acknowledge AstraZeneca for the funding of this project.*

References: *Y. Long, R. A. Shanks and Z. H. Stachurski, Prog. Polym. Sci, 20 (1995) 651 – 701.*